



# Peaks in frequency, but not relative abundance, occur in the center of tree species distributions on climate gradients

PATRICK H. MARTIN<sup>1,†</sup> AND CHARLES D. CANHAM<sup>2</sup>

<sup>1</sup>*Department of Biological Sciences, University of Denver, Denver, Colorado 80210 USA*

<sup>2</sup>*Cary Institute of Ecosystem Studies, Box AB, Millbrook, New York 12545 USA*

**Citation:** Martin, P. H., and C. D. Canham. 2020. Peaks in frequency, but not relative abundance, occur in the center of tree species distributions on climate gradients. *Ecosphere* 11(6):e03149. 10.1002/ecs2.3149

**Abstract.** The abundant-center hypothesis posits species are most abundant in the center of their climatic range and forms a key assumption in many species distribution models. However, this hypothesis has not been rigorously evaluated in plant communities, in part because abundance as a fraction of dominance is rarely incorporated. Here, we ask whether tree species frequency and abundance peak in the center of their distributions on continental-scale climate gradients across the Rocky Mountains and Interior West, USA. We used forest inventory data to model frequency (percentage of plots in a given climate a species occurred in) and relative abundance (percentage of basal area in plots) as a flexible function of climate for the 20 most common tree species on temperature and precipitation gradients. Frequency patterns were predominately “bell-shaped” and centered for species in the middle of both gradients and monotonic toward the extremes. Relative abundance patterns were primarily monotonic, especially with precipitation. In the middle of the temperature gradient, however, it is notable that six dominant and widespread species had peaks in both frequency and abundance that were centered and symmetric. Only one species had this pattern with precipitation. When frequency is considered, evidence for the abundant-center hypothesis is robust, especially in the middle portion of each gradient, and indicates patch occupancy probability generally declines away from a species' climatic optimum. For relative abundance, the hypothesis is largely refuted, particularly on the precipitation gradient. Together, these results suggest that climate's influence on patch colonization and occupancy dynamics is a fundamental filter on distribution patterns in Rocky Mountain forests, but that climate gradients are only weakly related to relative abundance and hence provide limited insight into the ecological processes that determine local dominance once a species is present in a site.

**Key words:** abundant-center hypothesis; biogeography of temperate trees; climate niche breadth; climate niche dimensions; climatic suitability models; Forest Inventory and Analysis (FIA); frequency vs. relative abundance; species distribution models.

**Received** 7 August 2019; revised 17 March 2020; accepted 18 March 2020. Corresponding Editor: Julie A. Jones.

**Copyright:** © 2020 The Authors. This is an open access article under the terms of the Creative Commons Attribution License, which permits use, distribution and reproduction in any medium, provided the original work is properly cited.

† **E-mail:** patrick.h.martin@du.edu

## INTRODUCTION

Ecologists have long assumed that climate is the overarching control on tree species distributions (Woodward 1987, Pacala and Hurtt 1993, Martin et al. 2007, Sherman et al. 2012), yet our quantitative understanding of how climate

structures the niches and distributions of tree species is incomplete (Rehfeldt et al. 2008, Canham and Thomas 2010, Clark et al. 2011, Dallas et al. 2017). Numerous approaches have been developed to model species climate distributions and to forecast species distributions along spatial or climatic gradients (Box et al. 1999, Iverson

et al. 2004, Hijmans and Graham 2006, Phillips and Dudík 2008, Elith and Leathwick 2009, Drake 2015), but these models are commonly based on presence–absence data (Thuiller 2003, Thuiller et al. 2006, McKenney et al. 2007), constrain the form the modeled niche can take (e.g., strictly bell-shaped, linear, and symmetric), and assume a species is most abundant in the center of its distribution (i.e., the “abundant-center hypothesis”; Sagarin and Gaines 2002).

Evidence for the abundant-center hypothesis is mixed in practice, however. Some studies provide strong support (VanDerWal et al. 2009, Gutiérrez et al. 2013), while others report that climatic distributions, at least those based on presence–absence data, do not predict patterns of species abundances (Nielsen et al. 2005, Filz et al. 2013, Dallas and Hastings 2018), casting doubt on the assumption that species are reliably most abundant in the center of their climatic distributions (Sagarin and Gaines 2002, Dallas et al. 2017). Furthermore, until recently our knowledge of species distribution patterns came primarily from faunal and marine communities (Lester et al. 2009), as distribution patterns in terrestrial plant communities along climate gradients were less studied. There is good reason to think distribution patterns in plant communities may be distinctive, with climate potentially shaping abundance patterns less than other ecological processes, especially for long-lived plant species. Dispersal and recruitment limitation, site disturbance history, topographic conditions, and biotic interactions such as competition (Canham et al. 2006, Bascombe 2009, HilleRisLambers et al. 2013) may all shift demographic rates and abundance patterns away from a species’ optimal climate. A number of recent studies on tree species distribution patterns have helped address this gap—characterizing tree probability of occurrence in relation to climate (Rehfeldt et al. 2006, 2008, Bell et al. 2014, Copenhaver-Parry et al. 2016, 2020), with one study in the eastern United States finding virtually no evidence of abundant-center relationships (Canham and Thomas 2010)—yet the relationship between patterns of abundance and climate in forests requires further inquiry.

In this study, we ask how the distribution, frequency, and abundance of Rocky Mountain tree species are structured on large gradients in climate using regional-scale forest inventory data,

and if there is evidence of functional groups of species with similar abundance and frequency patterns or a more individualistic distribution of species. Climate niche studies are needed in these forests, as temperatures are warming rapidly in the western United States (Pederson et al. 2010) and precipitation is changing in type, quantity, and seasonality (Mote 2006). We asked whether species are most abundant in the center of their climatic niches with symmetric distributions centered around the mode, as theory assumes. Do patterns of frequency and abundance vary similarly along climatic gradients? Are Rocky Mountain forests more structured by climate than forests in the eastern United States, or do we find similar patterns between biomes suggesting widespread and common dynamics between trees and climate? Given the steep climate gradients in the Rocky Mountains and the comparatively low number of tree species in the region, we expected that the climate niches of tree species would be well defined and display comparatively sharp transitions between species, and that peaks in abundance would be in the center of a species’ climatic distribution.

## METHODS

Our analyses are focused on the Interior West region of the U.S. Forest Service Forest Inventory and Analysis (FIA) program (Bechtold and Patterson 2005), encompassing Arizona, New Mexico, Colorado, Utah, Wyoming, Idaho, and Montana (<http://www.fs.fed.us/rm/ogden>). The region has a wide range in climate. There is a slight negative covariance between temperature and precipitation across the region, but there is a wide range of precipitation regimes for any given annual mean temperature, and vice versa. The region occurs entirely west of the historical dry boundary demarking the arid grasslands of the Great Plains (Salley et al. 2016). In the Interior West, the prairie–forest ecotone at lower elevations and the treeline ecotone at higher elevations occur widely on mountains throughout the region, frequently on the same landscape. Hence, the region’s mountainous terrain enables the full climatic distribution of extant tree species to be captured “locally” on the elevation gradient, often over small distances. Nevertheless, several dominant species in the region have distributions

that extend north or south of the Interior West FIA dataset (see *Results*) and care in the interpretation in their climatic distributions is warranted.

Forest Inventory and Analysis plots have four circular subplots (each 168.3 m<sup>2</sup>) with 36.6 m between subplot centers. All adult trees (stems  $\geq 12.7$  cm diameter at breast height [dbh]) are measured in the subplots, and saplings (stems  $\geq 2.5$  and  $< 12.7$  cm dbh) are measured in a 2.07 m radius microplot nested in each subplot. We combined data from the four microplots (for a total microplot area of 53.85 m<sup>2</sup>) and four subplots (for a total area of 673.2 m<sup>2</sup> per plot) to estimate presence and abundance of adults and saplings at the plot level. FIA plots are added to all public and private areas of “forest land” in the United States, which explicitly includes areas with small stems and sparse woody cover, defined as “at least 5% crown cover by live tally trees of any size or at least 5% cover of live tally species in the past (based on the presence of stumps, snags, or other evidence), or the presence of sufficient reproduction (40 tally tree species seedlings/saplings per acre).” Tally tree species are prioritized for sampling, usually because they occur in tree growth form throughout much of their range. “Forest land” includes transition zones, such as areas between forest and nonforest lands that meet the  $\geq 5\%$  tree crown cover criteria.

Because we required exact locations to extract climate data at the plot level, we limited our analyses to plots with exact locations provided via a security memorandum with the FIA program, and we also omitted plots with zero live saplings or adult trees due to either harvesting or natural disturbance. These criteria resulted in a total sample of 9543 plots, which span a wide range in latitude ( $\sim N 31^\circ$  to  $N 49^\circ$ ) and longitude ( $\sim W 102^\circ$  to  $W 117^\circ$ ) and climate (displayed in Appendix S1). The plots were censused over a wide range of years (1993–2009), but two-thirds of plots were measured between 2004 and 2009.

We compiled 10 yr of climate data up to the census date of each plot, using a bilinear interpolation of 800-m resolution PRISM climate data (<http://www.prism.oregonstate.edu/>). We focused our analyses on two climate variables, mean annual temperature and average annual precipitation during the 10 yr preceding the census, for reasons both pragmatic and principled. More

complex, derived climate variables (i.e., potential evaporation) could have a more mechanistic link to plant performance; however, the influence of specific derived climate variables likely varies idiosyncratically among species, making standard climate niche comparisons between species problematic. Moreover, much of the scientific and policy debate about climate change is couched in terms of annual mean temperature and total rainfall (Christensen et al. 2007).

We included all FIA tally tree species with sufficient sample sizes in the dataset for analysis (Table 1), dropping rare species which were insufficiently abundant for modeling and five species whose distribution is primarily outside the boundaries of the Interior West FIA region. These criteria resulted in a pool of 20 tree species for the analysis, capturing the vast majority of the biomass and individual trees in the region. We calculated presence and relative abundance separately for adults and saplings of each species in each plot, based on their percentage of adult or sapling basal area in the plot. We analyzed saplings separately as there is growing evidence of a divergence between the climate distributions of tree vs. sapling conspecifics as climate changes (Bell et al. 2014, Dobrowski et al. 2015); juveniles are more sensitive to climate than adult trees (Canham and Murphy 2016a) and hence may have different climate distributions; and adult-sized trees often take decades or longer to recruit into the canopy, and as such, the climate is often quite different now than when current adults were saplings.

In contrast to an analysis of FIA data in the eastern United States by Canham and Thomas (2010), which used a univariate symmetric Gaussian function (i.e., where temperature [ $T$ ] or precipitation [ $P$ ] was analyzed separately and functions were constrained to be symmetric around the mode), we modeled all species for presence and relative abundance with a bivariate symmetric Gaussian and a bivariate asymmetric Gaussian functional form, fitting for  $T$  and  $P$  simultaneously. The Gaussian function is widely used in describing niche dimensions, and our use of it here also reflects the flexible nature of the function: Depending on the values of the parameters, the shape of the function can be monotonically increasing, monotonically decreasing, or unimodal within a given range of  $T$  or  $P$ . In

Table 1. Study species, frequency of occurrence in FIA plots, model form, and goodness of fit ( $R^2$ ) as a bivariate function of temperature and precipitation for adult-sized tree species.

Tree species	Code	FIA plots frequency (%)	Adults		
			Functional form	Frequency ( $R^2$ )	Relative abundance ( $R^2$ )
<i>Abies concolor</i>	ABCO	3.7	Symmetric	0.777	0.043
<i>Abies lasiocarpa</i>	ABLA	23.2	Asymmetric	0.949	0.094
<i>Abies lasiocarpa</i> v. <i>arizonica</i>	ABAR	1.1	Asymmetric	0.248	0.049
<i>Acer grandidentatum</i>	ACGR	0.6	Symmetric	0.018	-0.026
<i>Cercocarpus ledifolius</i>	CELE	1.2	Symmetric	0.543	0.018
<i>Juniperus depeana</i>	JUDE	5.7	Asymmetric	0.949	-0.002
<i>Juniperus monosperma</i>	JUMO	4.1	Asymmetric	0.922	0.215
<i>Juniperus osteosperma</i>	JUOS	5.1	Asymmetric	0.765	0.076
<i>Juniperus scopulorum</i>	JUSC	4.7	Symmetric	0.793	-0.002
<i>Picea engelmannii</i>	PIEN	22.9	Asymmetric	0.965	0.126
<i>Pinus albicaulis</i>	PIAL	5.4	Asymmetric	0.904	0.143
<i>Pinus contorta</i>	PICO	20.1	Symmetric	0.945	0.083
<i>Pinus edulis</i>	PIED	9.4	Symmetric	0.928	0.011
<i>Pinus flexilis</i>	PIFL	4.5	Symmetric	0.880	0.024
<i>Pinus ponderosa</i>	PIPO	15.1	Asymmetric	0.972	0.077
<i>Populus tremuloides</i>	POTR	11.7	Symmetric	0.954	0.042
<i>Pseudotsuga menziesii</i>	PSME	26.9	Asymmetric	0.961	0.052
<i>Quercus arizonica</i>	QUAZ	3.5	Symmetric	0.908	0.082
<i>Quercus emoryi</i>	QUEM	1.6	Asymmetric	0.359	0.053
<i>Quercus gambelii</i>	QUGA	4.6	Symmetric	0.739	0.015

Note: Frequency of occurrence was calculated for each species based on its presence in the 9543 FIA plots in the analysis. The functional form of the best model was determined with AIC<sub>c</sub>. We evaluated goodness of fit of predicted frequency by binning the data into intervals of predicted frequency and comparing the average predicted frequency in that bin to the actual fraction of those plots in which the species was present. Goodness of fit of predictions of relative abundance when present was assessed using  $R^2$  calculated on the subset of plots in which a species was present;  $R^2$  values are low given the gamma distribution and wide scatter in the points.

fitting  $T$  and  $P$  simultaneously, our bivariate model allows for a more realistic estimate of how  $T$  and  $P$  interact to shape species distributions, and the asymmetric model provides superior realism in estimating niche dimensions by not assuming that upper and lower segments of a climate niche are identical. Bell-shaped curves and distributions are given a variety of names (e.g., normal distribution, normal curve, bell curve, Gaussian curve). Even when bell-shaped, however, our models do not necessarily describe a normal probability distribution, and as noted, Gaussian distributions can assume non-bell-shaped curves. Hence, in our results we refer to distributions with a clear mode or peak and symmetric or asymmetric declines around the mode as “bell-shaped.”

Species abundance distributions were all left-skewed and zero-inflated (i.e., non-normal, with a large number of plots with zero abundance). Thus, our model simultaneously estimates the

two components of abundance: (1) presence, modeled as a Bernoulli process, and (2) relative abundance when present, under a gamma distribution to account for the skew in the distribution of abundance. The data also displayed clear evidence of range limits along the gradients, so we thus incorporated a third component to estimate upper and lower range limits, that is, points along the temperature and precipitation gradients beyond which the probability of presence was effectively zero (set at less than 0.000001) and predicted relative abundance was 0.

The symmetric form was a simple bivariate Gaussian function:

$$\text{RA or Presence} = \left\{ a_{\max} e^{-0.5 \left( \frac{T-t_m}{t_v} \right)^2} e^{-0.5 \left( \frac{P-p_m}{p_v} \right)^2} \right\}$$

if  $T_{\min} < T \leq T_{\max}$  and  $P_{\min} < P \leq P_{\max}$ ,

otherwise RA or Presence = 0

(1)



The bivariate asymmetric Gaussian function:

$$\text{RA or Presence} = \left\{ \begin{array}{l} a_{\max} e^{-0.5 \left( \frac{T-t_m}{t_{lo}} \right)^2} \text{ if } T \leq t_m \\ a_{\max} e^{-0.5 \left( \frac{T-t_m}{t_{hi}} \right)^2} \text{ if } T > t_m \end{array} \right\} \times \left\{ \begin{array}{l} a_{\max} e^{-0.5 \left( \frac{P-p_m}{p_{lo}} \right)^2} \text{ if } P \leq p_m \\ a_{\max} e^{-0.5 \left( \frac{P-p_m}{p_{hi}} \right)^2} \text{ if } P > p_m \end{array} \right\}$$

if  $T_{\min} < T \leq T_{\max}$  and  $P_{\min} < P \leq P_{\max}$ ,  
 otherwise RA or Presence = 0 (2)

In both forms,  $T$  is mean annual temperature and  $P$  is average annual precipitation in a plot, and  $T_{\min}$ ,  $T_{\max}$ ,  $P_{\min}$  and  $P_{\max}$  were the estimated lower and upper range limits for temperature and precipitation, respectively, and  $a_{\max}$ ,  $t_m$ ,  $t_v$ ,  $p_m$ , and  $p_v$  are estimated parameters. Relative abundance is assumed to be zero below or above estimated climate limits ( $T_{\min}$  and  $T_{\max}$  and  $P_{\min}$  and  $P_{\max}$  respectively). Note: Relative abundance was scaled from 0 to 100, so  $a_{\max}$  is the predicted presence or abundance (in percentage of basal area) in the optimal environment (i.e., when  $T = t_m$  and  $P = p_m$ ). The symmetric function (Eq. 1) simply estimates a single value for niche breadth for presence and a single value of niche breadth for relative abundance when present (i.e.,  $t_v$  instead of  $t_{lo}$  and  $t_{hi}$ , and  $p_v$  instead of  $p_{lo}$  and  $p_{hi}$ ), while the asymmetric function (Eq. 2) estimates the modal temperature ( $t_m$ ) and precipitation ( $p_m$ ), and then allows different niche breadths and shapes below and above that mode ( $t_{lo}$  and  $t_{hi}$  and  $p_{lo}$  and  $p_{hi}$  respectively).

These equations were truncated to zero for plots outside the estimated range limits of a given species. We defined a climatic range limit statistically as the value on a gradient beyond which the probability of observing a nonzero abundance in a plot is highly unlikely. Setting this likelihood to zero (i.e., an absolute limit) is problematic for both computational reasons (generating underflows when taking the log of zero) and from a sampling perspective, since there can be errors in species identification outside the true range of a species. We set the likelihood to 1 in a million (0.000001) for the probability of observing a species in a plot outside the estimated range

limit for the species. We tested other thresholds which did not result in notable changes in estimated range limits, as range thresholds along both climate gradients were quite abrupt.

The overall likelihood function was as follows:

$$\text{Prob}(y|\theta) = \begin{cases} 0.000001 & a \\ P_z (= 1 - \text{Prob}(\text{presence})) & b \\ (1 - P_z) \text{Gamma}(y|\theta) & c \end{cases}$$

<sup>a</sup>if  $T < T_{\min}$  or  $T > T_{\max}$  or  $P < P_{\min}$  or  $P > P_{\max}$   
<sup>b</sup>if  $y = 0$   
<sup>c</sup>if  $y > 0$  (3)

where  $y$  was the observed relative abundance of a given species in a plot;  $T$  was the mean annual temperature and  $P$  the average annual precipitation in the plot;  $T_{\min}$ ,  $T_{\max}$ ,  $P_{\min}$  and  $P_{\max}$  were the estimated lower and upper range limits for  $T$  and  $P$ , respectively; and  $\text{Gamma}(y|\theta)$  is the probability of observing a (nonzero) abundance of  $y$  given a gamma distribution and the estimated parameters of the model ( $\theta$ ).

We used simulated annealing, a global optimization algorithm, to find the maximum likelihood estimates of the parameters for both functions for each species as a function of  $T$  and  $P$ , using the *likelihood* package (version 1.7) in R (R Core Team 2014). We compared the symmetric and asymmetric models, and present results from the model with the lower AIC<sub>c</sub> (Tables 1, 2). We calculated two-unit support intervals to evaluate strength of evidence for the parameter estimates (shown in Appendices S2, S3). Analogous to a 95% confidence interval, two-unit support intervals are common in likelihood methods and calculate the range of parameter values in which the likelihood of the model is within two units of likelihood of the best model. We evaluated goodness of fit of the predicted presence by binning the data into intervals of predicted presence and then comparing the average predicted presence in that bin to the actual fraction of those observations in which the species was present; goodness of fit of the predictions of relative abundance when present was assessed using  $R^2$  calculated on the subset of plots in which a species was present (Tables 1, 2).

Table 2. Study species, frequency of occurrence in all FIA plots, model form, and goodness of fit ( $R^2$ ) as a bivariate function of temperature and precipitation for sapling-sized individuals.

Tree species	Code	FIA plots frequency (%)	Saplings		
			Functional form	Frequency ( $R^2$ )	Relative abundance ( $R^2$ )
<i>Abies concolor</i>	ABCO	1.7	Asymmetric	0.777	0.010
<i>Abies lasiocarpa</i>	ABLA	14.8	Asymmetric	0.941	0.043
<i>Abies lasiocarpa</i> v. <i>arizonica</i>	ABAR	0.6	Symmetric	0.491	0.006
<i>Acer grandidentatum</i>	ACGR	0.7	Symmetric	0.650	-0.019
<i>Cercocarpus ledifolius</i>	CELE	0.6	Symmetric	0.346	-0.027
<i>Juniperus depepeana</i>	JUDE	1.4	Asymmetric	0.697	-0.019
<i>Juniperus monosperma</i>	JUMO	1.0	Symmetric	-0.612	0.161
<i>Juniperus osteosperma</i>	JUOS	1.4	Symmetric	-0.018	0.073
<i>Juniperus scopulorum</i>	JUSC	1.3	Symmetric	0.380	-0.031
<i>Picea engelmannii</i>	PIEN	10.1	Asymmetric	0.950	0.041
<i>Pinus albicaulis</i>	PIAL	2.3	Asymmetric	0.655	0.135
<i>Pinus contorta</i>	PICO	8.8	Symmetric	0.943	0.009
<i>Pinus edulis</i>	PIED	5.1	Asymmetric	0.862	0.041
<i>Pinus flexilis</i>	PIFL	1.2	Symmetric	0.563	-0.002
<i>Pinus ponderosa</i>	PIPO	4.4	Symmetric	0.883	-0.001
<i>Populus tremuloides</i>	POTR	6.2	Symmetric	0.896	-0.011
<i>Pseudotsuga menziesii</i>	PSME	9.6	Asymmetric	0.957	0.018
<i>Quercus arizonica</i>	QUAZ	1.5	Symmetric	0.679	-0.004
<i>Quercus emoryi</i>	QUEM	0.5	Symmetric	0.275	0.066
<i>Quercus gambelii</i>	QUGA	6.0	Asymmetric	0.948	0.013

Note: See legend in Table 1 for full description.

We used output from these models to visually classify the shape of each species climate niche into one of three basic patterns: flat; monotonically peaking toward either end of the gradient; or showing a clear mode or peak on the gradient with an approximately symmetric or bell shape to the pattern. Distribution patterns for temperature and precipitation were evaluated separately. For each species, we also visually determined whether its frequency and abundance distributions (1) peak together with a bell shape at or near the center of its climate range, (2) peak together outside of the center of its climate range, or (3) peak separately on different sections of its climate range. By definition, flat or monotonic changes in frequency and abundance distributions cannot satisfy scenario 1.

## RESULTS

The FIA plots of the Interior West region encompass a wide range of temperatures (mean annual temperatures (MATs) from  $-4.5^{\circ}\text{C}$  to  $22.5^{\circ}\text{C}$ ) and precipitation (155–2350 mm/yr). See Appendix S1 for the full climate space of the study system. Based on our analysis of range

limits, this FIA dataset appears to encompass the complete climatic range of nearly all of the study species (see Appendix S1 for individual species climate space diagrams). A few species with substantial distributions outside of the Interior West region may experience climate conditions not covered in this dataset. *Abies lasiocarpa*, *Picea engelmannii*, and *Pinus albicaulis* may experience lower MATs and higher precipitation north and west of the study area, and *Juniperus monosperma* may extend into higher temperatures than captured in our study (Figs. 1, 2).

*Pseudotsuga menziesii* occurred most frequently (adult-sized PSME occurred in 26.9% of the FIA plots), and *Acer grandidentatum* was the least frequent (0.6%; see Tables 1, 2 for all species). There was no evident pattern between frequency or relative abundance (hereafter, abundance) and niche breadth, as the niche breadths of subdominant and rarer species were generally as wide as dominant species on both temperature and precipitation gradients (Figs. 1–3).

### Frequency and temperature

Frequency, that is, the percentage of plots in a given climate in which a species occurred,

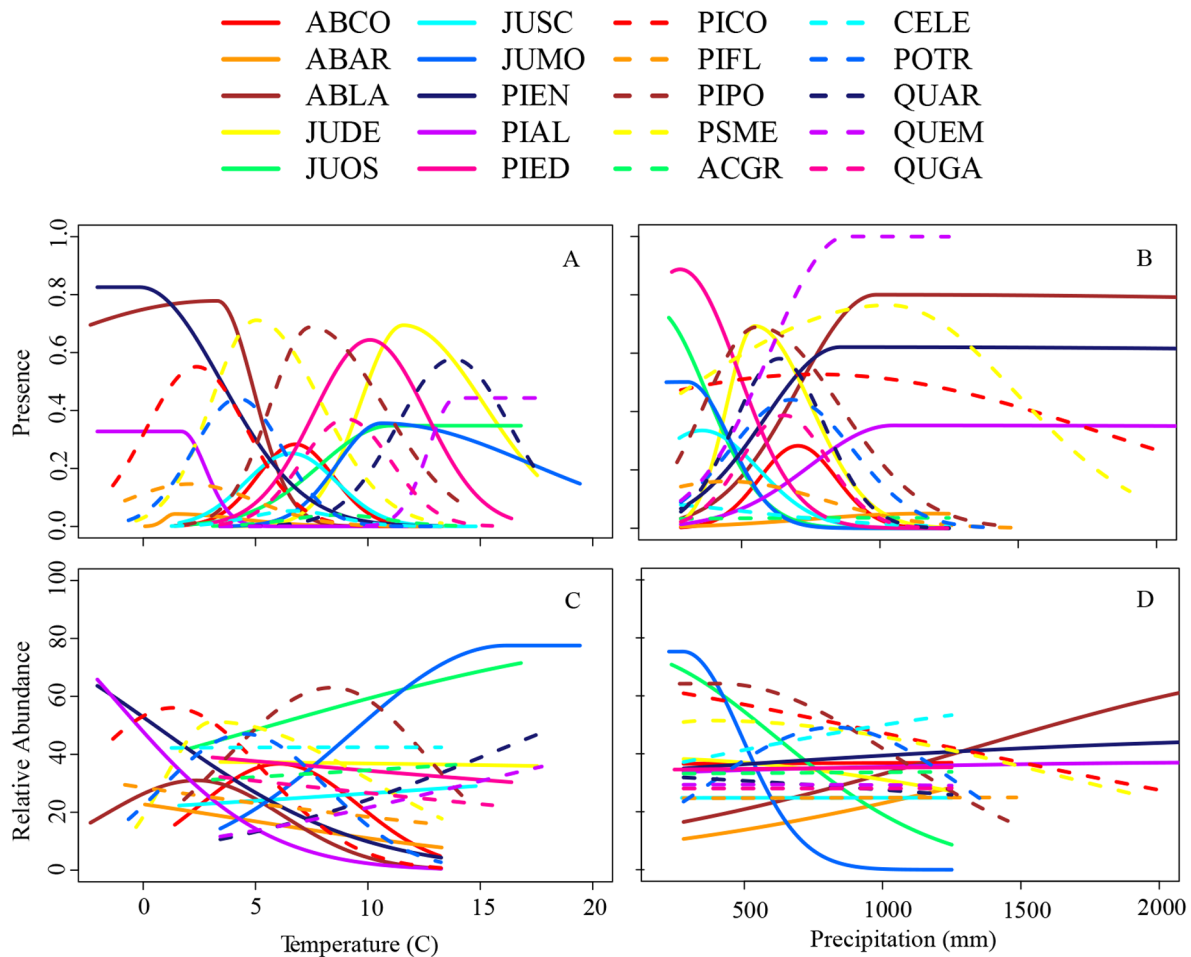


Fig. 1. Distribution, frequency, and abundance of adult-sized tree species as a function of annual mean temperature and precipitation for the 20 most abundant tree species in the Interior West region. Curves show predicted variation in presence (the percentage of plots in which the species occurs) and relative abundance (percentage of basal area, when present) as a function of climate. Temperature patterns are displayed with precipitation held at the mean level for that species and vice-a-versa. Patterns for each species individually with two-unit support intervals are shown in Appendices S2, S3. Species abbreviations consist of the first two letters of the genus and specific epithet, for example, *Abies concolor*, ABCO. Full species names are listed in Table 1.

varied strongly with mean annual temperature for nearly all species (Figs. 1A, 2A; Appendix S2). Indeed, while climatic range limits were quite broad for most species, the range in climate in which a species was common was much narrower. Frequency patterns on the temperature gradient were individualistic, with no obvious clusters or ecotones of species groups (Fig. 3A). The adults of eight species dominate regional frequency, each with the highest frequency on some portion of the temperature gradient. The six species of adults that

dominate the middle of the gradient display classic patterns of turnover, partitioning the niche space with nearly identical, non-overlapping peaks in frequency, while the species that dominate the ends of the gradient—*A. lasiocarpa*, *P. albicaulis*, and *P. engelmannii* at  $<2\text{--}3^\circ\text{C}$ , *Juniperus osteosperma* and *Quercus emoryi* at  $>15^\circ\text{C}$ —show no declines in frequency past a threshold temperature (Fig. 1A).

Frequency patterns with temperature for the adults of 15 species and saplings of 17 species showed a clearly defined peak, including both

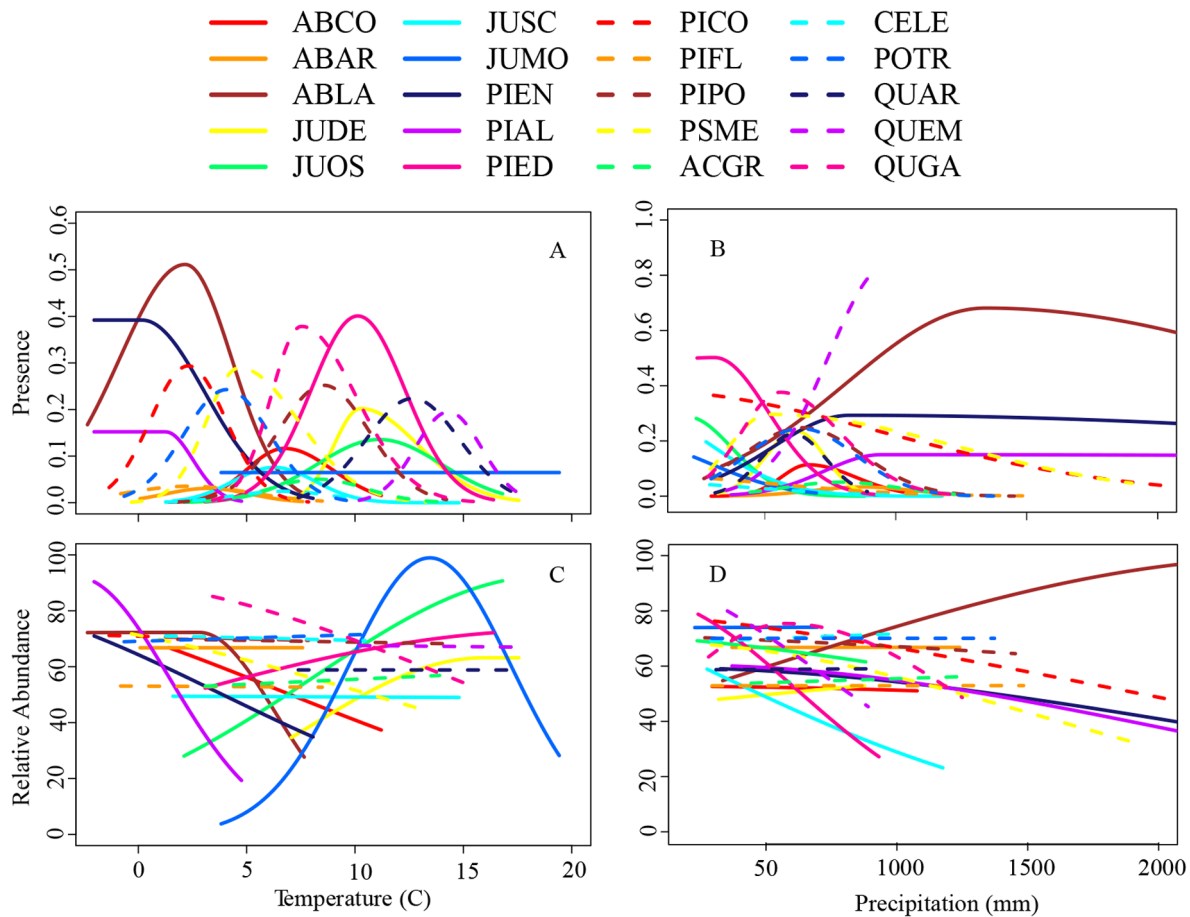


Fig. 2. Distribution, frequency, and abundance of sapling-sized tree species as a function of annual mean temperature and precipitation for the 20 most abundant tree species in the Interior West region. Note the different scales between temperature and precipitation for presence. Patterns for each species individually and two-unit support intervals are provided in Appendices S2, S3. See Fig. 1 legend for full details.

very common (e.g., peak frequency of 50–80%) and less common species (e.g., peak frequencies <40%). Moreover, frequencies of adults of 12 species and saplings of 15 species were both bell-shaped and symmetric—that is, clearly unimodal with approximately identical distributions around the mode—on the temperature gradient. Of the remaining species, all five species of adults and two of the three species of saplings with non-bell-shaped frequencies had strongly curvilinear distributions (i.e., not flat) with temperature, but were highly asymmetric around the peak. Only *J. monosperma* saplings had a flat, invariant frequency with temperature.

#### Frequency and precipitation

Frequency patterns with precipitation also varied markedly for nearly all species (Figs. 1B, 2B; Appendix S3), but the shapes of frequency distributions were more varied in shape and less individually spaced on the gradient compared to temperature (Fig. 3B). The species can be visually classed into three functional groups along the precipitation gradient: (1) nine species of adults and nine of saplings, all with bell-shaped patterns, clustered at intermediate precipitation levels, of which five species of adults and eight of saplings were symmetric; (2) on the wet end, five species had a monotonic increase in



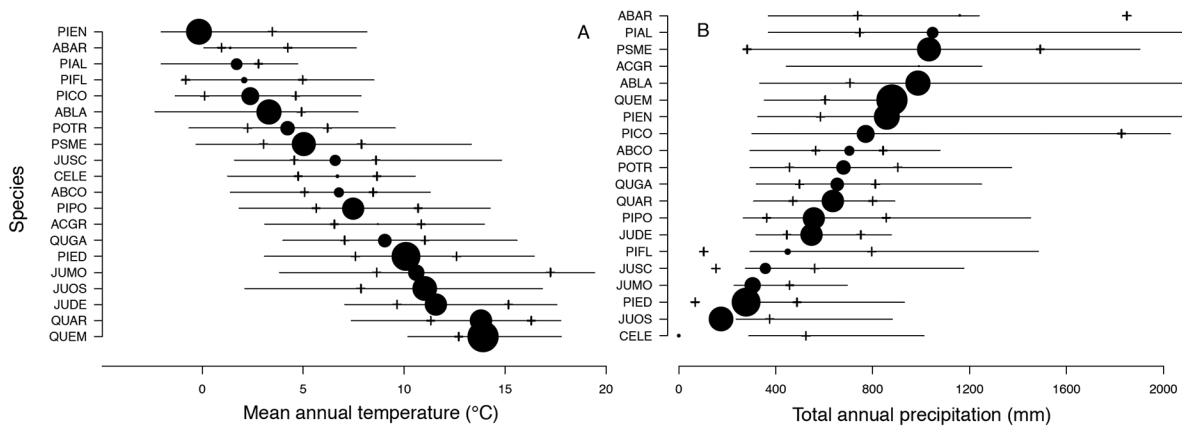


Fig. 3. (A) The mean annual temperature and (B) average annual precipitation at which species reached their peak estimated frequency (location and size of circular symbol), the range of temperatures and precipitations within which species were present (solid lines), and the estimated niche breadth for presence along the temperature or precipitation gradient (indicated by the range between the crosses). Niche breadths were the estimated standard deviations of the Gaussian distributions (Eq. 2). For asymmetric models, the niche breadths are different above and below peak frequency. No niche breadth shown on one end of the gradient indicates that niche breadth exceeded the observed range of temperature or precipitation on that end of the gradient. Frequency in several species did not reach a clear peak within the observed range of precipitation (i.e., JUOS and CELE). The size of the circular symbol is proportional to the highest estimated peak frequency among the 20 species. Species codes are given in Table 1.

frequency at higher levels of precipitation, up to a threshold level where frequency plateaued; and (3) on the dry end, five species showed a monotonic or nearly monotonic increase in frequency at lower levels of precipitation. The frequency of a single species (*A. grandidentatum*) was effectively flat. The composition of these groups is generally congruent with conventional wisdom on the drought tolerance and the distribution of the species along moisture gradients in the region, for example, three species of juniper and the two-needle pinyon (*Pinus edulis*) showed peak frequencies at the low end, while all species with peak frequencies at high precipitation are dominant in snowy, high elevation forests.

Overall, departures from symmetric frequency distributions occurred entirely at the extreme ends of both climate gradients, although the distributions of a few species did remain bell-shaped and symmetric at the extremes. In the center of each climate gradient, temperature and precipitation frequencies were symmetric for all but two rare species, which were flat. The precipitation niche for most species, as a portion of the total gradient, was narrower than temperature,

with 14 species limited to the lower half of the precipitation gradient (~250–1000 mm/yr). Additionally, there was much more overlap in peak frequencies along the precipitation than temperature gradient, highlighting how moisture requirements are fundamentally shared by groups of western tree species.

#### Relative abundance and temperature

Abundance patterns showed highly individualistic variation (i.e., bell-shaped, negative, positive, neutral; Figs. 1C, 2C) along climatic gradients, varying markedly for the adults of 15 species. Five species showed modest-to-no variation. The adults of only six species (*Abies concolor*, *A. lasiocarpa*, *Pinus contorta*, *Pinus ponderosa*, *Populus tremuloides*, and *P. menziesii*) and the saplings of only one species displayed strongly bell-shaped abundance patterns with temperature, all occurring entirely in the middle portion of the gradient; only three species of adults and none of the saplings were both bell-shaped and symmetric. The abundance of the 12 adults that dominate the hot or cold extremes of the gradient all rapidly and monotonically decline as

temperatures moderate. Five of the 10 species that are common (frequencies >40%) on the temperature gradient also have the high abundance with temperature (Fig. 1; Appendix S2). For most species, peaks in abundance were visually wider than peak frequencies on both gradients.

#### Relative abundance and precipitation

Abundance on the precipitation gradient displayed little niche structuring or interspecific partitioning (Figs. 1D, 2D), with nine adult-sized species showing effectively no variation in abundance across their entire precipitation range. The abundance of only one species of adult and one species of sapling was both bell-shaped and symmetric with precipitation. Six species declined monotonically in abundance with higher precipitation (all were from driest end of the gradient), while four species monotonically increased with precipitation, two of which dominate the wet end.

#### Abundant-center relationships

We found evidence of “full” abundance-center relationships—when the center of a species’ climatic distribution, peak frequency, and peak abundance all coincide on the climate gradient—for adults of six species and no saplings on the temperature gradient, and only adults of one species (*P. tremuloides*) and saplings of one species (*Quercus gambelii*) on the precipitation gradient. All but one of these species have ranges that appear entirely encompassed by the climate space in our dataset, and the adults of all of these species are abundant, regional dominants (*A. lasiocarpa*, *P. contorta*, *P. ponderosa*, *P. tremuloides*, and *P. menziesii*) or subdominants (*A. concolor*), as defined by species with peak frequencies and peak relative abundances >40%. Dominance is not inevitably associated with these relationships, however, as there were five dominant species (*Juniperus deppeana*, *P. edulis*, *P. engelmannii*, *Quercus arizonica*, and *Q. emoryi*) on the temperature gradient whose abundance either peaked at the extremes or was invariant. Moreover, these relationships were nonexistent on both gradients for the adults of rarer species and saplings of nearly all species irrespective of dominance. Many of these rarer species and saplings either showed little variation in abundance over their

entire range or increased monotonically in abundance toward one end of their range.

Coincident peaks in frequency and abundance that occur away from the center of a species’ climatic distribution were more common than “full” abundant-center patterns. Such non-centered peaks occurred for 11 species of adults and 3 species of saplings on the temperature gradient (all on the coldest end), and 8 species of adults (mostly peaking on the wet or dry extremes) and 4 species of saplings (3 of which peak on the dry end) on the precipitation gradient.

Finally, a number of species have centered peaks in frequency but not abundance: Adults of 15 species and saplings of 18 species have peak frequencies in the center of their temperature ranges, and adults of 10 species and saplings of 9 species have peak frequencies in the center of their precipitation ranges. The remaining species either had peak frequencies that did not coincide with their range centers—all dominate the hot or cold ends of the gradient—or had no variation in frequency.

## DISCUSSION

#### Abundant-center relationships

Our two components of species abundance, frequency and relative abundance when present, generally showed divergent patterns along climate gradients. When only frequency is considered, the hypothesis that abundance is highest near the center of a species’ climatic range (Dallas and Hastings 2018) is robust for most species, especially along temperature gradients. When abundance as a fraction of stem basal area is included, however, the hypothesis is refuted for most species, especially at the extremes on the temperature and precipitation gradients. In particular, our analyses indicate that on the precipitation gradient in the Interior West region, neither the center of a species’ climatic distribution nor its peak frequency is associated with a species’ peak abundance, with the exception of adults of *P. tremuloides*, which showed full abundant-center patterns on both temperature and precipitation gradients. Only in the middle of the temperature gradient (with MATs from ~0°C to ~15°C) did species commonly have symmetric, bell-shaped, and coincident peaks in range, frequency, and abundance. The opposite pattern

occurred at the extremes of the climate gradients; where abiotic stress is high and biotic pressure typically declines (Liancourt et al. 2005), stress-tolerant species become hyper-dominant at the edge of their range. Together, these patterns suggest that where temperature stress is low or absent, biotic interactions increase (Canham et al. 2006, HilleRisLambers et al. 2013) and foster bell-shaped patterns in abundance, particularly for dominant species.

The general absence of abundant-center relationships between climatic distributions and relative abundance suggests that climate gradients, and species distribution and climatic suitability models based on them, are not consistently predictive of abundance patterns across tree species. Indeed, abundance–climate relationships were effectively flat for around half of the species, with little-to-no variation in relative abundance (<10% change in total) over their entire distribution for seven species of adults and 10 species of saplings with temperature, and 11 species of adults and 11 species of saplings with precipitation. This suggests that climate gradients provide limited insight into the ecological and demographic processes that determine the relative abundance of a species within a stand.

These patterns correspond with mounting evidence of a general decoupling of tree species climatic distributions from key components of tree demography which determine abundance. A large study using forest inventory data found that climates with the highest frequencies of a species were negatively correlated with those species' population growth rates (Thuiller et al. 2014), a pattern that could cause a disconnect between frequency and abundance. Other studies report modest or nonexistent variation in tree growth rates along wide gradients of temperature in the Rockies (Buechling et al. 2017) and precipitation in the eastern United States (Canham and Murphy 2016b). Certainly, some elements of tree demography such as fecundity are strongly associated with climate (Buechling et al. 2016), but considerable evidence indicates once a species is present in a site, demographic processes in forests in western North America are predominately determined by non-climatic factors (Zhang et al. 2015).

Demographic decoupling from climate could occur for a number of reasons, including when local adaptation to climate is pronounced (Buechling et al. 2017, Canham et al. 2018) or when the effects of climate on growth are abated by strong ecophysiological acclimation potential, as seen in photosynthesis rates of many tree species that can rapidly acclimate to local conditions, particularly temperature (Smith and Dukes 2013, Carroll et al. 2017). Furthermore, while a strong climate signal on frequency patterns can be readily explained by the importance on climate-sensitive recruitment processes, such as seed germination and first-year seedling survival (Foster et al. 2020), post-establishment abundance of seedlings is poorly explained by climate in western forests (Kroiss and HilleRisLambers 2015, Dallas and Hastings 2018, Redmond and Kelsey 2018, Copenhagen-Parry et al. 2020), indicating that the weakening of climatic influences on abundance begins early in a tree's life cycle. Nevertheless, given the general aridity of the region and the bell-shaped growth response of dominant tree species on precipitation gradients in the Rockies (Buechling et al. 2017), it remains notable that the relative abundance of 15 adult and 19 sapling species monotonically declines or shows no change at higher levels of precipitation.

The frequency and pervasiveness of natural disturbances such as fire and bark beetles in the forests of western North America (Veblen et al. 2003, Raffa et al. 2008) suggest that the average stand condition in these forests is likely to be in an early post-disturbance stage compared with many other forest biomes. Overall, this should mean that climatic influences important in early successional processes, like seedling germination, should predominate and that the role of non-climatic influences common in later stages of stand dynamics (e.g., biotic influences like crowding; Buechling et al. 2017) might be less important in western forests. Furthermore, we anticipate regular natural disturbances weaken the compositional inertia of forests to climate change by removing canopy dominants (Canham et al. 2006). However, by themselves disturbances and mortality agents typically do not change a species' distribution, but rather alter local and landscape abundance episodically across a portion of a species' range.

Despite weak or nonexistent abundant-center relationships for many of the species in this study, it is notable that six of the most dominant and widespread species in the region—five of which have their full climatic distribution captured in the dataset—showed abundance and frequency patterns on the temperature gradient consistent with the abundant-center hypothesis. Given the importance of non-climatic influences on tree demography, which weaken the climatic signal in tree distributions, and other broad-scale studies that found no evidence for the abundant-center hypothesis (Thuiller et al. 2014, Dallas and Hastings 2018), the symmetric and coincident abundance patterns in these six dominant species are significant. We hypothesize that the strength of these patterns is due in part to the low alpha diversity in the forest communities of the Interior West region, which allows one or two species to become unusually dominant along a portion of the climatic gradient. However, the population dynamics that create high abundance also require a species have high frequency, and hence, the patterns are synchronized along the gradient. The centered and symmetric nature of this dynamic, however, breaks down at the extremes of the gradient where biotic pressure is weaker (Buechling et al. 2017).

#### *Niche patterns*

The incidence of distributions with a clear peak and symmetrical distributions depended primarily on (1) frequency vs. abundance patterns, (2) temperature vs. precipitation gradients, and (3) where a species is distributed (center vs. extremes) on the climate gradient. The majority of species had frequency patterns that were both bell-shaped and symmetric with temperature as adults, but only 25% of species of adults did with precipitation. Most species with non-bell-shaped and non-symmetric frequencies had peak frequencies at the extremes on both gradients. The abundance of nearly all species of adults and saplings on both gradients was neither bell-shaped nor symmetrically distributed.

Bell-shaped frequency patterns along a gradient indicate that a species' probability of patch occupancy declines when moving away from its climatic optimum, mostly likely via changes to colonization, recruitment, or survivorship rates. These patterns suggest that climate's influence on

presence-absence dynamics across patches is a fundamental filter on tree species distribution patterns in Rocky Mountain forests. Using FIA data in the eastern United States, Canham and Thomas (2010) also found strong bell-shaped patterns in frequency, particularly as a function of temperature, suggesting that the processes that structure tree species frequency patterns on temperature gradients are similar across regions.

The most likely influence of climate on patch occupancy probability is on seedling recruitment. Seedling recruitment in the Rockies is highly sensitive to climatic conditions (Foster et al. 2020), and pulsed seedling recruitment episodes synchronized to decadal-scale variation in climate are common (Brown and Wu 2005, Gray et al. 2006, Andrus et al. 2018). In the eastern United States, Canham and Murphy (2016a, b) also concluded that seedling recruitment, compared to growth and mortality of saplings and adults, is the most climate-sensitive component of tree demography. These patterns suggest that processes that influence the frequency of a species across patches (e.g., fecundity, germination, seedling recruitment) will be particularly important in determining how tree species respond to climate change (Canham and Murphy 2016a).

Tree species abundance patterns in contrast indicate that once any barriers to patch occupancy are passed and a species is present in a site, relative abundance along the climate gradient generally decouples from frequency. As a result, abundance-climate relationships overall are weak for many species in the region. Nevertheless, western species overall displayed much stronger climate patterning in abundance than eastern species, as Canham and Thomas (2010) found little-to-no variation in abundance for any species along climate gradients. Western species also had much less niche overlap in peak frequencies than eastern species, perhaps due to lower species richness and higher dominance in western forests.

#### *Climate change implications*

If temperatures continue to warm as predicted in the Rockies (Christensen and Lettenmaier 2006) and species distributions closely track changes in climate, substantial shifts in species frequencies in a given area are likely to occur, particularly for dominant species. Yet, given



wide range limits and generally non-overlapping peak frequencies, it does not appear that forest communities as a whole in the Rocky Mountain region will require long-range dispersal to persist even under substantial warming, as there are a variety of species adapted to warmer conditions already present within a stand or nearby along elevation gradients across most of the region. Hence, as a dominant species declines in an area due to warmer temperatures, another species already present in a lower frequency can increase. The likelihood of this scenario, however, assumes that the response to warming is fairly consistent across subpopulations of a species; the patterns of response could be more idiosyncratic if local adaptation to climate is pronounced, a distinct possibility for temperate tree species (Rehfeldt et al. 1999, Buechling et al. 2017, Canham et al. 2018).

Of course, if extreme warming happens and the climatic range limits of tree species are exceeded—many forecasts project much faster warming in both montane and high-latitude forests compared to the global average (Giorgi et al. 1997, Chen et al. 2003, Christensen et al. 2007)—a far more general disruption of forests communities will occur. Indeed, there are portions of the Rockies where warming of  $\sim 5^{\circ}\text{C}$  could produce dramatic effects, particularly in forests occurring in the hottest portions of the region ( $>15^{\circ}\text{C}$  MAT), which could transition to grasslands as warming pushes pinyon–juniper forests into cooler areas. Similarly, subalpine forests in the coldest forested areas of the American Rockies, which are likely to remain forested under substantial warming, eventually could lose their dominant species (i.e., *P. engelmannii* and *A. lasiocarpa*) as their peak frequencies and abundances shift further north. *Pinus albicaulis* in particular looks like it will be disproportionately impacted by further warming, as it experiences a sharp decline in frequency in temperatures above  $2^{\circ}\text{C}$  and its abundance drops steeply and monotonically at higher temperatures.

Changes in moisture will likely have greater effects on the region's forests than increases in temperature, as so many species share a common, narrow niche around 600–700 mm in average annual precipitation. Forecasts of future precipitation regimes in the Rockies have considerable uncertainty in both magnitude

and direction (Christensen and Lettenmaier 2006), but long-term decreases in precipitation as little as 200 mm/yr could cause wholesale changes in community composition, decreasing the amount of forests dominated entirely by subalpine tree species while converting mixed conifer communities (currently occurring at  $\sim 600$  mm/yr) to ponderosa pine and pinyon–juniper communities. Changes in moisture also are likely to have important indirect effects on tree communities, most notably by altering the frequency and severity of fires in the Rockies (Veblen et al. 2003) and the dynamics of bark beetle outbreaks (Negron et al. 2009), which are widely predicted to increase under climate change as drought stress impairs host tree defenses and higher temperatures accelerate beetle population growth (Temperli et al. 2015). Overall, our results suggest that species found at the drier and colder ends of these climate gradients will be most sensitive to future climate change, given their steep and mostly monotonic drops in frequency and abundance with even small shifts in climate.

#### ACKNOWLEDGMENTS

We thank the U.S. Forest Service Forest Inventory and Analysis Program staff for making the FIA data available and their assistance in compiling the dataset.

#### LITERATURE CITED

- Andrus, R. A., B. J. Harvey, K. C. Rodman, S. J. Hart, and T. T. Veblen. 2018. Moisture availability limits subalpine tree establishment. *Ecology* 99:567–575.
- Bascompte, J. 2009. Mutualistic networks. *Frontiers in Ecology and the Environment* 7:429–436.
- Bechtold, W. A., and P. L. Patterson. 2005. The enhanced forest inventory and analysis program: national sampling design and estimation procedures. General Technical Report SRS-80. USDA Forest Service, Southern Research Station, Asheville, North Carolina, USA.
- Bell, D. M., J. B. Bradford, and W. K. Lauenroth. 2014. Early indicators of change: Divergent climate envelopes between tree life stages imply range shifts in the western United States. *Global Ecology and Biogeography* 23:168–180.
- Box, E. O., D. W. Crumpacker, and E. D. Hardin. 1999. Predicted effects of climatic change on distribution of ecologically important native tree and shrub species in Florida. *Climate Change* 41:213–248.



- Brown, P. M., and R. Wu. 2005. Climate and disturbance forcing of episodic tree recruitment in a southwestern ponderosa pine landscape. *Ecology* 86:3030–3038.
- Buechling, A., P. H. Martin, and C. D. Canham. 2017. Climate and competition effects on tree growth in Rocky Mountain forests. *Journal of Ecology* 105:1636–1647.
- Buechling, A., P. H. Martin, C. D. Canham, W. D. Sheperd, and M. A. Battaglia. 2016. Climate drivers of seed production in *Picea engelmannii* and response to warming temperatures in the southern Rocky Mountains. *Journal of Ecology* 104:1051–1062.
- Canham, C. D., and L. Murphy. 2016a. The demography of tree species response to climate: seedling recruitment and survival. *Ecosphere* 7:e01424.
- Canham, C. D., and L. Murphy. 2016b. The demography of tree species response to climate: sapling and canopy tree growth. *Ecosphere* 7:e01474.
- Canham, C. D., L. Murphy, R. Riemann, R. McCullough, and E. Burrill. 2018. Local differentiation in tree growth responses to climate. *Ecosphere* 9:e02368.
- Canham, C. D., M. J. Papaik, M. Uriarte, W. H. McWilliams, J. C. Jenkins, and M. J. Twery. 2006. Neighborhood analyses of canopy tree competition along environmental gradients in New England forests. *Ecological Applications* 16:540–554.
- Canham, C. D., and R. Q. Thomas. 2010. Frequency, not relative abundance, of temperate tree species varies along climate gradients in eastern North America. *Ecology* 91:3433–3440.
- Carroll, C. J. W., A. K. Knapp, and P. H. Martin. 2017. Dominant tree species of the Colorado Rockies have divergent physiological and morphological responses to warming. *Forest Ecology and Management* 402:234–240.
- Chen, B., W. C. Chao, and X. Liu. 2003. Enhanced climatic warming in the Tibetan plateau due to doubling CO<sub>2</sub>: a model study. *Climate Dynamics* 20:401–413.
- Christensen, J. H., et al. 2007. Regional climate projections. Pages 847–940 in S. Solomon, D. Qin, M. Manning, Z. Chen, M. Marquis, K. B. Averyt, M. Tignor, and H. L. Miller, editors. *Climate Change, 2007: The Physical Science Basis. Contribution of Working Group I to the Fourth Assessment Report of the Intergovernmental Panel on Climate Change*. Cambridge University Press, Cambridge, UK.
- Christensen, N., and D. P. Lettenmaier. 2006. A multi-model ensemble approach to assessment of climate change impacts on the hydrology and water resources of the Colorado River basin. *Hydrology and Earth System Sciences Discussions* 3:3737–3770.
- Clark, J. S., D. Bell, M. H. Hersh, and L. Nichols. 2011. Climate change vulnerability of forest biodiversity: climate and competition tracking of demographic rates. *Global Change Biology* 17:1834–1849.
- Copenhaver-Parry, P. E., S. E. Albeke, and D. B. Tinker. 2016. Do community-level models account for the effects of biotic interactions? A comparison of community-level and species distribution modeling of Rocky Mountain conifers. *Plant Ecology* 217:533–547.
- Copenhaver-Parry, P. E., C. J. Carroll, P. H. Martin, and M. V. Talluto. 2020. Multi-scale integration of tree recruitment and range dynamics in a changing climate. *Global Ecology and Biogeography* 29:102–116.
- Dallas, T. A., R. R. Decker, and A. Hastings. 2017. Species are not most abundant in the center of their geographic range or climatic niche. *Ecology Letters* 20:1526–1533.
- Dallas, T. A., and A. Hastings. 2018. Habitat suitability estimated by niche models is largely unrelated to species abundance. *Global Ecology and Biogeography* 27:1448–1456.
- Dobrowski, S. Z., A. K. Swanson, J. T. Abatzoglou, Z. A. Holden, H. D. Safford, M. K. Schwartz, and D. G. Gavin. 2015. Forest structure and species traits mediate projected recruitment declines in western US tree species. *Global Ecology and Biogeography* 24:917–927.
- Drake, J. M. 2015. Range bagging: a new method for ecological niche modelling from presence-only data. *Journal of the Royal Society Interface* 12:20150086.
- Elith, J., and J. R. Leathwick. 2009. Species distribution models: ecological explanation and prediction across space and time. *Annual Review of Ecology, Evolution, and Systematics* 40:677–697.
- Filz, K. J., T. Schmitt, and J. O. Engler. 2013. How fine is fine-scale? Questioning the use of fine-scale bioclimatic data in species distribution models used for forecasting abundance patterns in butterflies. *European Journal of Entomology* 110:311.
- Foster, A. C., P. H. Martin, and M. D. Redmond. 2020. Soil moisture strongly limits Douglas-fir seedling establishment near its upper altitudinal limit in the southern Rocky Mountains. *Canadian Journal of Forest Research*. <https://doi.org/10.1139/cjfr-2019-0296>
- Giorgi, F., J. W. Hurrell, M. R. Marinucci, and M. Beniston. 1997. Elevation dependency of the surface climate change signal: a model study. *Journal of Climate* 10:288–296.
- Gray, S. T., J. L. Betancourt, S. T. Jackson, and R. G. Eddy. 2006. Role of multidecadal climate variability

- in a range extension of pinyon pine. *Ecology* 87:1124–1130.
- Gutiérrez, D., J. Harcourt, S. B. Díez, J. G. Illán, and R. J. Wilson. 2013. Models of presence–absence estimate abundance as well as (or even better than) models of abundance: the case of the butterfly *Par-nassius apollo*. *Landscape Ecology* 28:401–413.
- Hijmans, R. J., and C. H. Graham. 2006. The ability of climate envelope models to predict the effect of climate change on species distributions. *Global Change Biology* 12:2272–2281.
- HilleRisLambers, J., M. A. Harsch, A. K. Ettinger, K. R. Ford, and E. J. Theobald. 2013. How will biotic interactions influence climate change–induced range shifts? *Annals of the New York Academy of Sciences* 1297:112–125.
- Iverson, L. R., M. W. Schwartz, and A. M. Prasad. 2004. How fast and far might tree species migrate in the eastern United States due to climate change? *Global Ecology and Biogeography* 13:209–219.
- Kroiss, S. J., and J. HilleRisLambers. 2015. Recruitment limitation of long-lived conifers: implications for climate change responses. *Ecology* 96:1286–1297.
- Lester, S. E., B. S. Halpern, K. Grorud-Colvert, J. Lubchenco, B. I. Ruttenberg, S. D. Gaines, S. Aïramé, and R. R. Warner. 2009. Biological effects within no-take marine reserves: a global synthesis. *Marine Ecology Progress Series* 384:33–46.
- Liancourt, P., R. M. Callaway, and R. Michalet. 2005. Stress tolerance and competitive-response ability determine the outcome of biotic interactions. *Ecology* 86:1611–1618.
- Martin, P. H., R. E. Sherman, and T. J. Fahey. 2007. Tropical montane forest ecotones: climate gradients, natural disturbance, and vegetation zonation in the Cordillera Central, Dominican Republic. *Journal of Biogeography* 34:1792–1806.
- McKenney, D. W., J. H. Pedlar, K. Lawrence, K. Campbell, and M. F. Hutchinson. 2007. Potential impacts of climate change on the distribution of North American trees. *AIBS Bulletin* 57:939–948.
- Mote, P. W. 2006. Climate-driven variability and trends in mountain snowpack in western North America. *Journal of Climate* 19:6209–6220.
- Negron, J. F., J. D. McMillin, J. A. Anhold, and D. Coulson. 2009. Bark beetle-caused mortality in a drought-affected ponderosa pine landscape in Arizona, USA. *Forest Ecology and Management* 257:1353–1362.
- Nielsen, S. E., C. J. Johnson, D. C. Heard, and M. S. Boyce. 2005. Can models of presence-absence be used to scale abundance? Two case studies considering extremes in life history. *Ecography* 28:197–208.
- Pacala, S. W., and G. C. Hurtt. 1993. Terrestrial vegetation and climate change: integrating models and experiments. Pages 57–74 in P. Kareiva, J. G. Kingsolver, and R. B. Huey, editors. *Biotic interactions and global change*. Sinauer, Sunderland, Massachusetts, USA.
- Pederson, G. T., L. J. Graumlich, D. B. Fagre, T. Kipfer, and C. C. Muhlfeld. 2010. A century of climate and ecosystem change in western Montana: What do temperature trends portend? *Climatic Change* 98:133–154.
- Phillips, S. J., and M. Dudík. 2008. Modeling of species distributions with maxent: new extensions and a comprehensive evaluation. *Ecography* 31:161–175.
- R Core Team 2014. R: A language and environment for statistical computing. R Foundation for Statistical Computing, Vienna, Austria.
- Raffa, K. F., B. H. Aukema, B. J. Bentz, A. L. Carroll, J. A. Hicke, M. G. Turner, and W. H. Romme. 2008. Cross-scale drivers of natural disturbances prone to anthropogenic amplification: the dynamics of bark beetle eruptions. *BioScience* 58:501–517.
- Redmond, M. D., and K. C. Kelsey. 2018. Topography and overstory mortality interact to control tree regeneration in spruce-fir forests of the southern Rocky Mountains. *Forest Ecology and Management* 427:106–113.
- Rehfeldt, G. E., N. L. Crookston, M. V. Warwell, and J. S. Evans. 2006. Empirical analyses of plant-climate relationships for the western United States. *International Journal of Plant Sciences* 167:1123–1150.
- Rehfeldt, G. E., D. E. Ferguson, and N. L. Crookston. 2008. Quantifying the abundance of co-occurring conifers along inland northwest (USA) climate gradients. *Ecology* 89:2127–2139.
- Rehfeldt, G. E., C. C. Ying, D. L. Spittlehouse, and D. A. Hamilton Jr. 1999. Genetic responses to climate in *Pinus contorta*: niche breadth, climate change, and reforestation. *Ecological Monographs* 69:375–407.
- Sagarin, R. D., and S. D. Gaines. 2002. The “abundant centre” distribution: To what extent is it a biogeographical rule? *Ecology Letters* 5:137–147.
- Salley, S. W., R. O. Sleezer, R. M. Bergstrom, P. H. Martin, and E. F. Kelly. 2016. A long-term analysis of the historical dry boundary for the Great Plains of North America: implications of climatic variability and climatic change on temporal and spatial patterns in soil moisture. *Geoderma* 274:104–113.
- Sherman, R. E., T. J. Fahey, P. H. Martin, and J. J. Battles. 2012. Patterns of growth, recruitment, mortality and biomass across an altitudinal gradient in a neotropical montane forest, Dominican Republic. *Journal of Tropical Ecology* 28:483–495.

- Smith, N. G., and J. S. Dukes. 2013. Plant respiration and photosynthesis in global-scale models: incorporating acclimation to temperature and CO<sub>2</sub>. *Global Change Biology* 19:45–63.
- Temperli, C., T. T. Veblen, S. J. Hart, D. Kulakowski, and A. J. Tepley. 2015. Interactions among spruce beetle disturbance, climate change and forest dynamics captured by a forest landscape model. *Ecosphere* 6:1–20.
- Thuiller, W. 2003. BIOMOD—optimizing predictions of species distributions and projecting potential future shifts under global change. *Global Change Biology* 9:1353–1362.
- Thuiller, W., et al. 2014. Does probability of occurrence relate to population dynamics? *Ecography* 37:1155–1166.
- Thuiller, W., S. Lavorel, M. T. Sykes, and M. B. Araújo. 2006. Using niche-based modelling to assess the impact of climate change on tree functional diversity in Europe. *Diversity and Distributions* 12:49–60.
- VanDerWal, J., L. P. Shoo, C. N. Johnson, and S. E. Williams. 2009. Abundance and the environmental niche: Environmental suitability estimated from niche models predicts the upper limit of local abundance. *American Naturalist* 174:282–291.
- Veblen, T. T., W. L. Baker, G. Montenegro, and T. W. Swetnam. 2003. Fire regimes and climatic change in temperate ecosystems of the western Americas. Springer-Verlag, New York, New York, USA.
- Woodward, F. I. 1987. *Climate and plant distribution*. Cambridge University Press, Cambridge, UK.
- Zhang, J., S. Huang, and F. He. 2015. Half-century evidence from western Canada shows forest dynamics are primarily driven by competition followed by climate. *Proceedings of the National Academy of Sciences USA* 112:4009–4014.

### SUPPORTING INFORMATION

Additional Supporting Information may be found online at: <http://onlinelibrary.wiley.com/doi/10.1002/ecs2.3149/full>

# **Ecosphere**

Peaks in frequency, but not relative abundance, occur in the center of tree species distributions on climate gradients

Patrick H. Martin and Charles D. Canham

## **Appendix S1**

-Figure S1. FIA plot locations across the Interior West region.

-Figures S2-S21. Observed data of individual tree species climate distributions (nested in the climate space of the full dataset), observed presence data for each species on temperature and precipitation gradients, and maps of each individual species' occurrence in FIA plots.

# All FIA plot locations -- Interior West Region

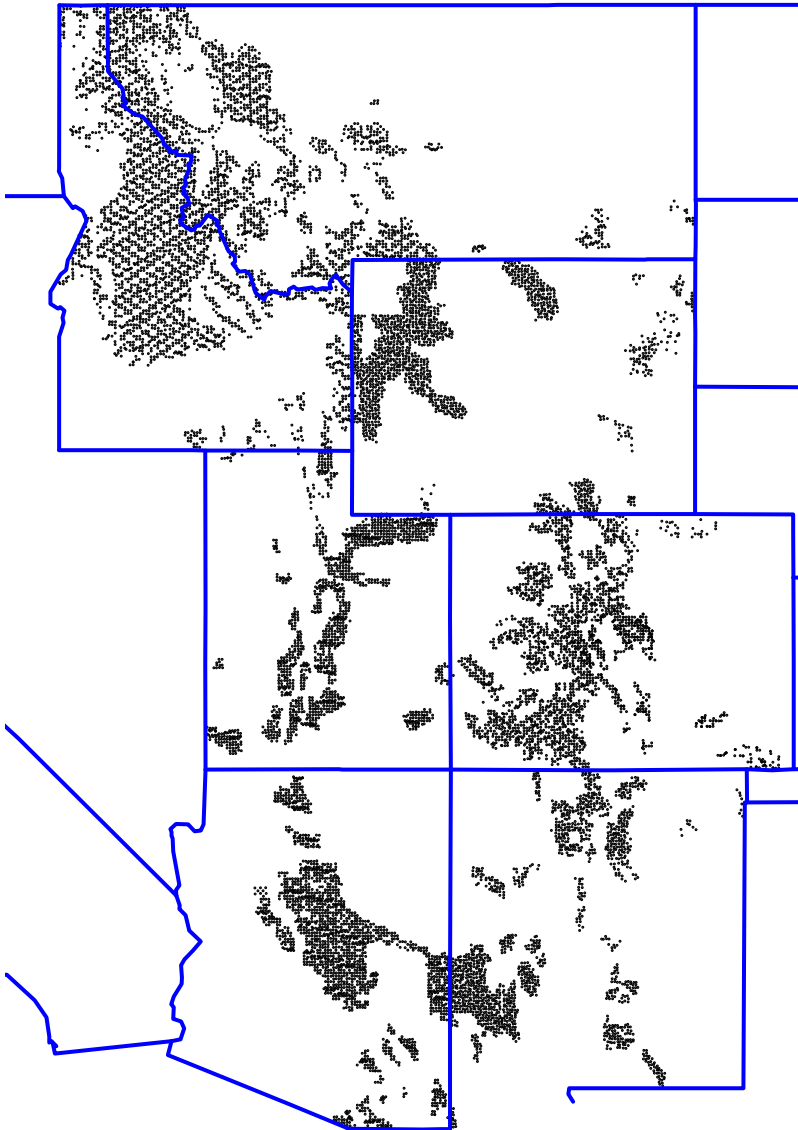
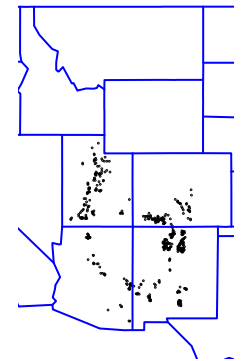
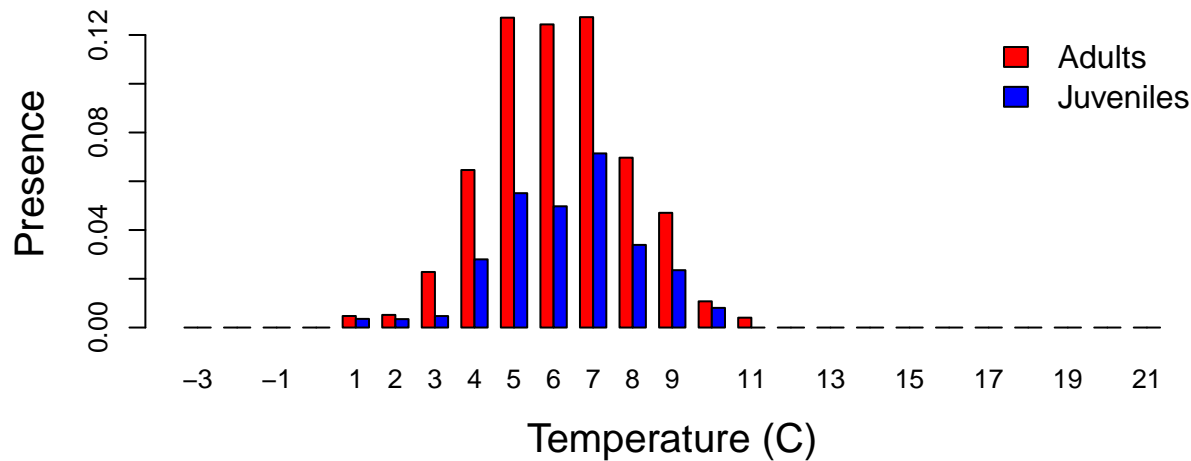
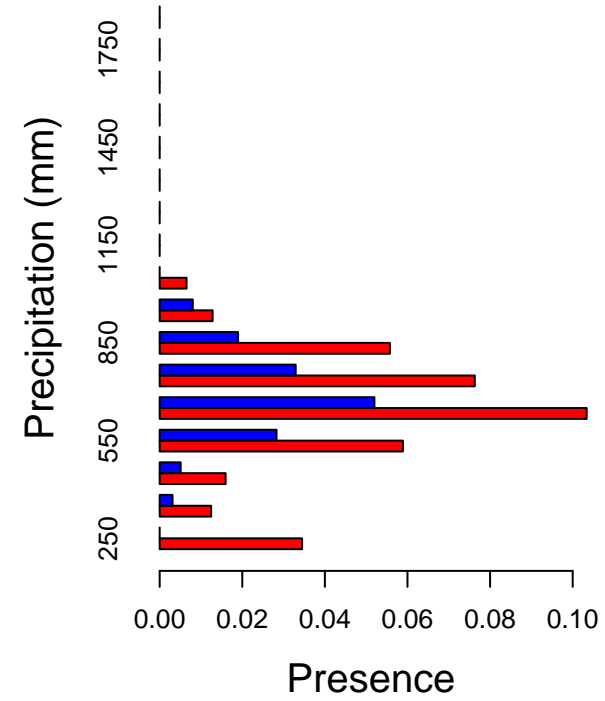
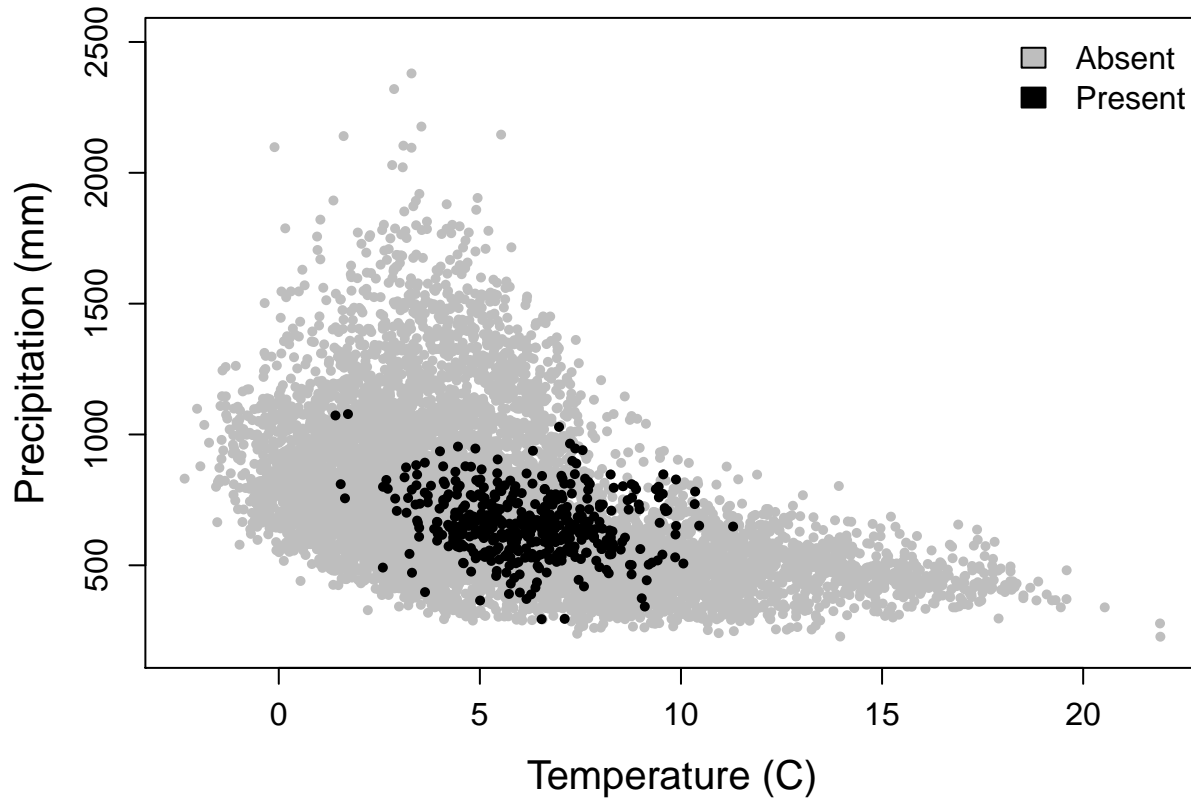


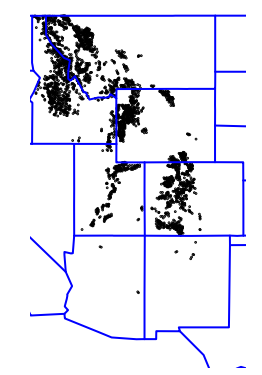
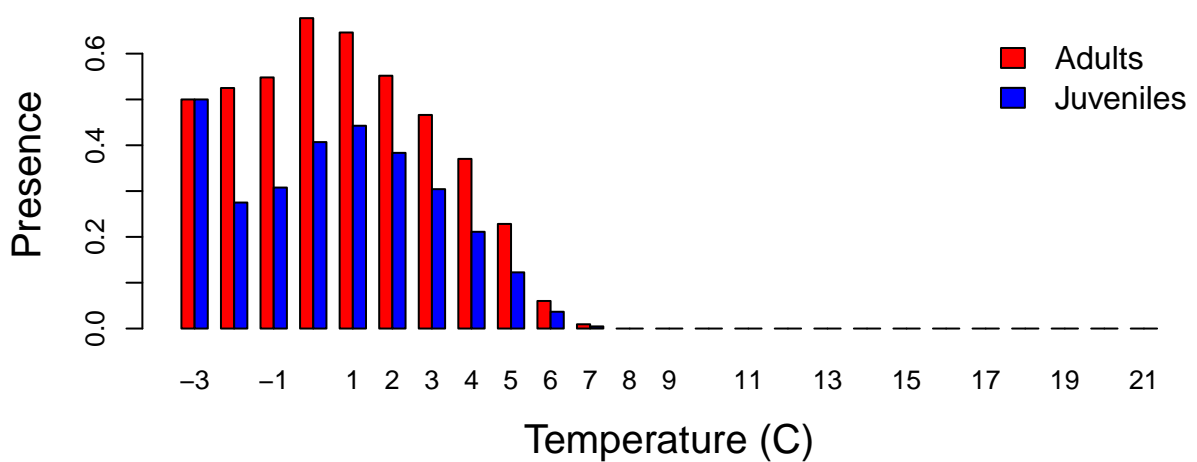
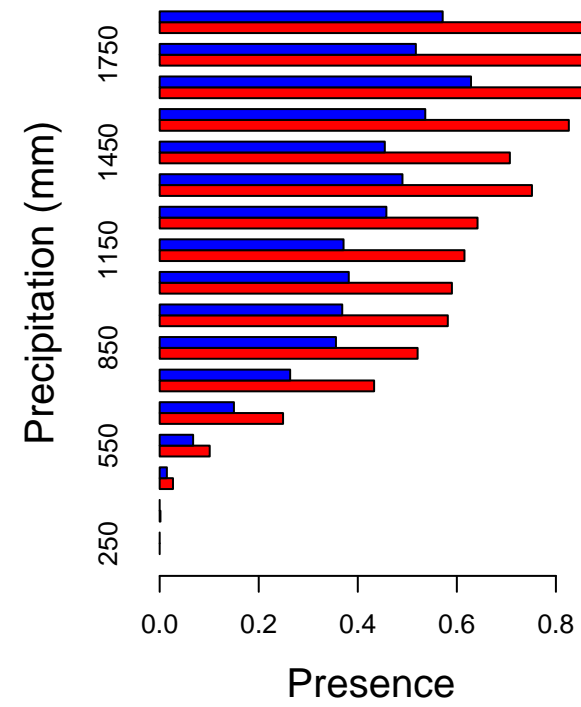
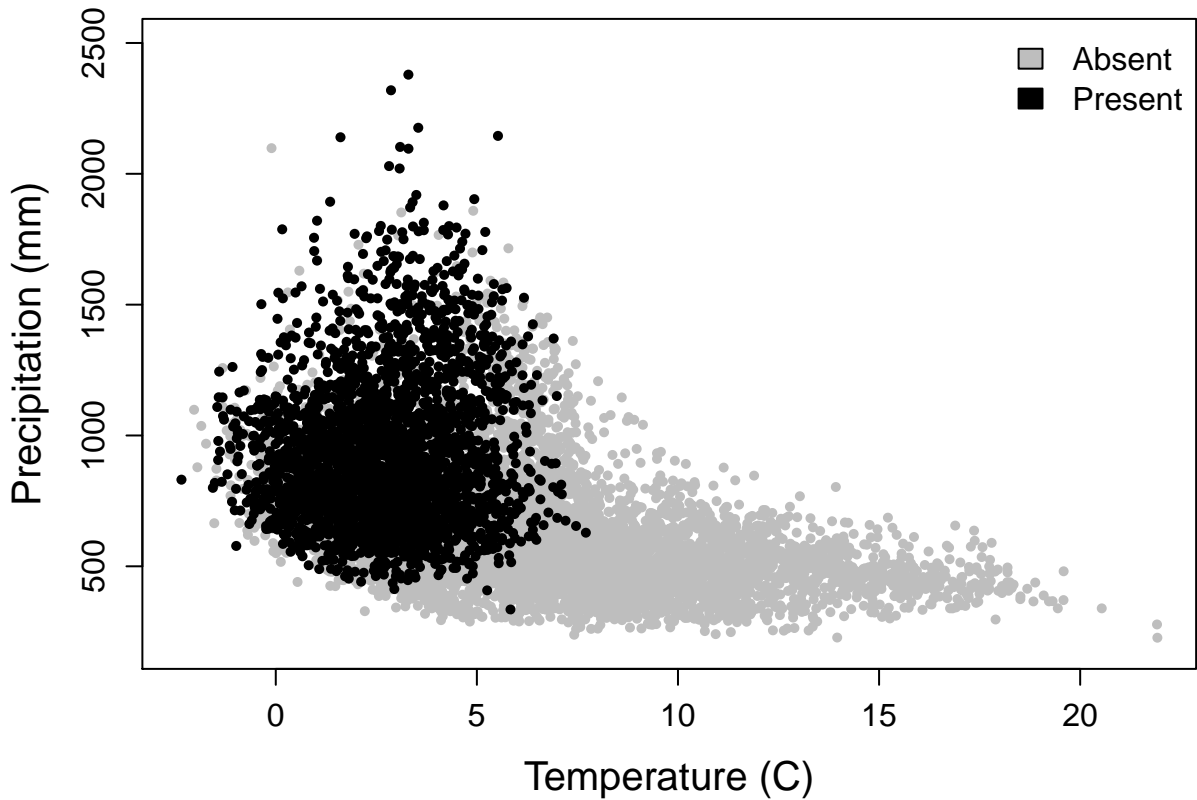
Figure S1. Per our security memorandum with the FIA program, the FIA plot displayed here are the publicly available "fuzzed and swapped" locations, not the true plot locations used in our analysis.



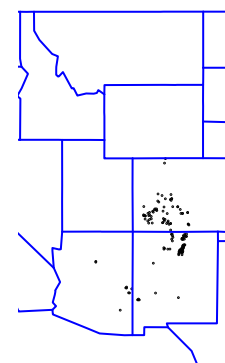
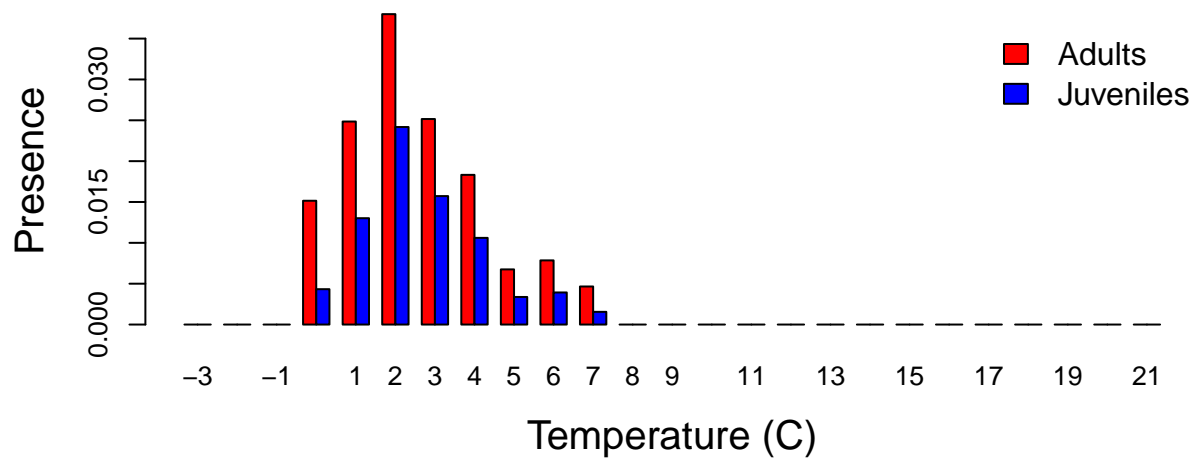
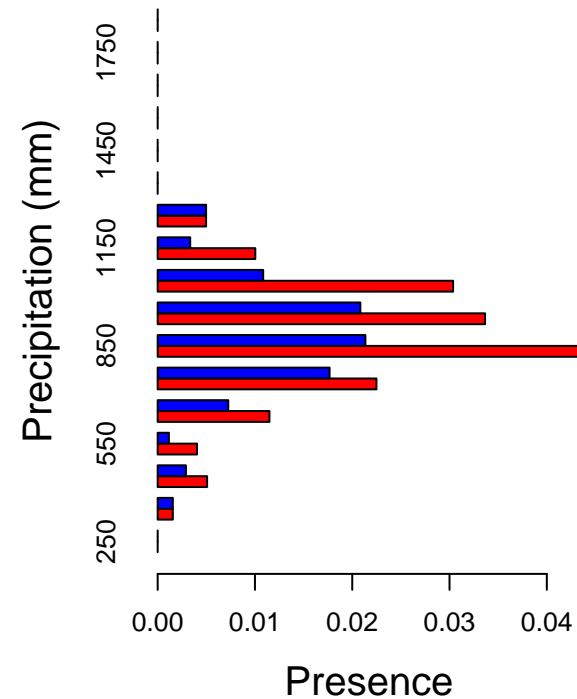
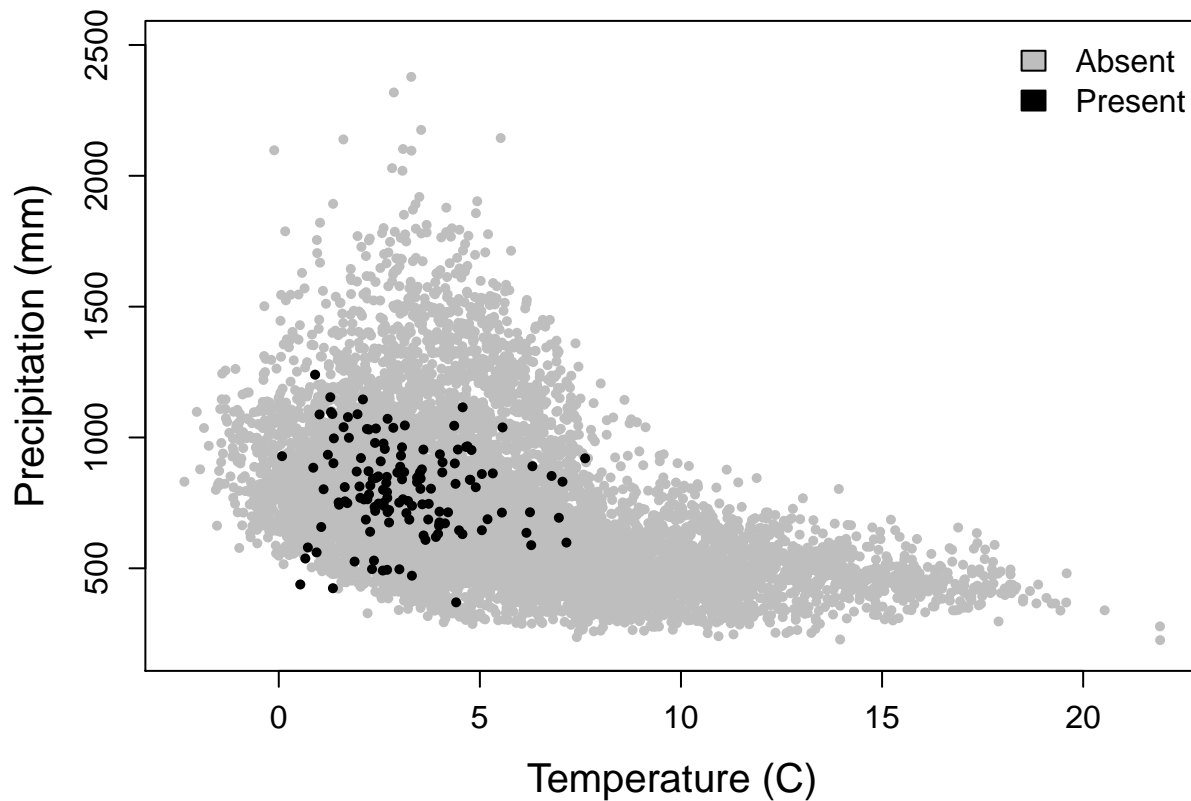
# Abies concolor – white fir



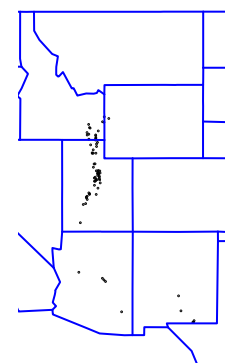
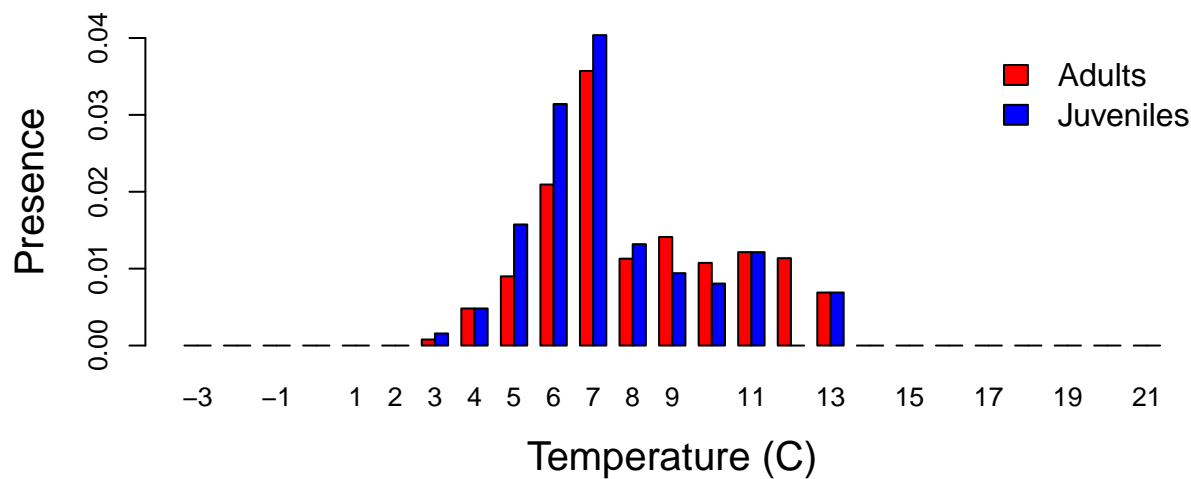
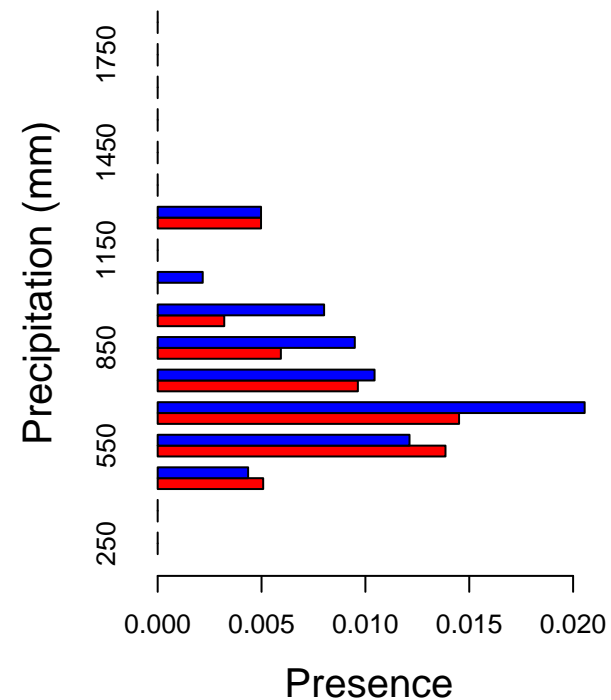
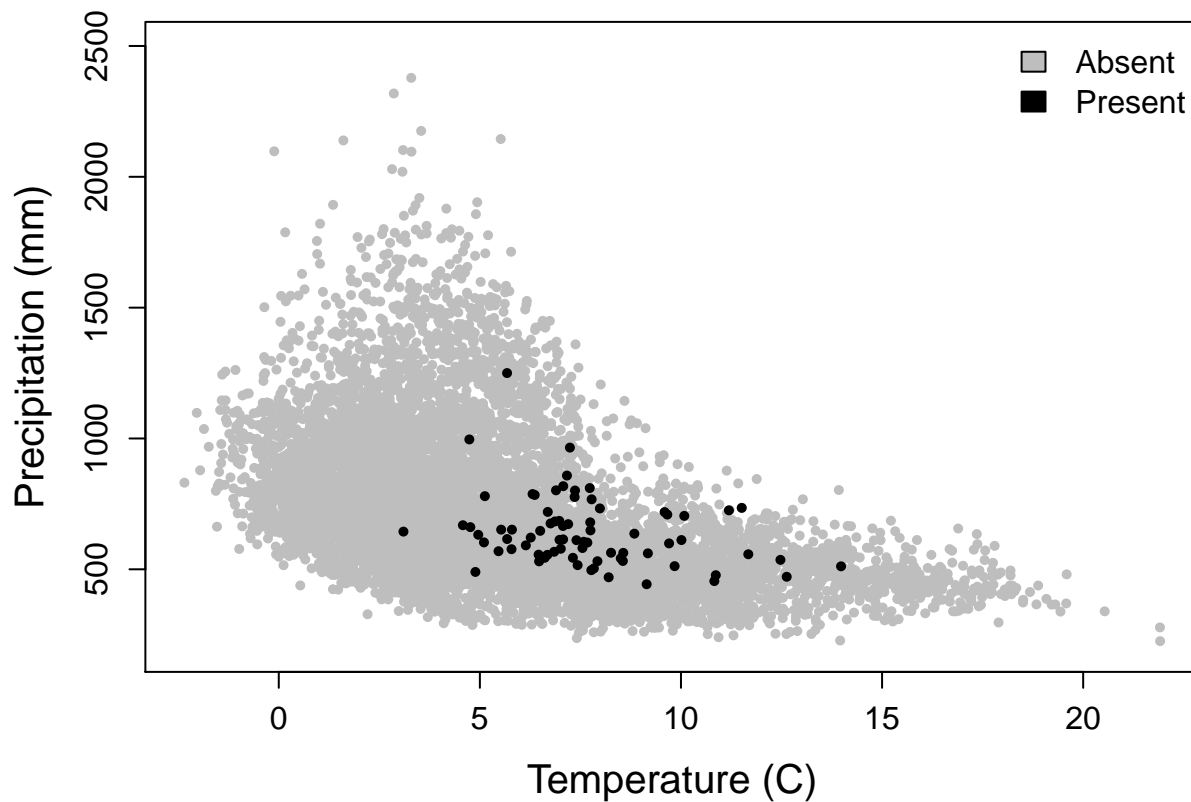
# Abies lasiocarpa – subalpine fir



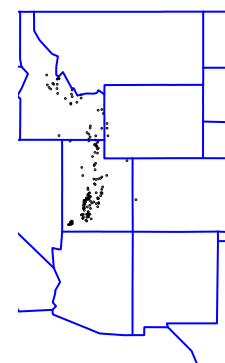
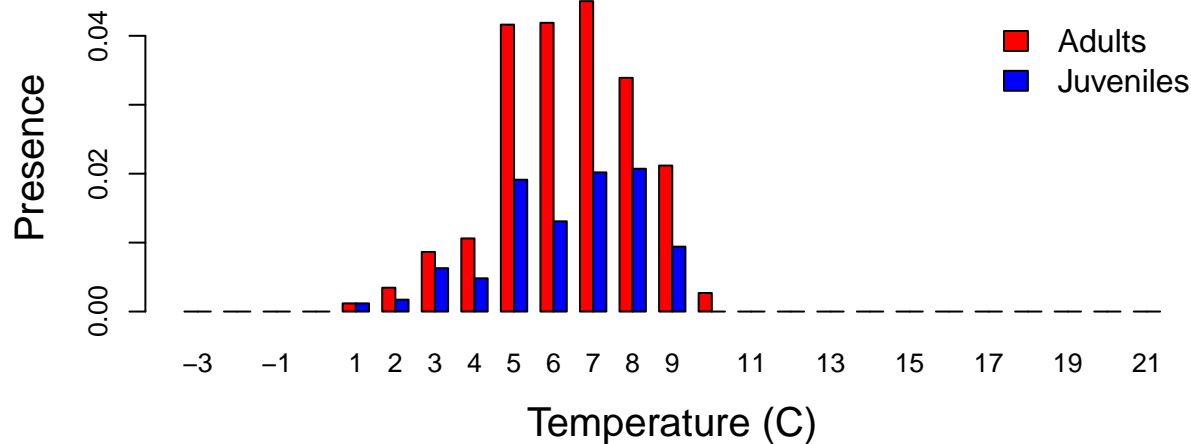
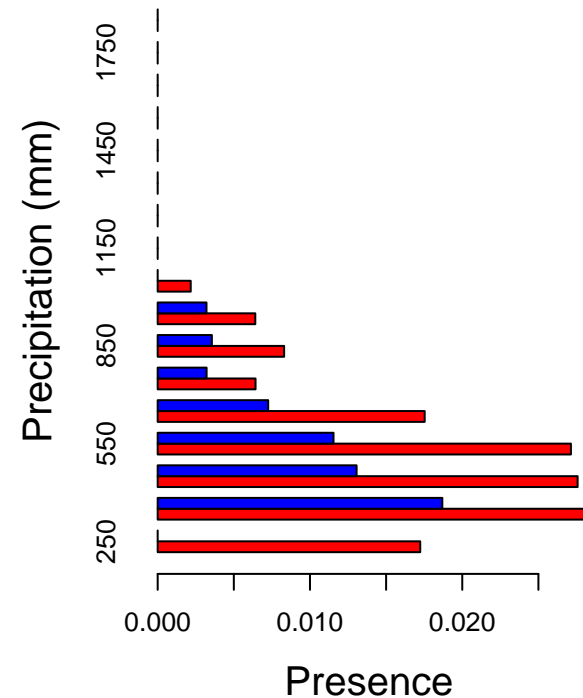
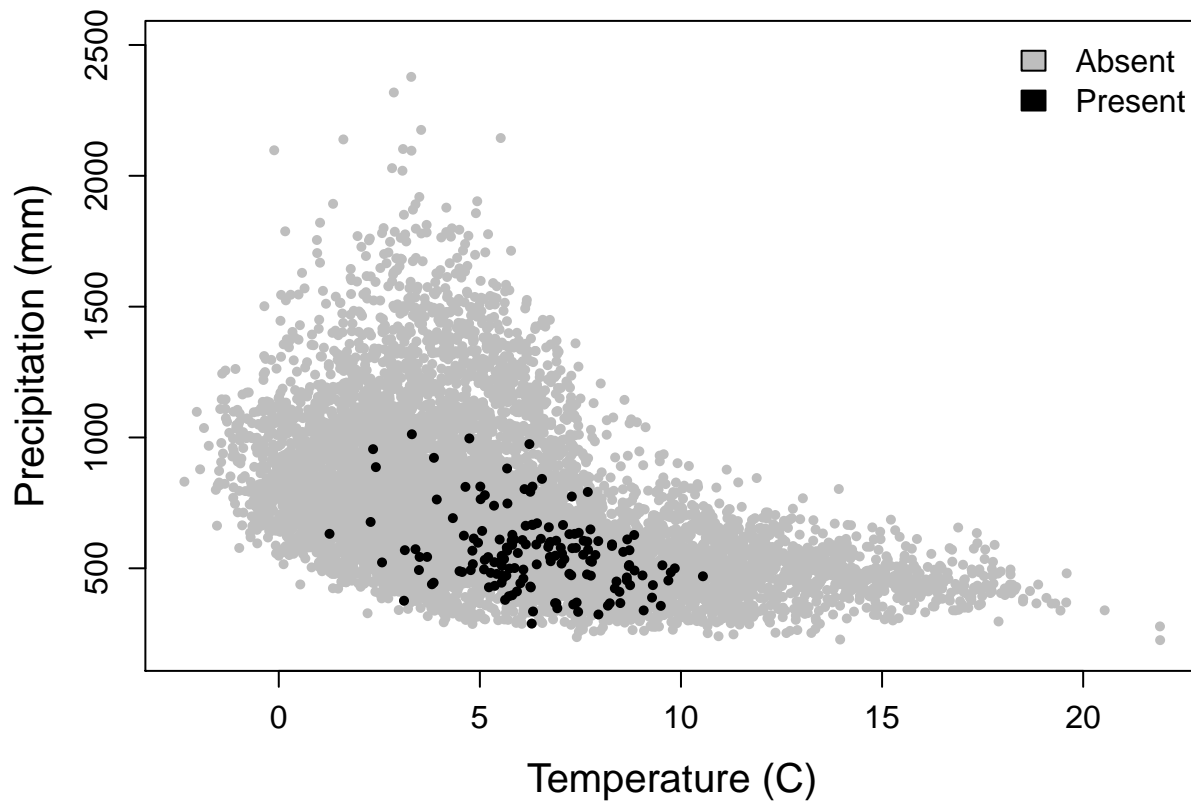
# Abies lasiocarpa var. arizonica – corkbark fir



# Acer grandidentatum – bigtooth maple

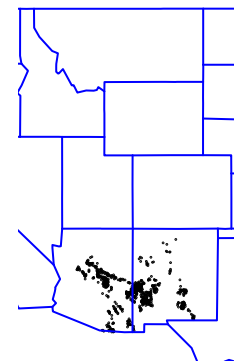
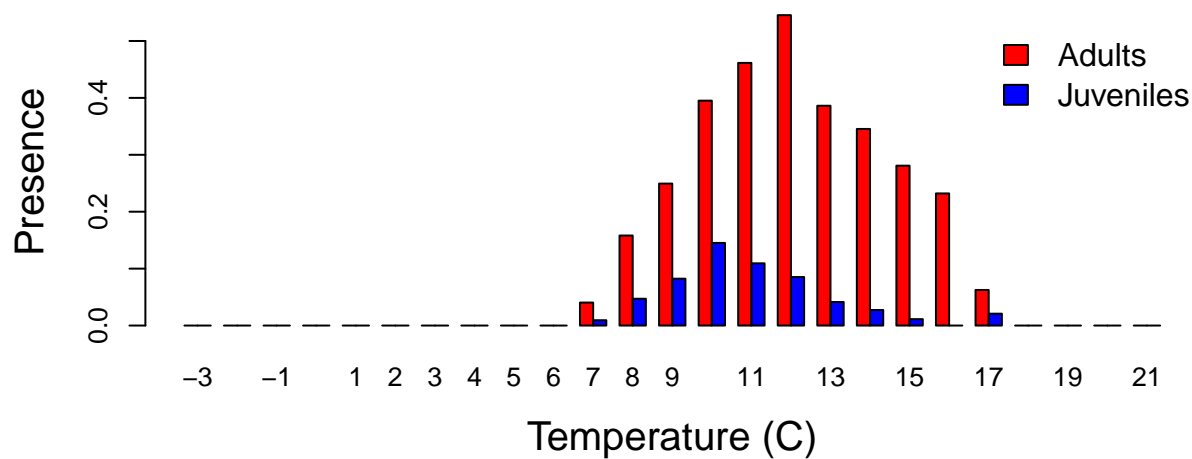
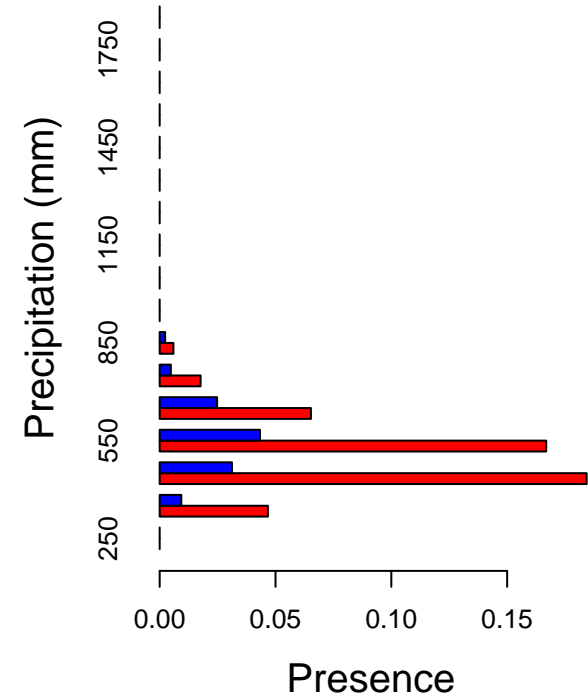
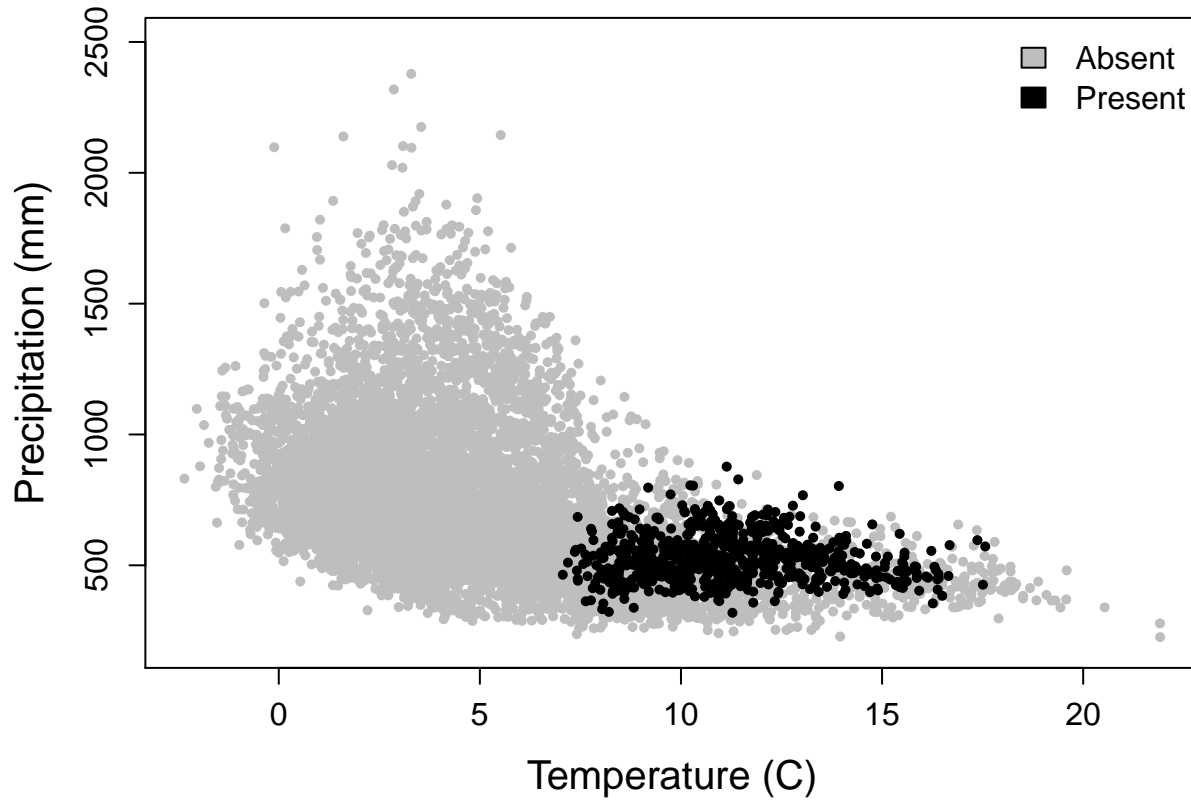


# Cercocarpus ledifolius – curleaf mountainmahogany

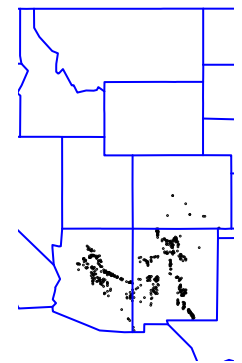
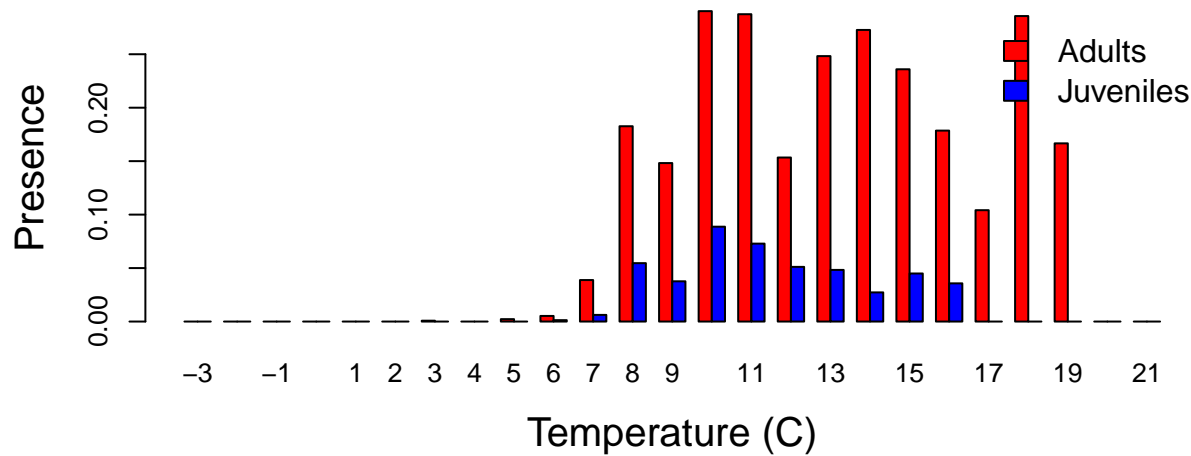
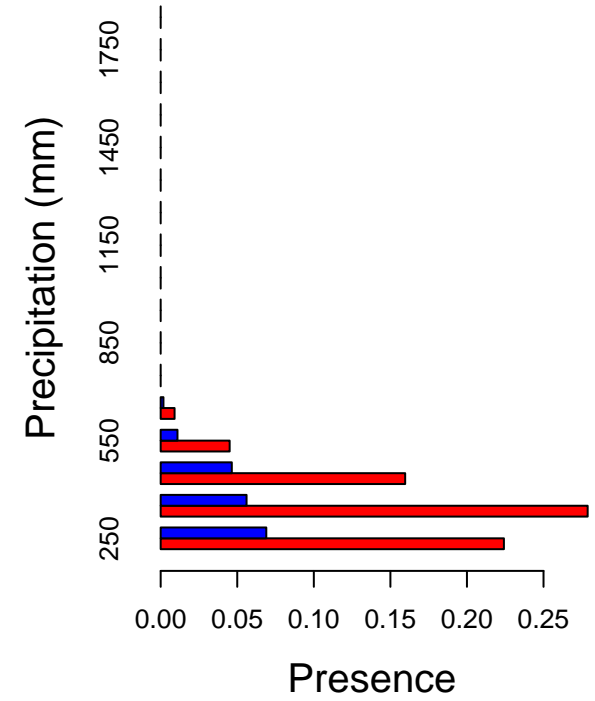
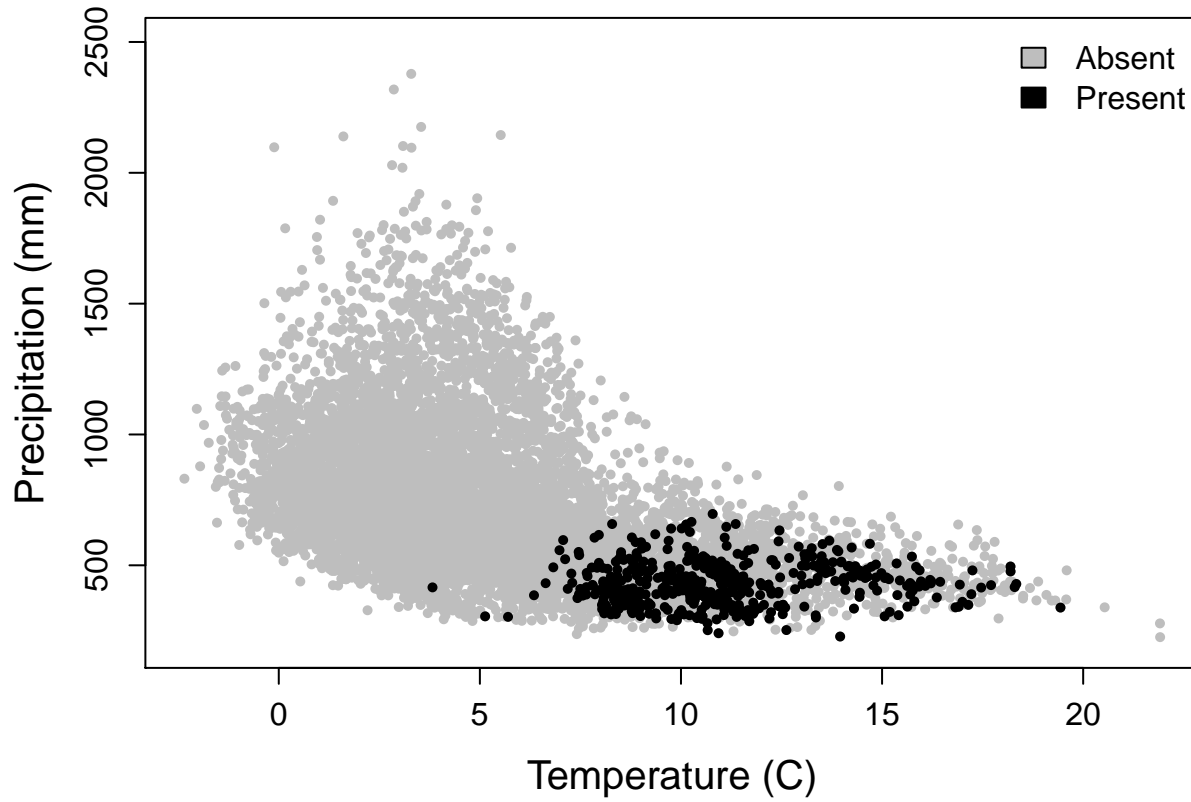




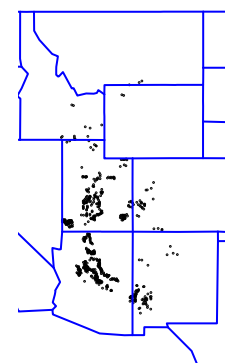
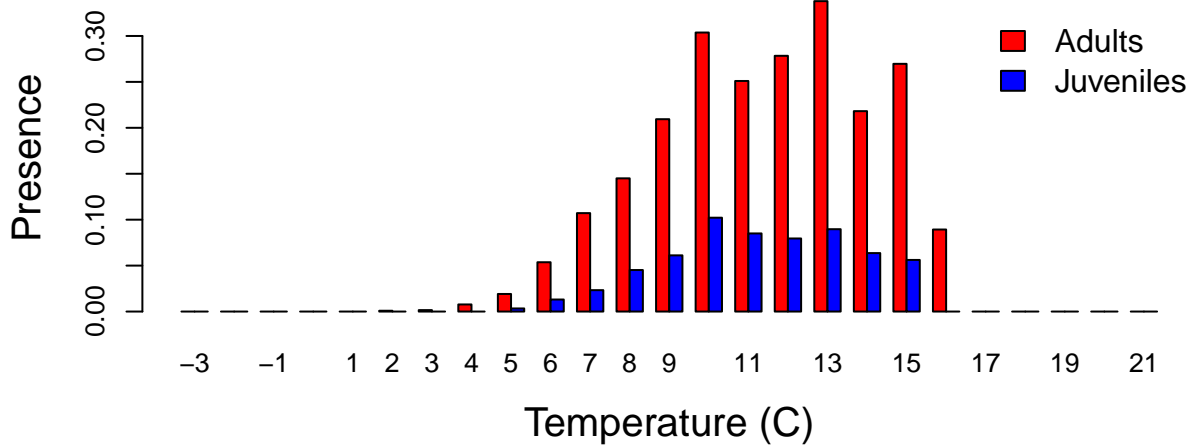
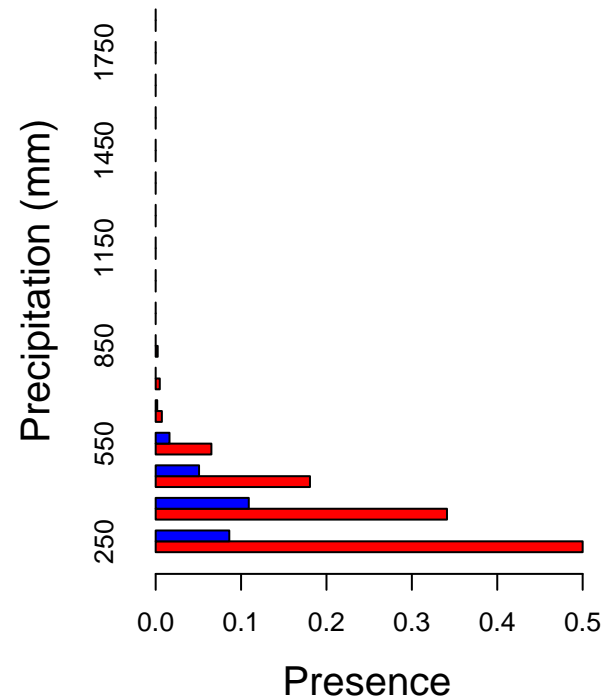
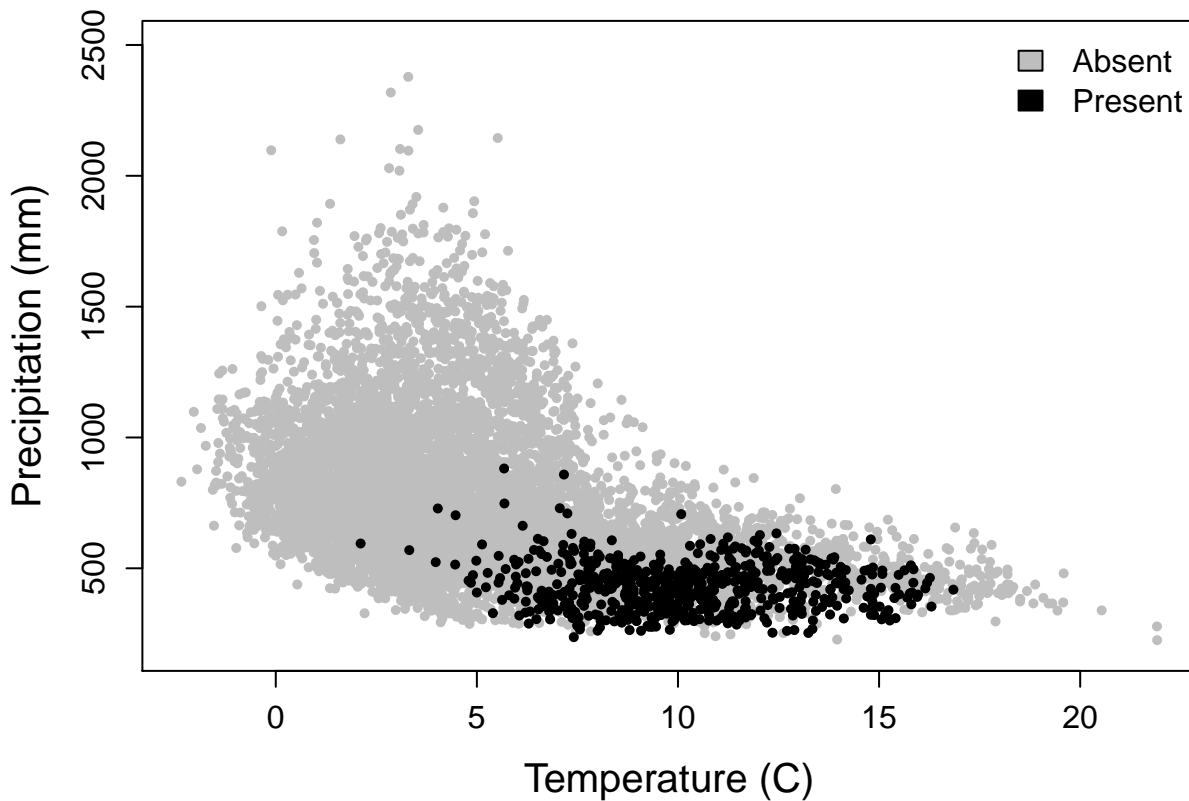
# Juniperus deppeana – alligator juniper



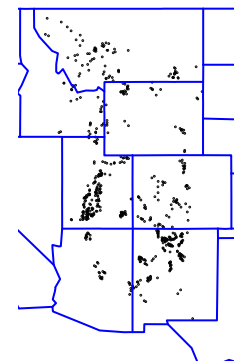
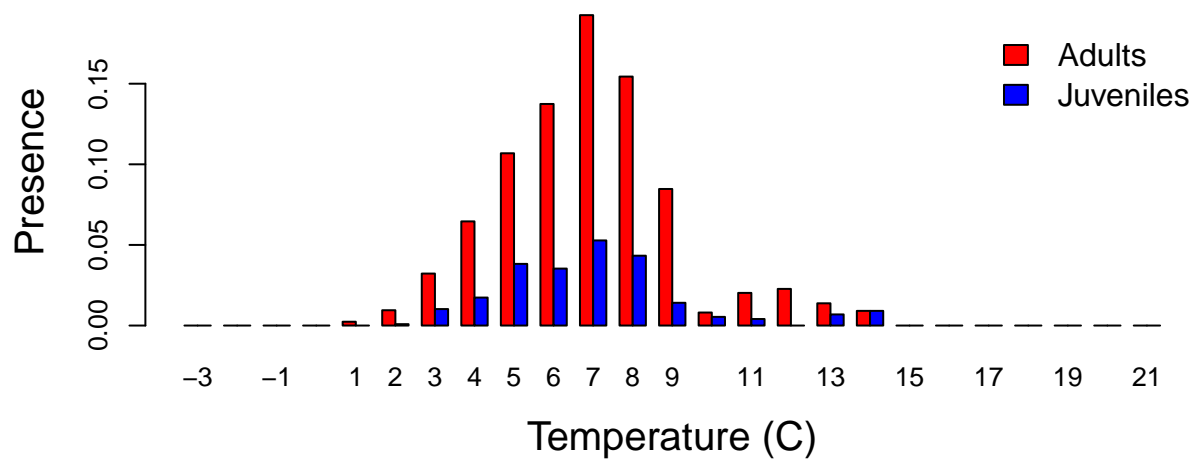
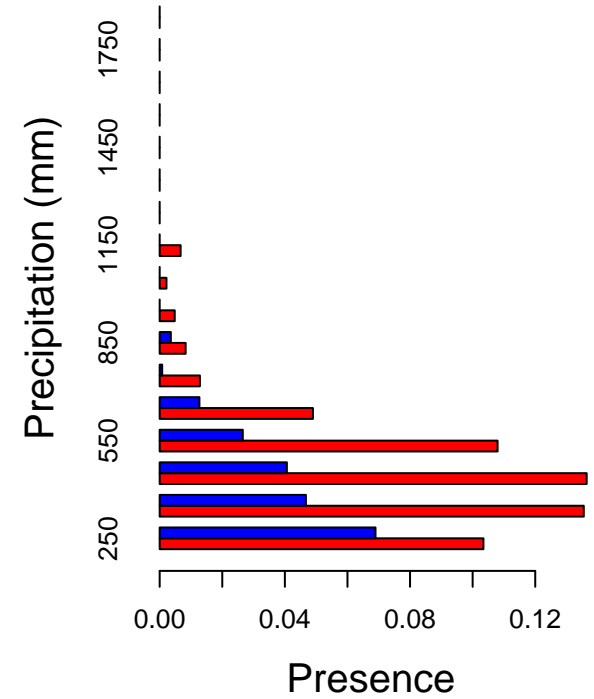
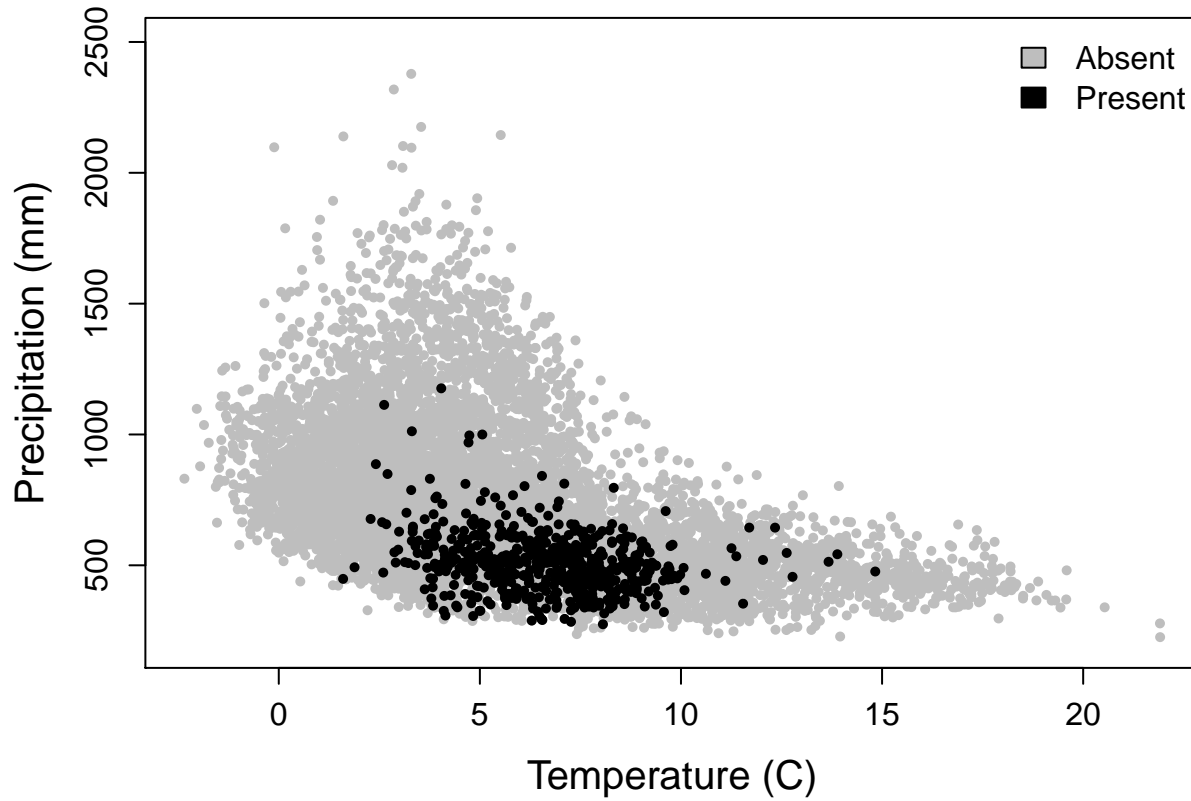
# Juniperus monosperma – oneseed juniper



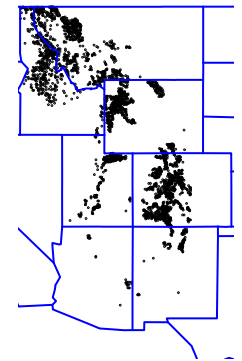
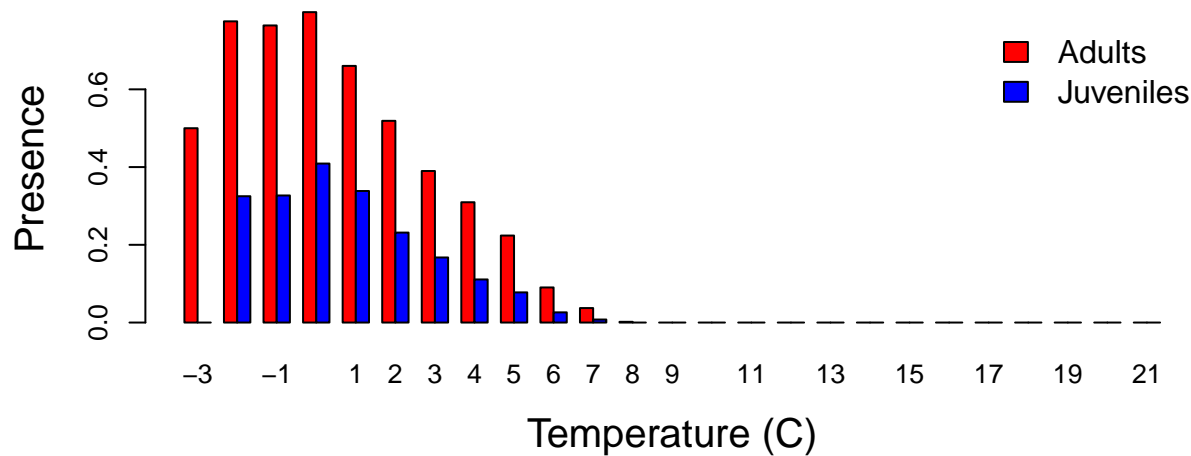
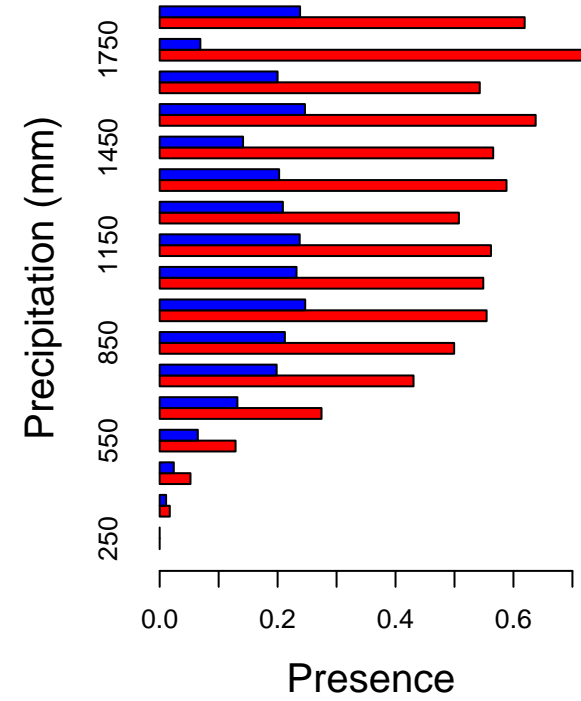
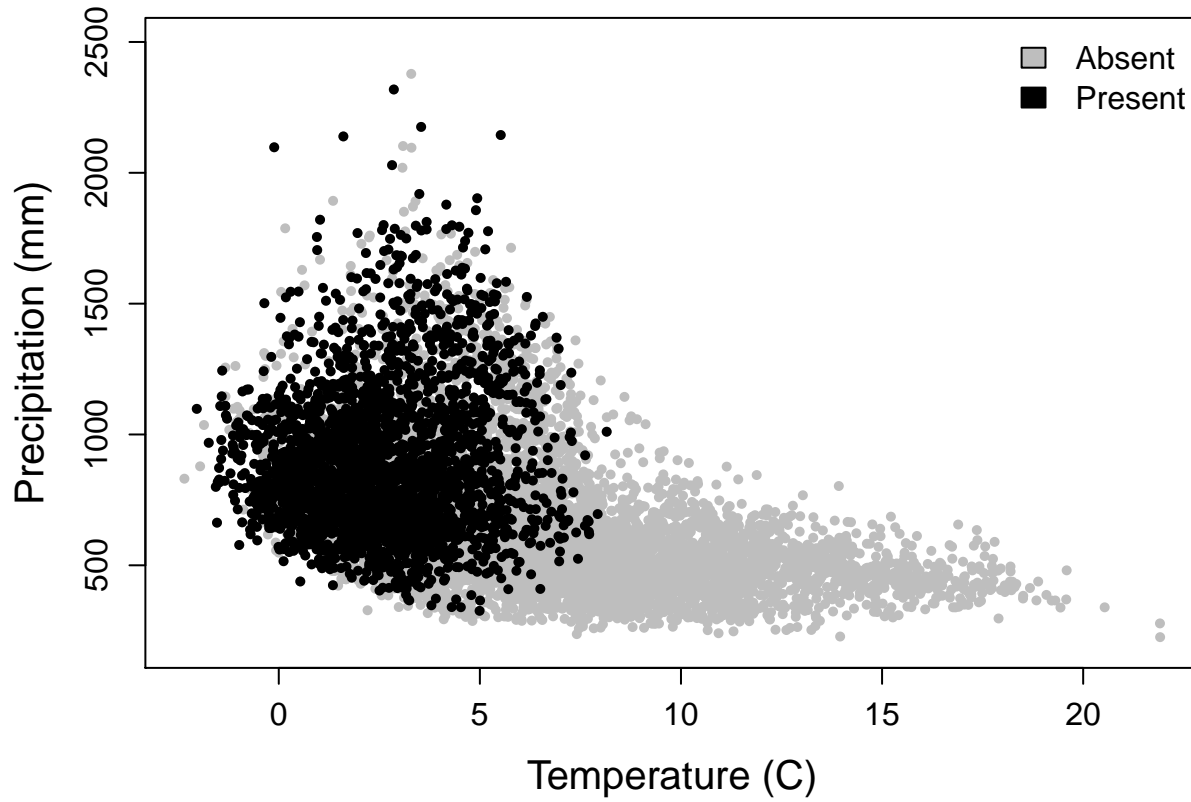
# Juniperus osteosperma – Utah juniper



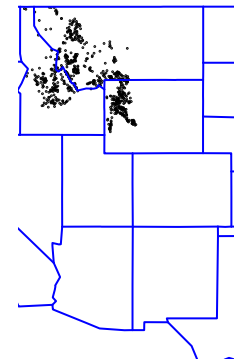
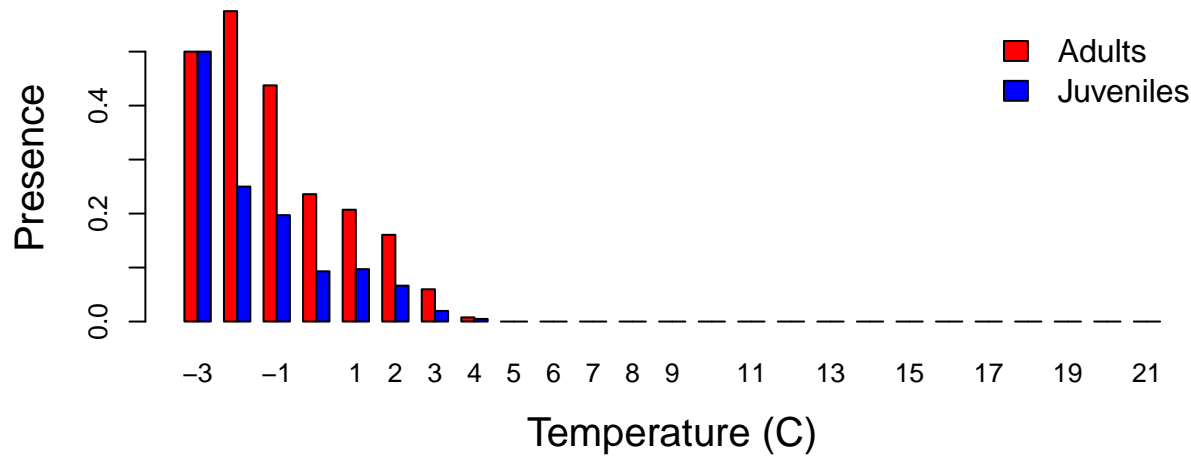
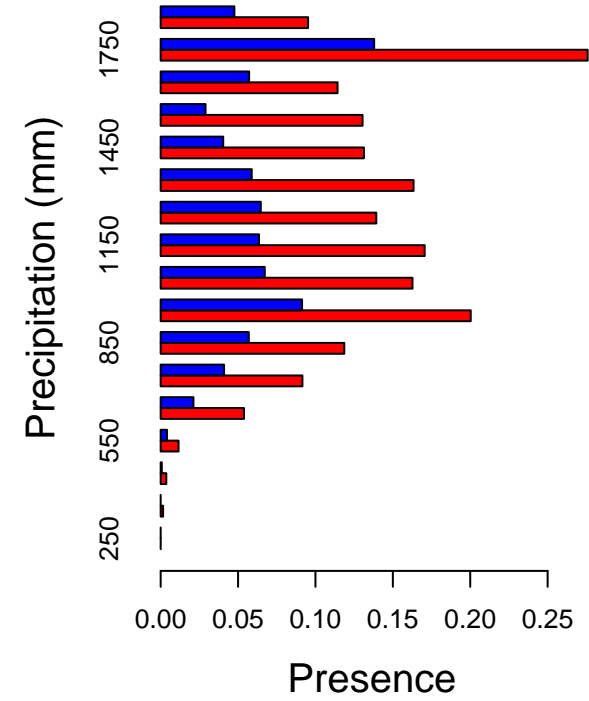
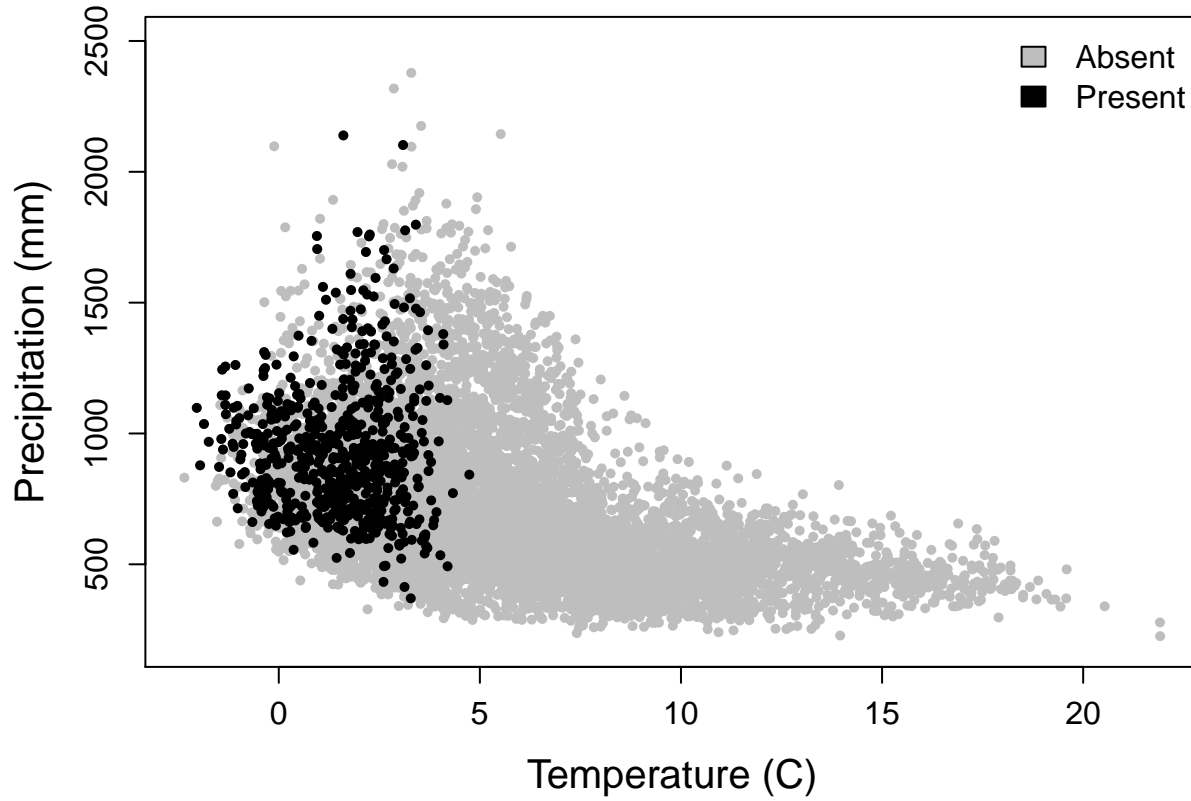
# Juniperus scopulorum – Rocky Mountain juniper



# Picea engelmannii – Engelmann spruce

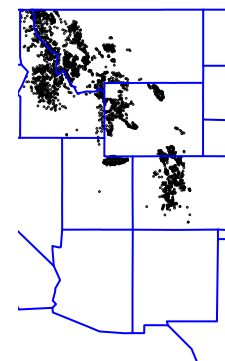
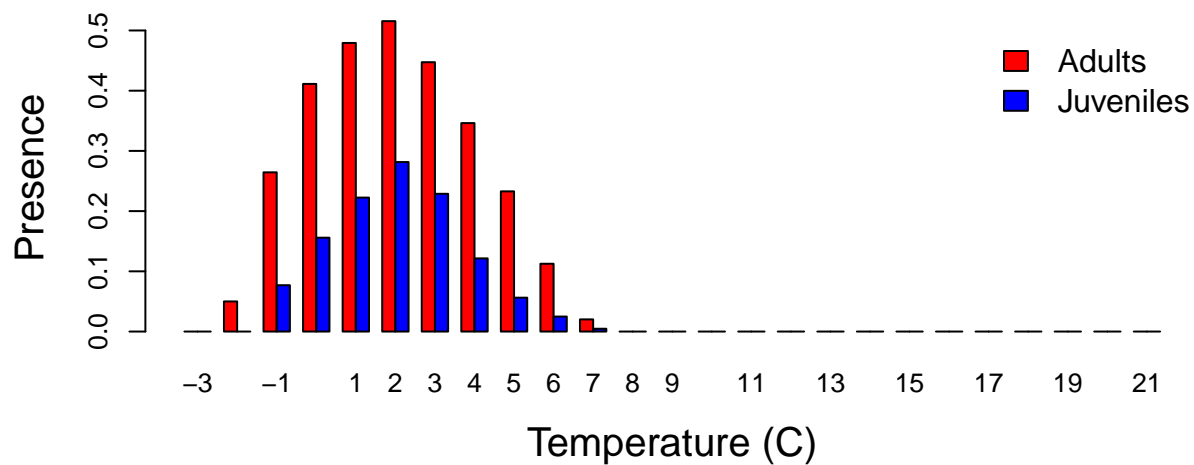
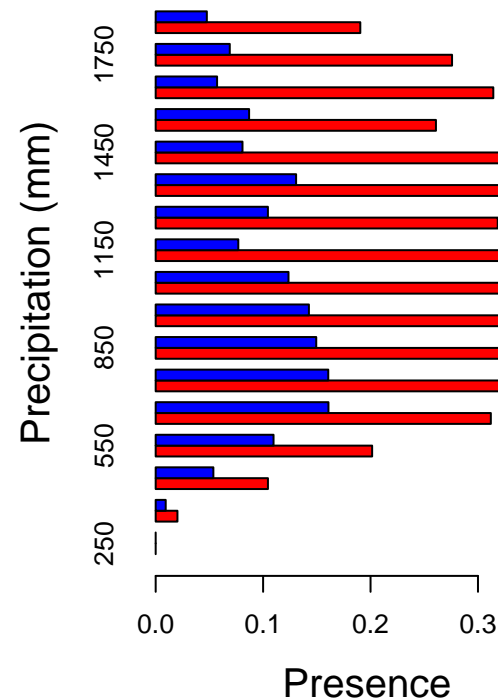
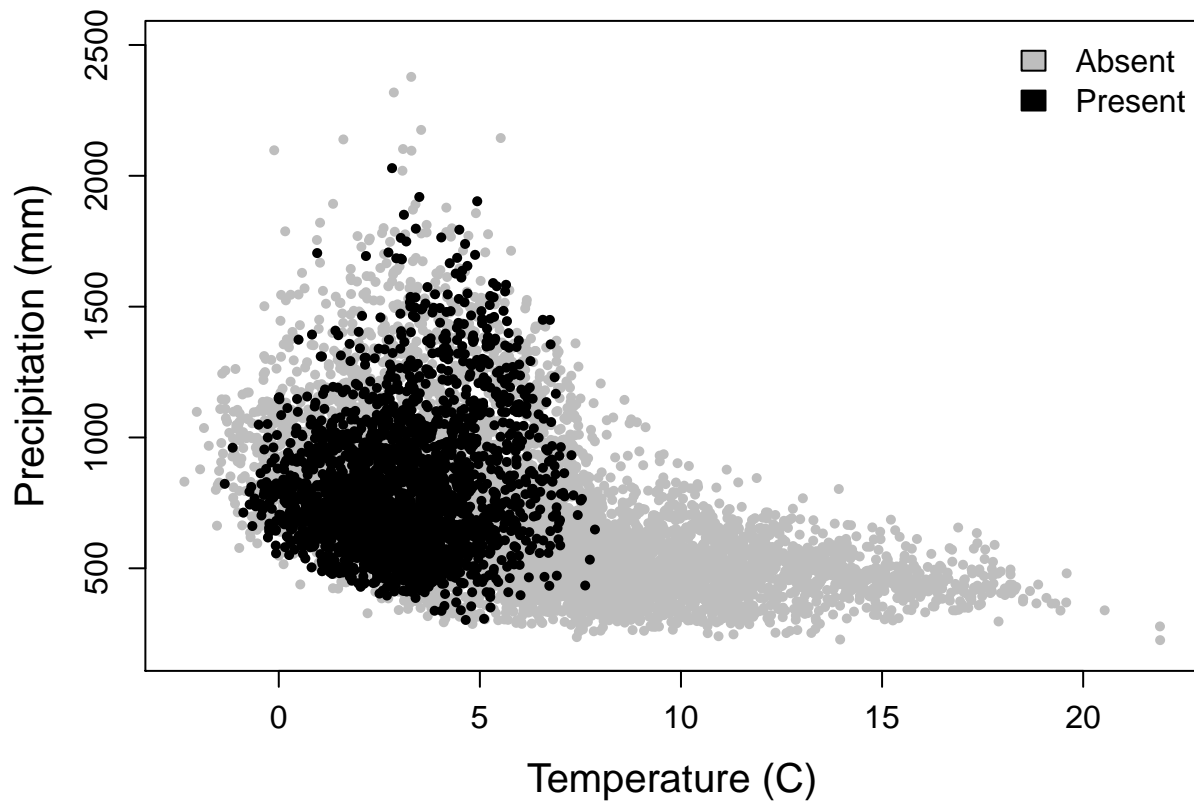


# Pinus albicaulis – whitebark pine

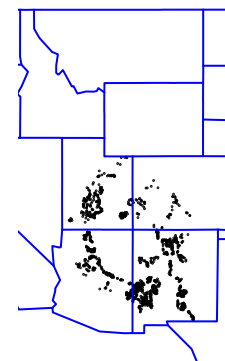
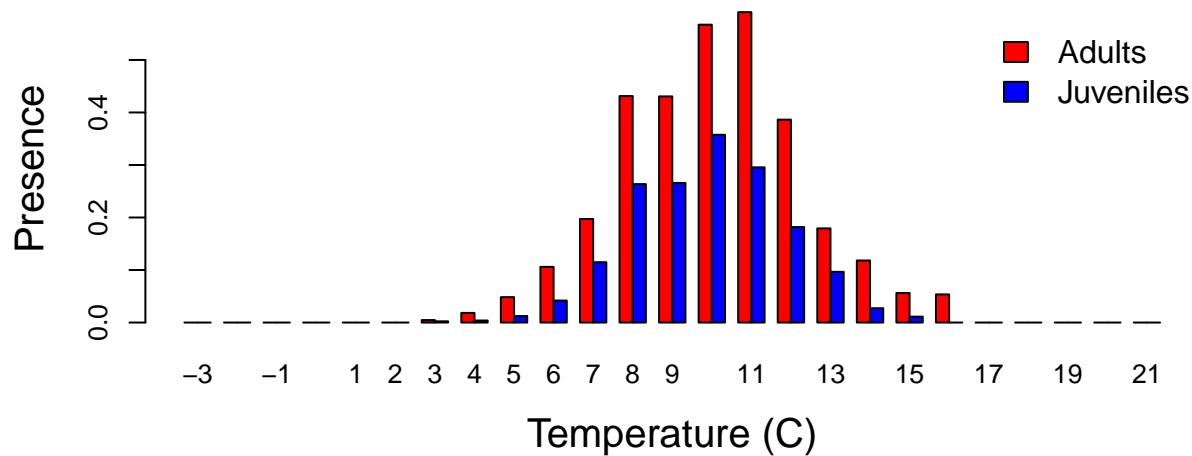
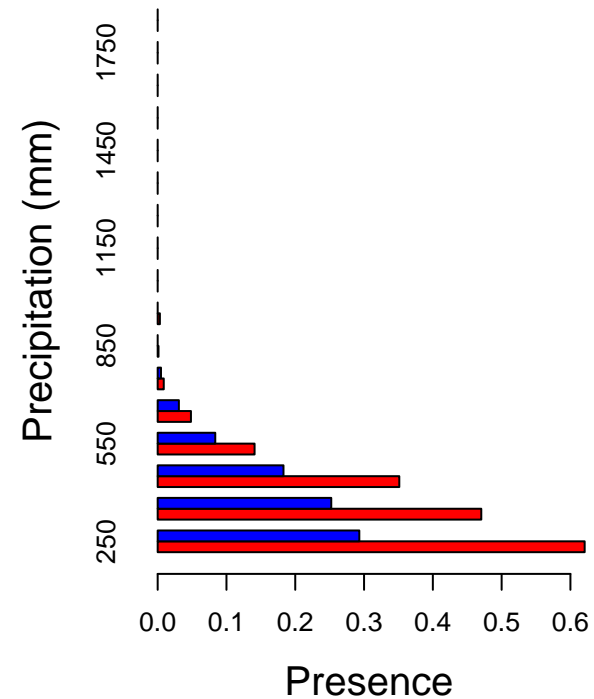
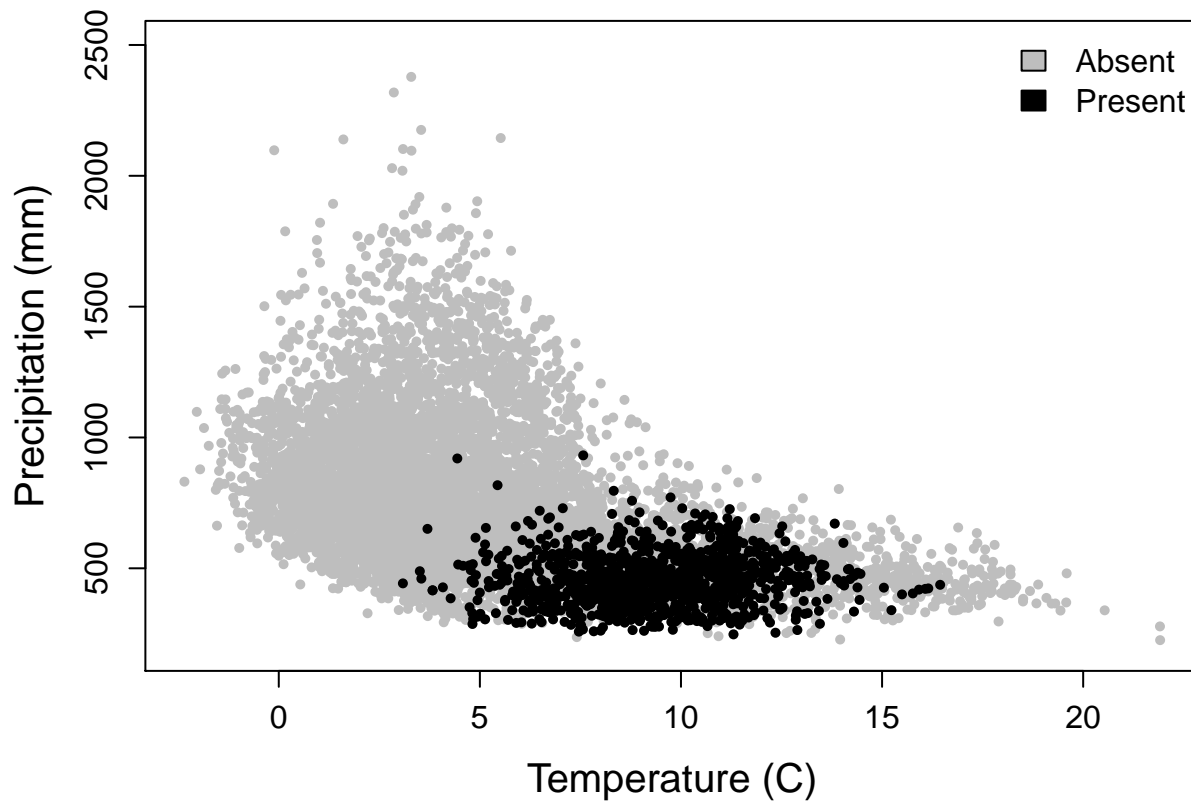




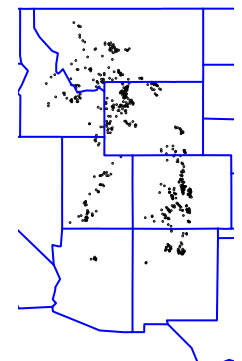
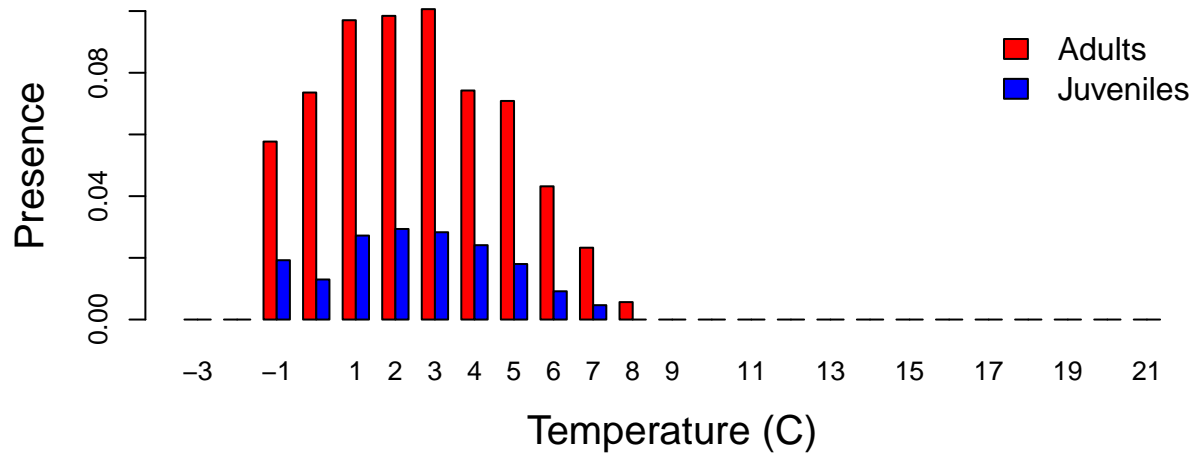
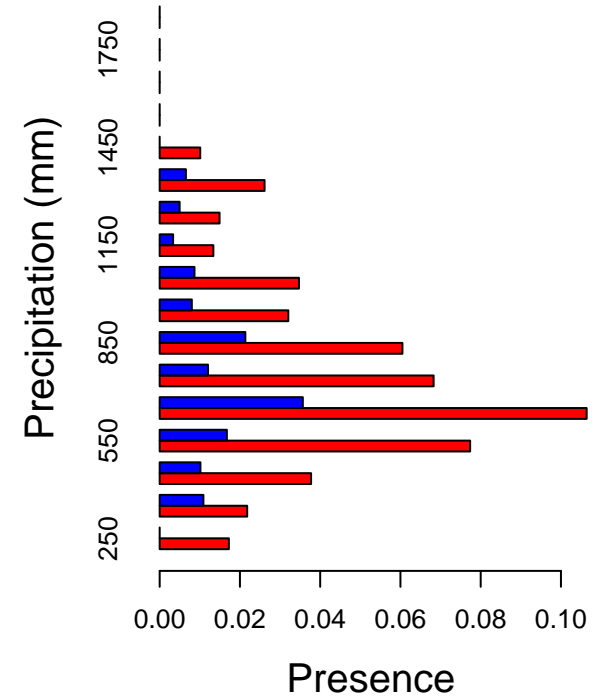
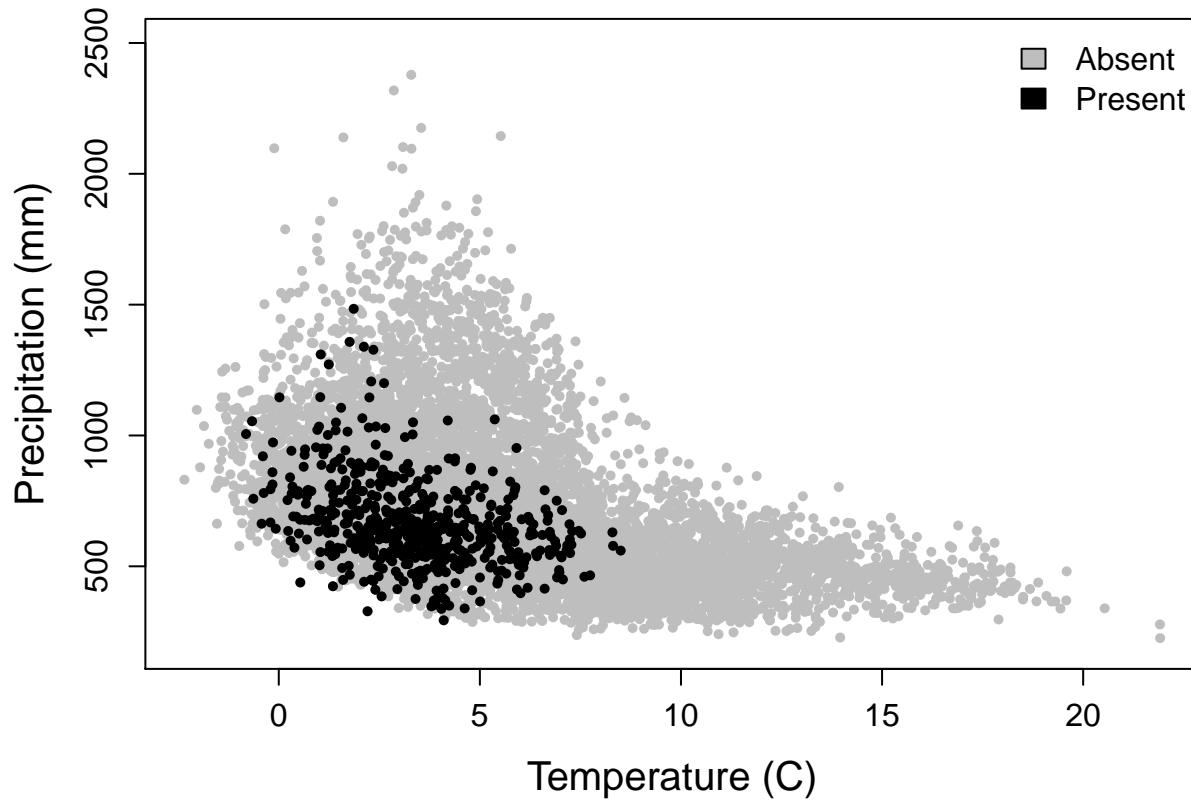
# Pinus contorta – lodgepole pine



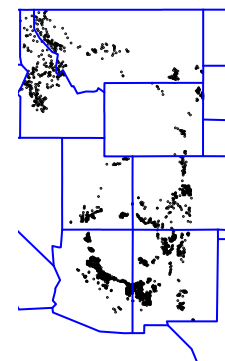
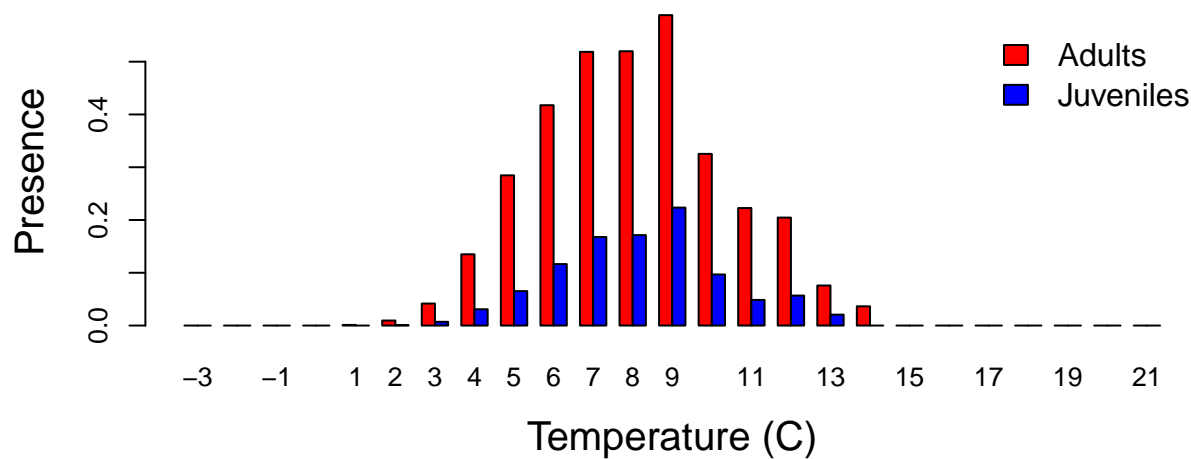
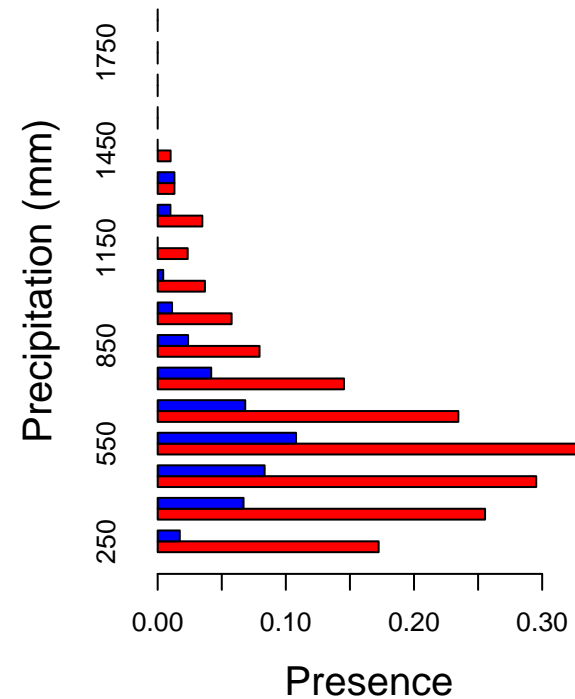
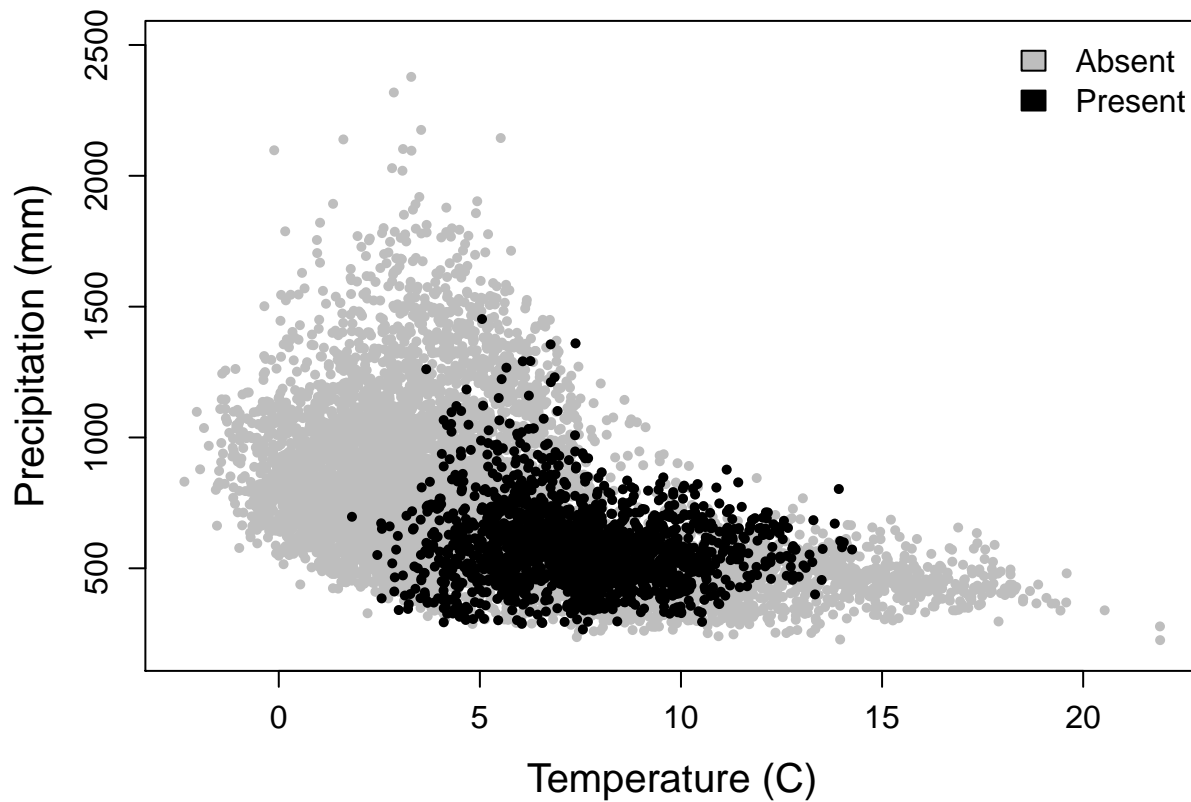
# Pinus edulis – Common or two-needle Pinyon



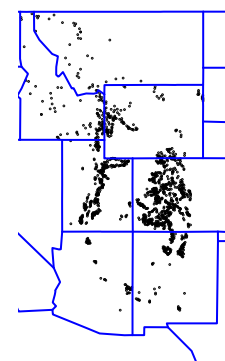
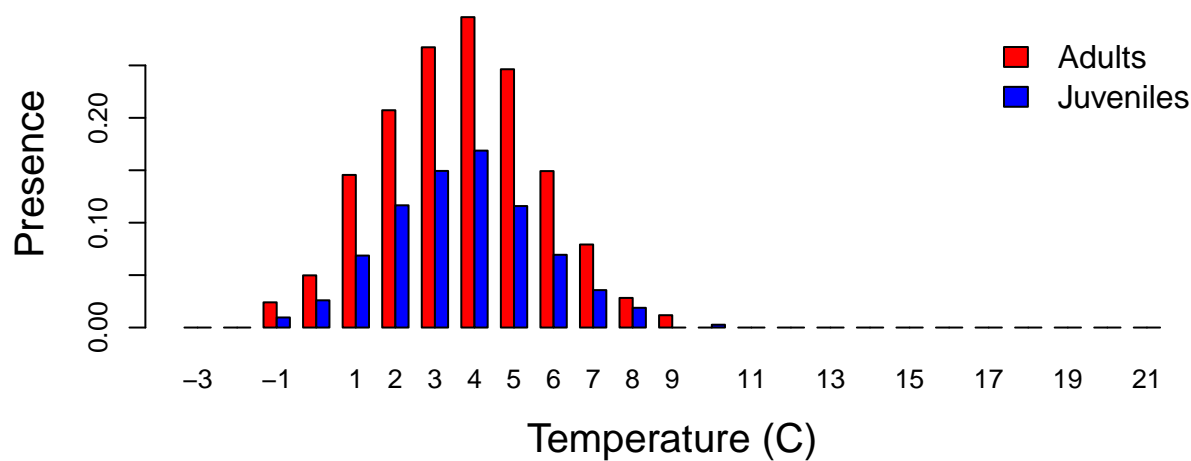
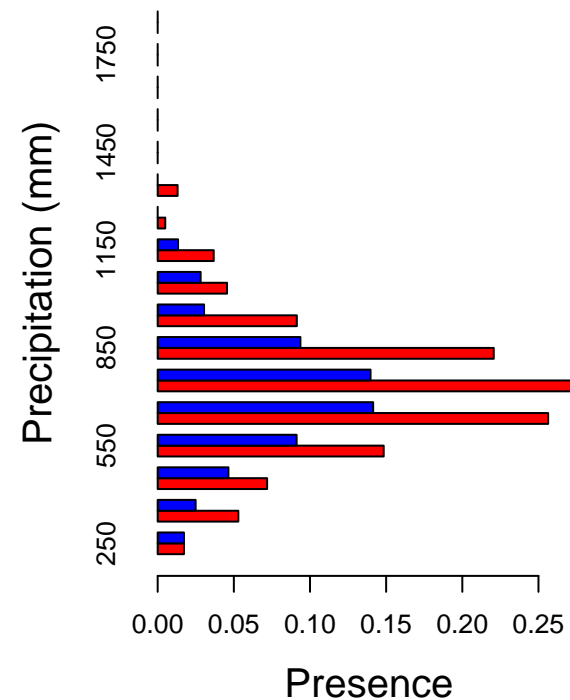
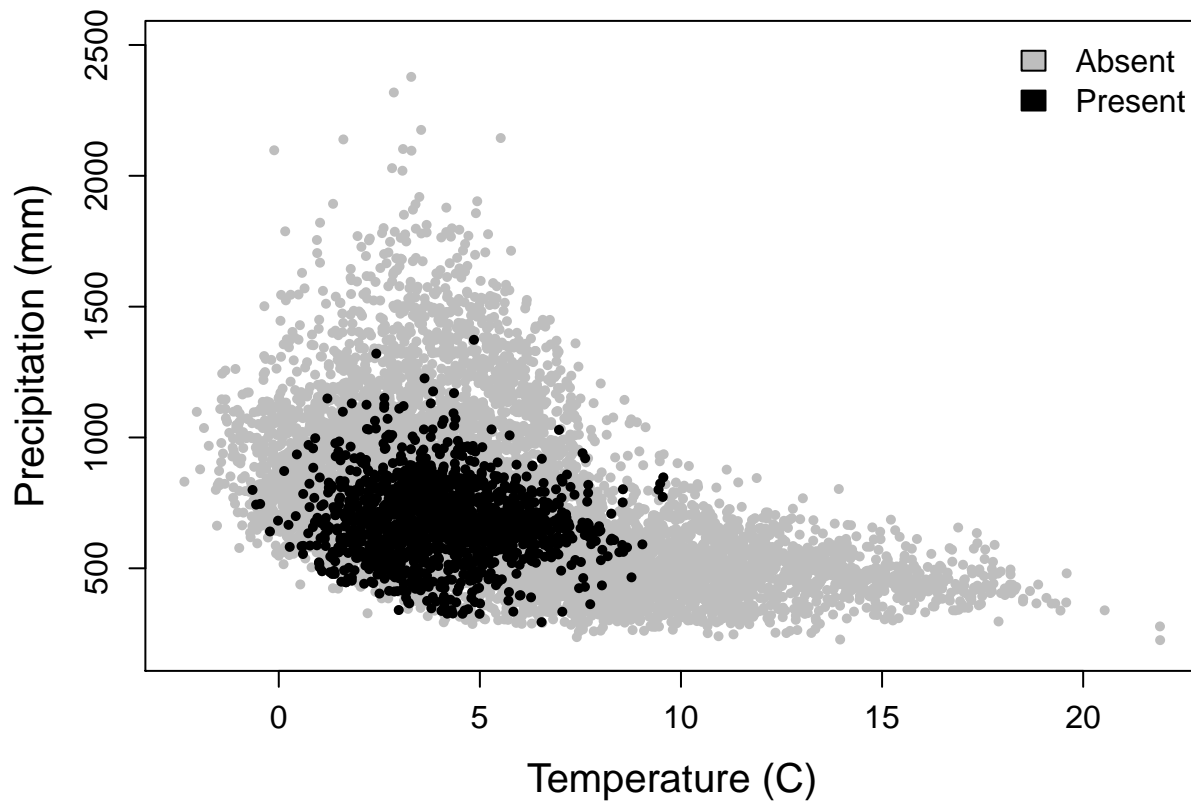
# Pinus flexilis – limber pine



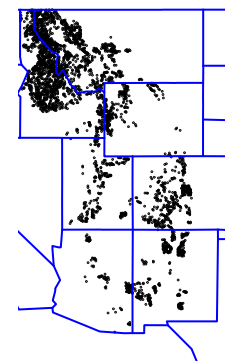
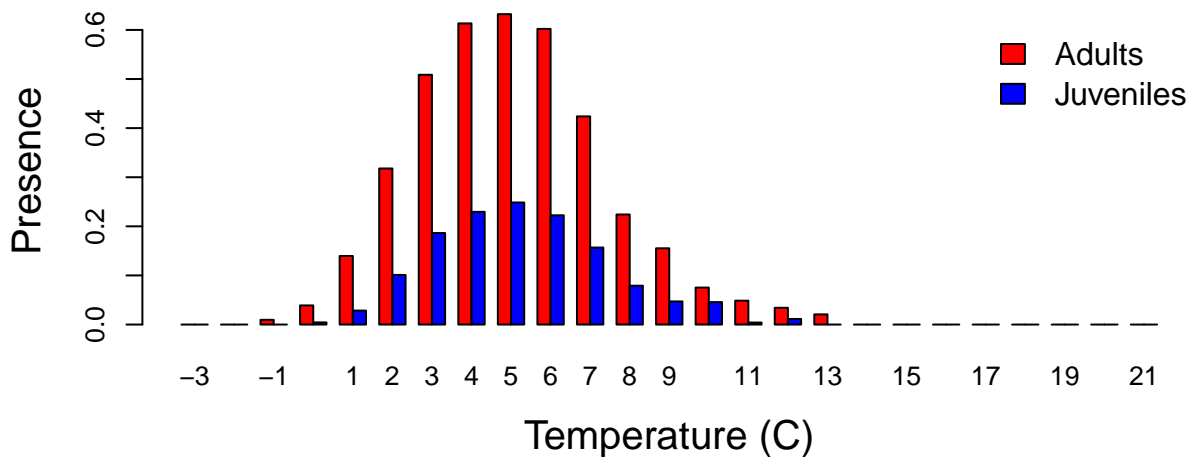
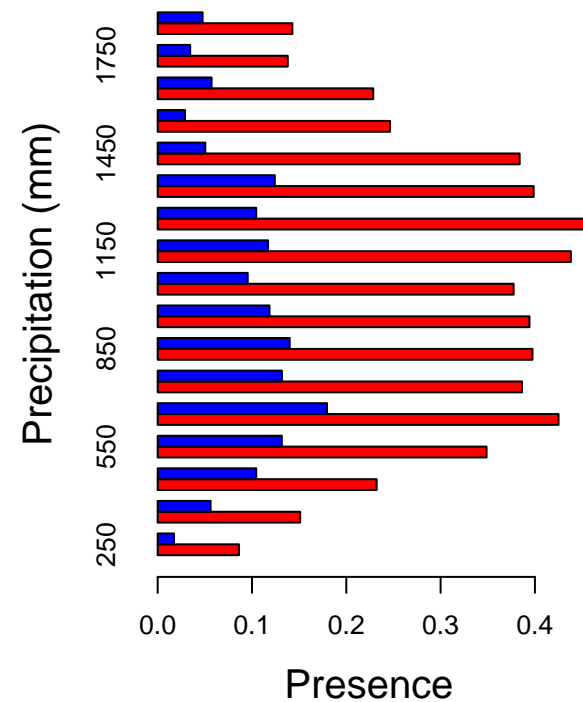
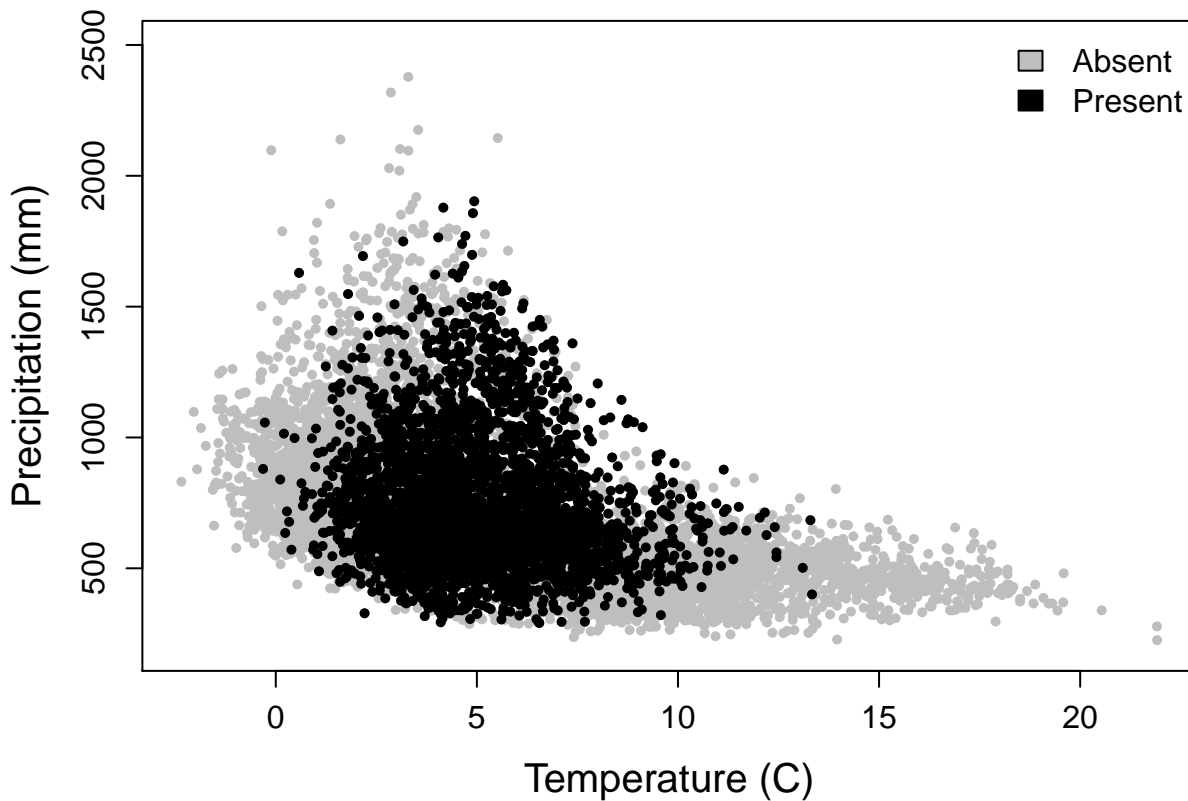
# Pinus ponderosa – ponderosa pine



# Populus tremuloides – quaking aspen

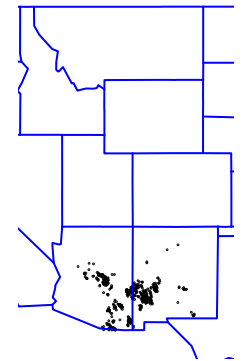
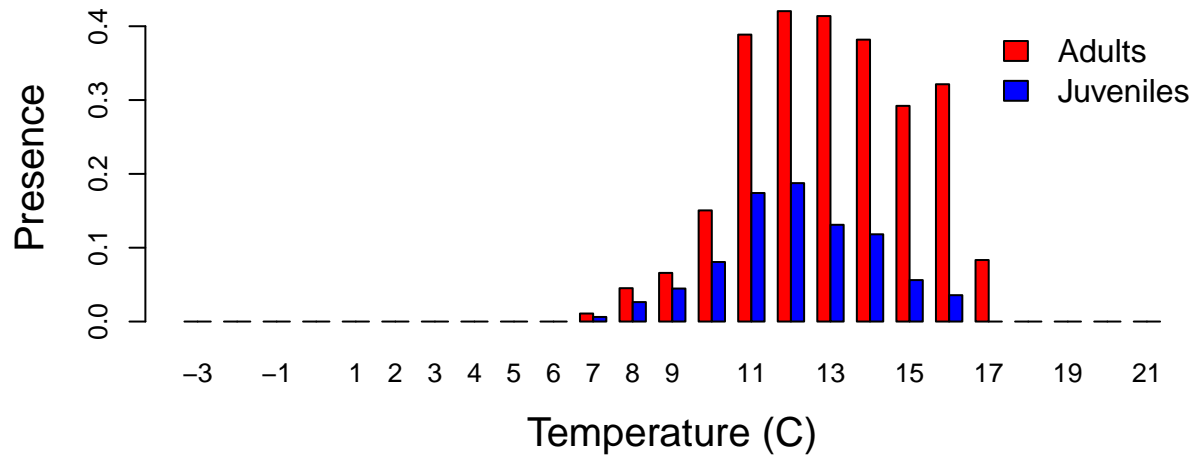
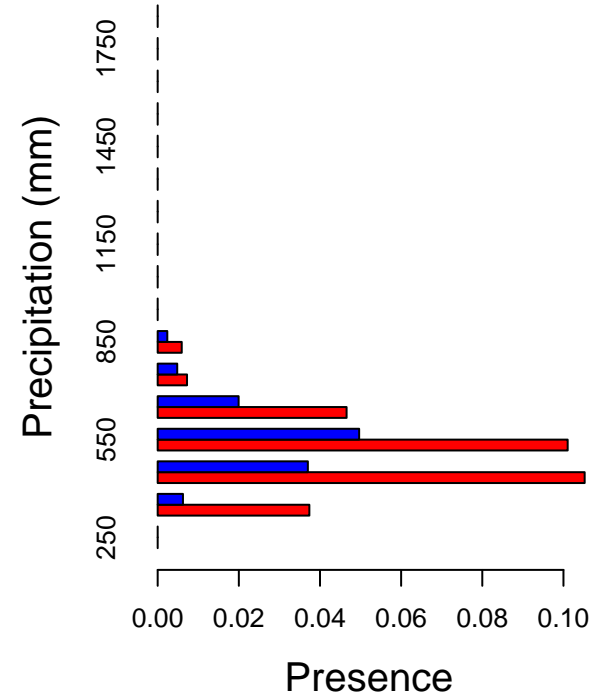
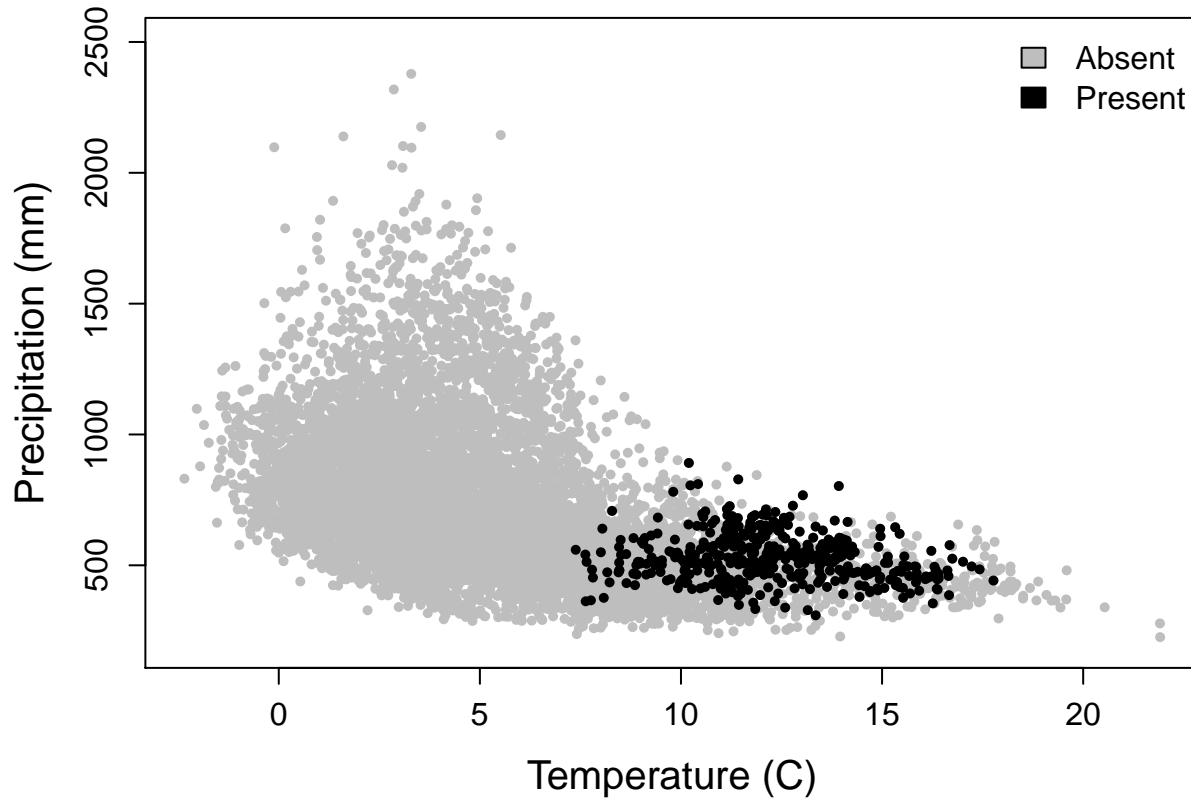


# *Pseudotsuga menziesii* – Douglas-fir

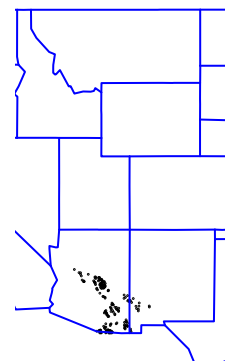
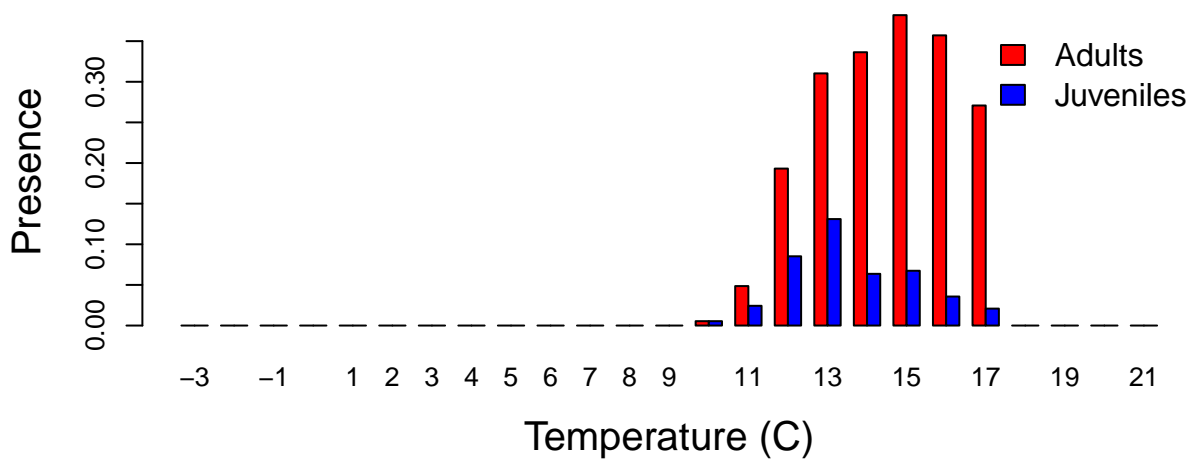
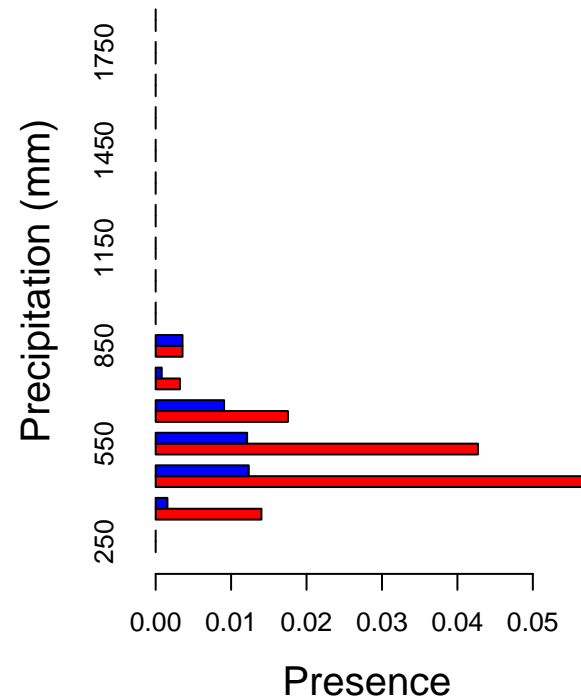
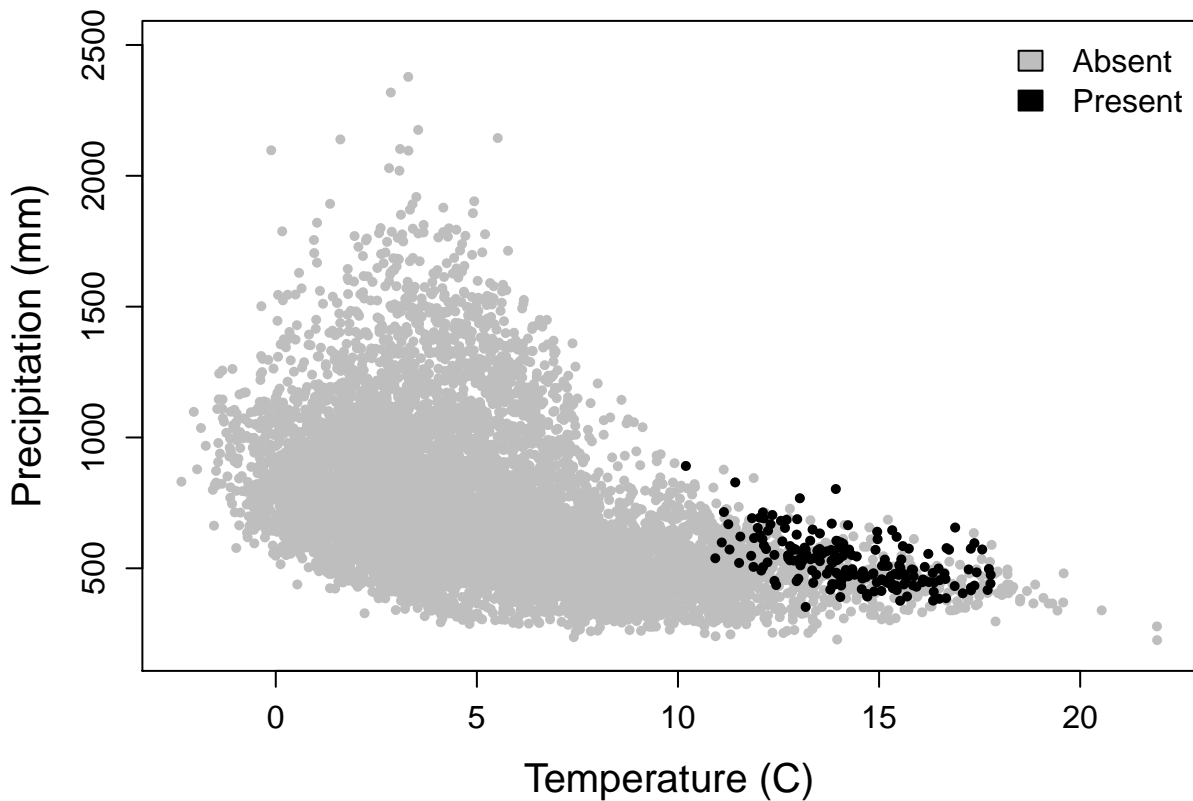




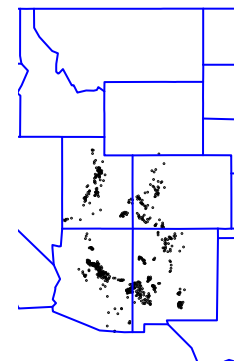
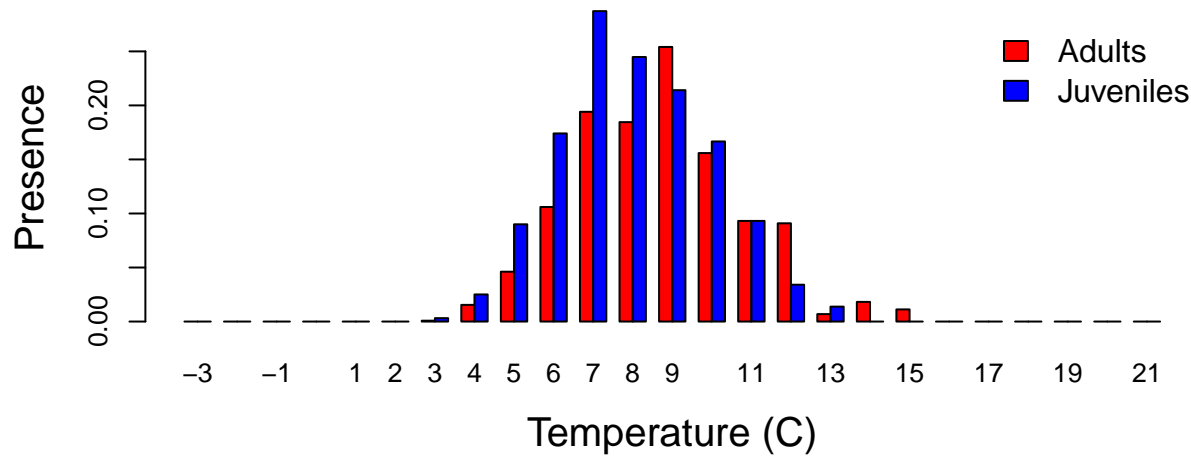
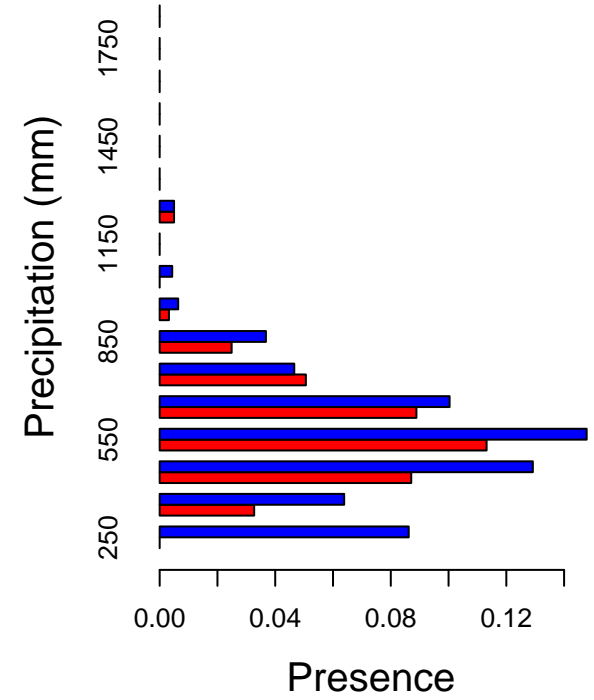
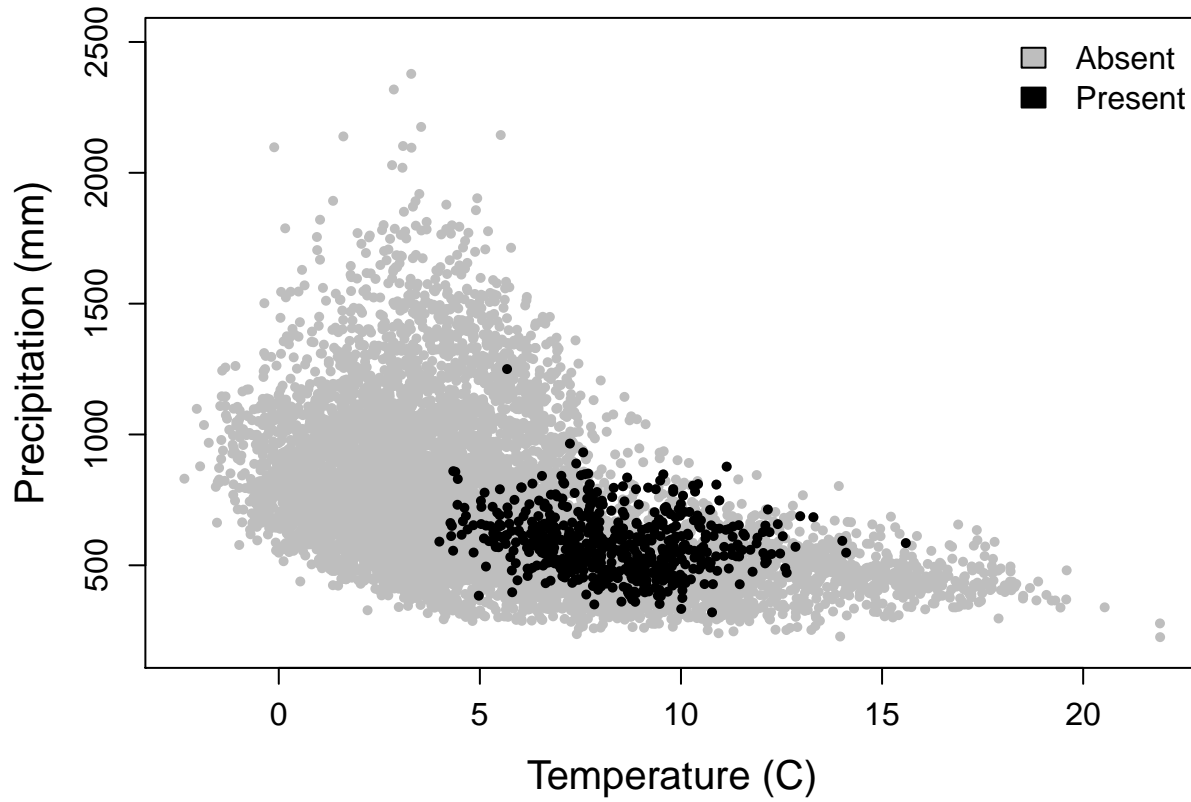
# Quercus arizonica – Arizona white oak



# Quercus emoryi – Emory oak



# Quercus gambelii – Gambel oak



# **Ecosphere**

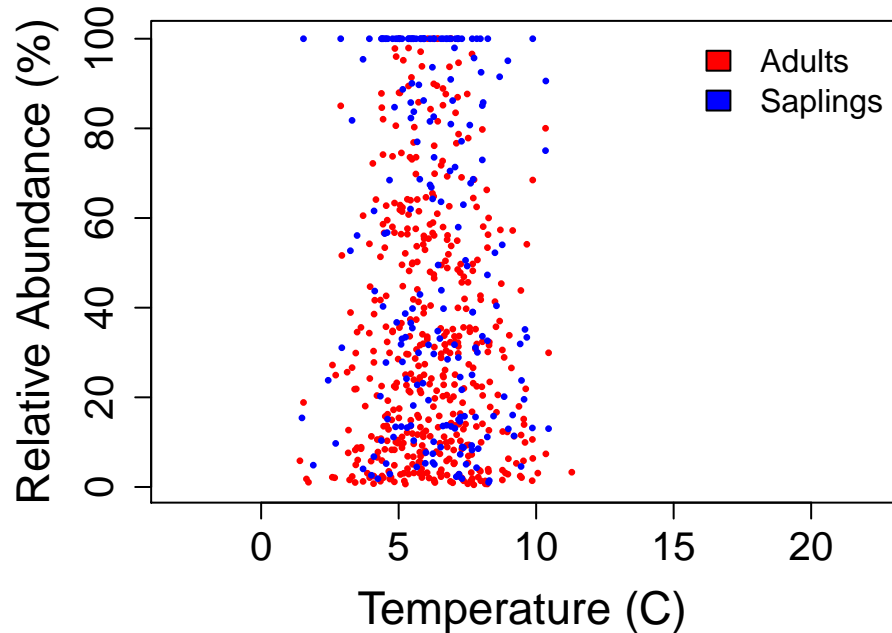
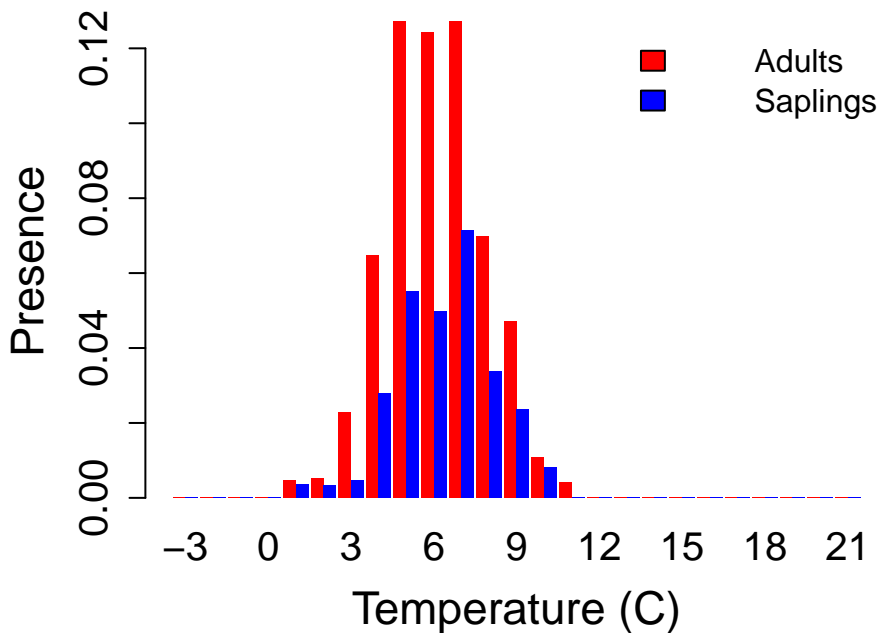
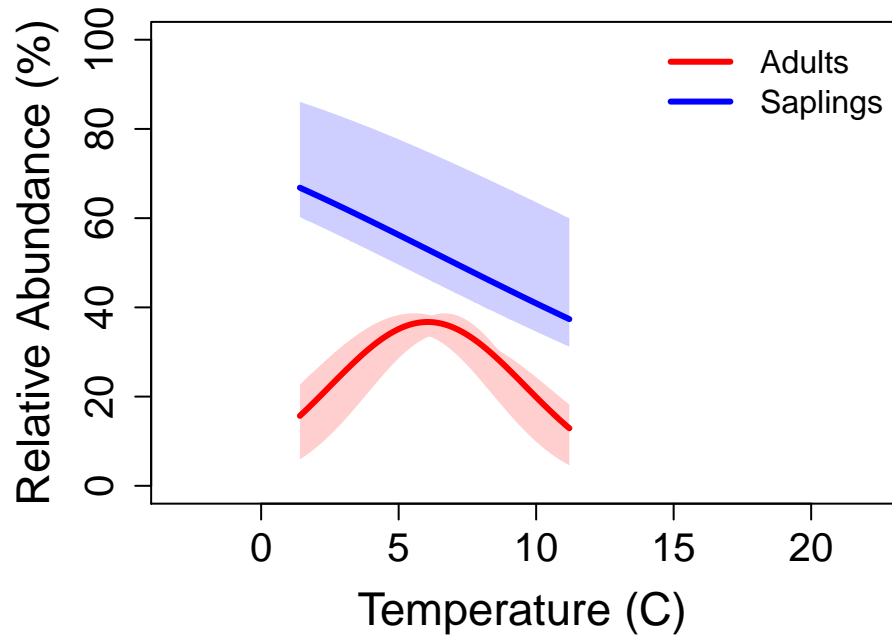
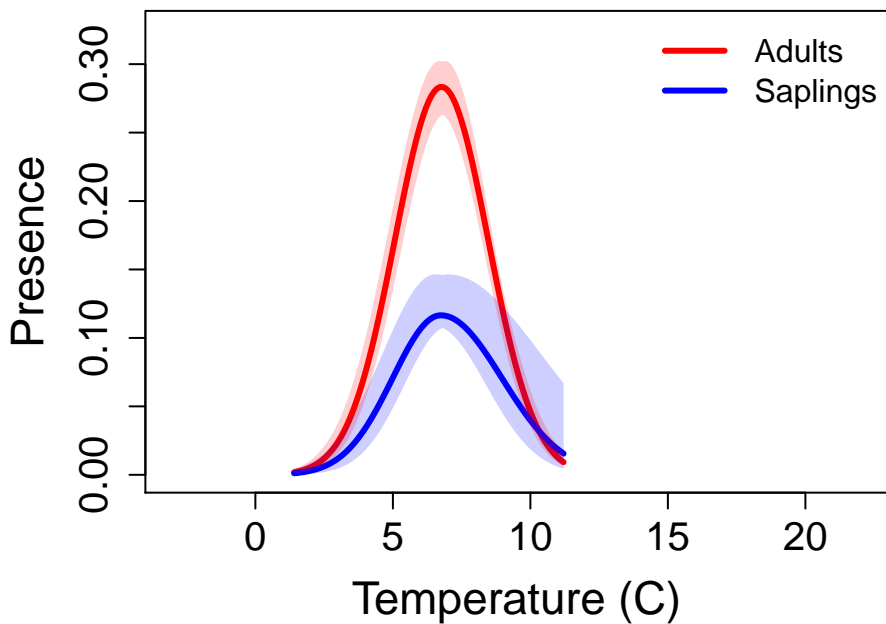
Peaks in frequency, but not relative abundance, occur in the center of tree species distributions on climate gradients

Patrick H. Martin and Charles D. Canham

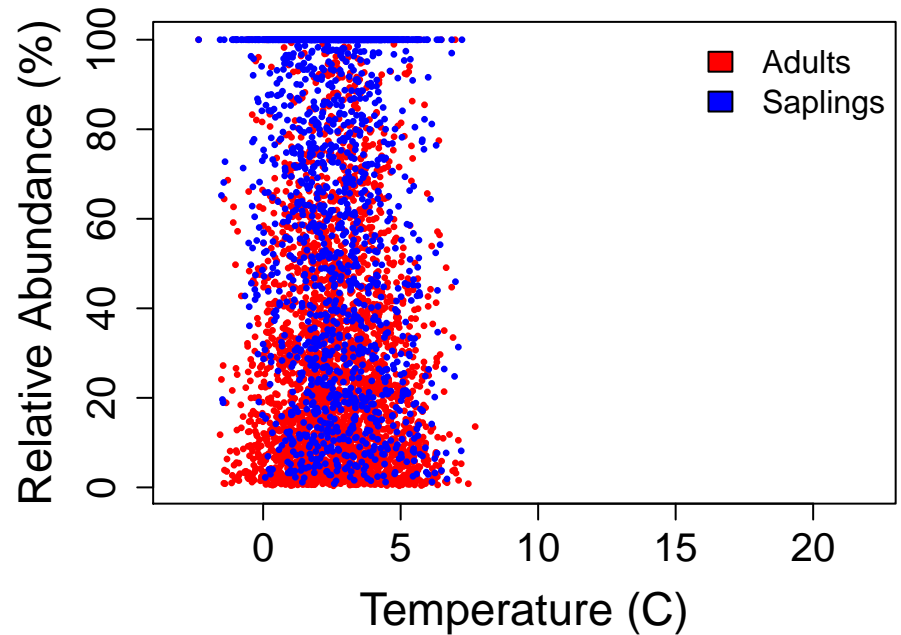
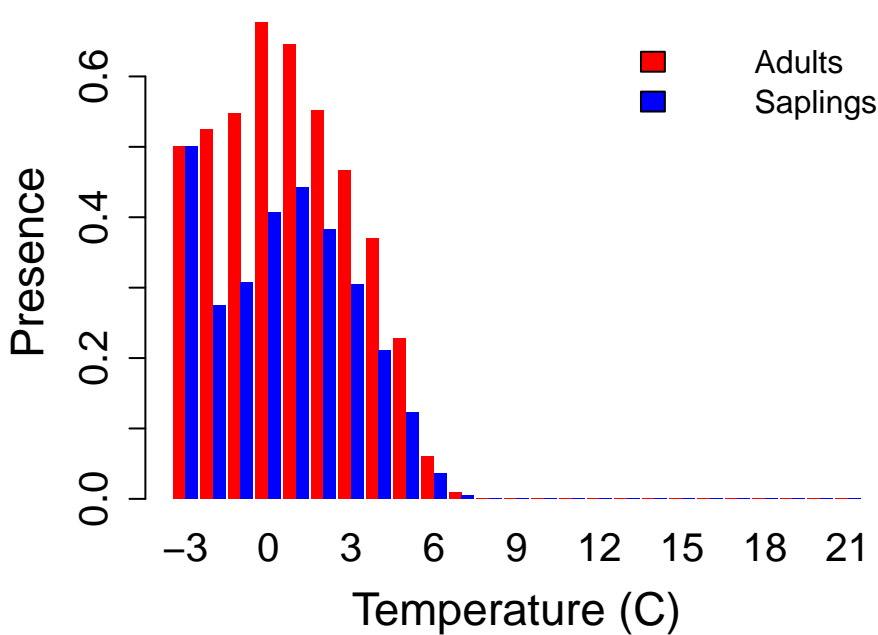
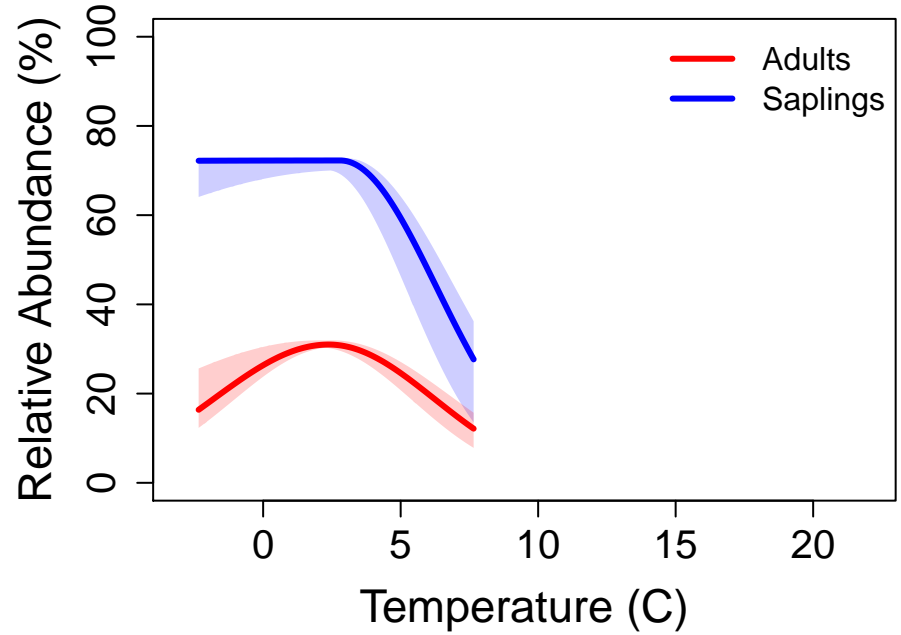
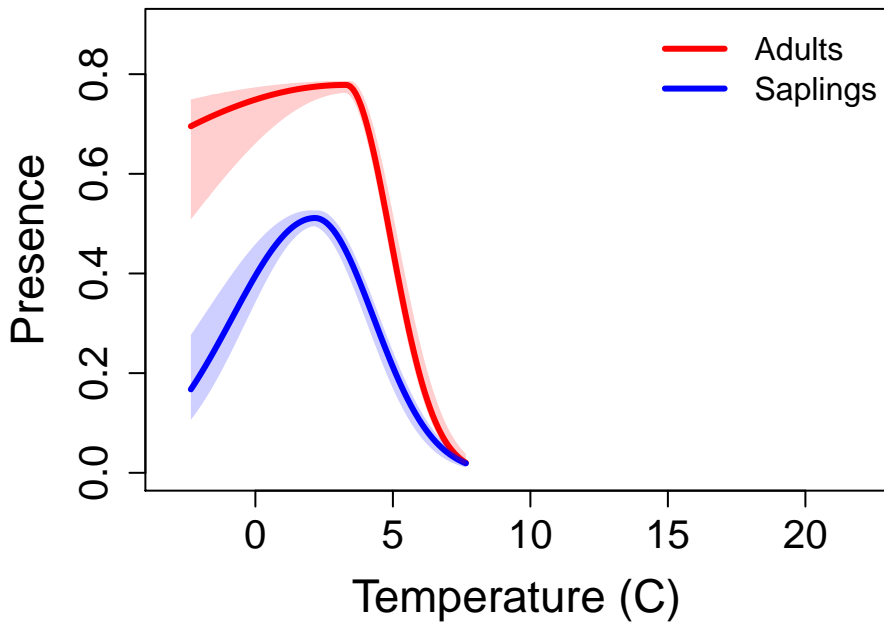
## **Appendix S2**

Temperature Distributions – Modeled presence and relative abundance distributions with 2-unit support intervals for adults and saplings of dominant tree species on temperature gradients in the Interior West Region, and observed presence and relative abundance in the FIA data.

# Abies concolor – white fir

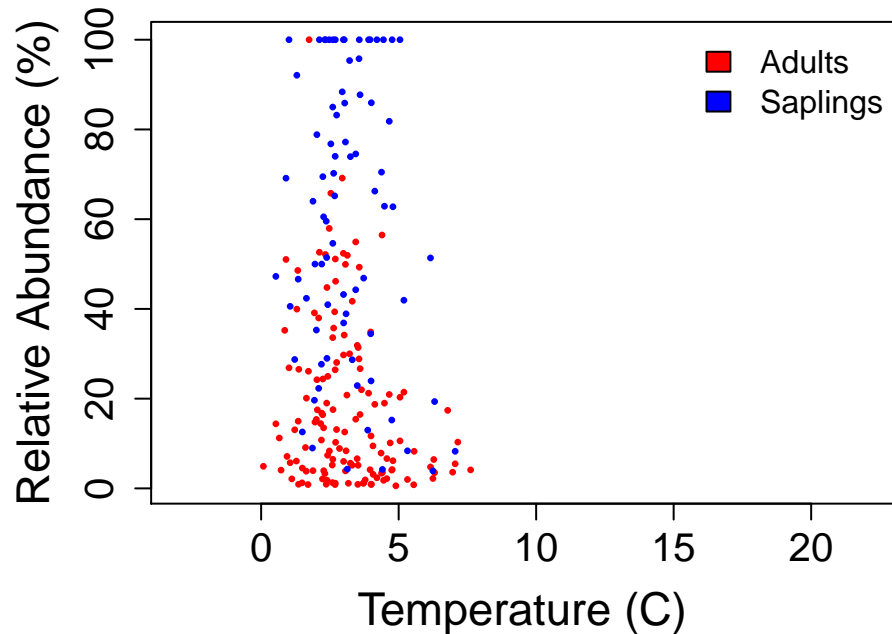
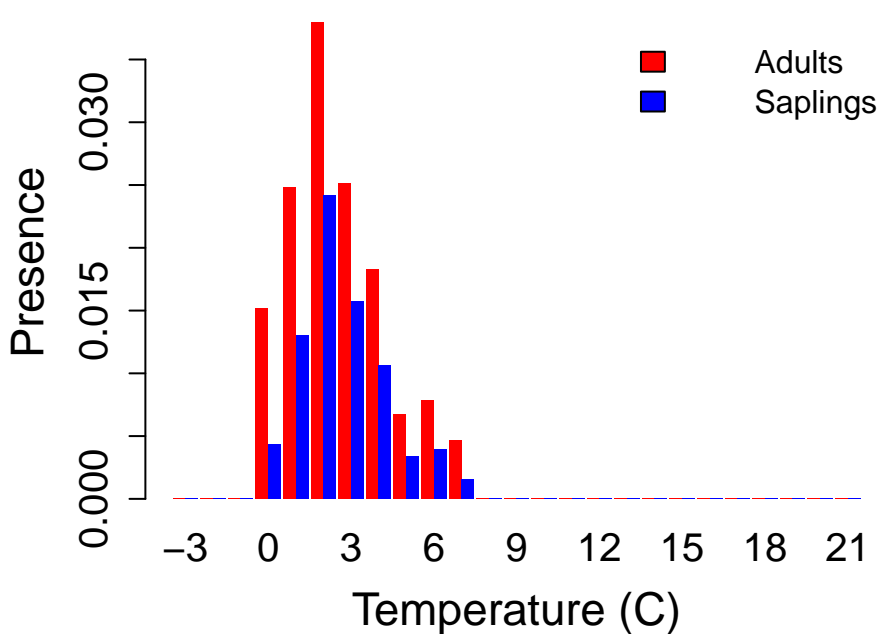
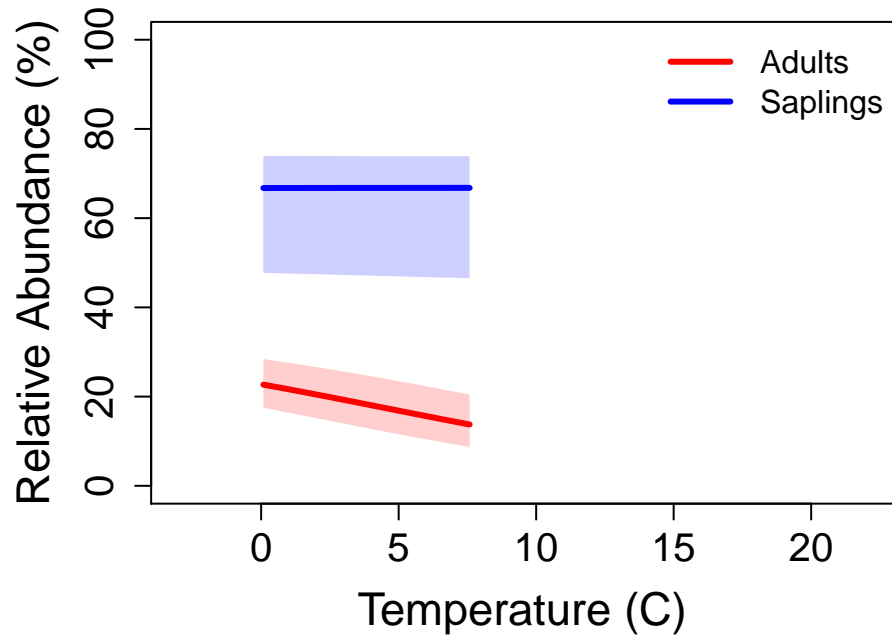
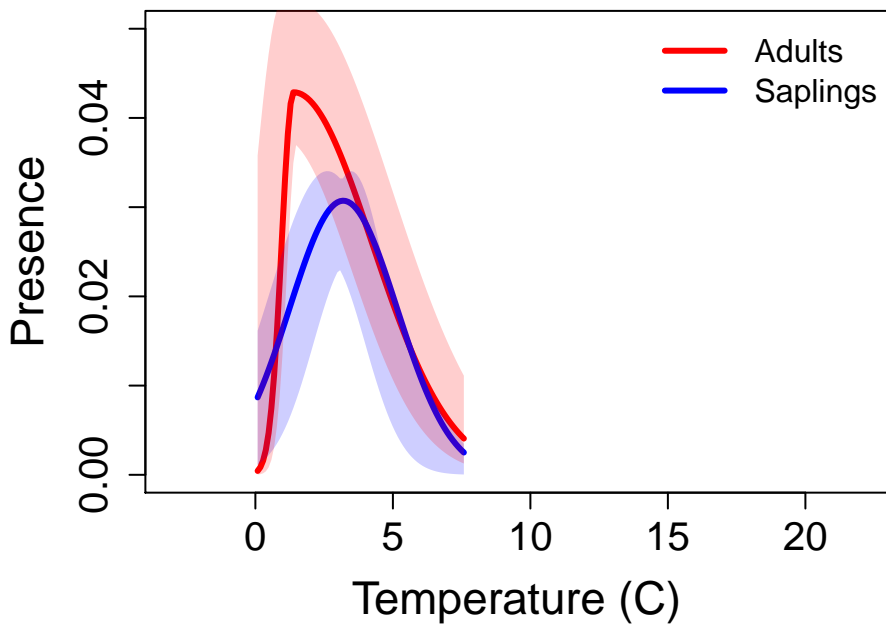


# Abies lasiocarpa - subalpine fir

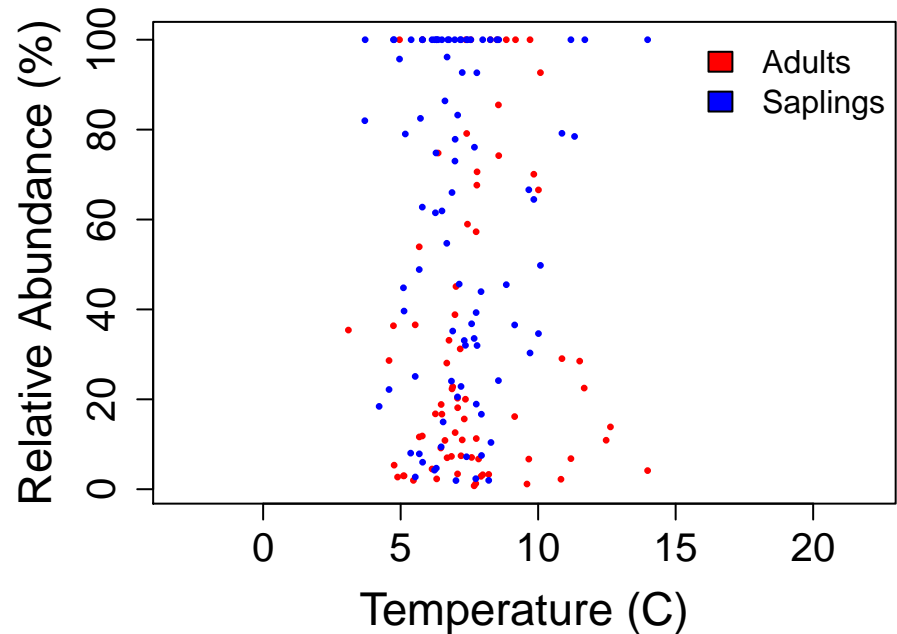
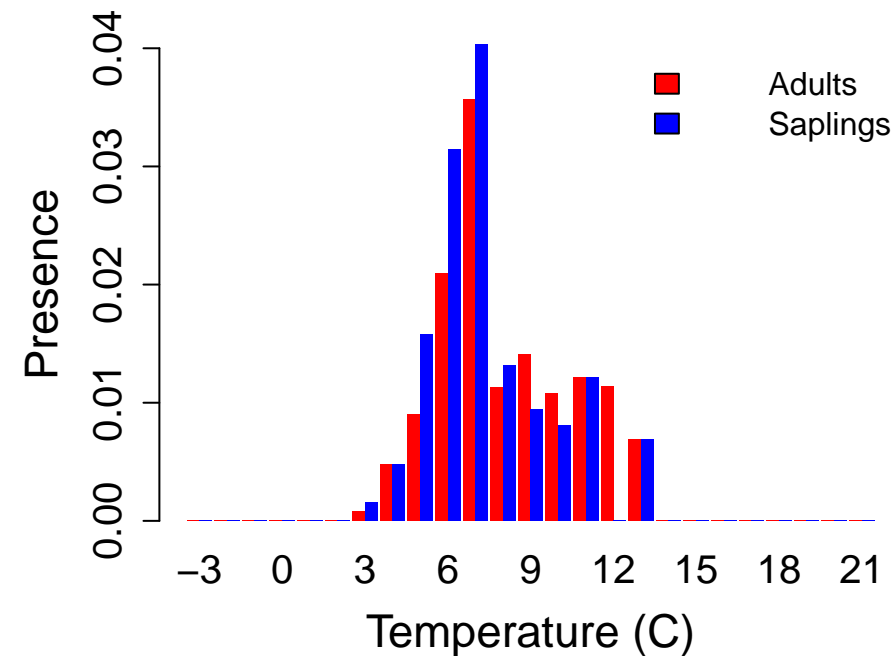
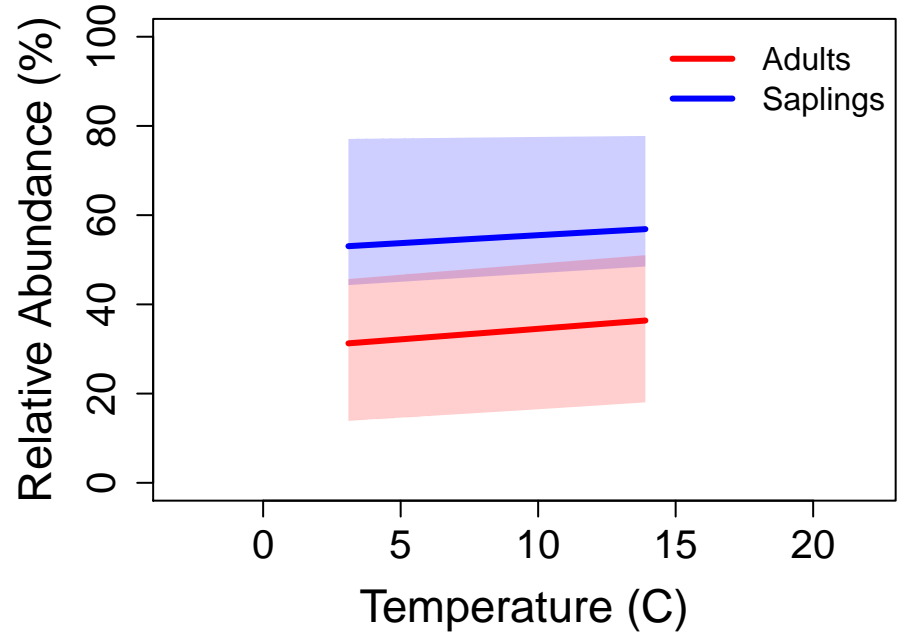
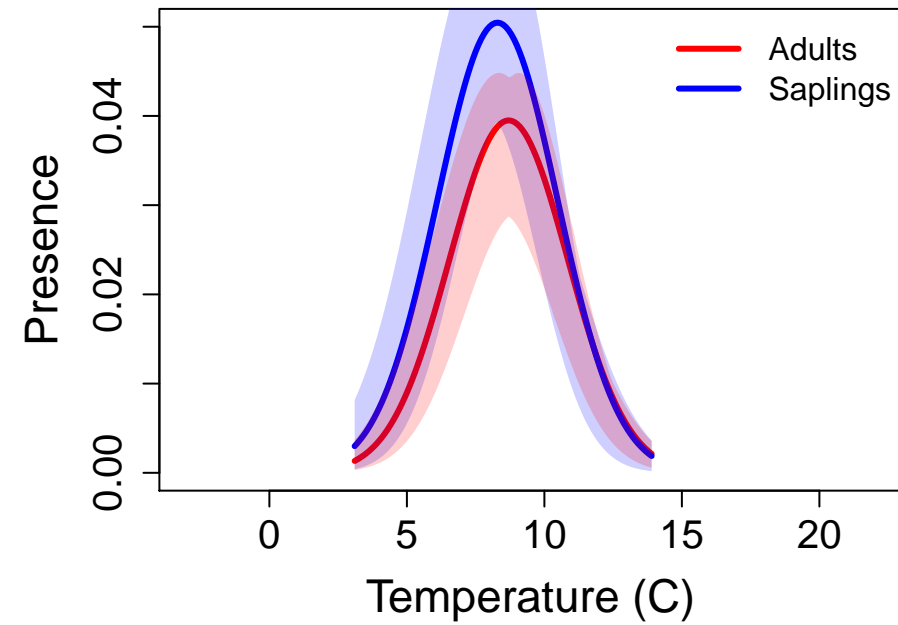




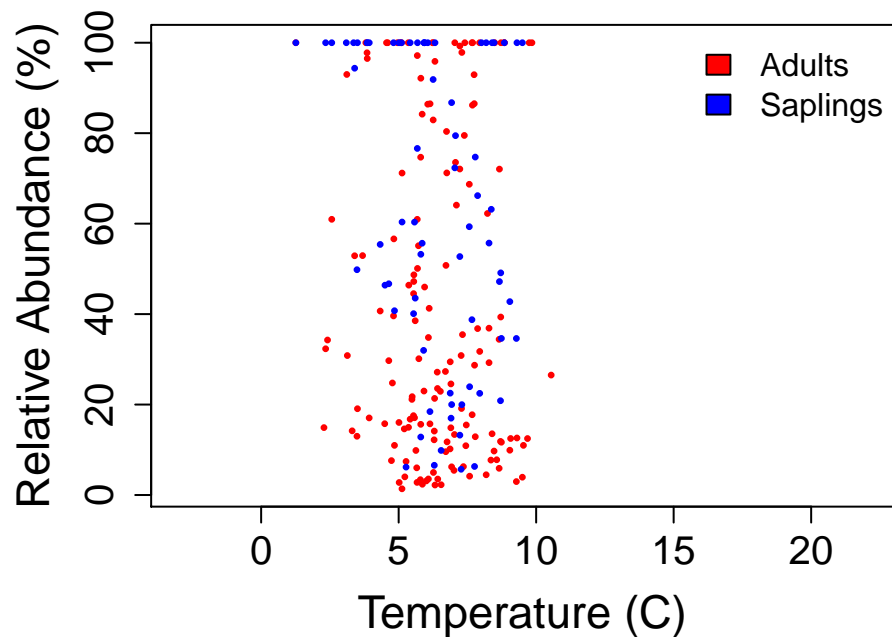
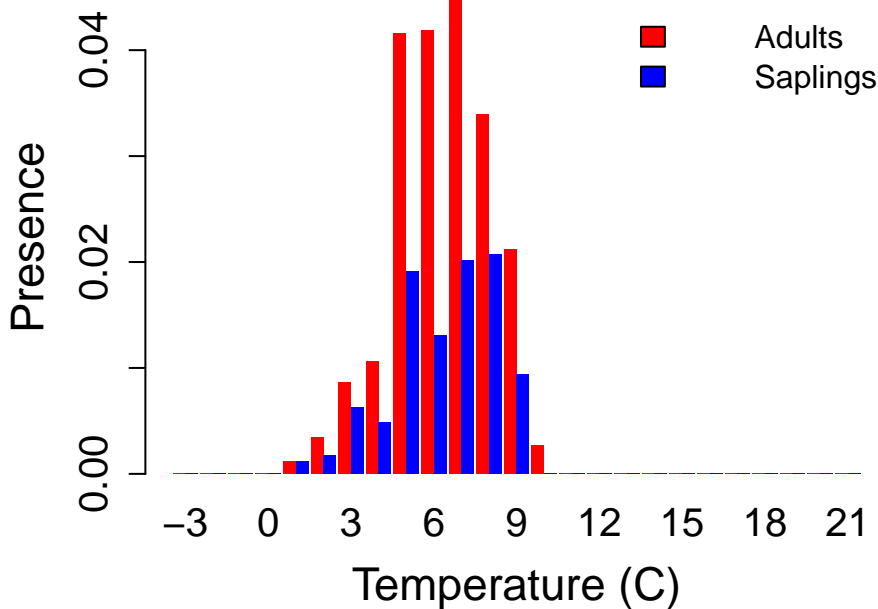
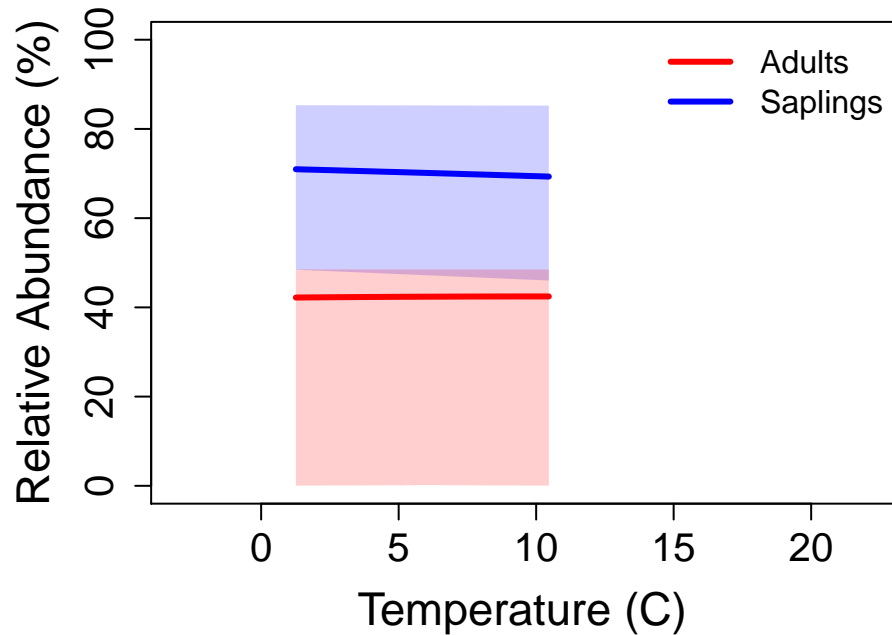
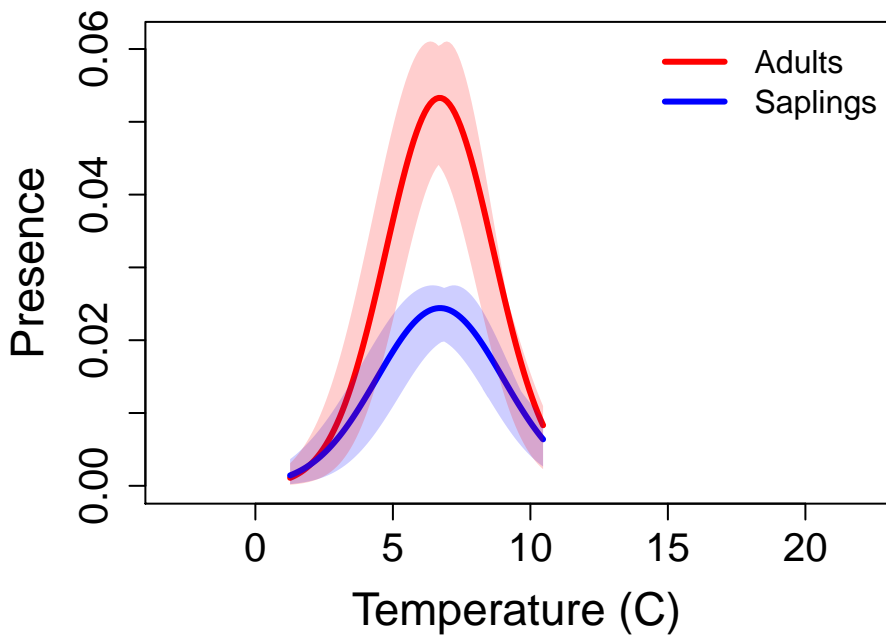
# Abies lasiocarpa var. arizonica – corkbark fir



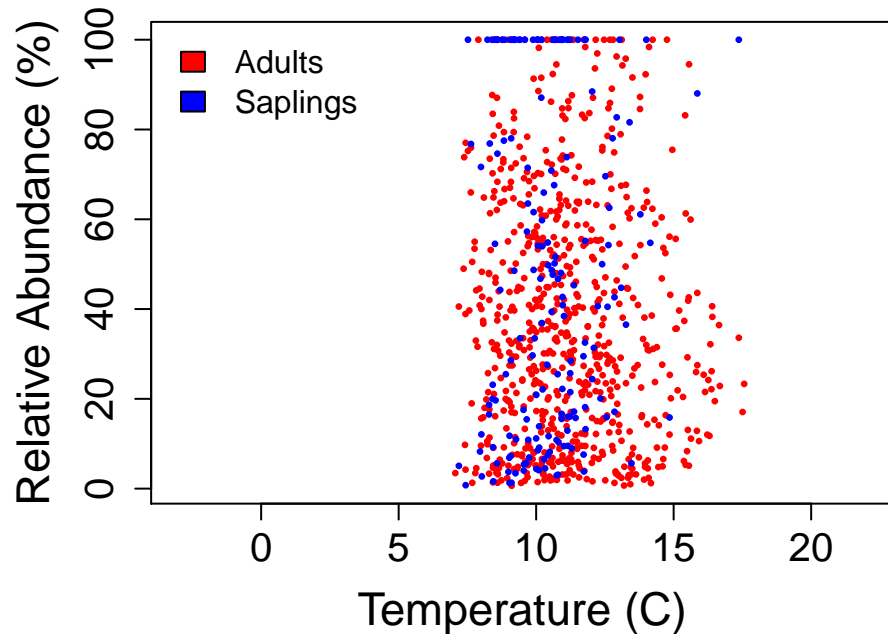
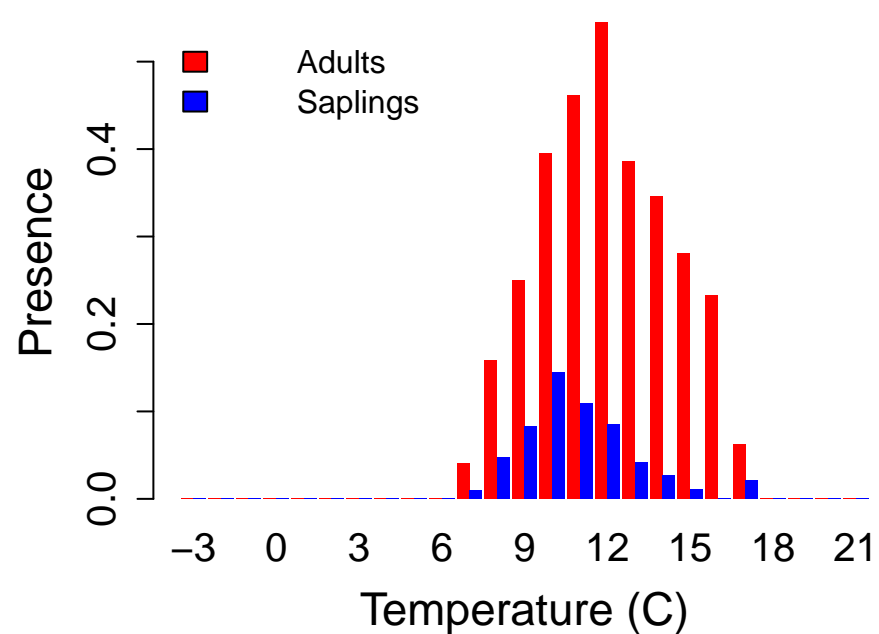
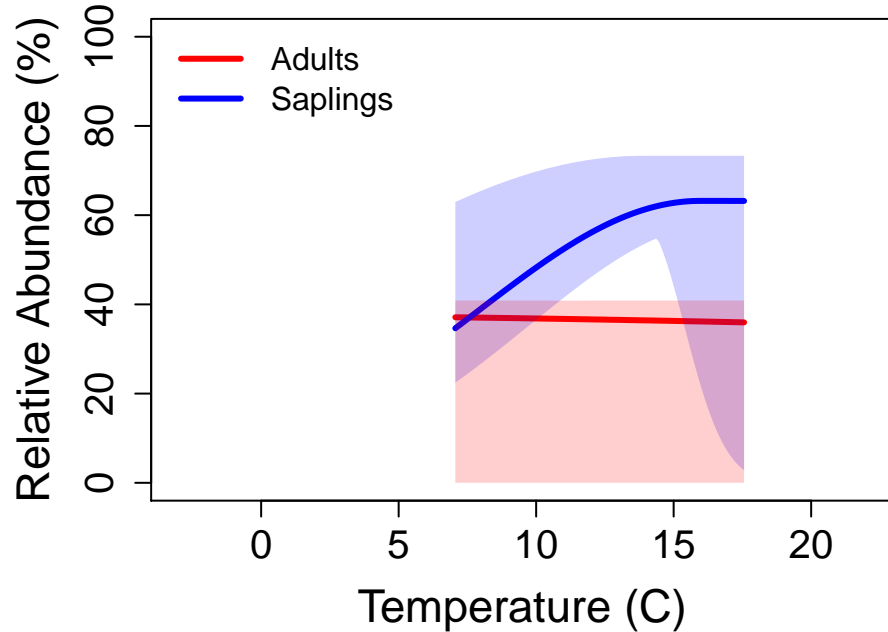
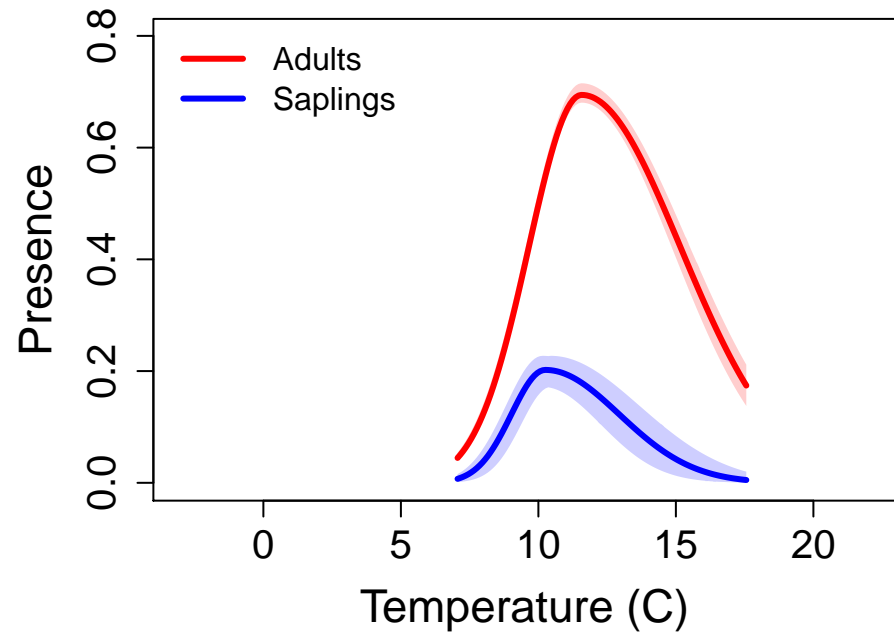
# Acer grandidentatum – bigtooth maple



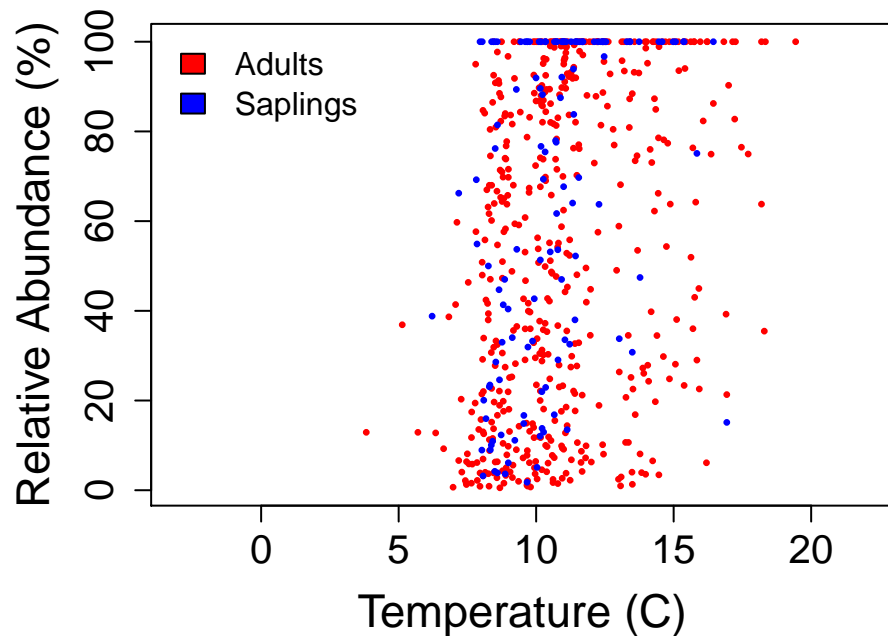
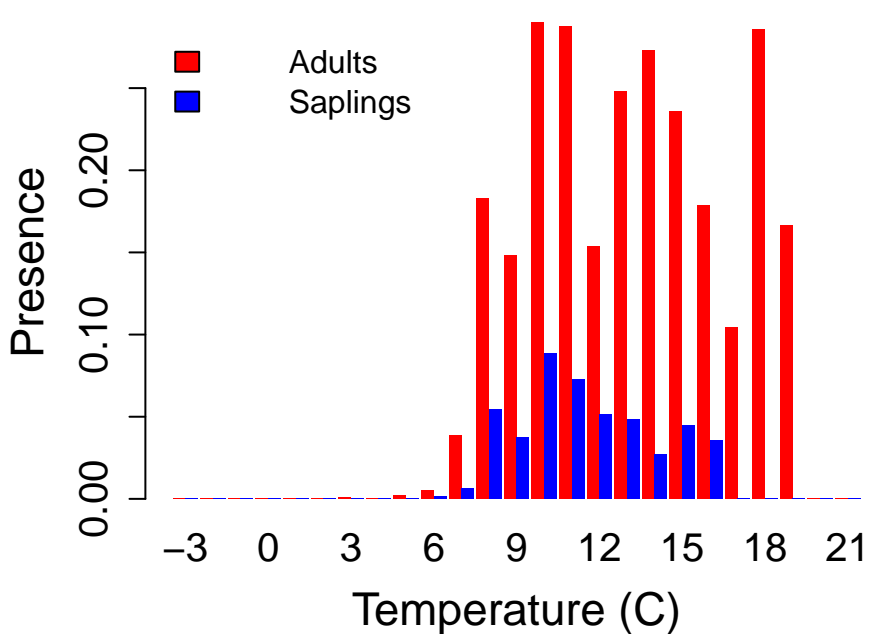
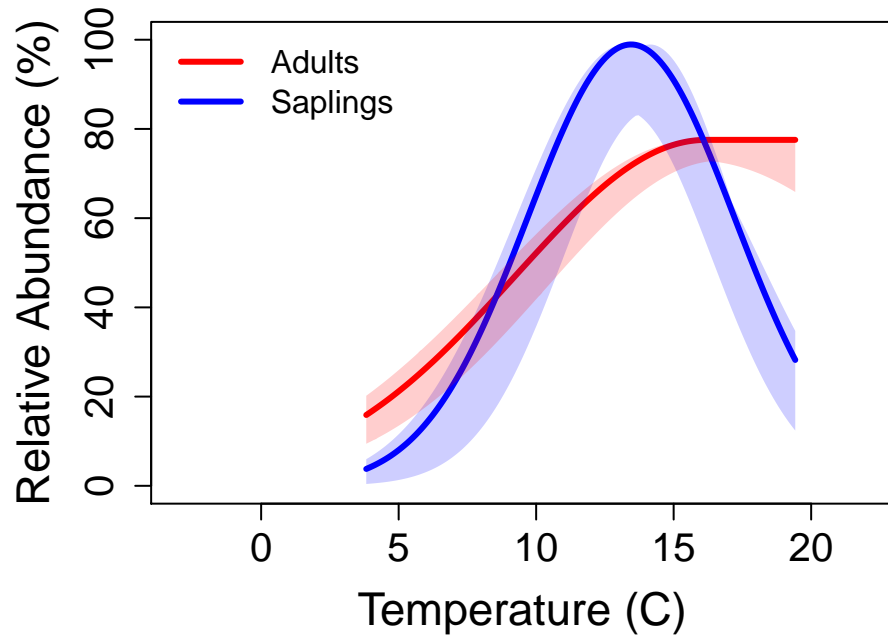
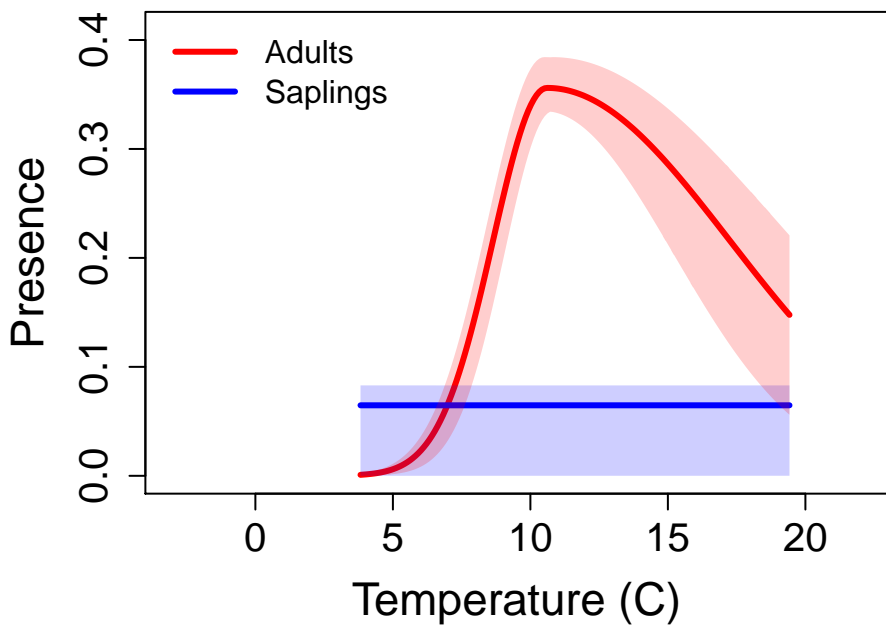
# Cercocarpus ledifolius – curleaf mountainmahogany



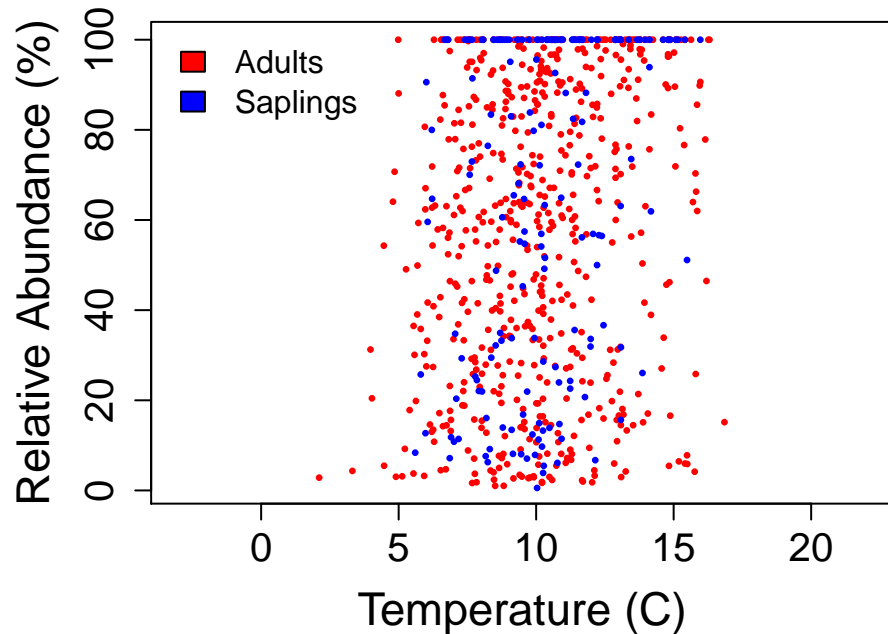
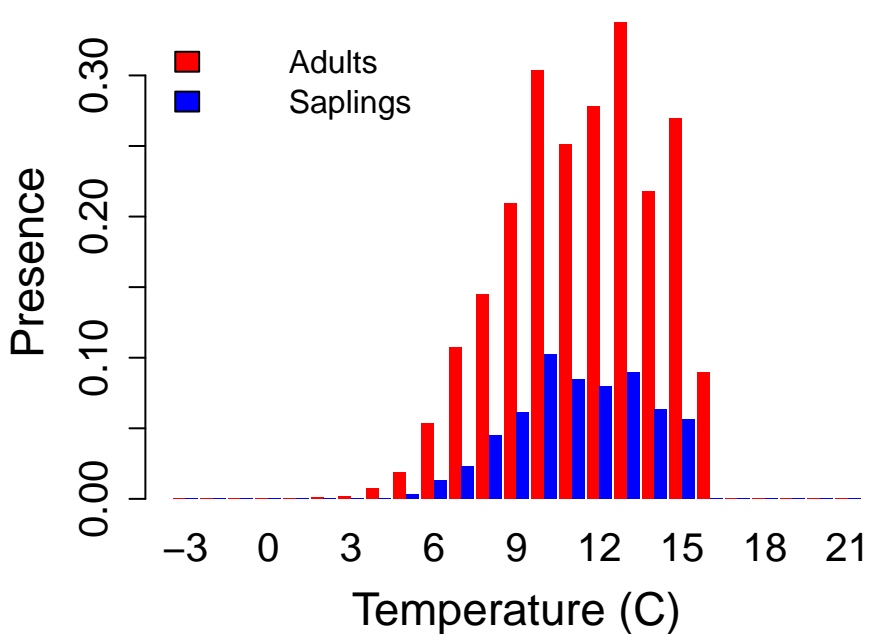
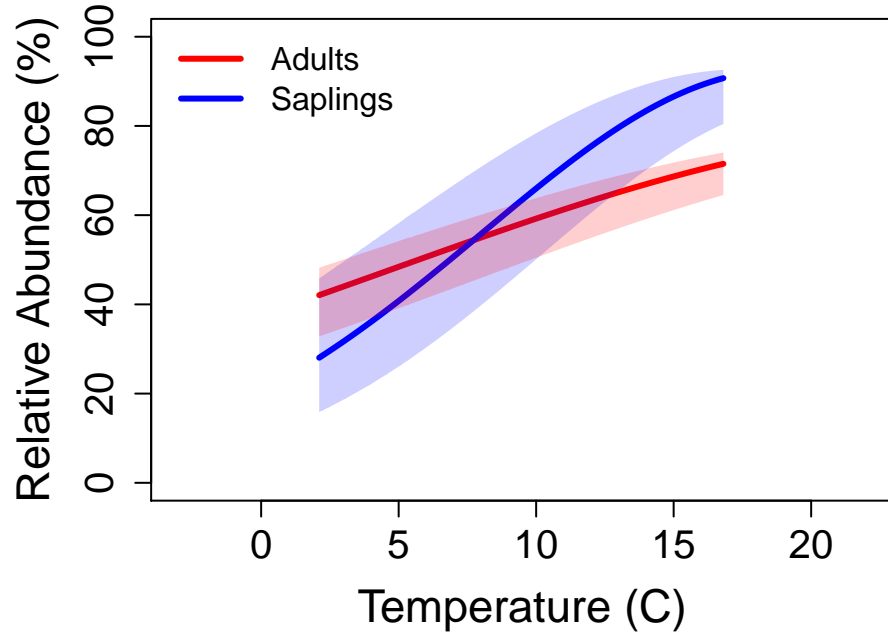
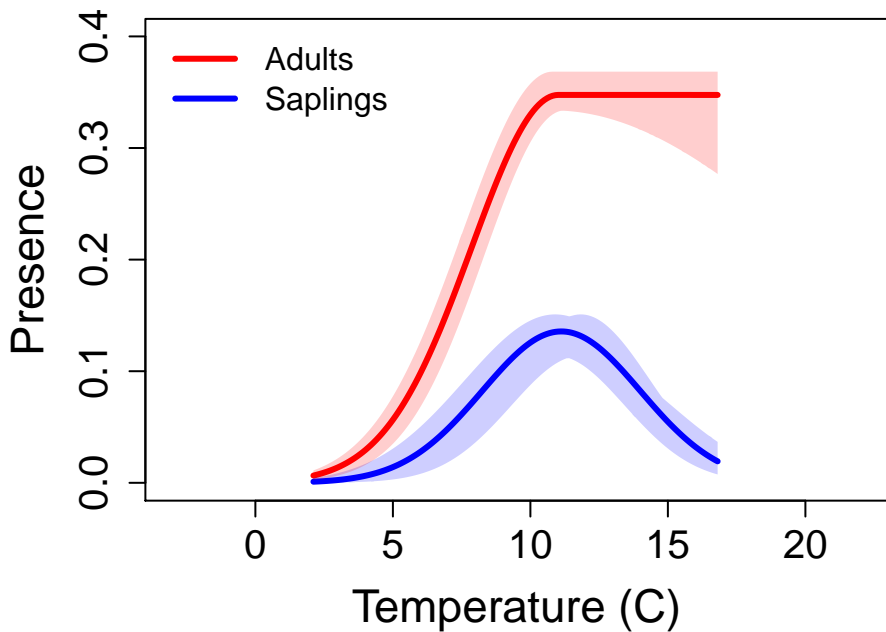
# Juniperus deppeana – alligator juniper



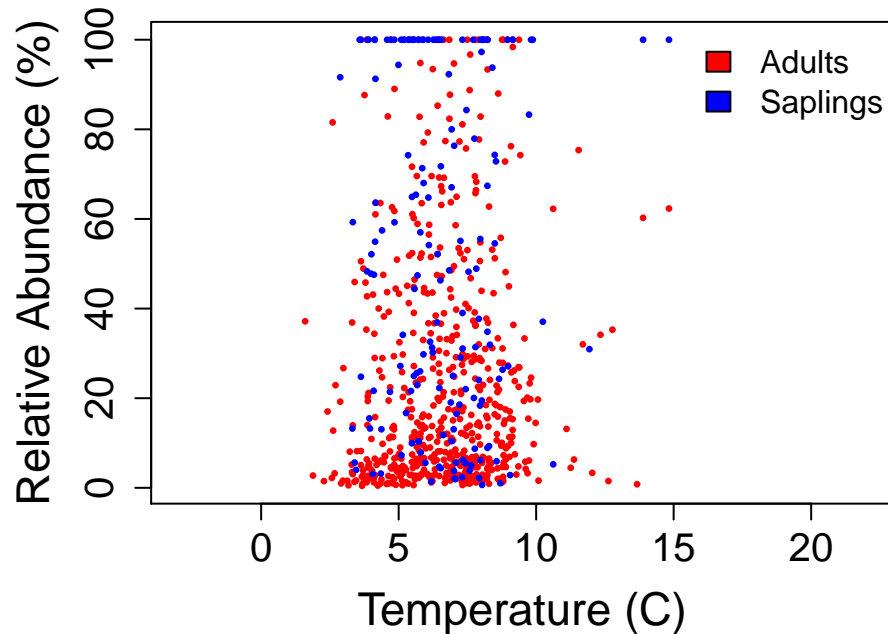
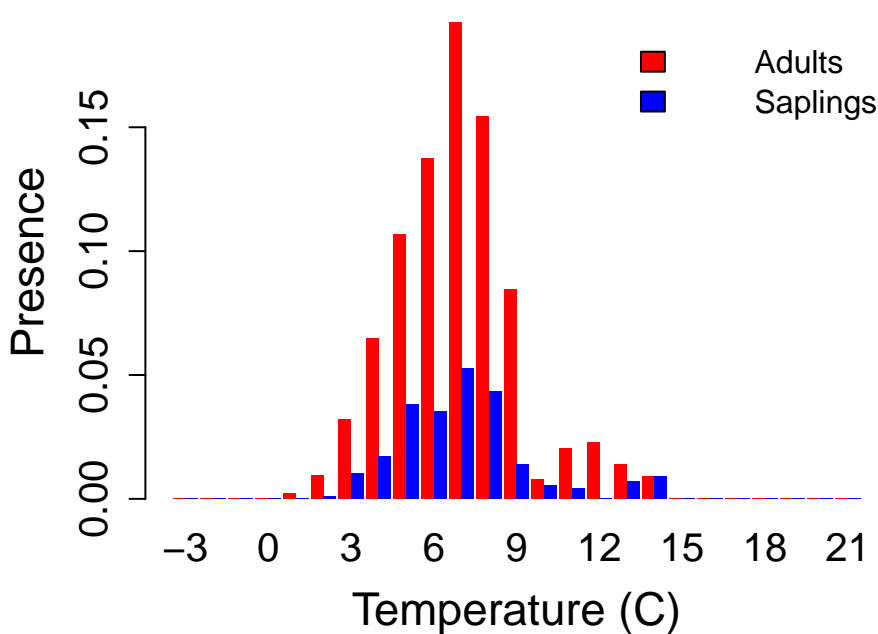
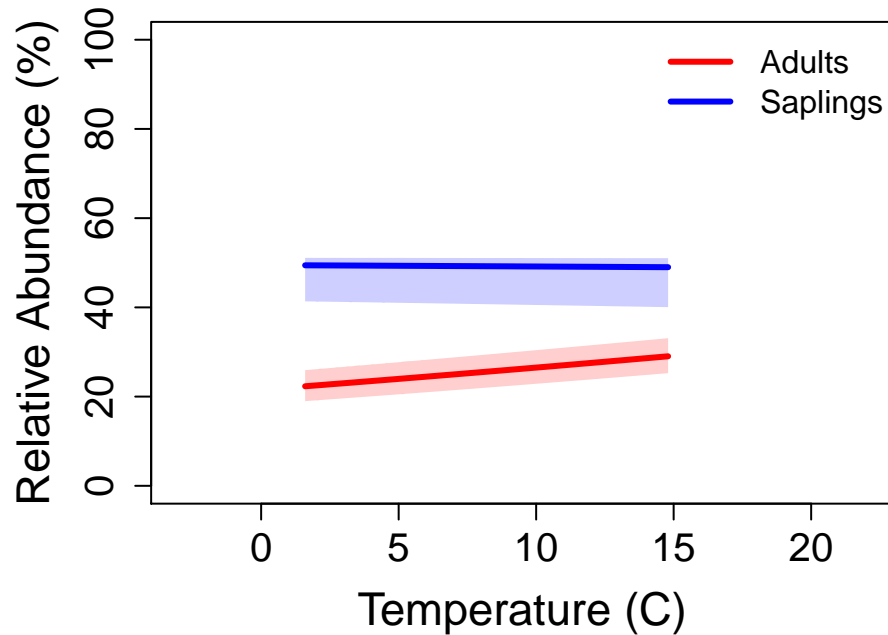
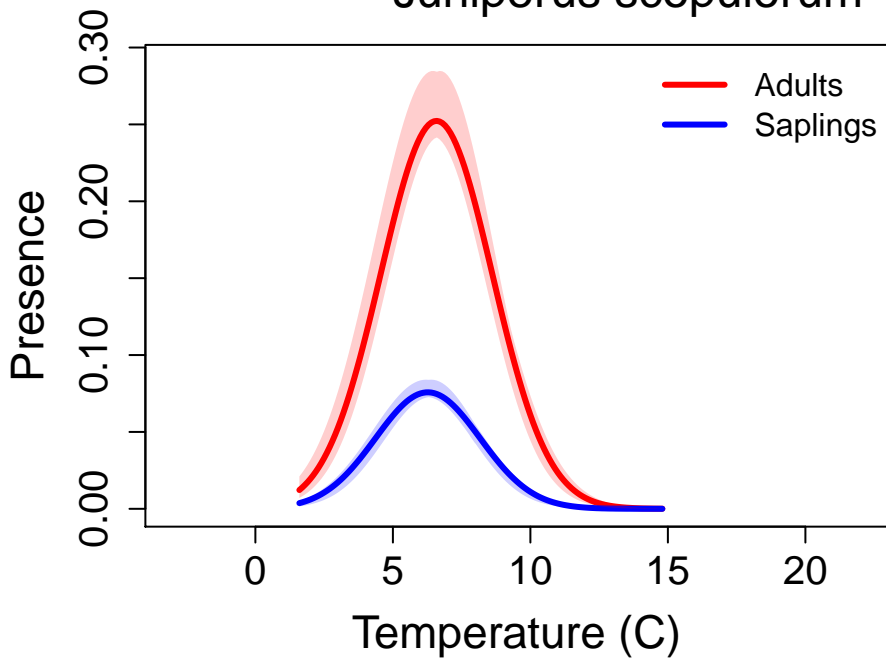
# Juniperus monosperma – oneseed juniper



# Juniperus osteosperma – Utah juniper

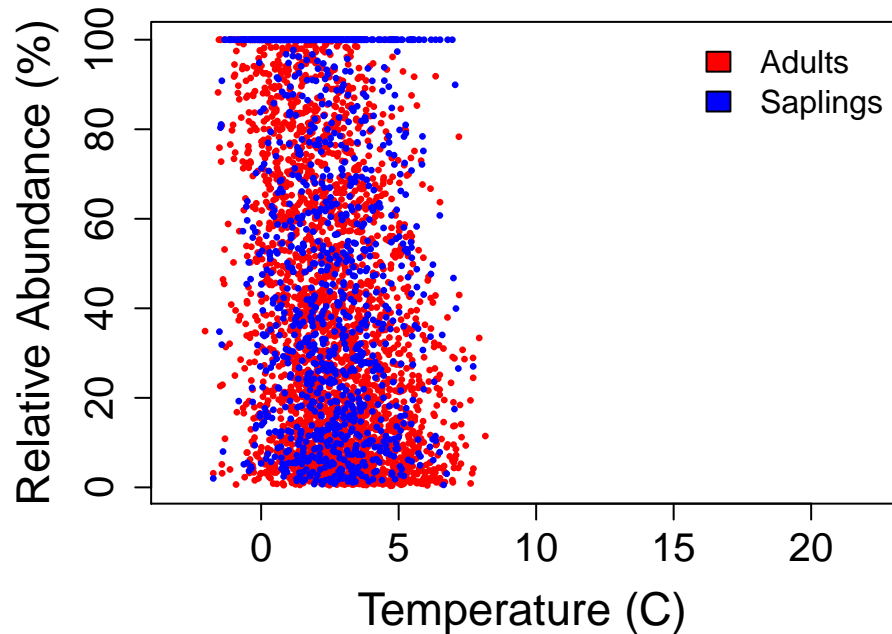
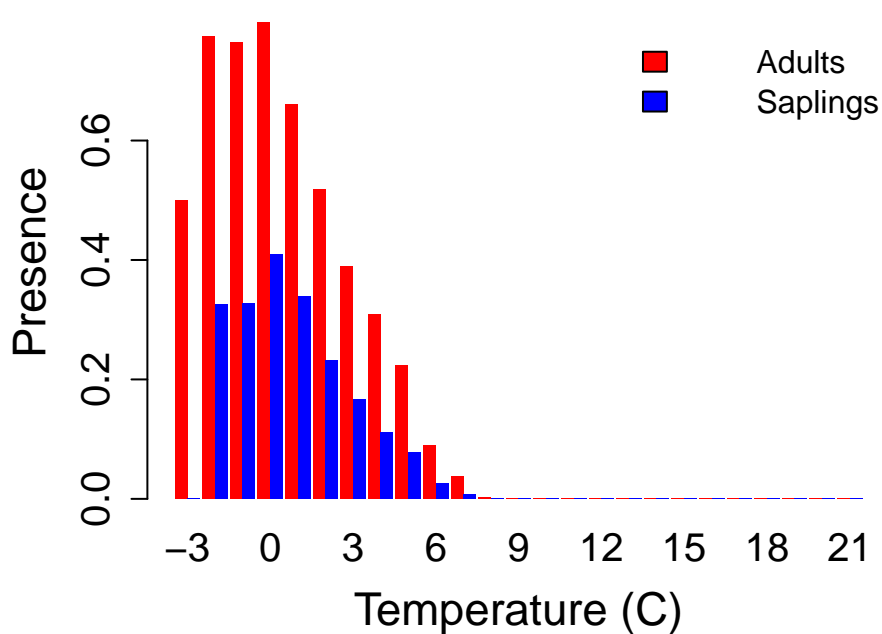
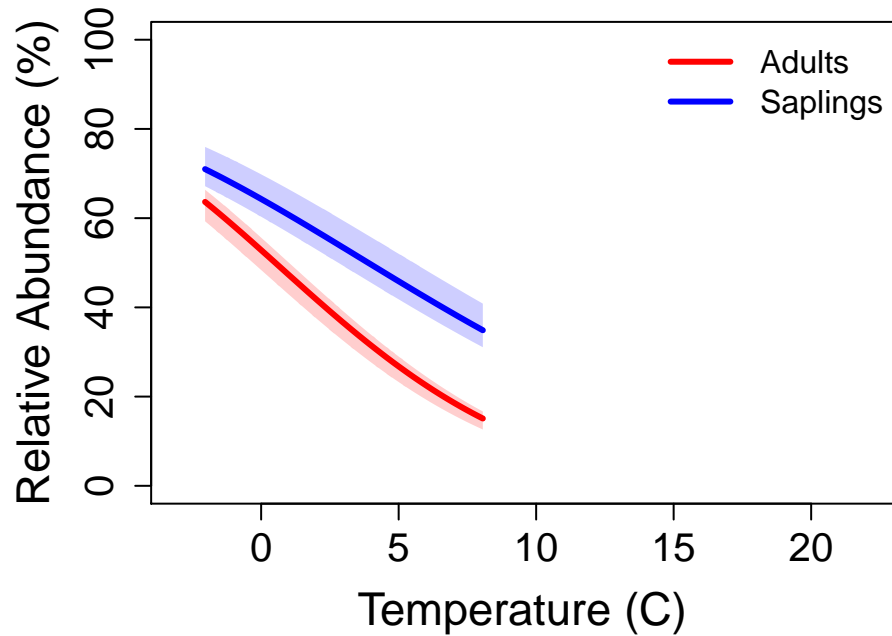
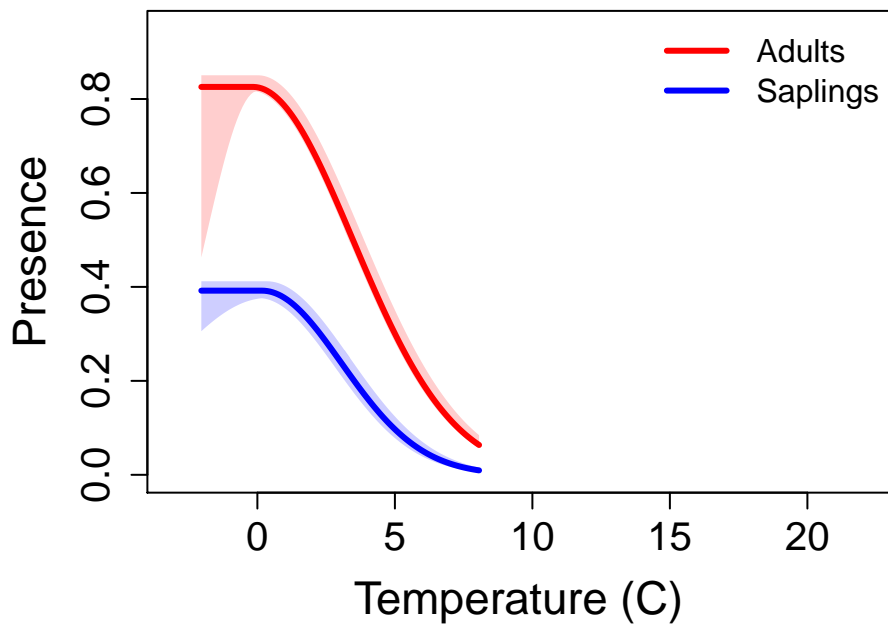


# Juniperus scopulorum – Rocky Mountain juniper

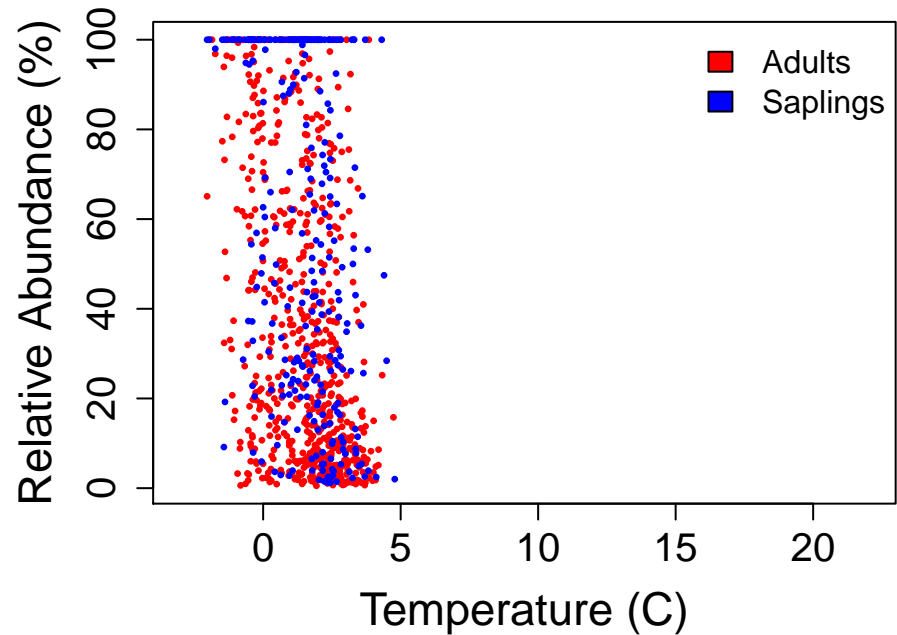
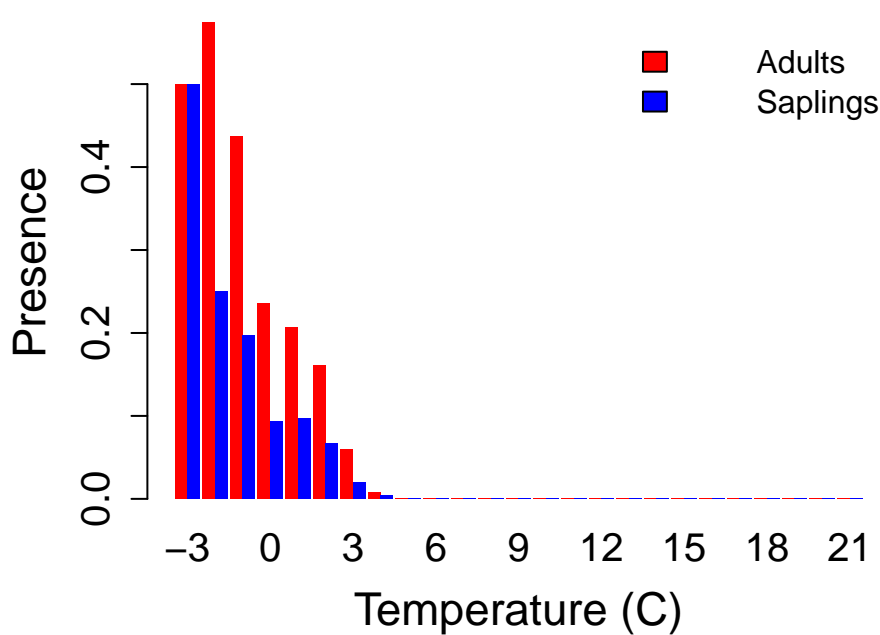
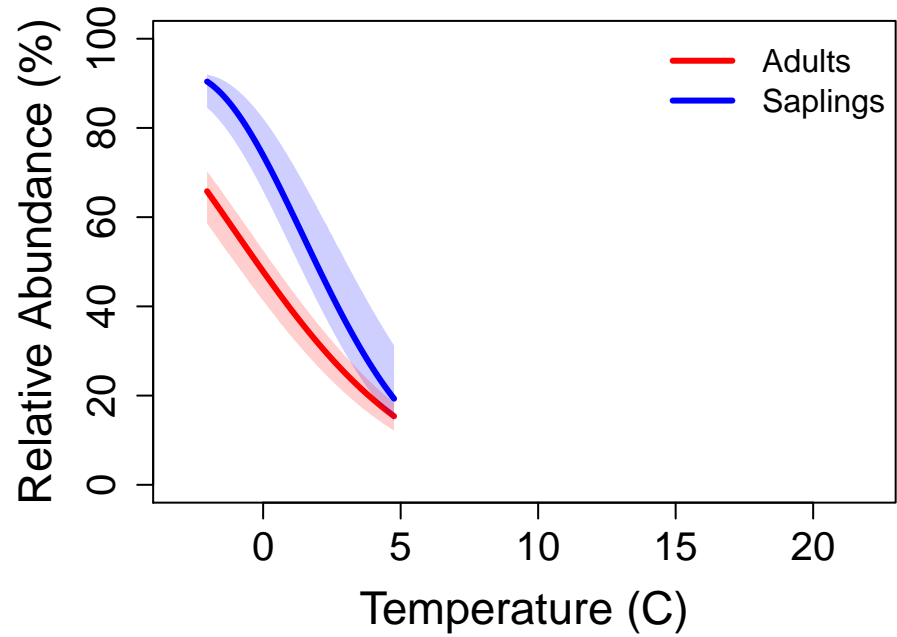
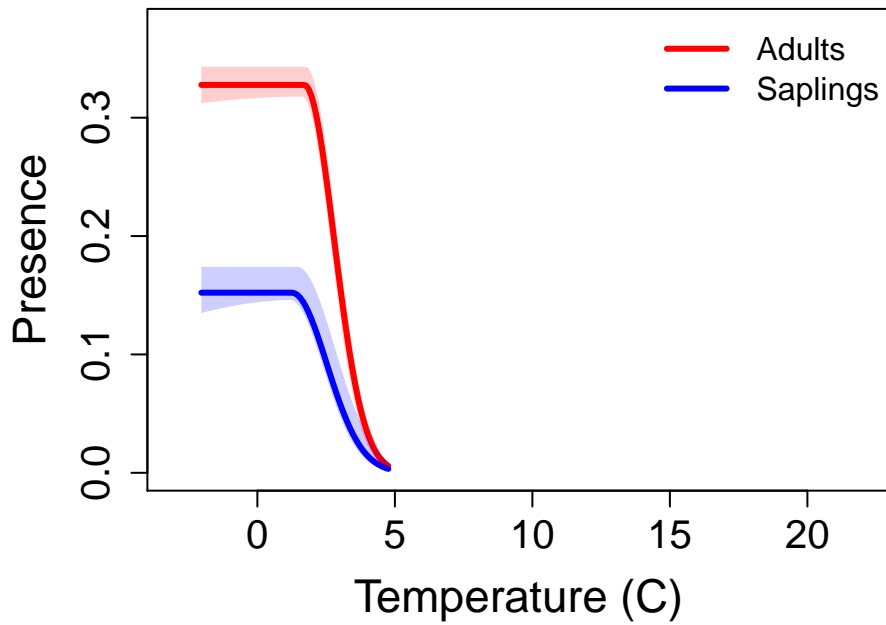




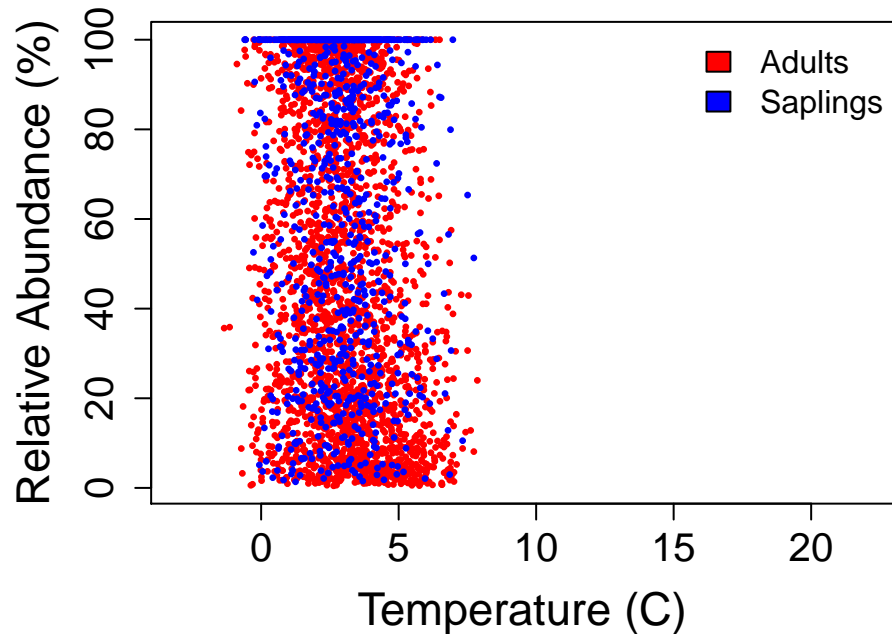
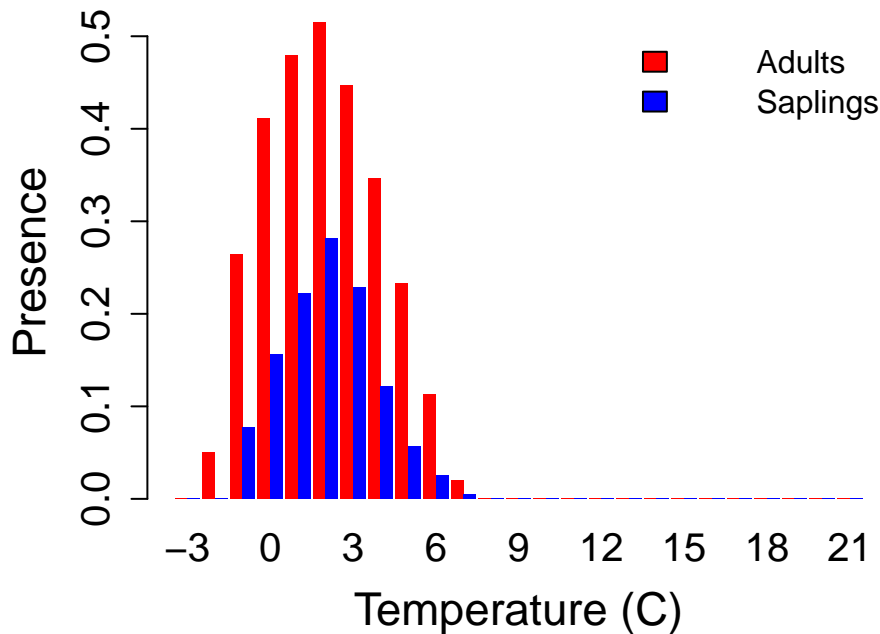
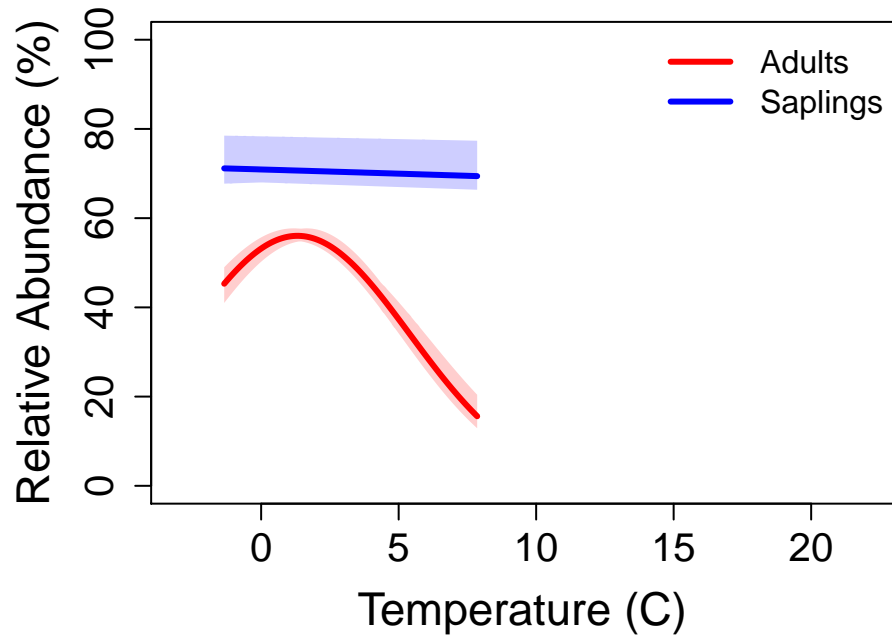
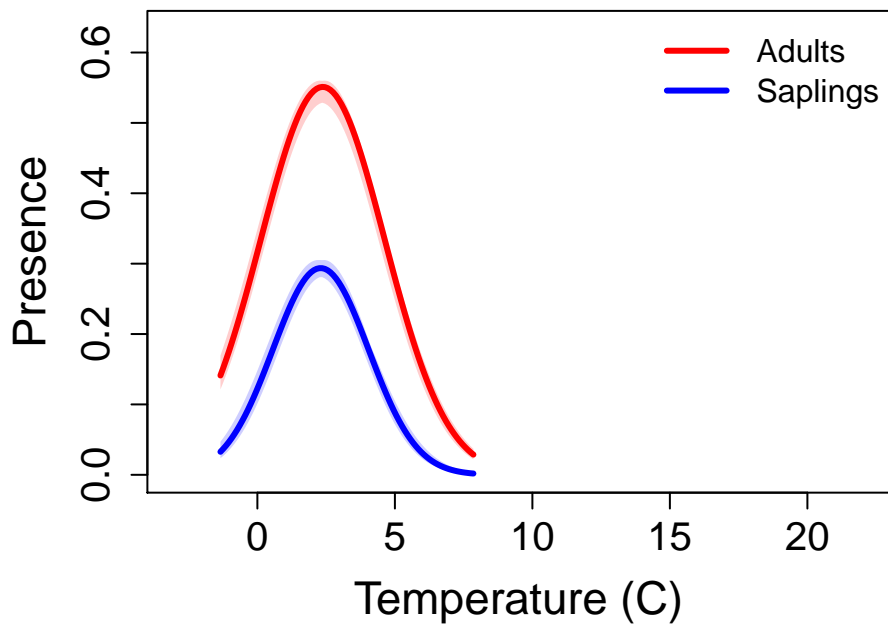
# *Picea engelmannii* – Engelmann spruce



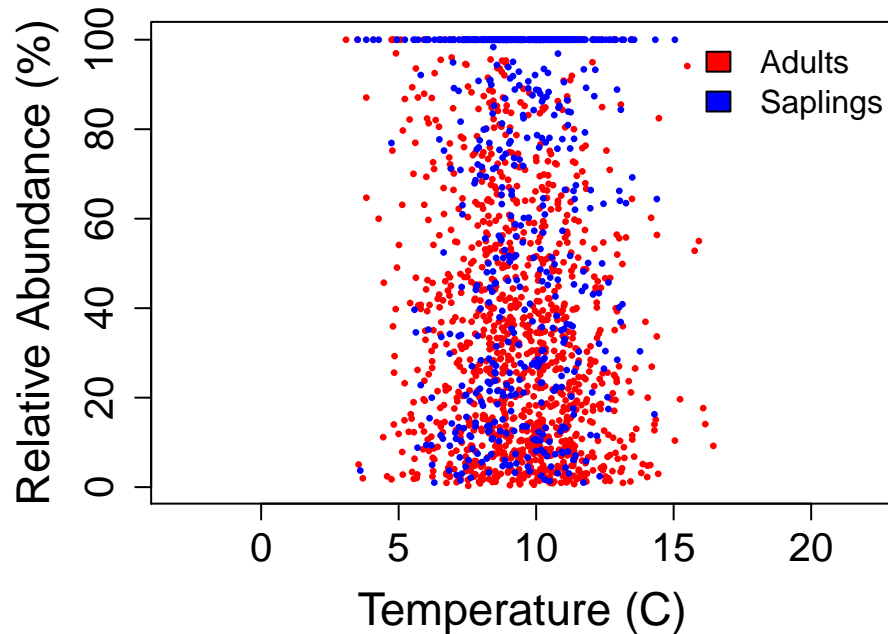
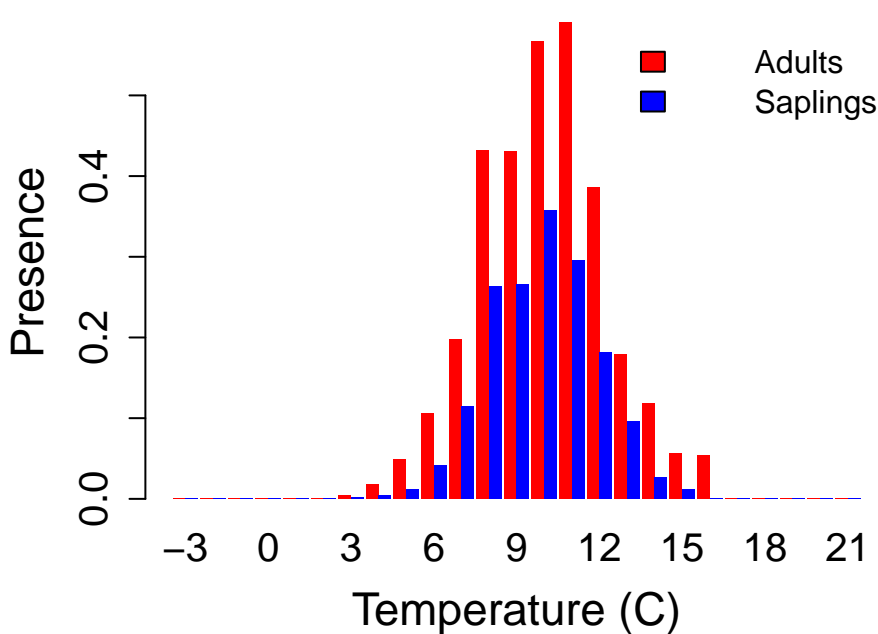
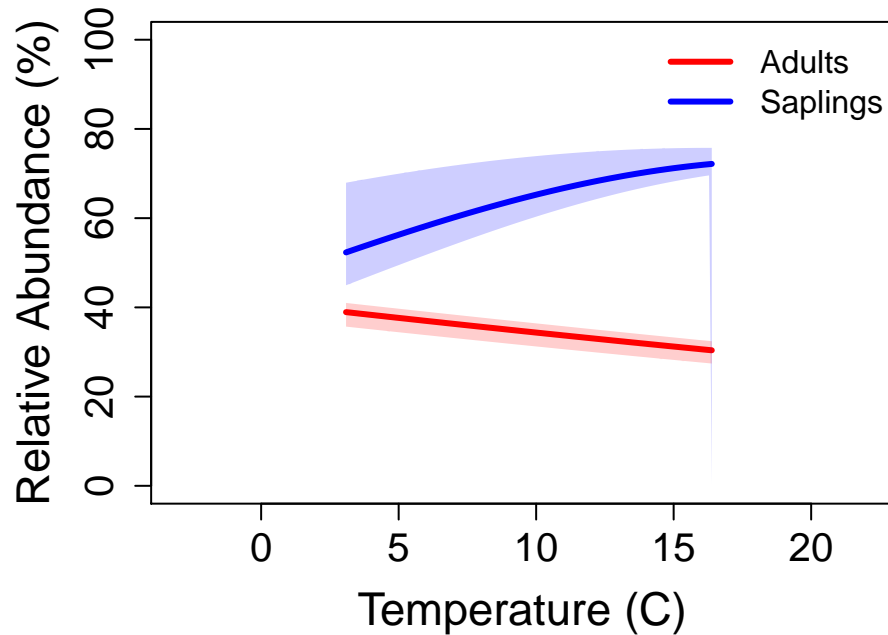
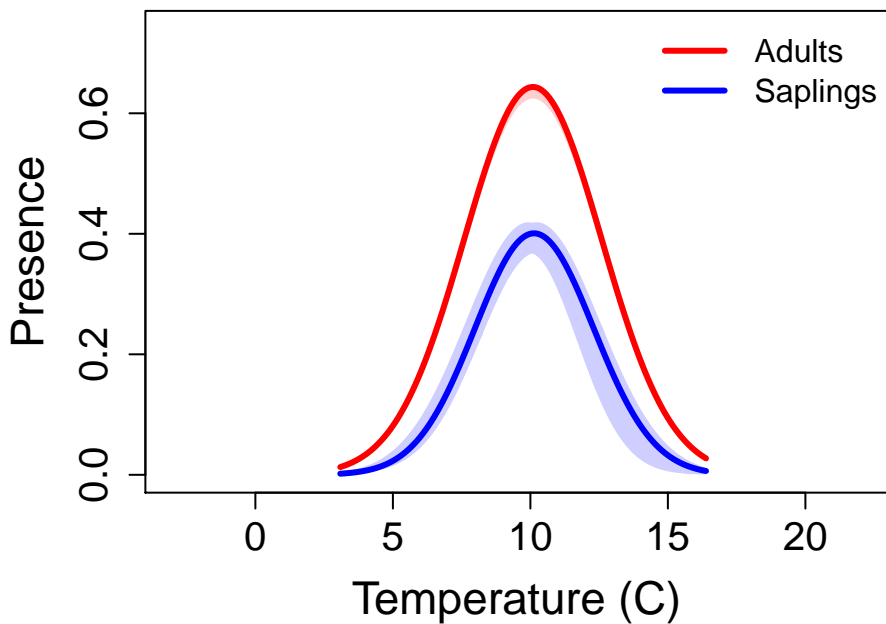
# Pinus albicaulis – whitebark pine



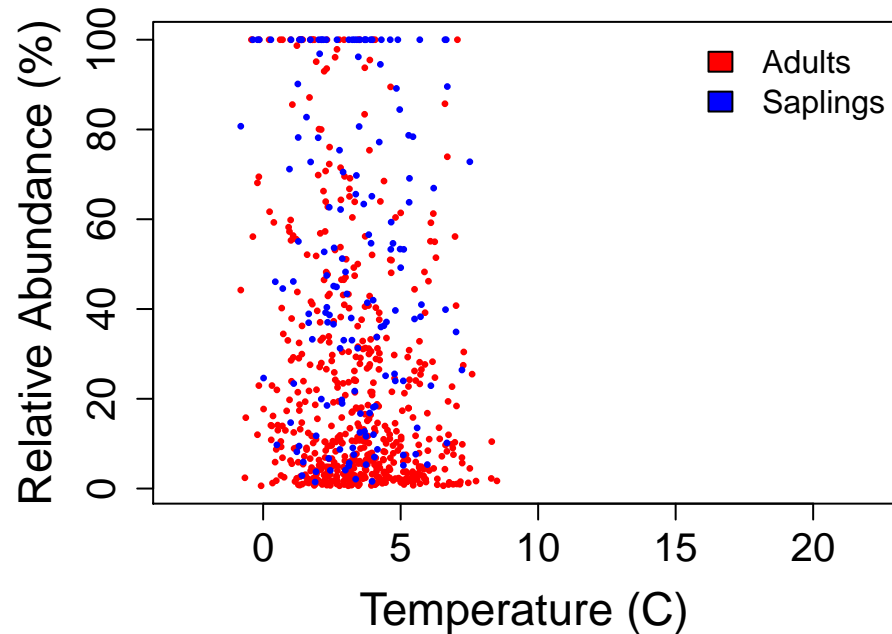
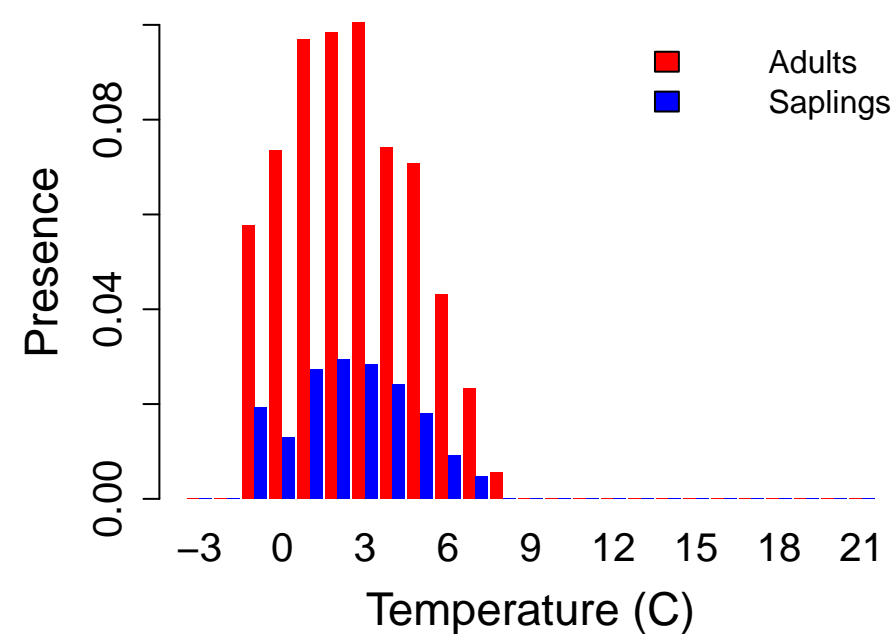
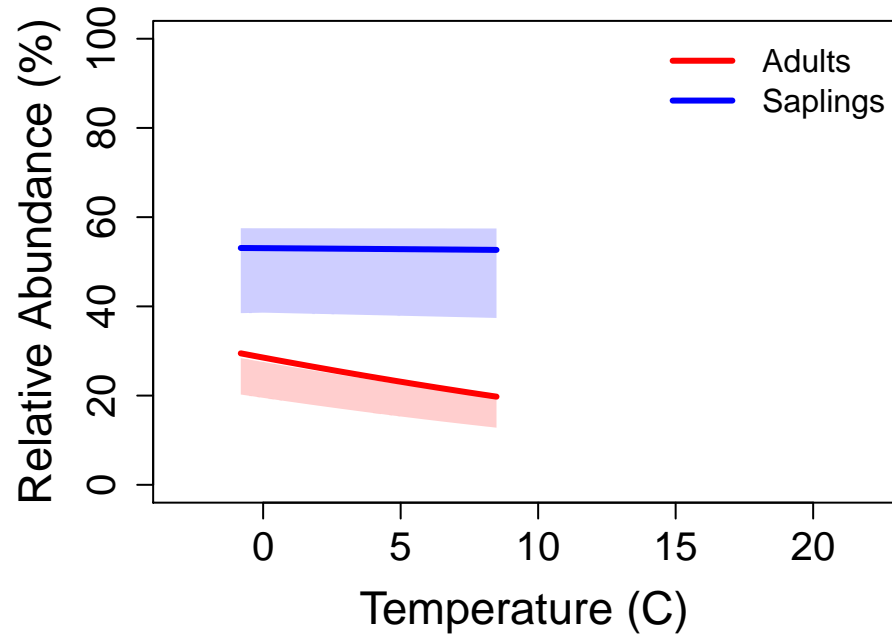
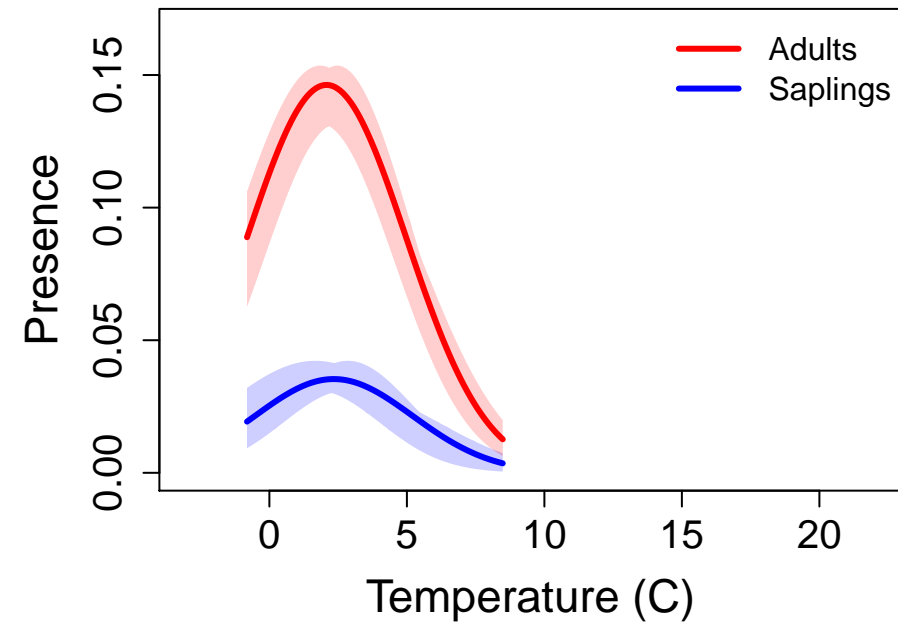
# Pinus contorta – lodgepole pine



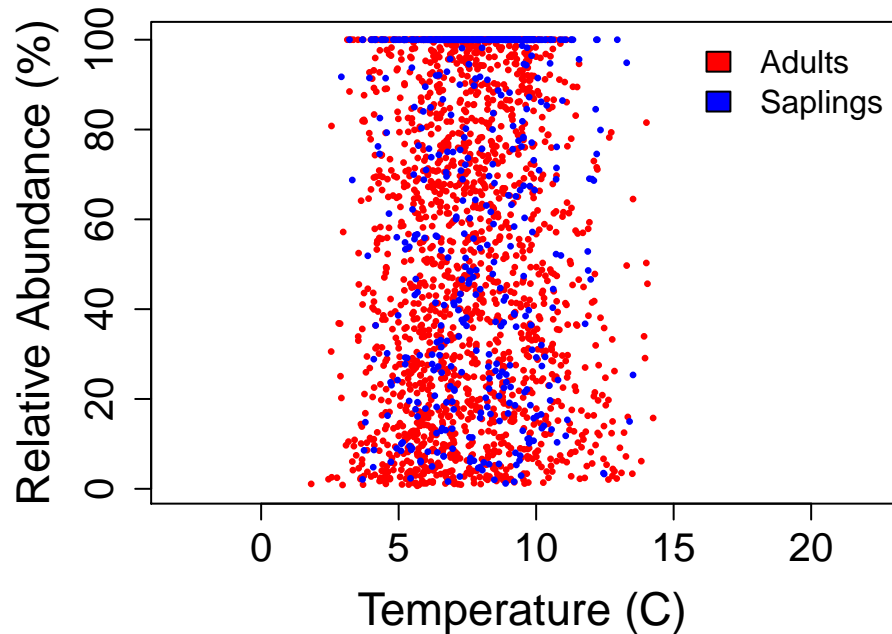
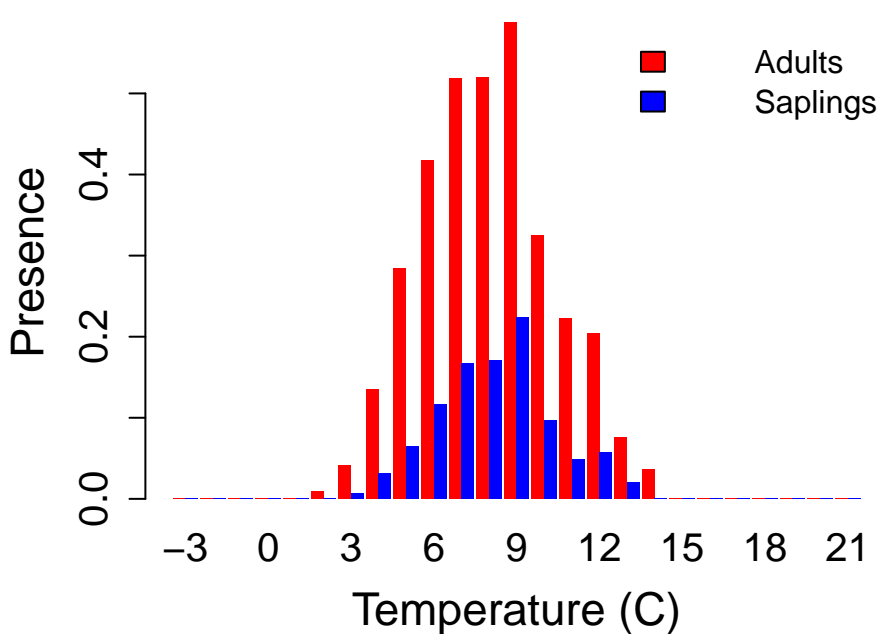
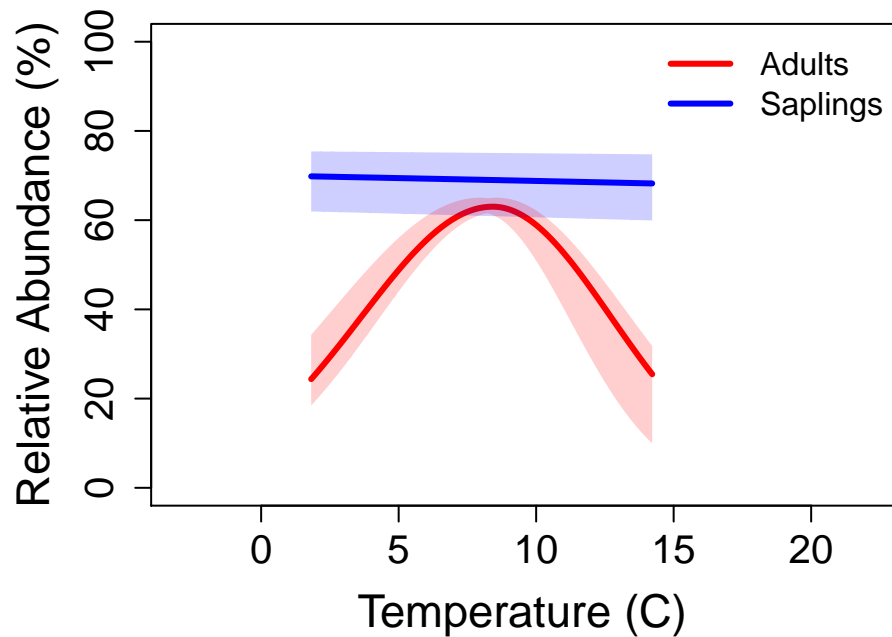
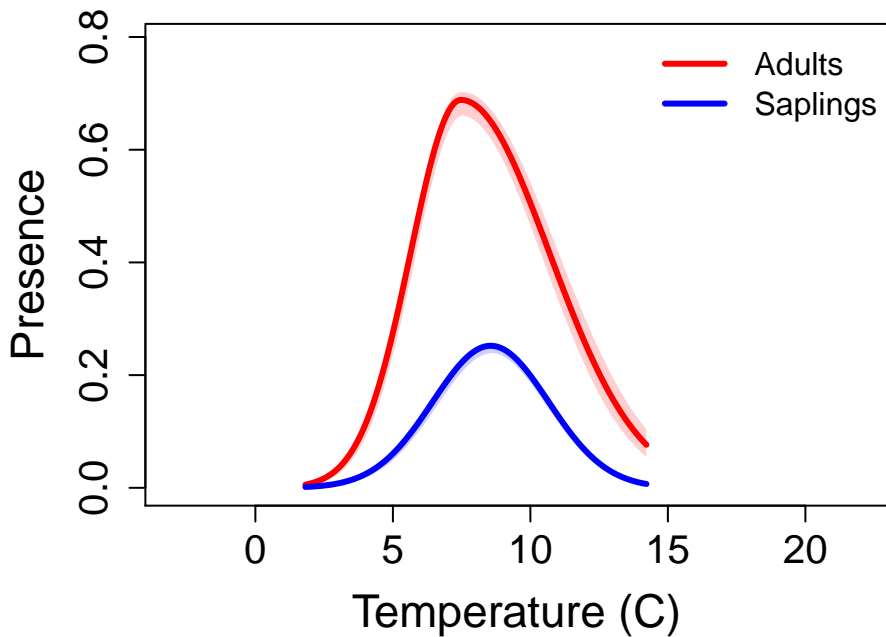
# Pinus edulis – Common or two-needle Pinyon



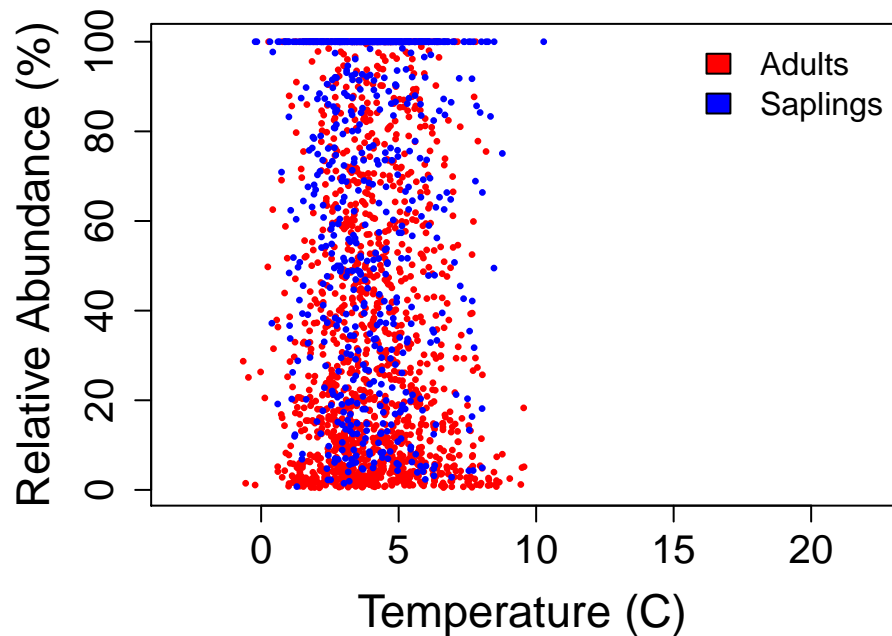
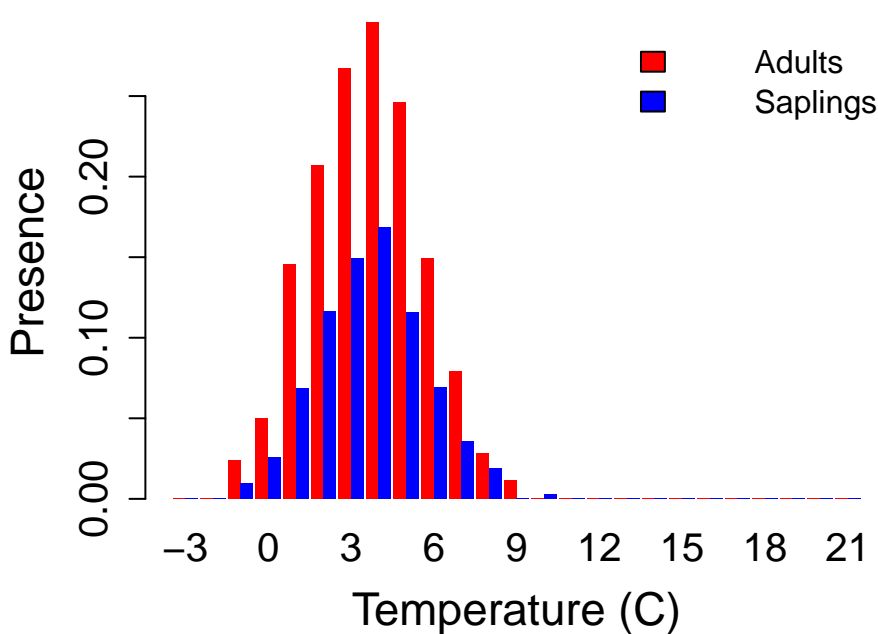
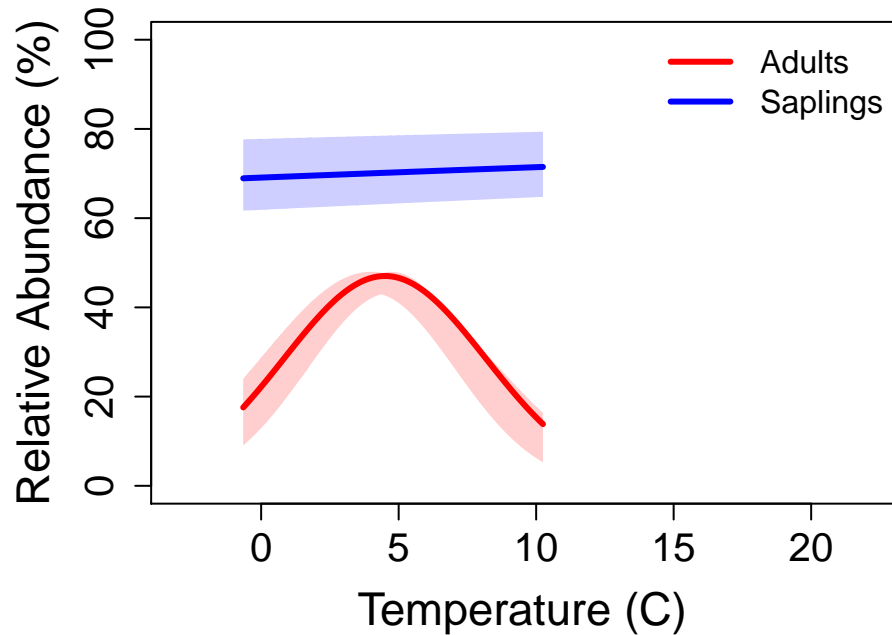
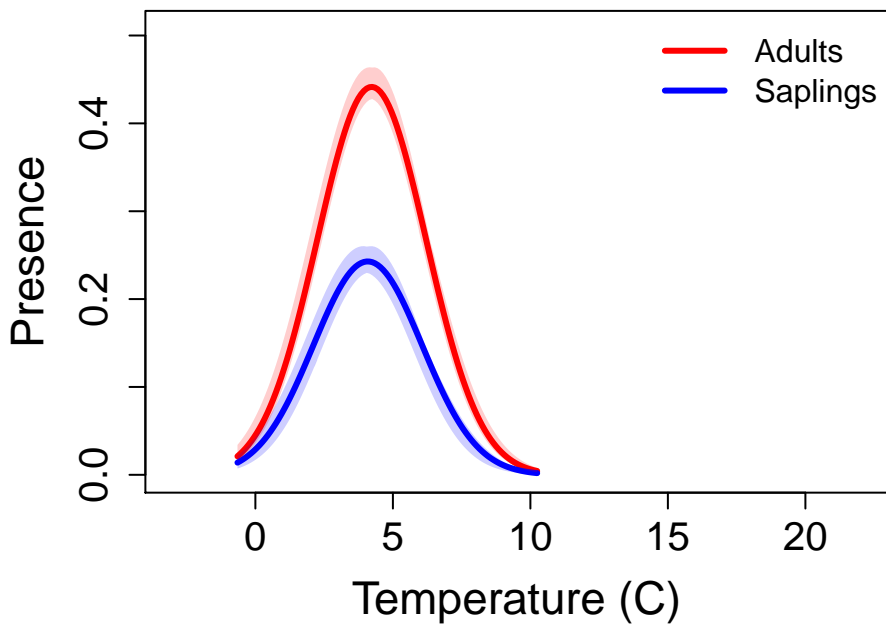
# Pinus flexilis – limber pine



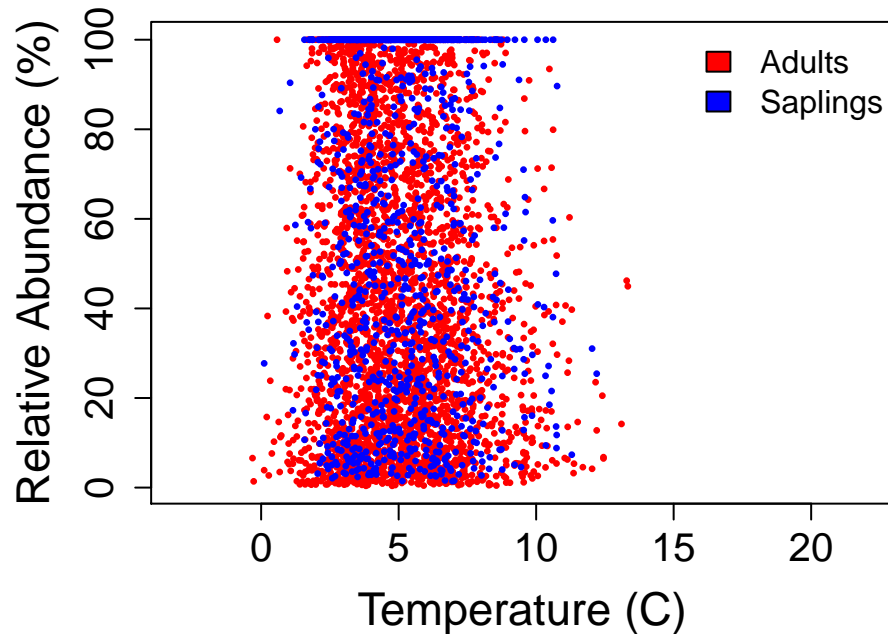
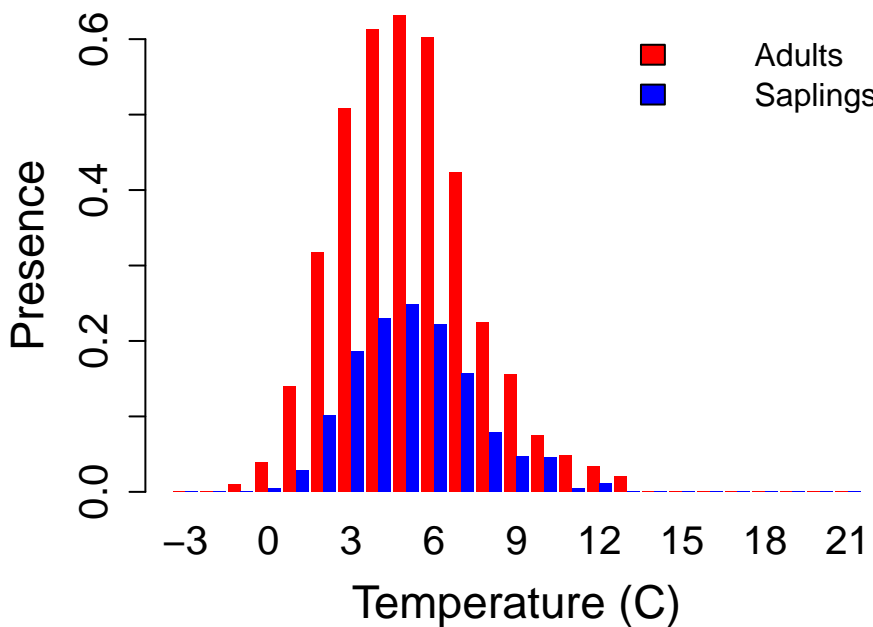
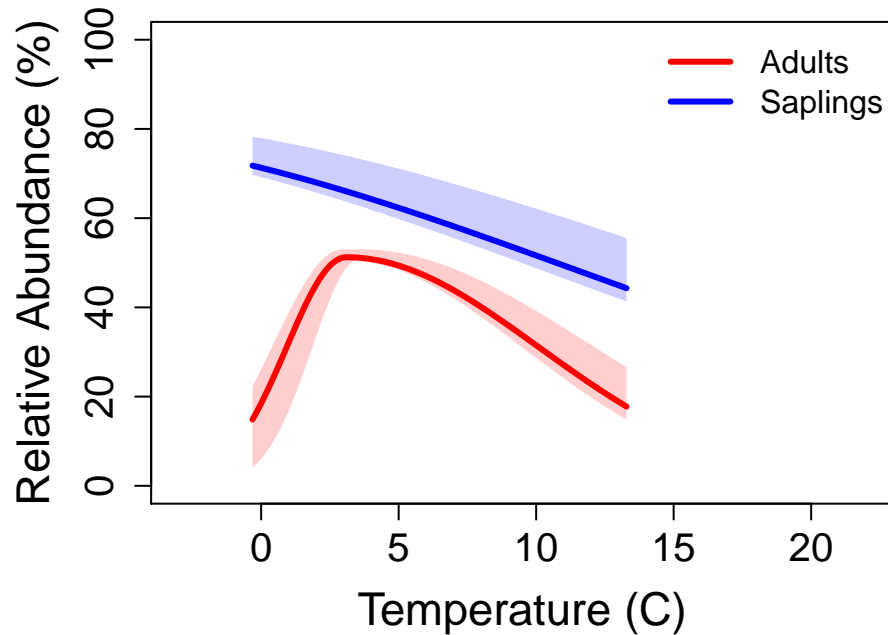
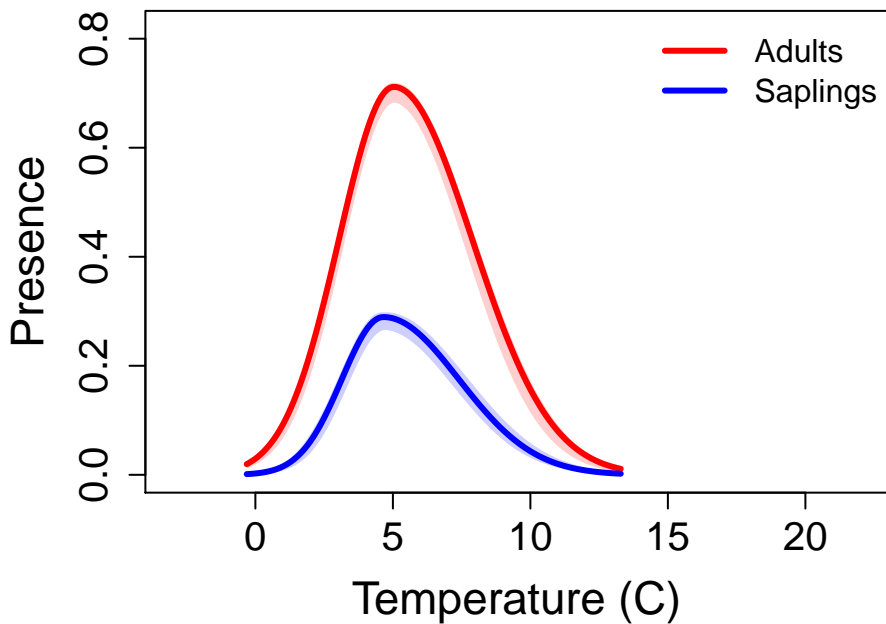
# Pinus ponderosa – ponderosa pine



# Populus tremuloides – quaking aspen

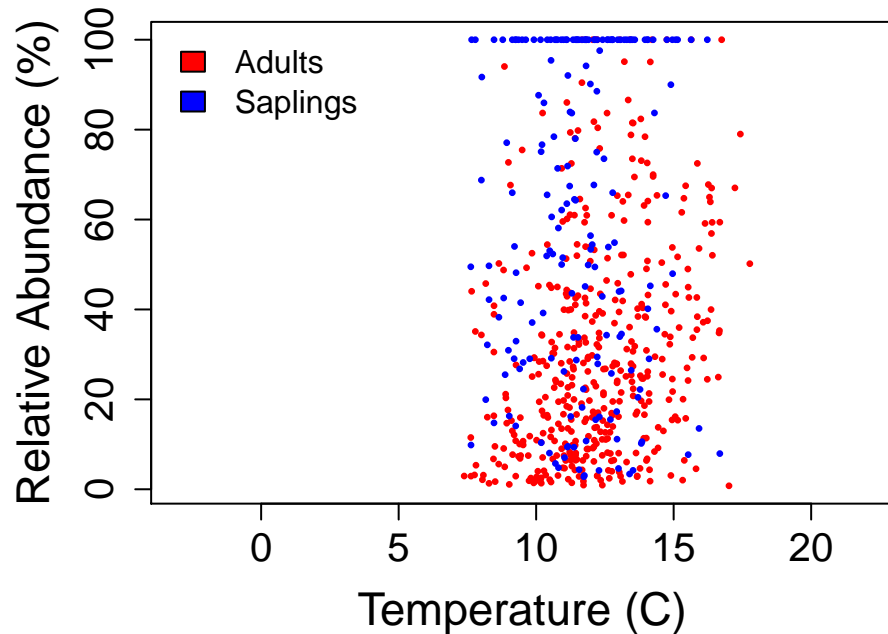
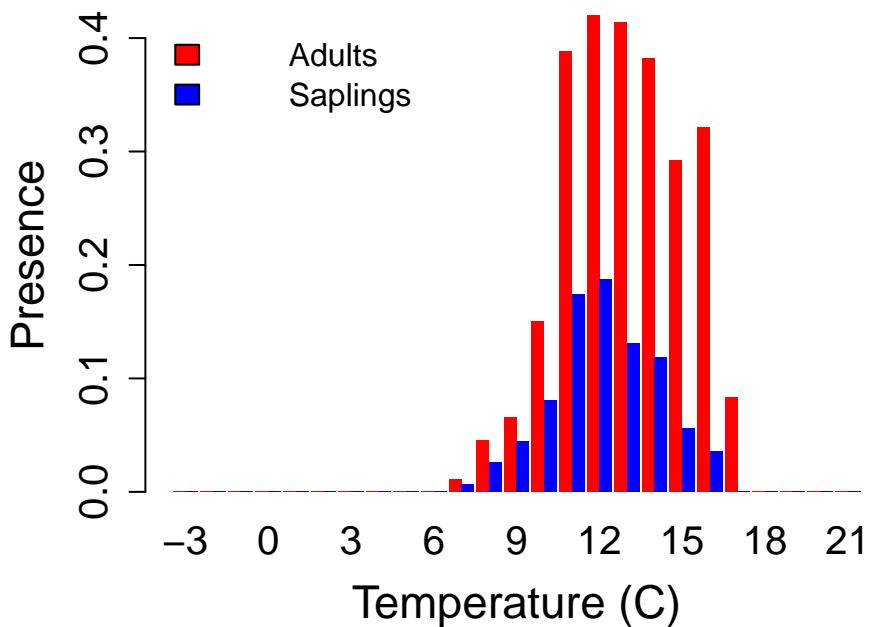
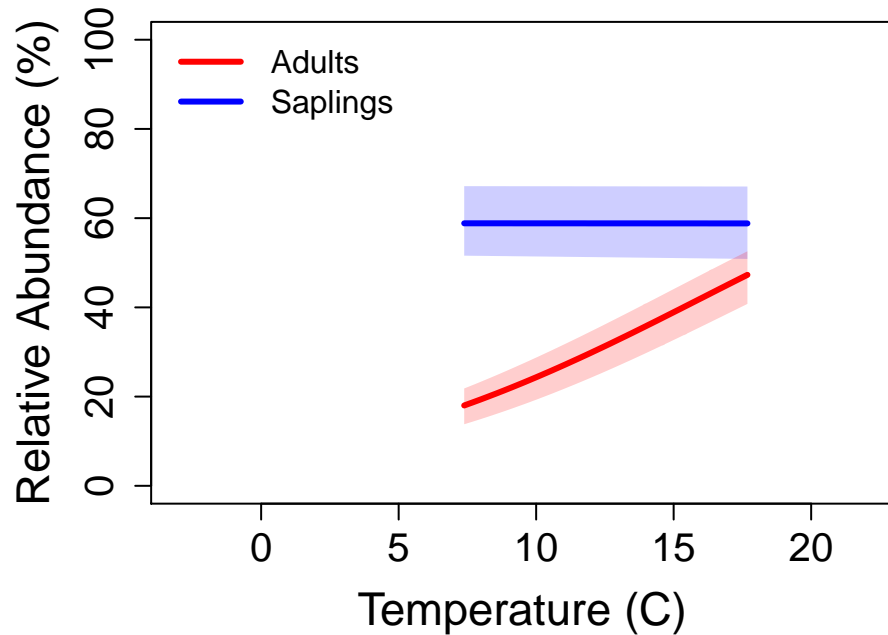
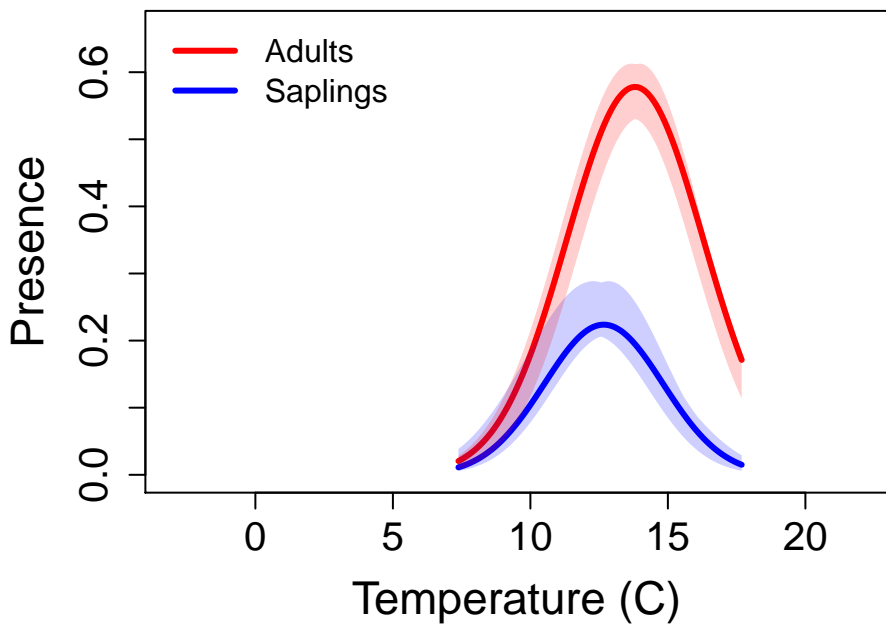


# *Pseudotsuga menziesii* – Douglas–fir

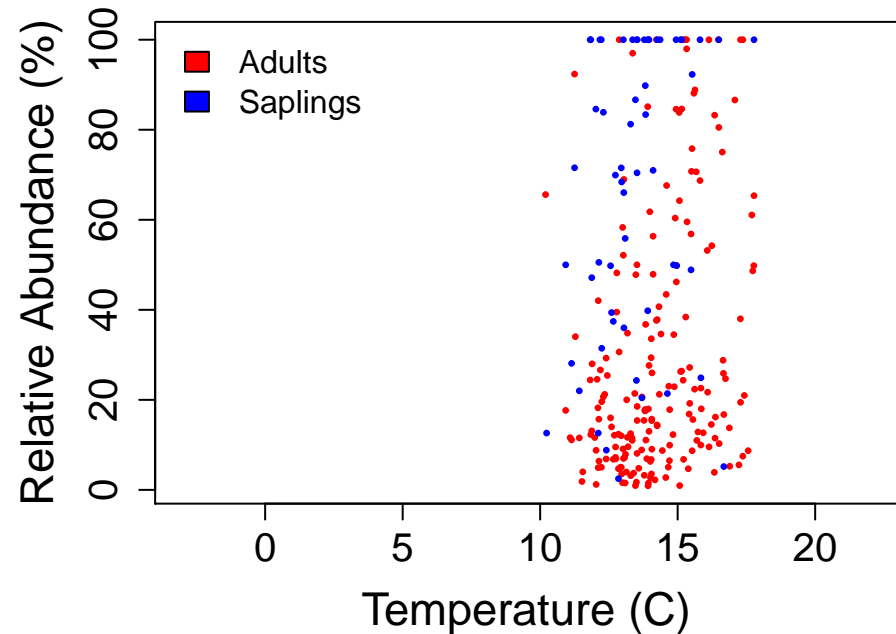
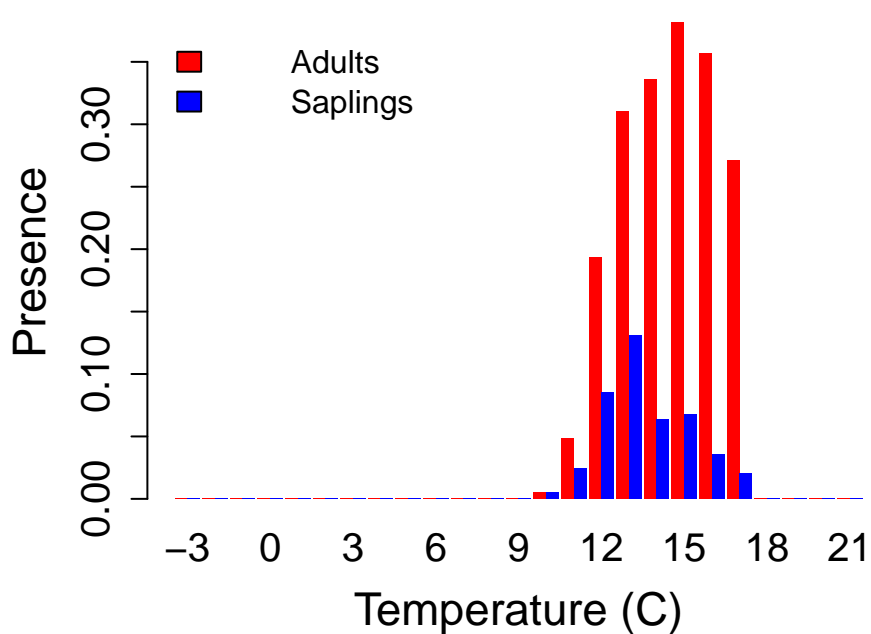
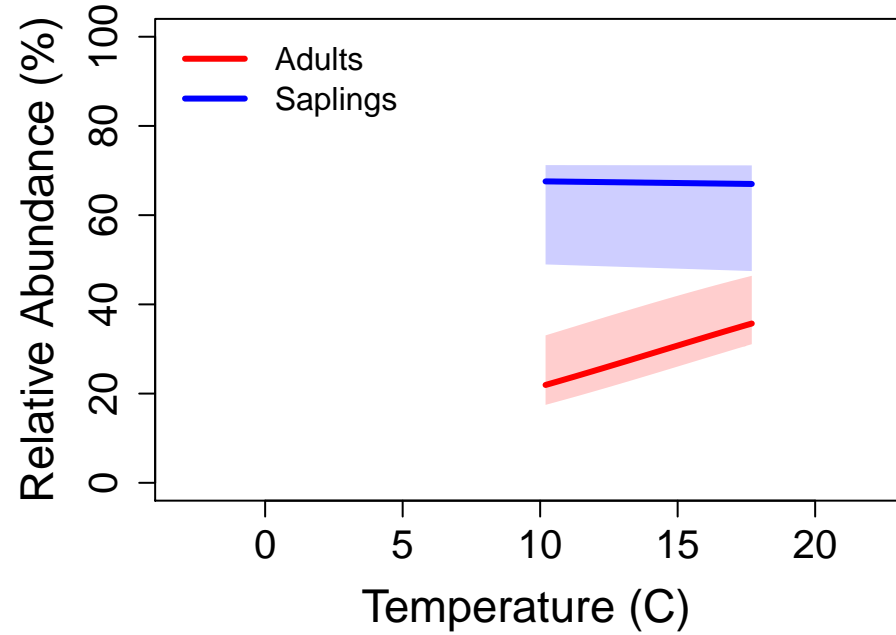
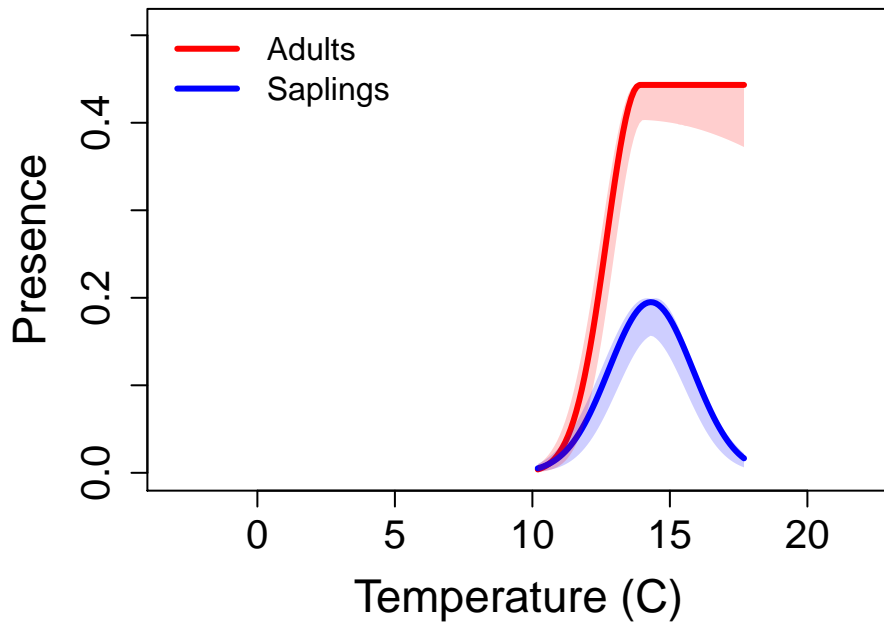




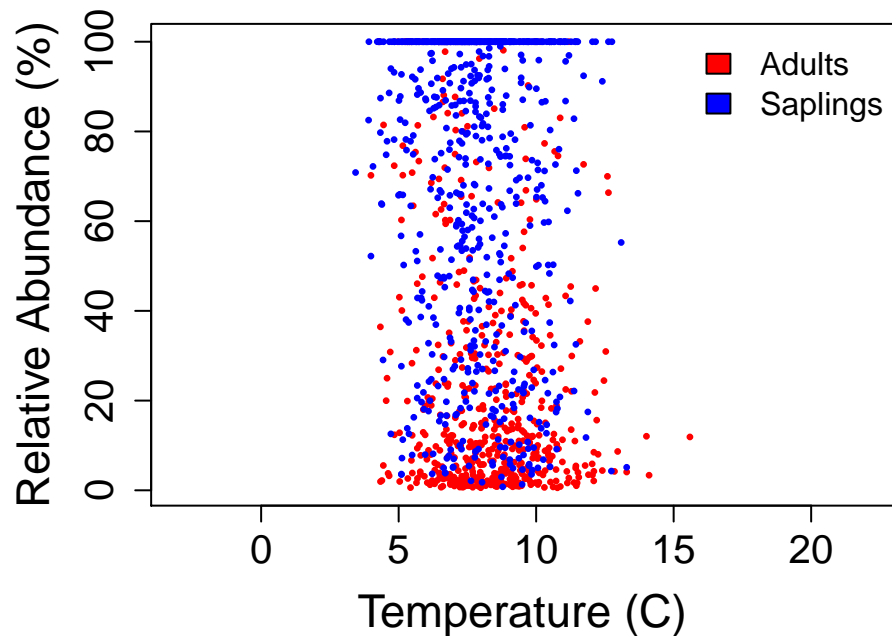
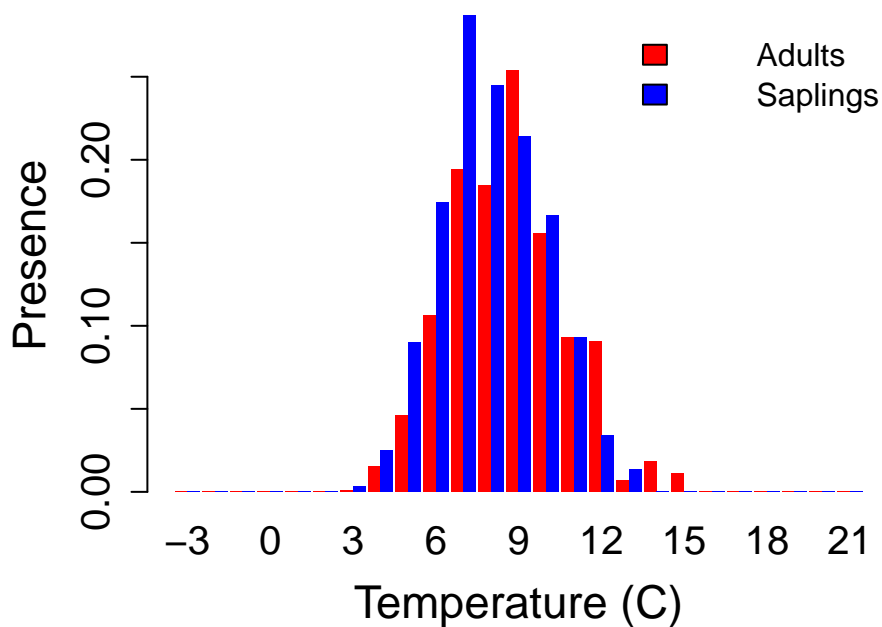
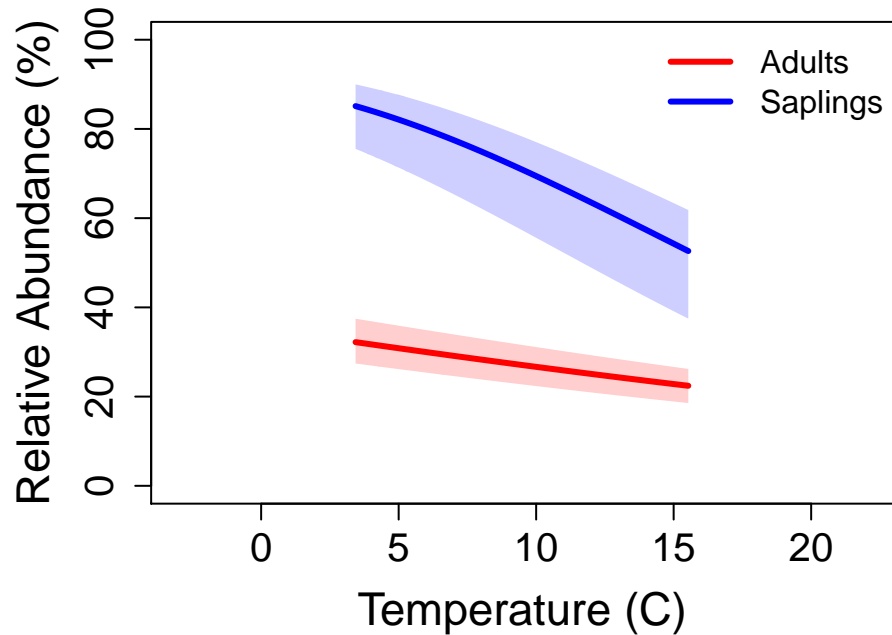
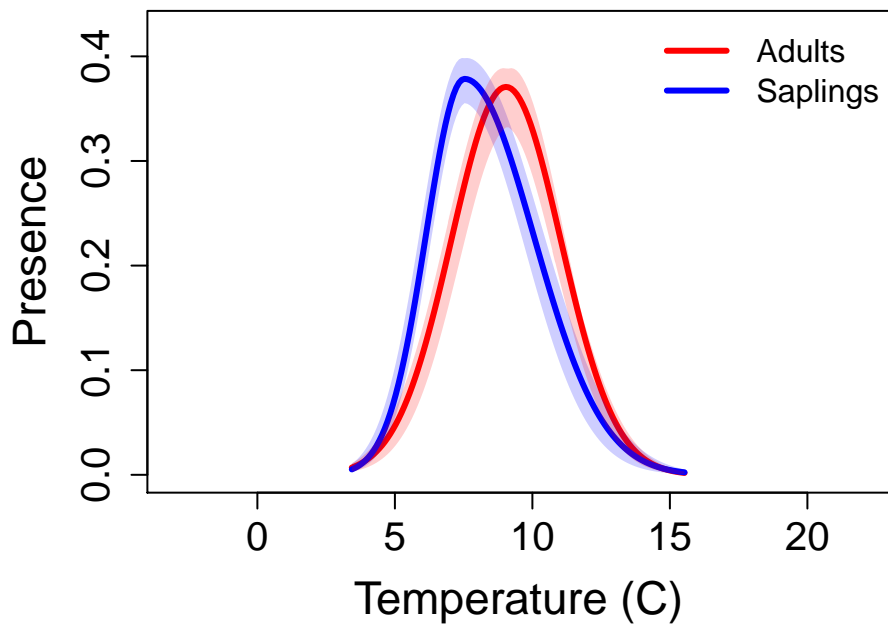
# Quercus arizonica – Arizona white oak



# Quercus emoryi - Emory oak



# Quercus gambelii – Gambel oak



# **Ecosphere**

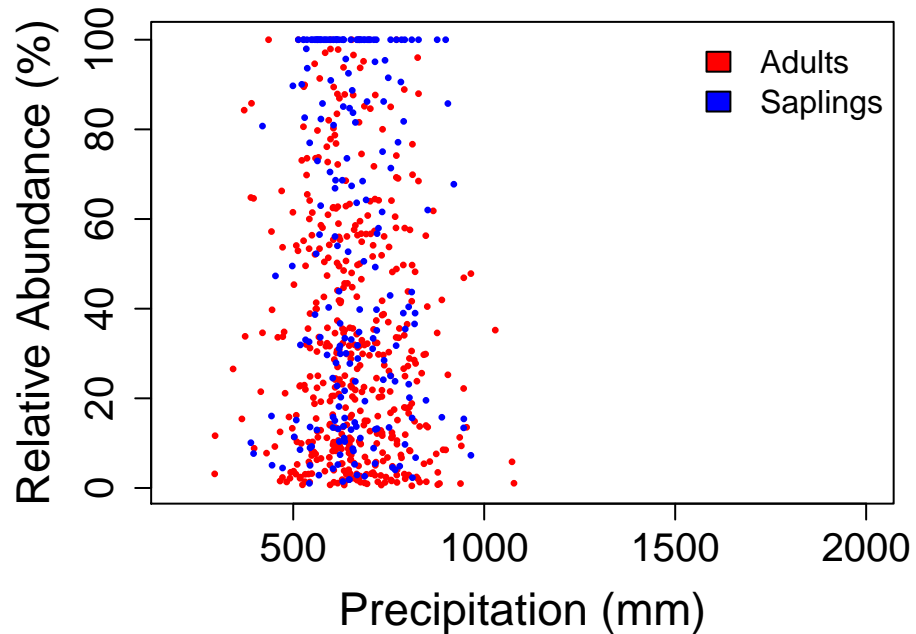
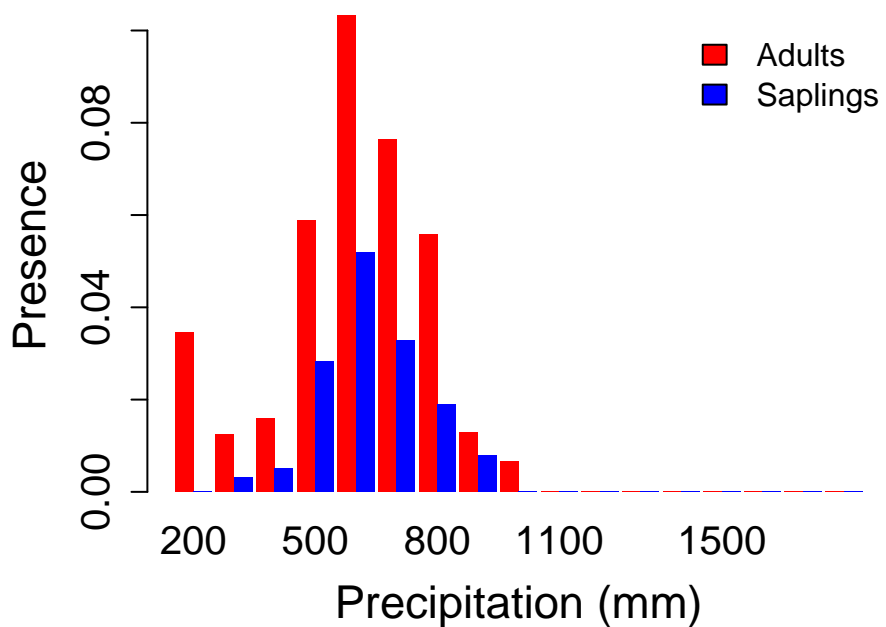
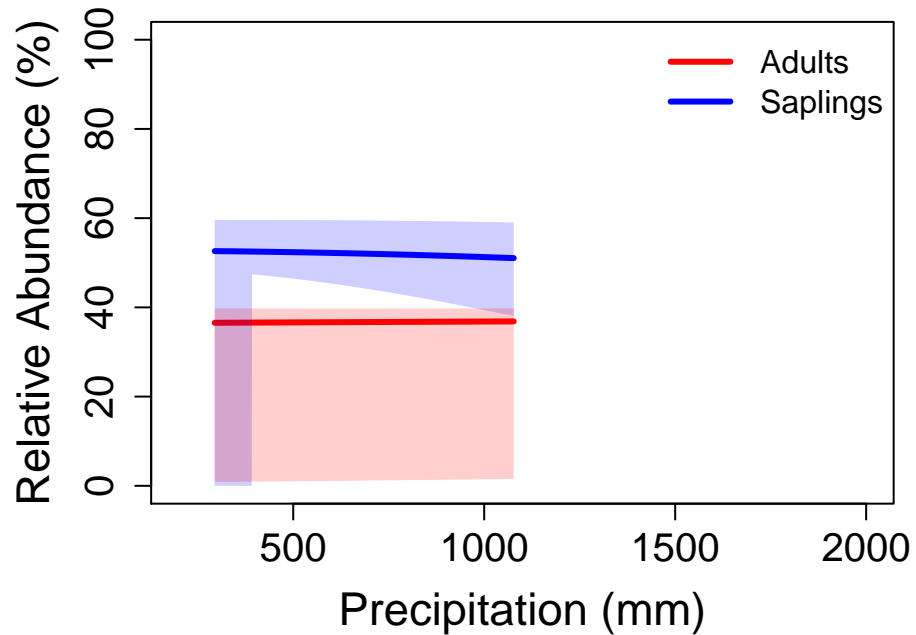
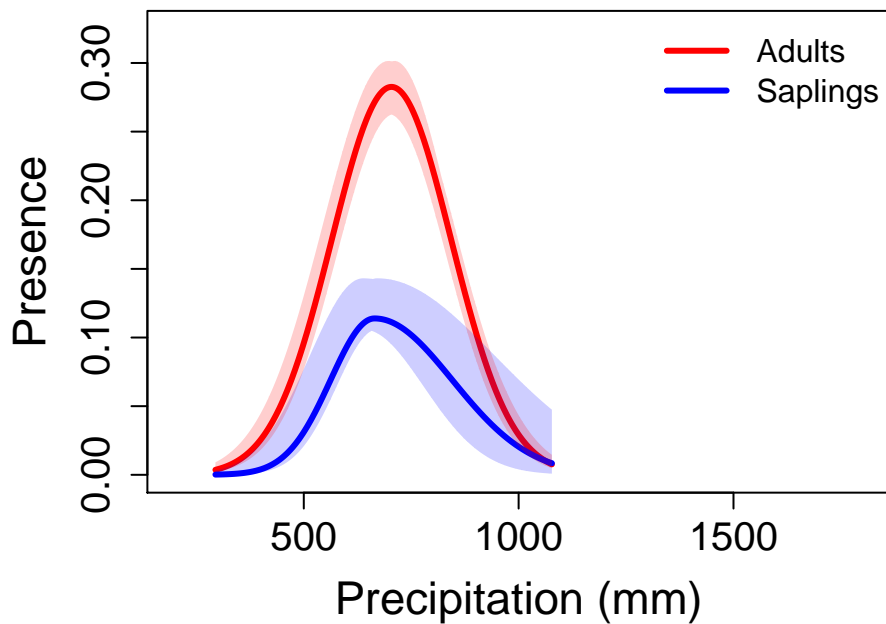
Peaks in frequency, but not relative abundance, occur in the center of tree species distributions on climate gradients

Patrick H. Martin and Charles D. Canham

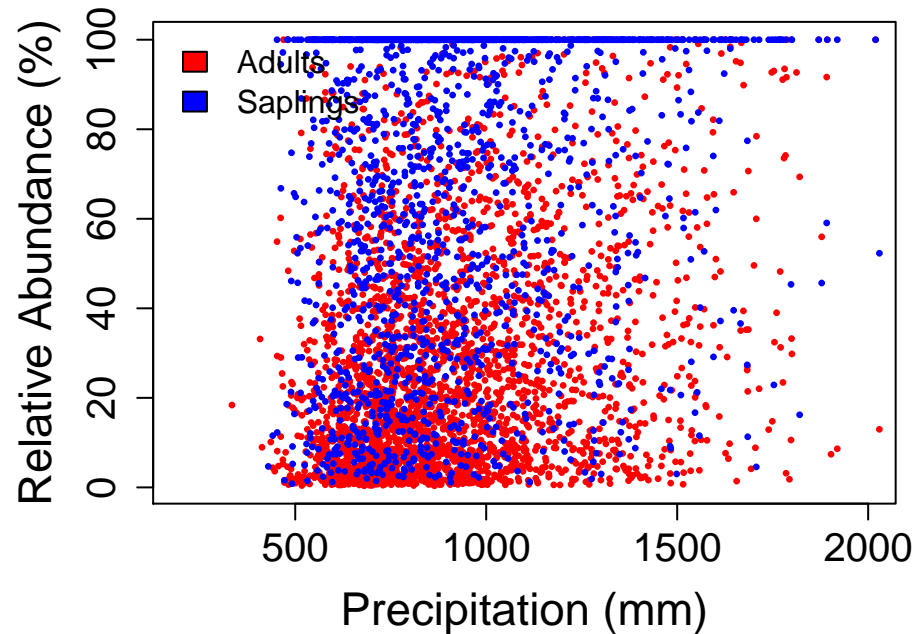
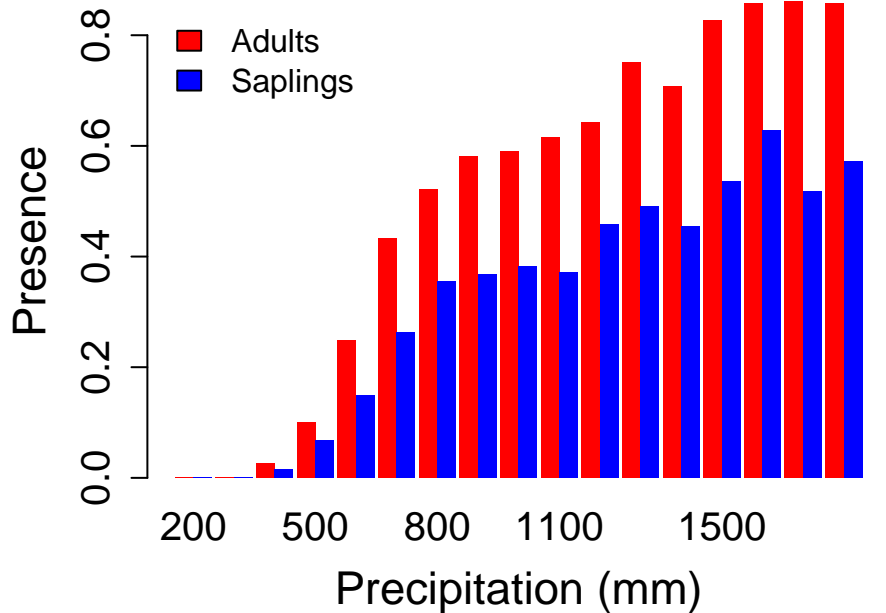
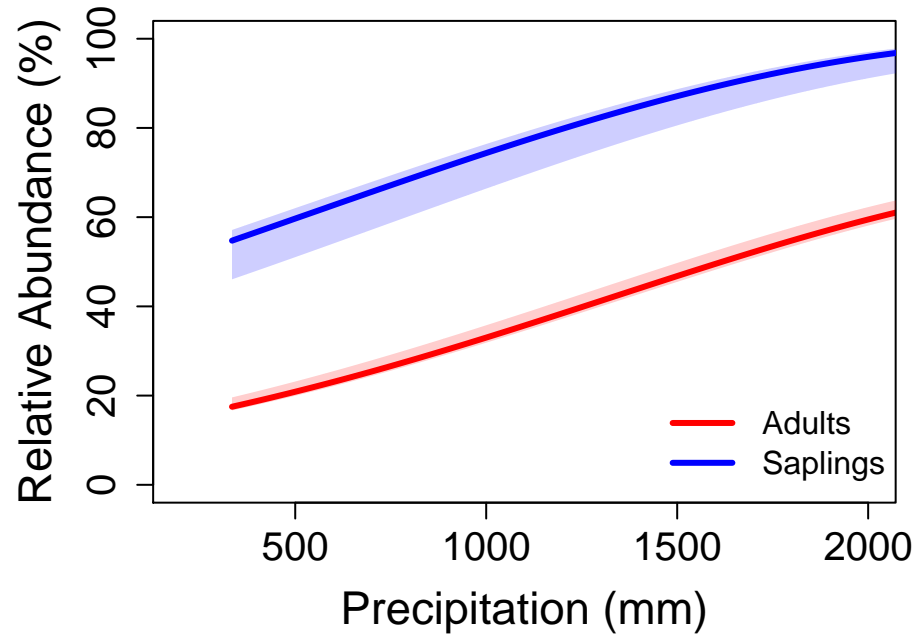
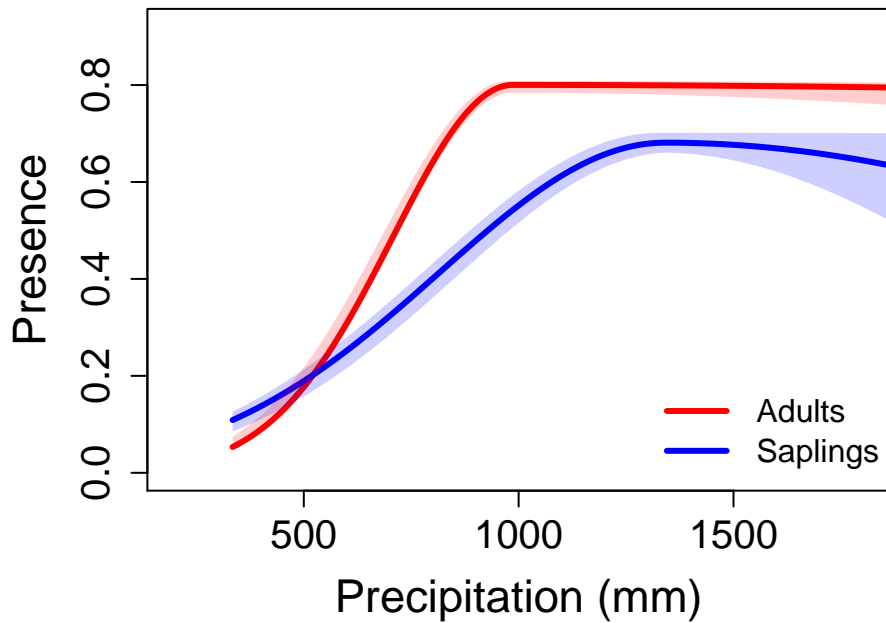
## **Appendix S3**

Precipitation Distributions – Modeled presence and relative abundance distributions with 2-unit support intervals for adults and saplings of dominant tree species on precipitation gradients in the Interior West Region, and observed presence and relative abundance in the FIA data.

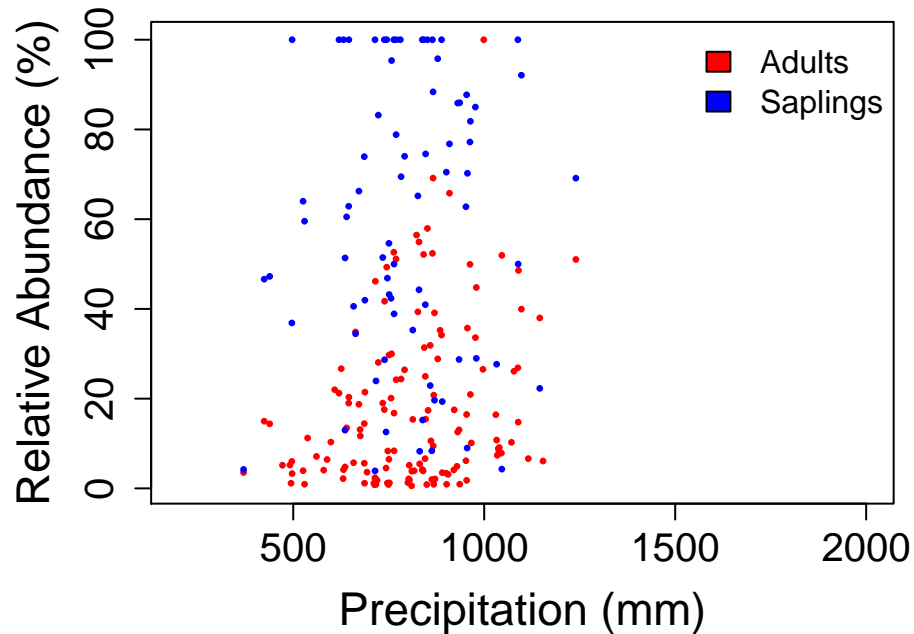
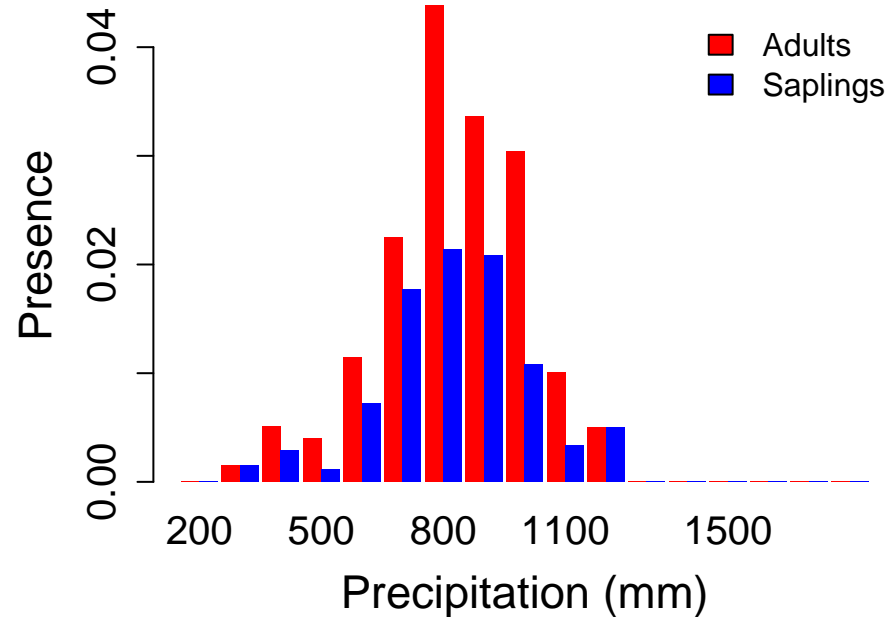
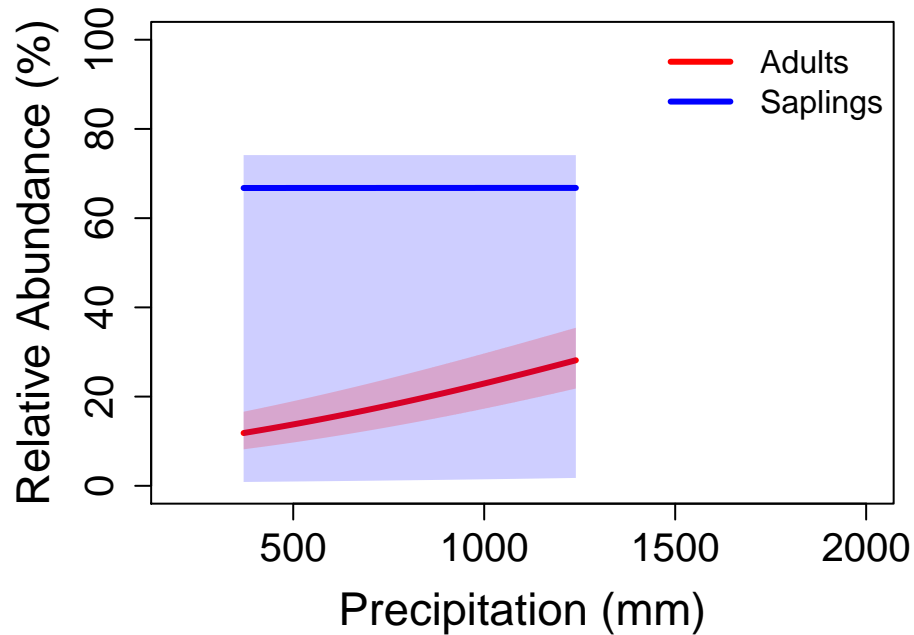
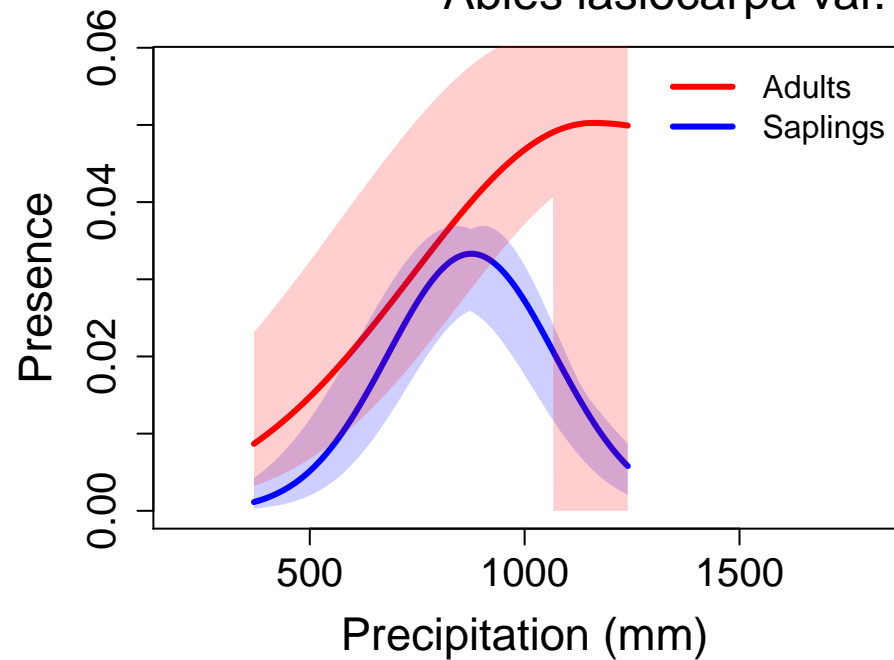
# Abies concolor – white fir



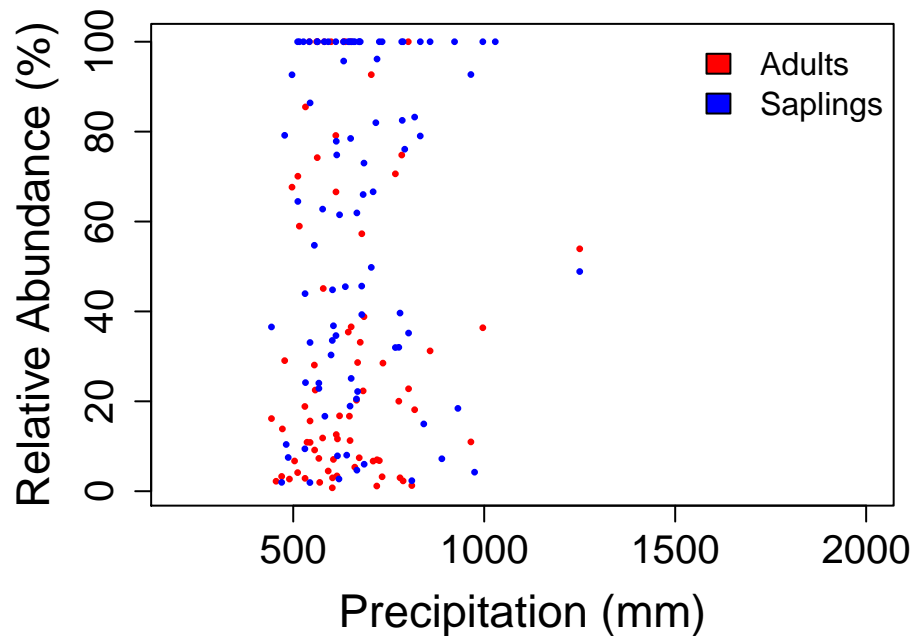
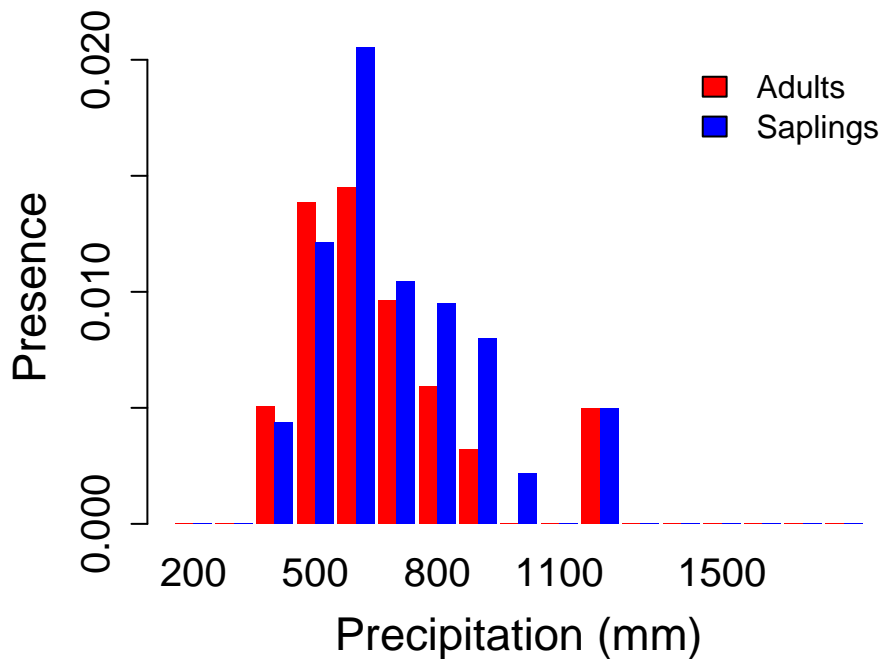
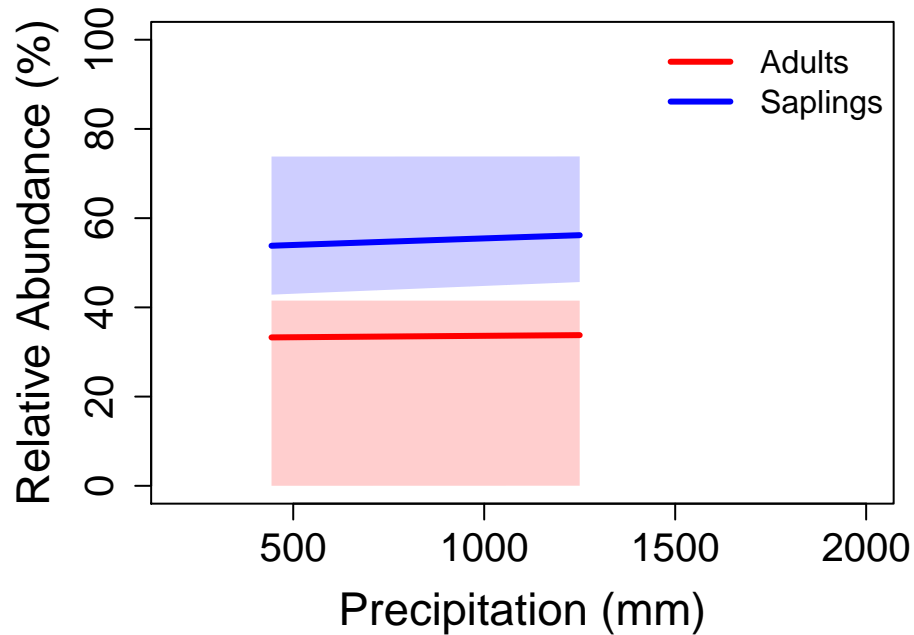
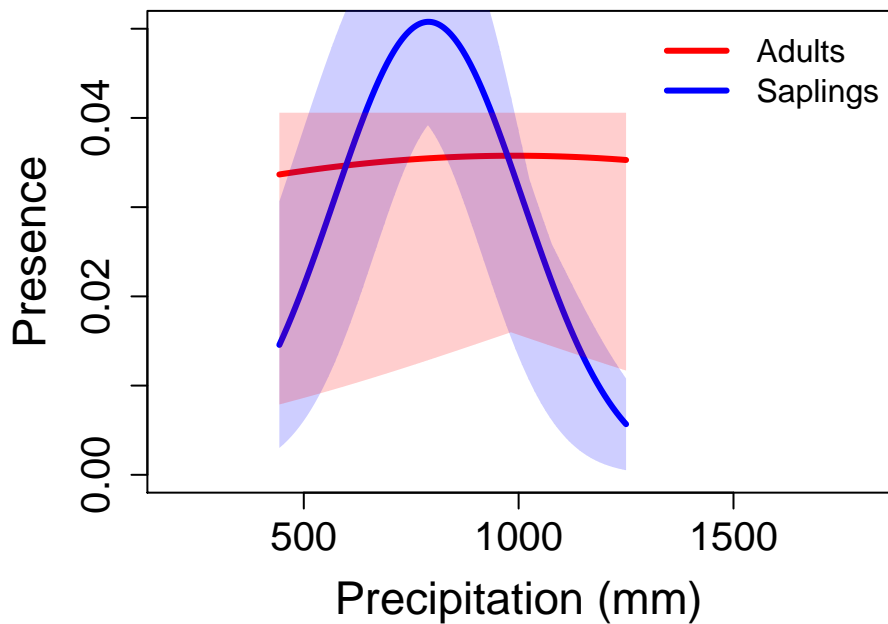
# *Abies lasiocarpa* - subalpine fir



# *Abies lasiocarpa* var. *arizonica* – corkbark fir

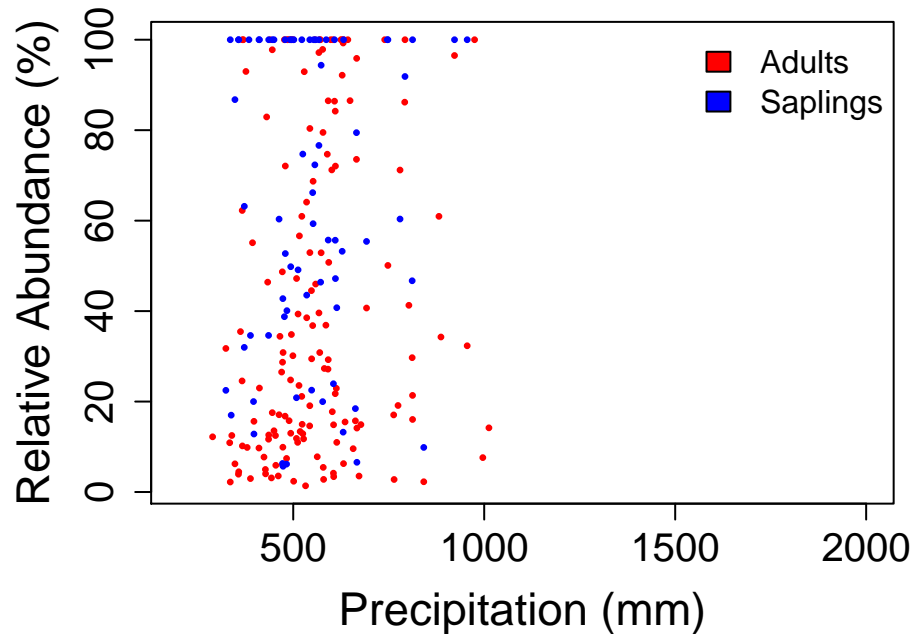
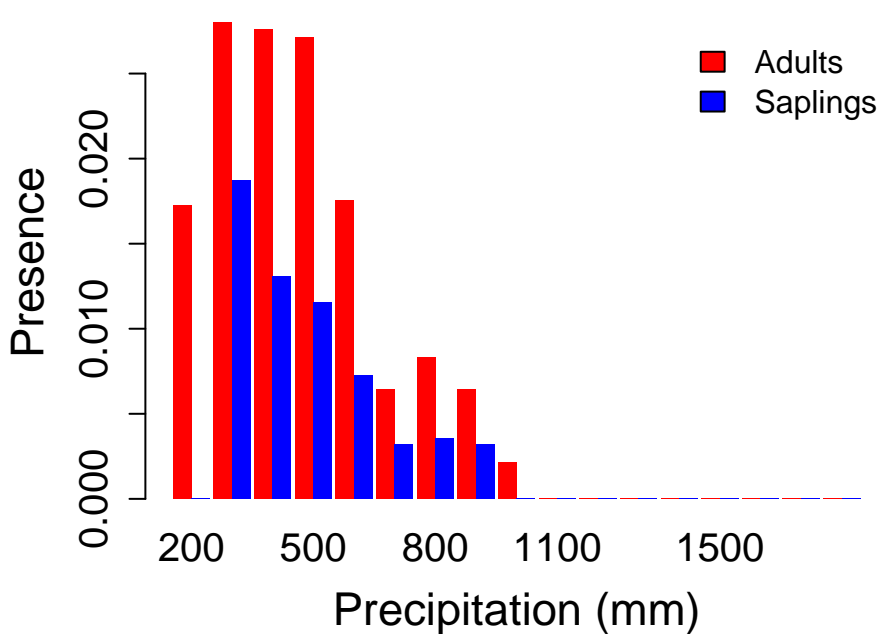
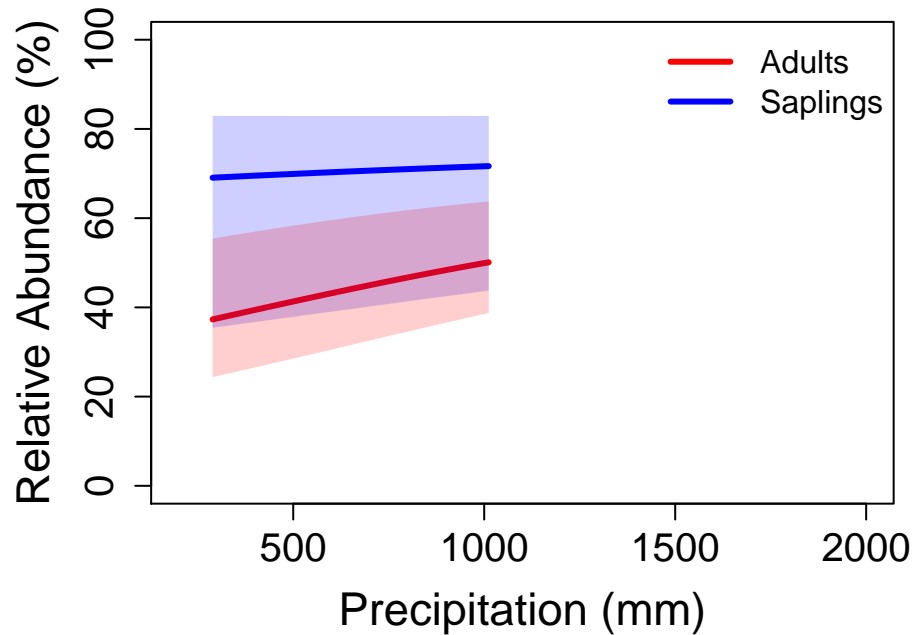
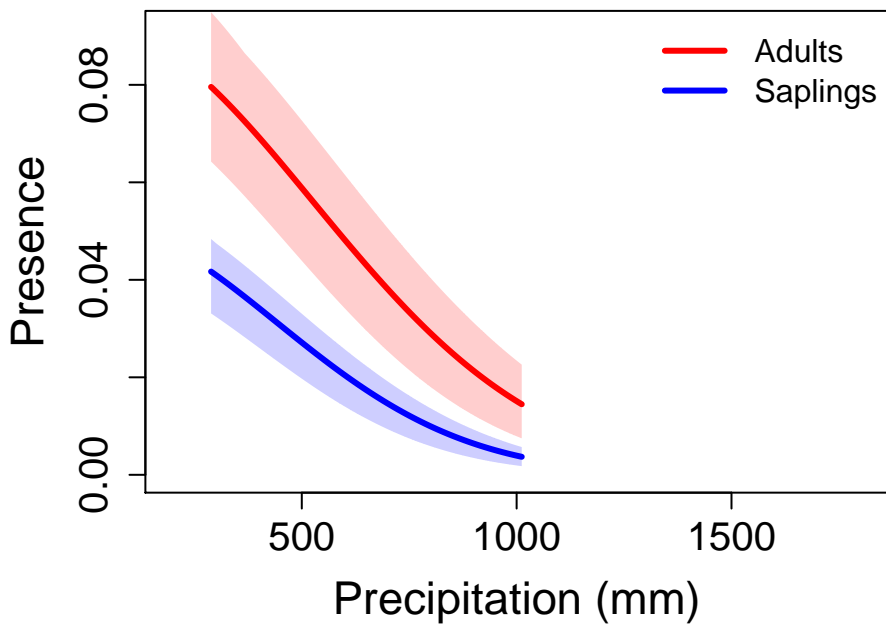


# Acer grandidentatum – bigtooth maple

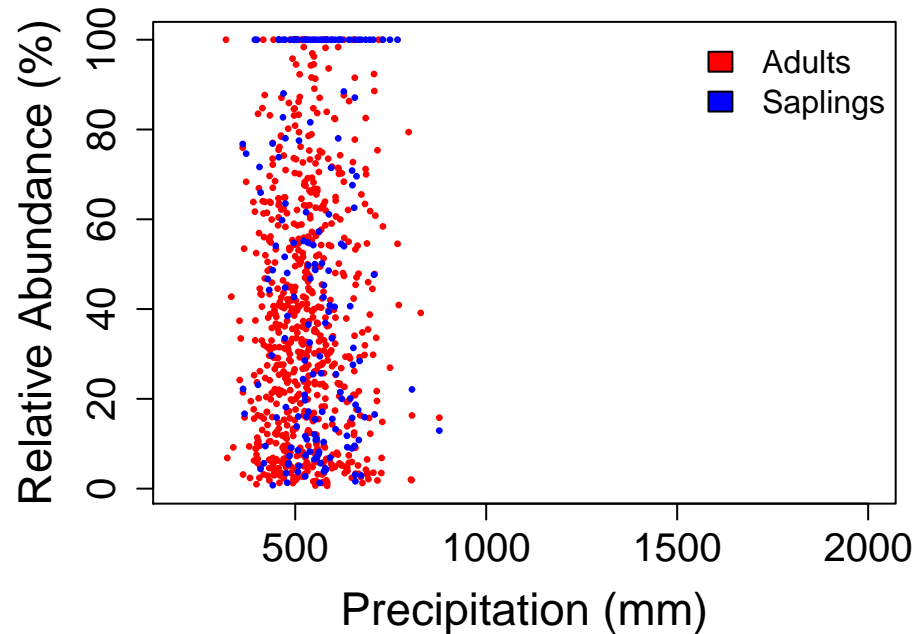
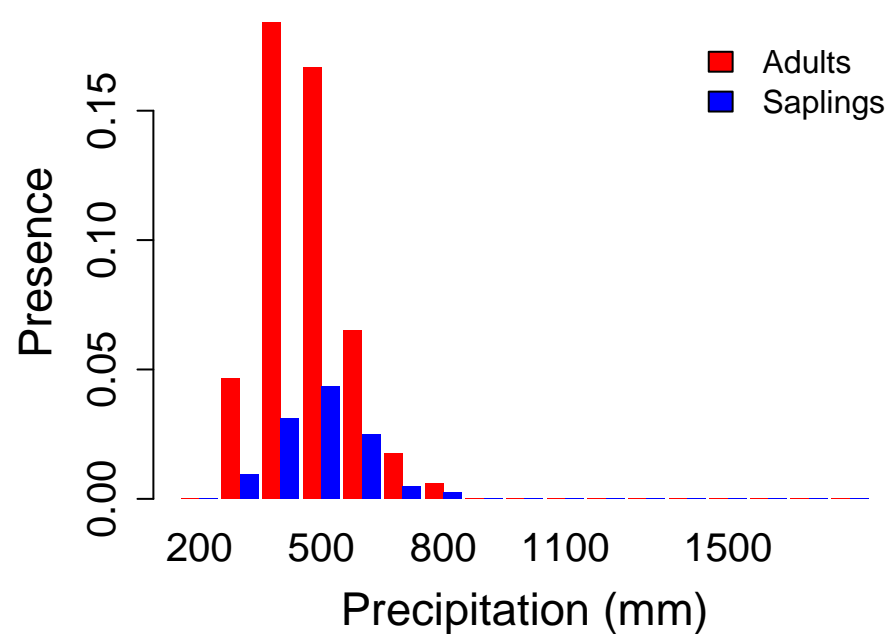
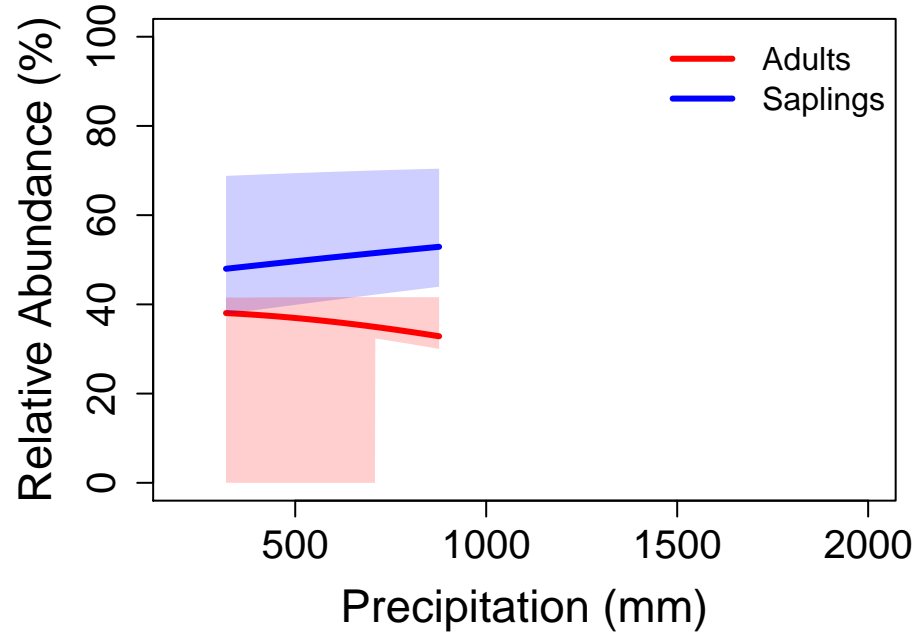
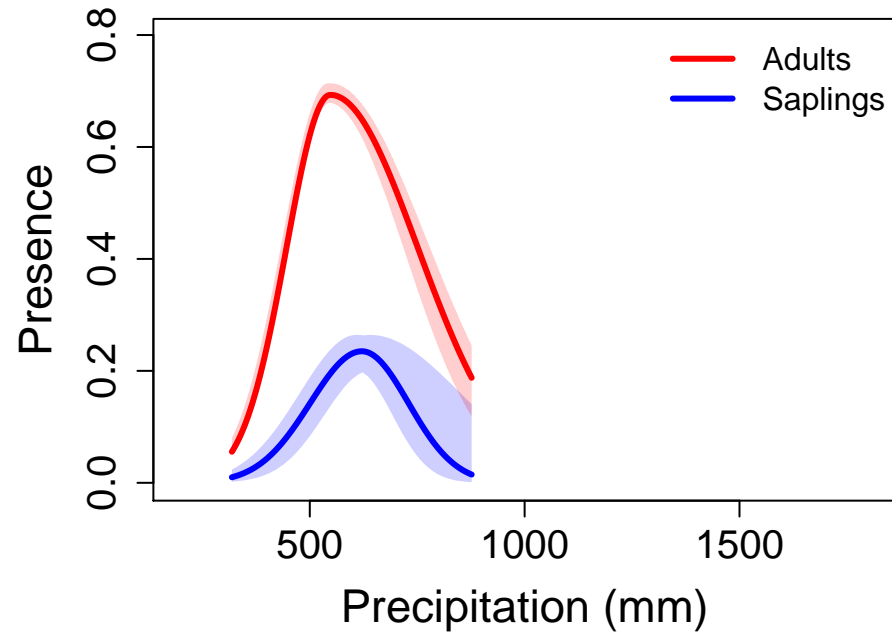




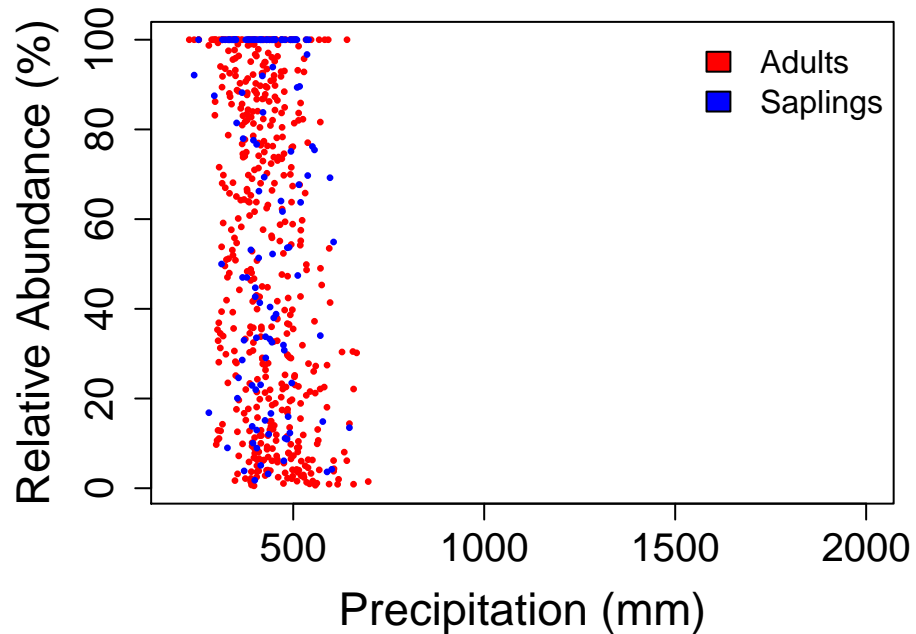
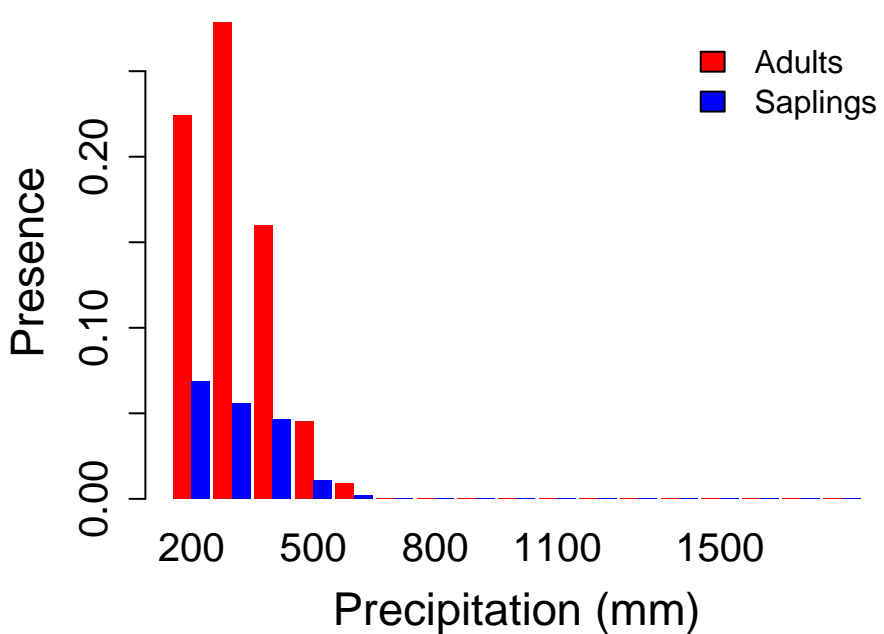
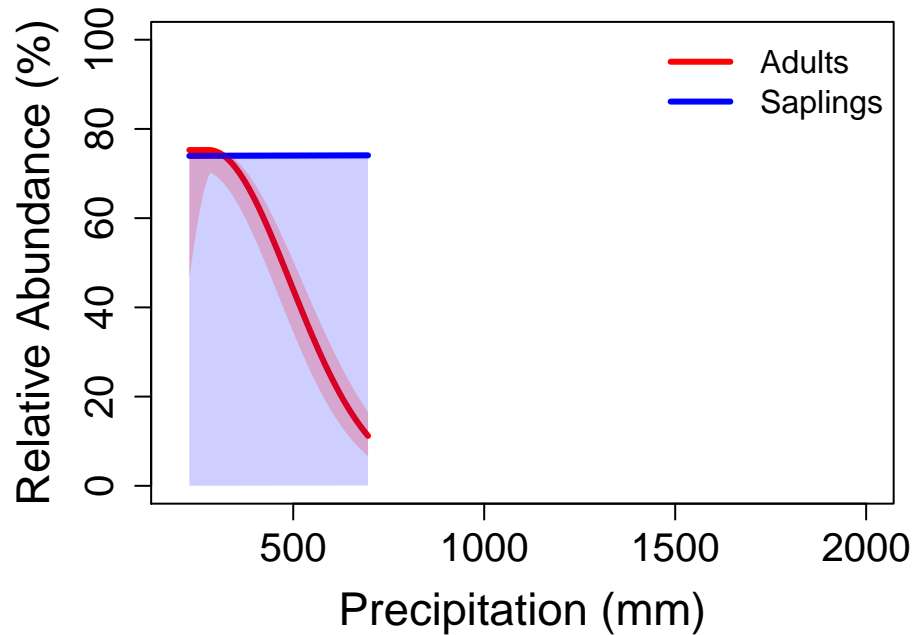
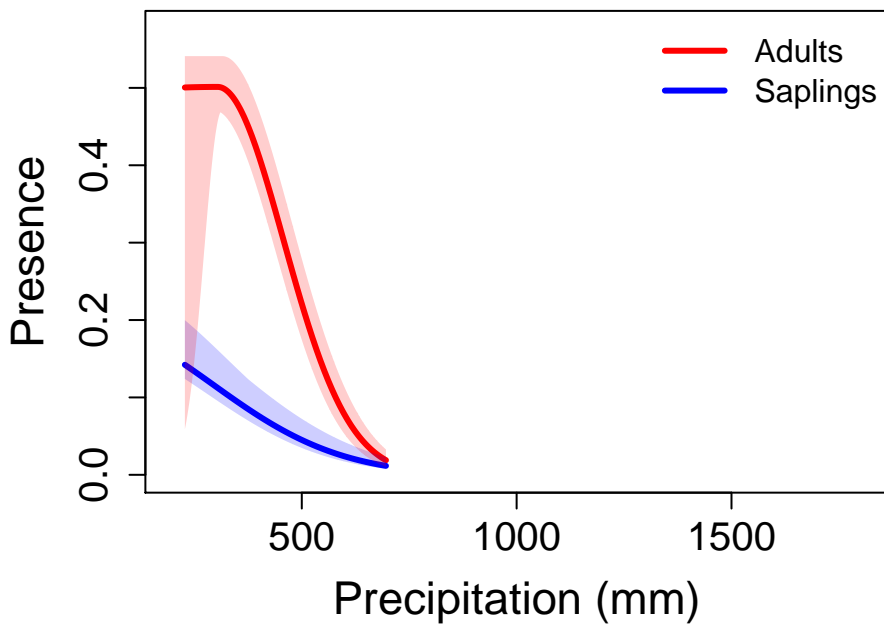
# Cercocarpus ledifolius – curleaf mountainmahogany



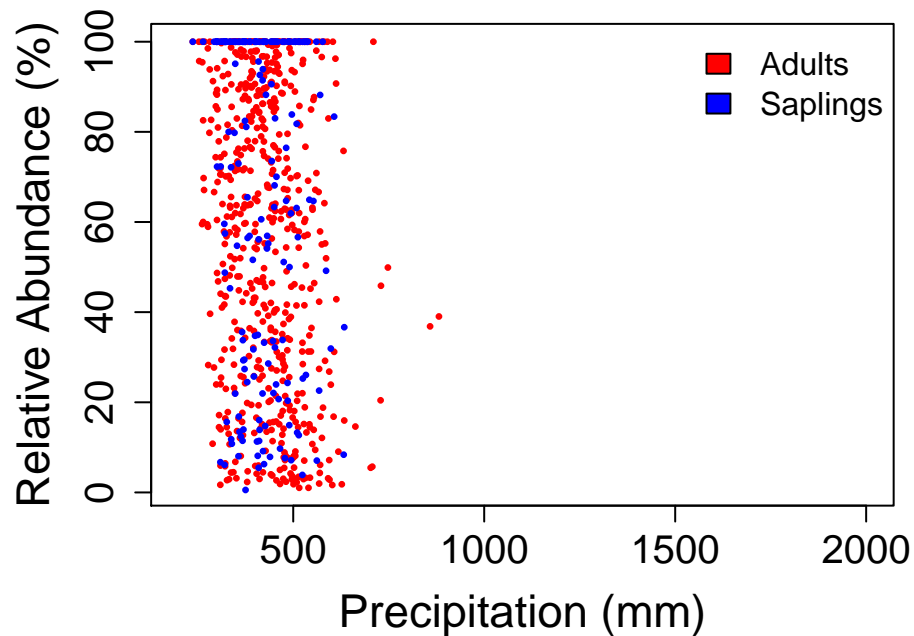
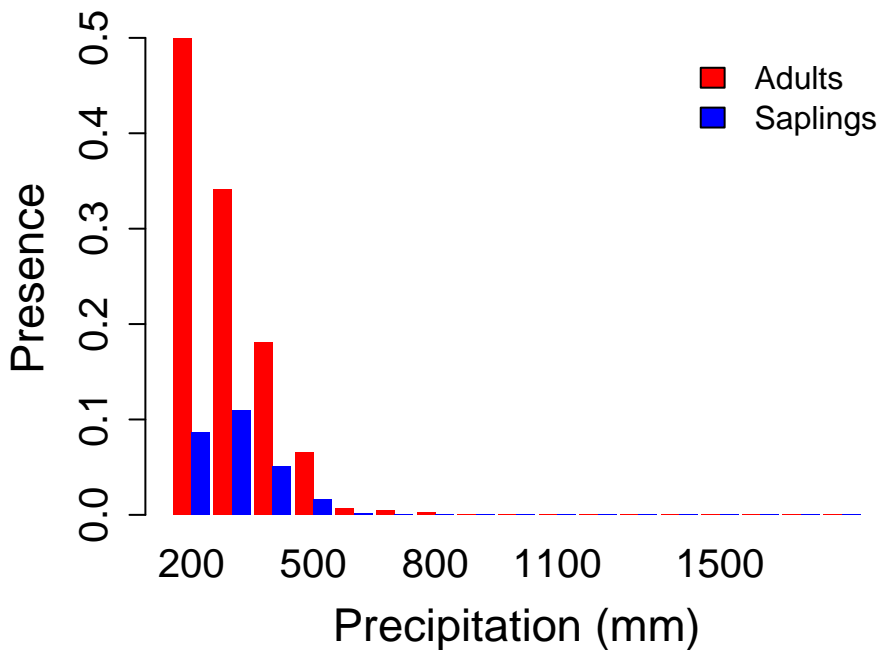
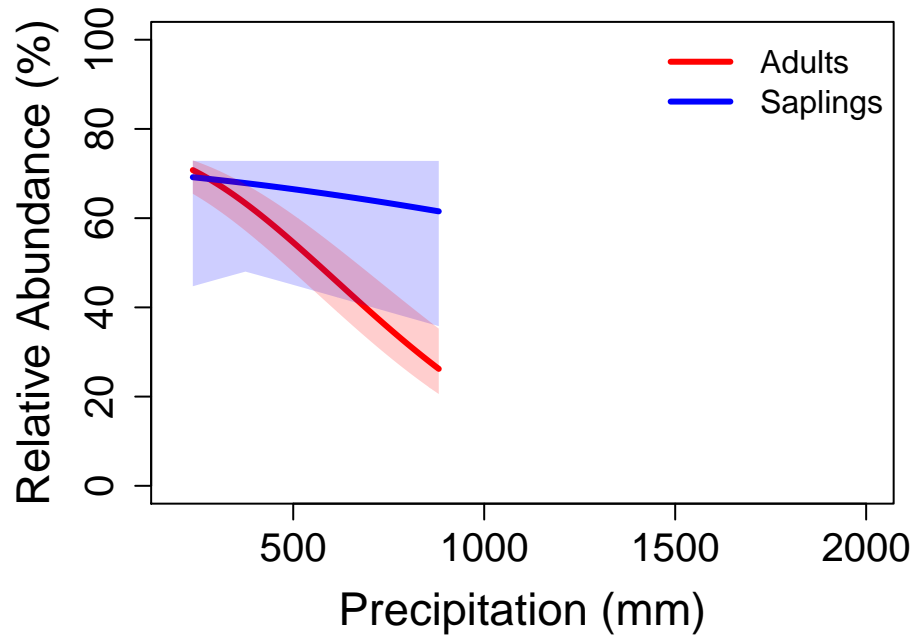
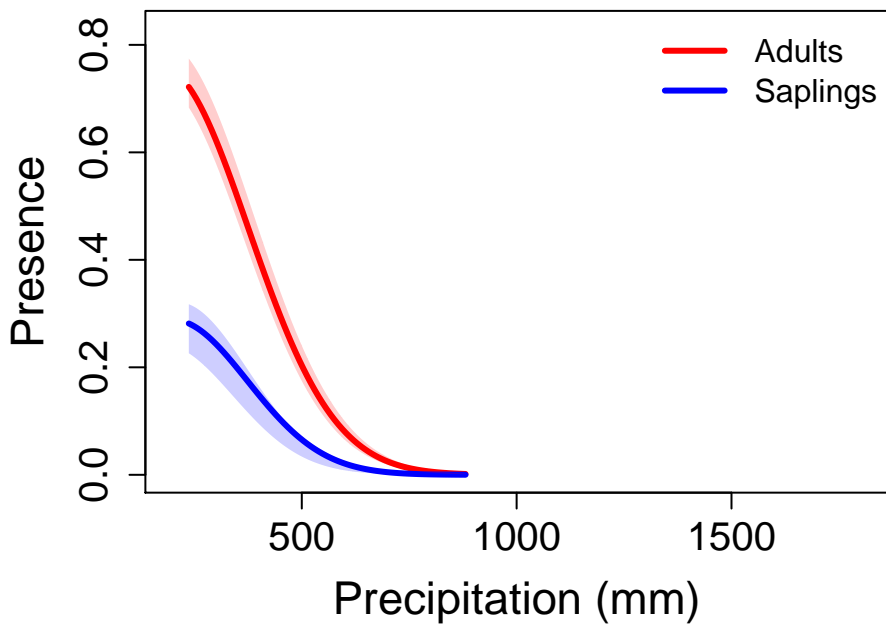
# Juniperus deppeana – alligator juniper



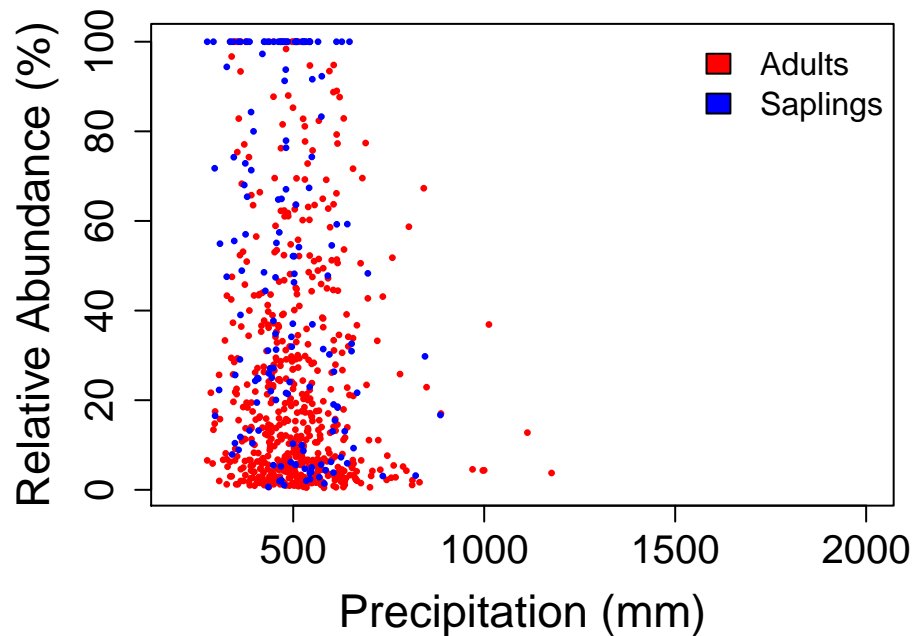
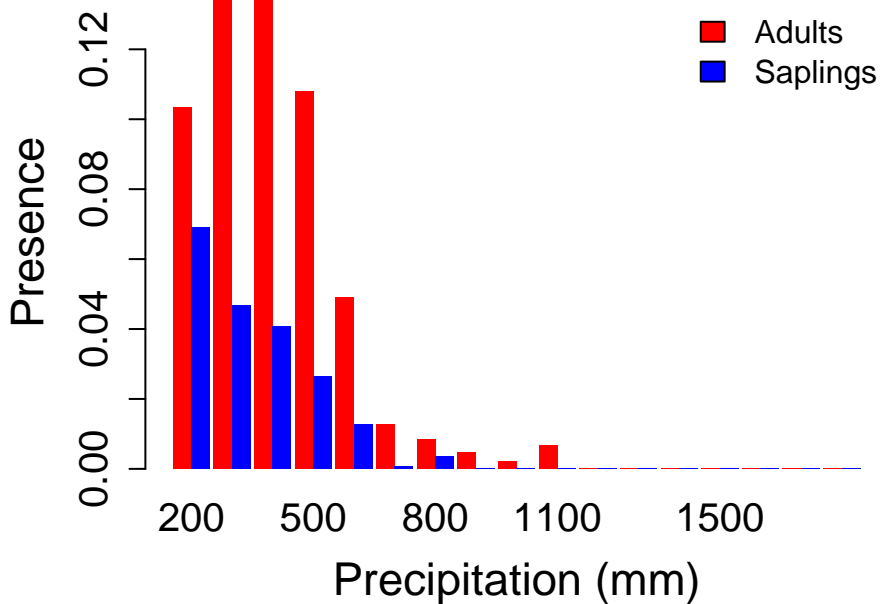
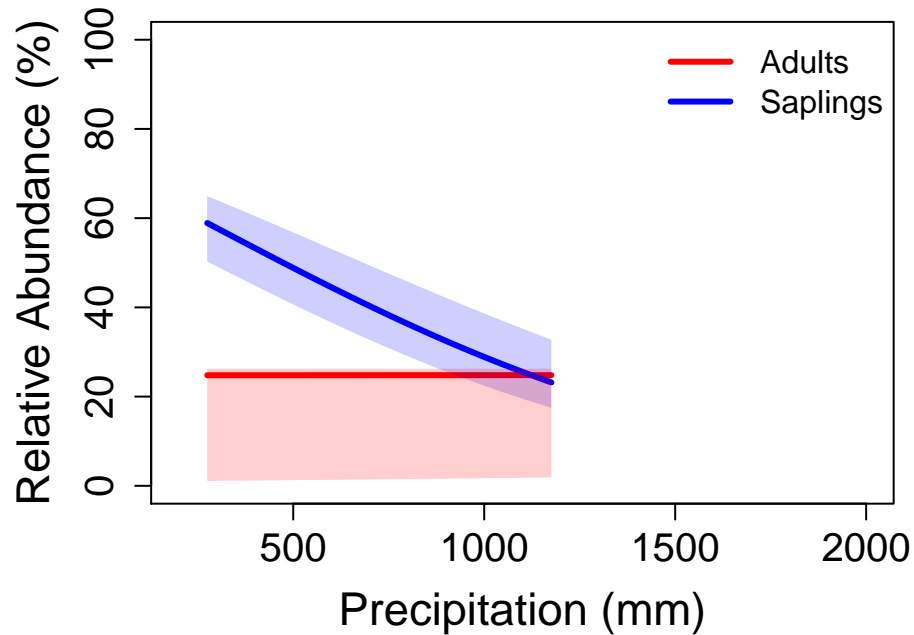
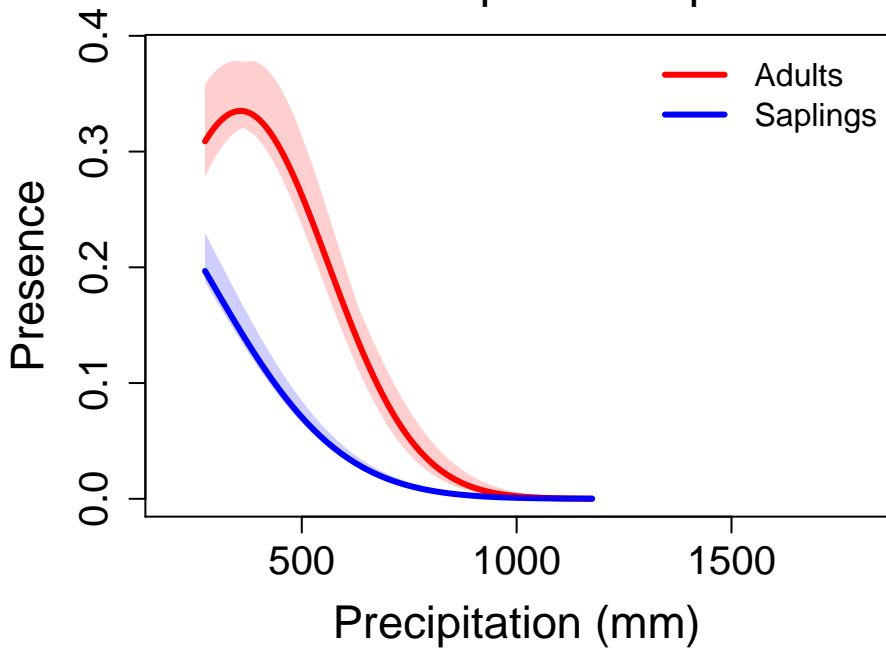
# Juniperus monosperma – oneseed juniper



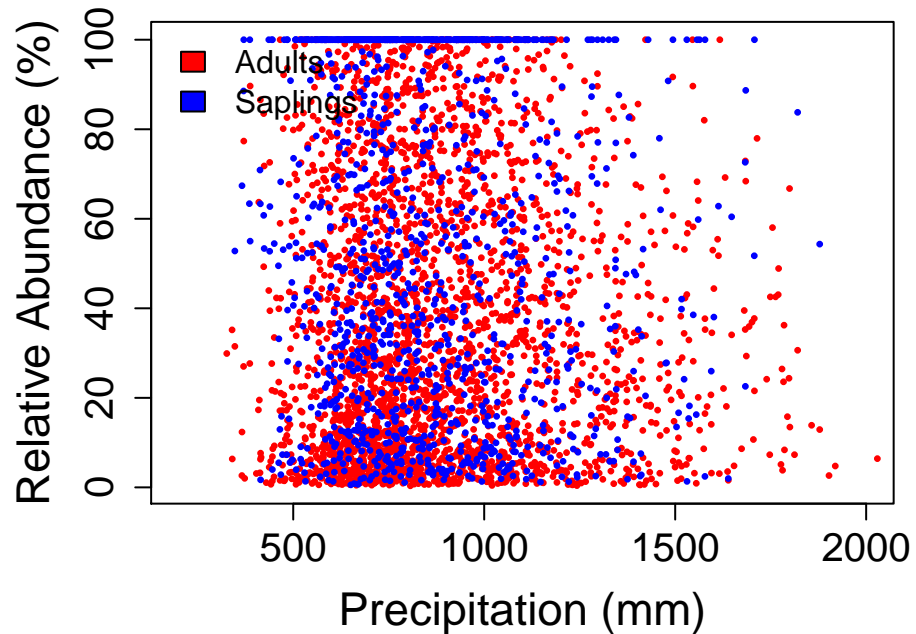
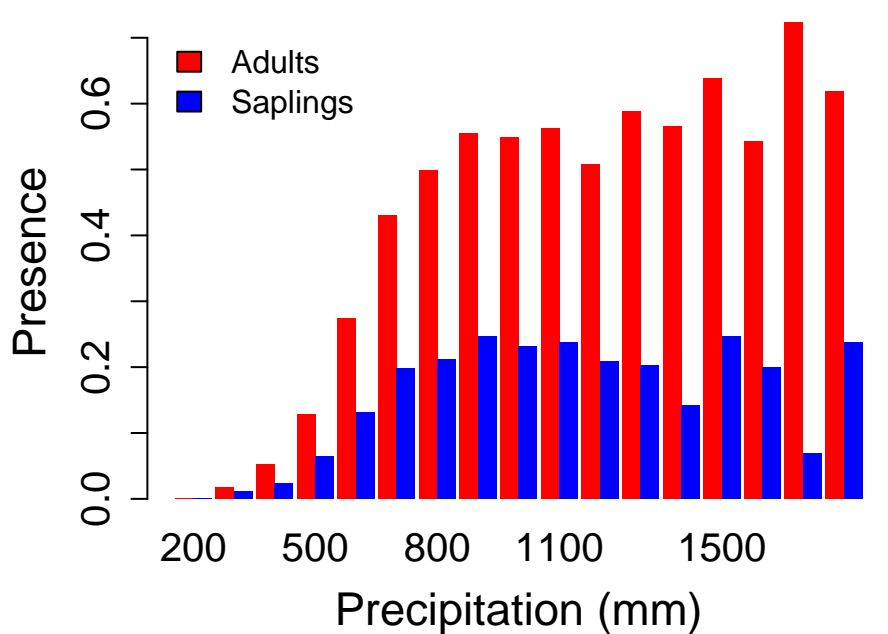
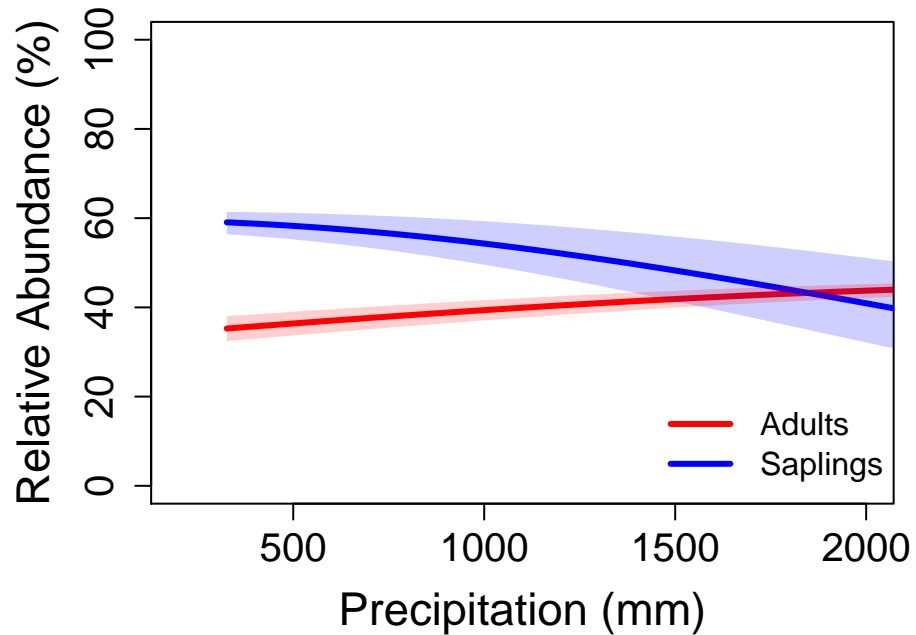
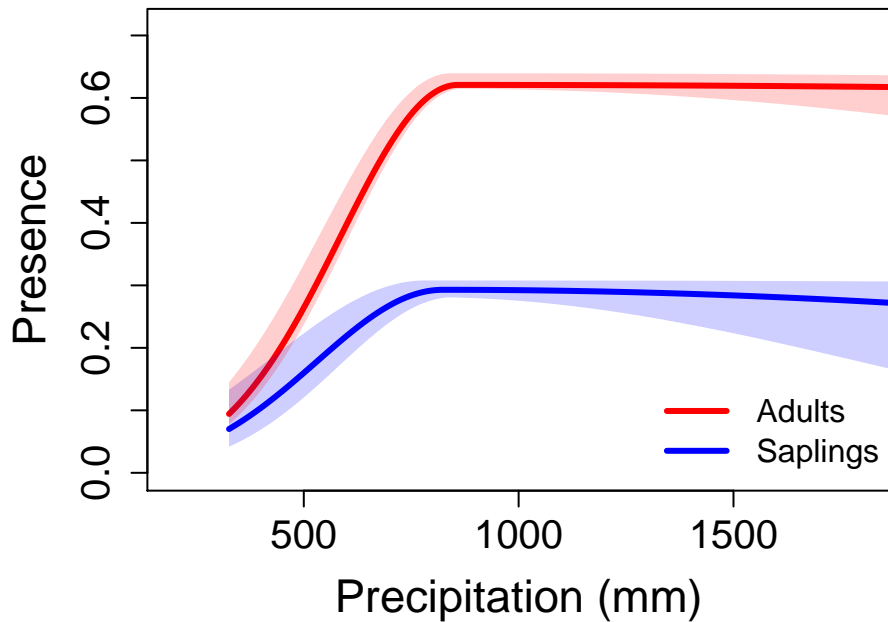
# Juniperus osteosperma – Utah juniper



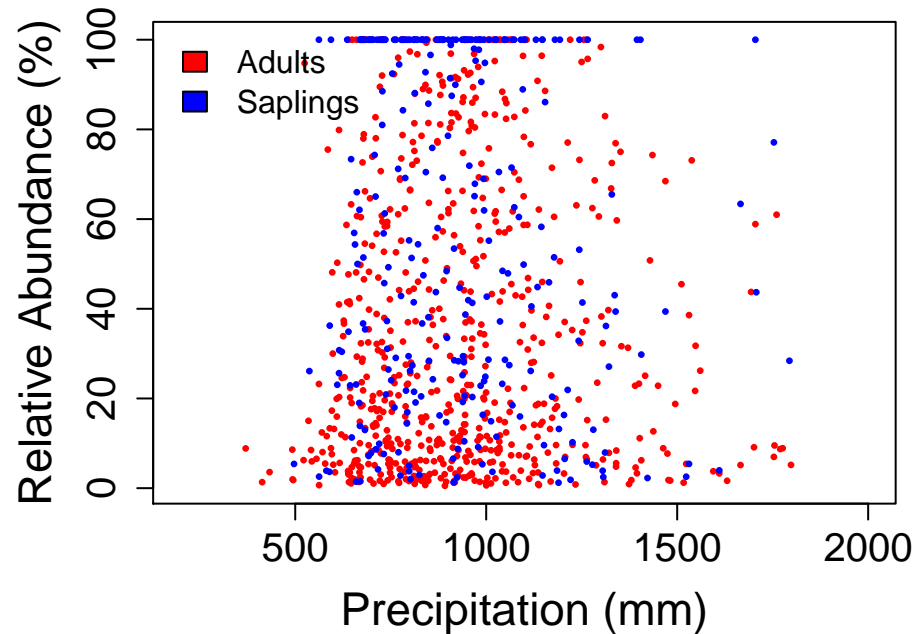
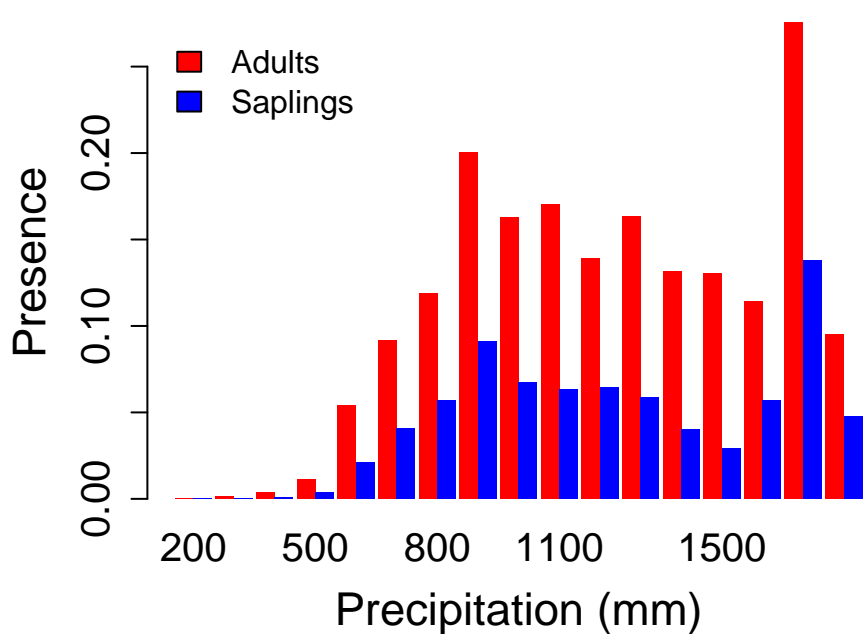
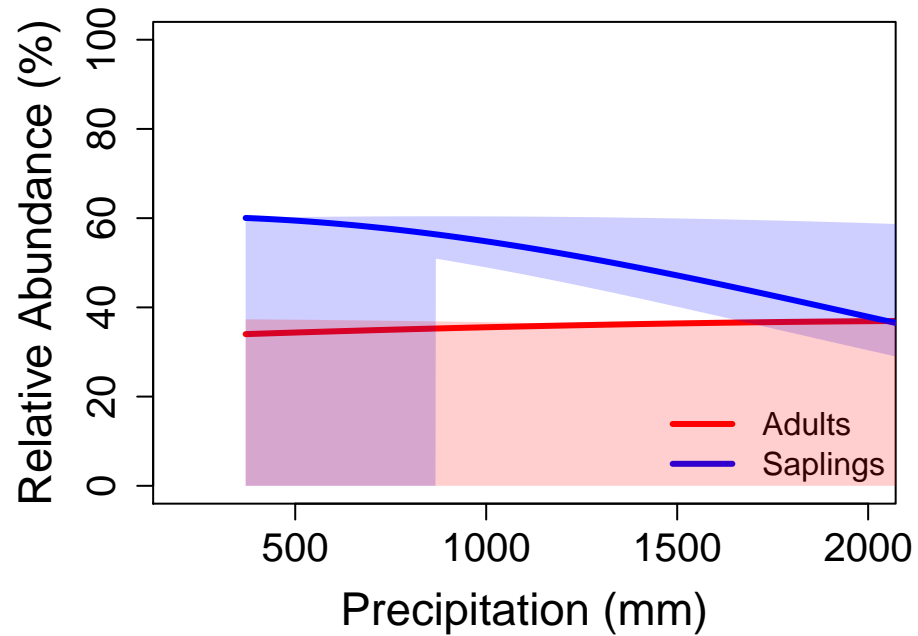
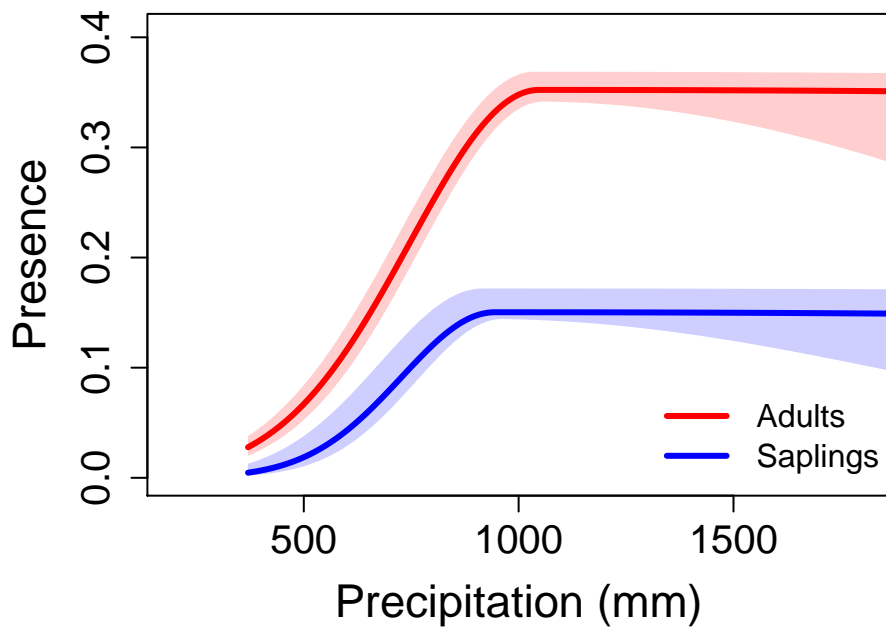
# Juniperus scopulorum – Rocky Mountain juniper



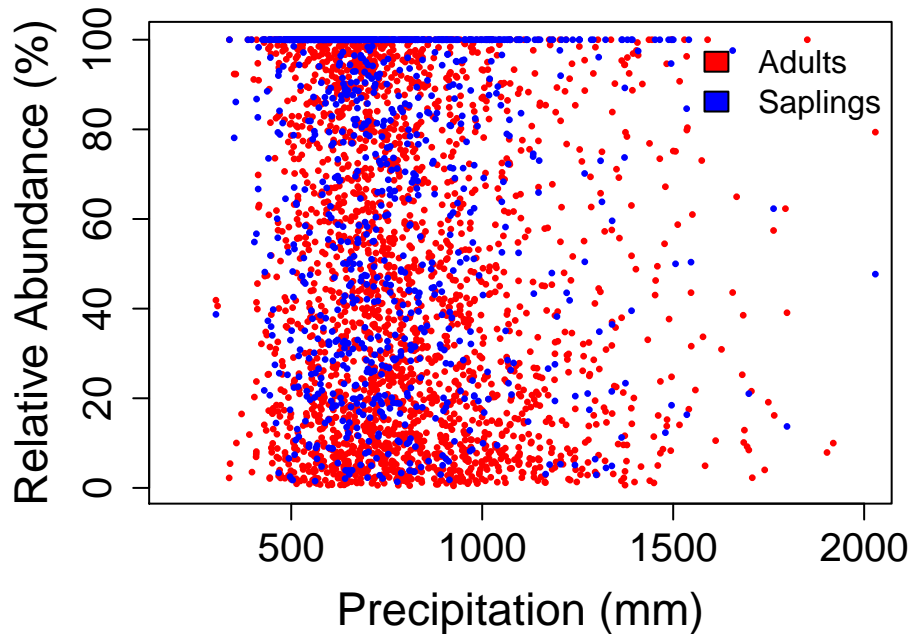
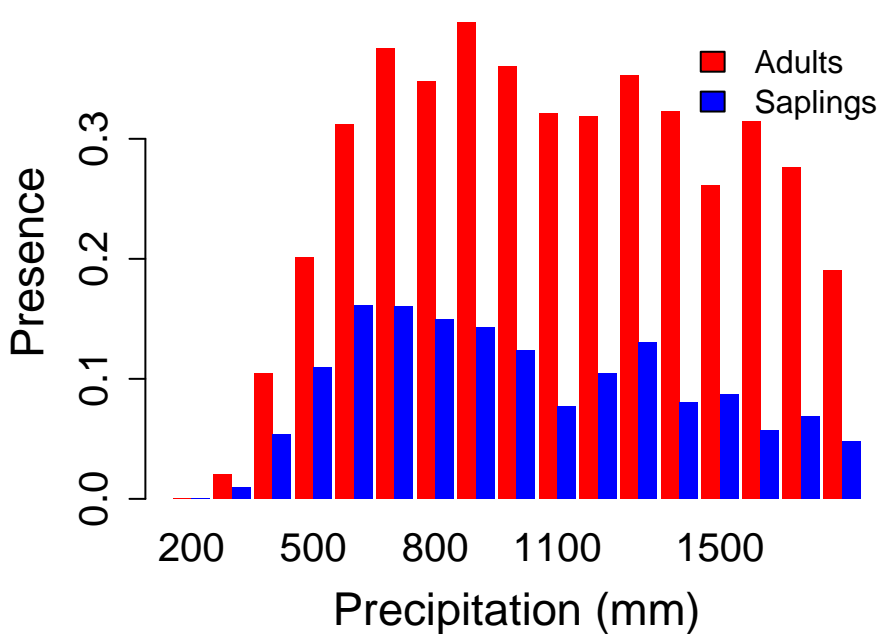
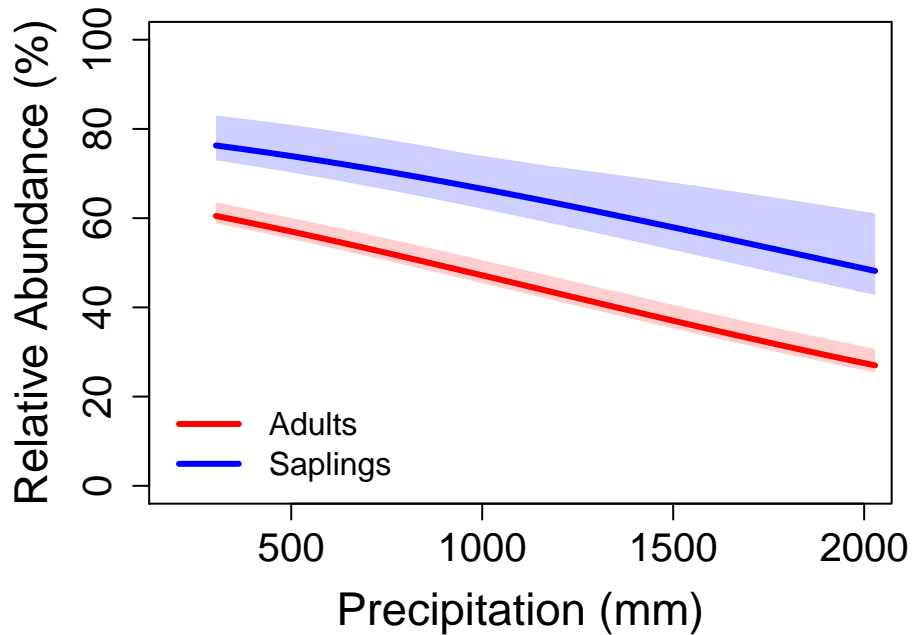
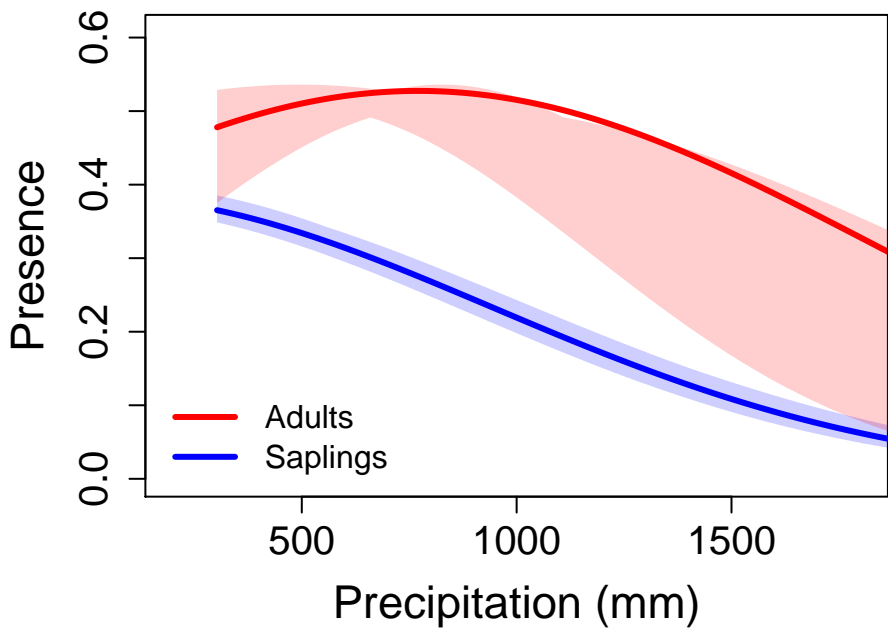
# *Picea engelmannii* – Engelmann spruce



# Pinus albicaulis – whitebark pine

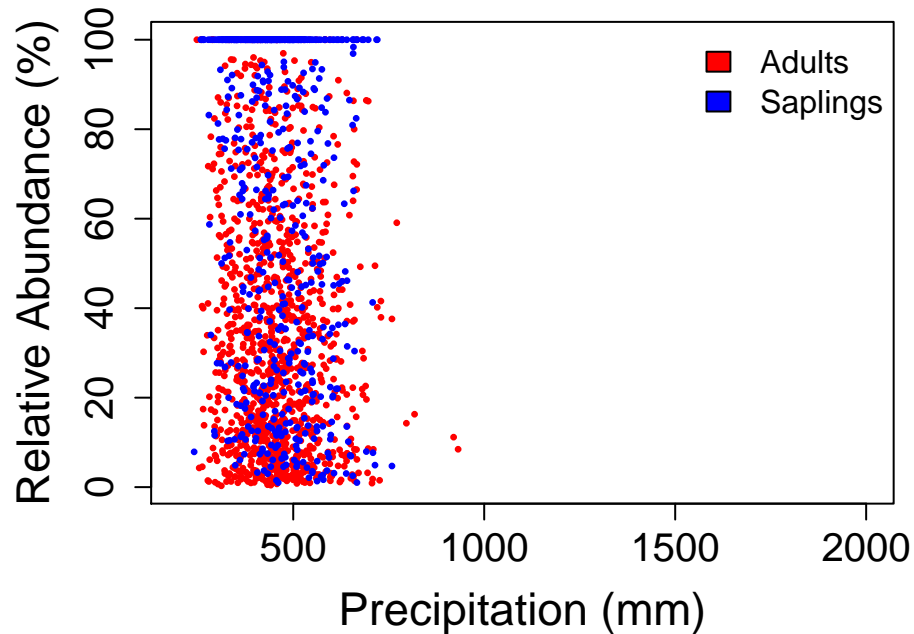
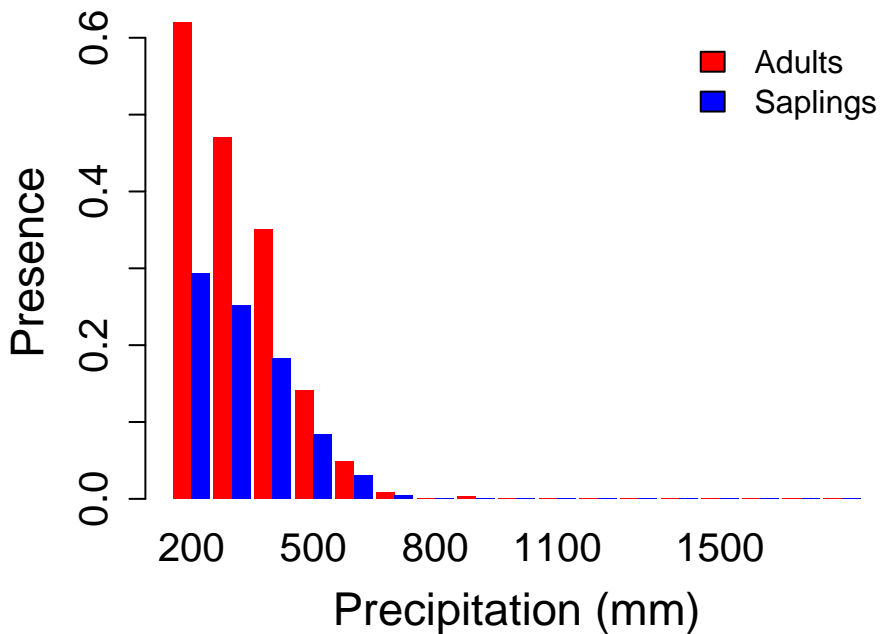
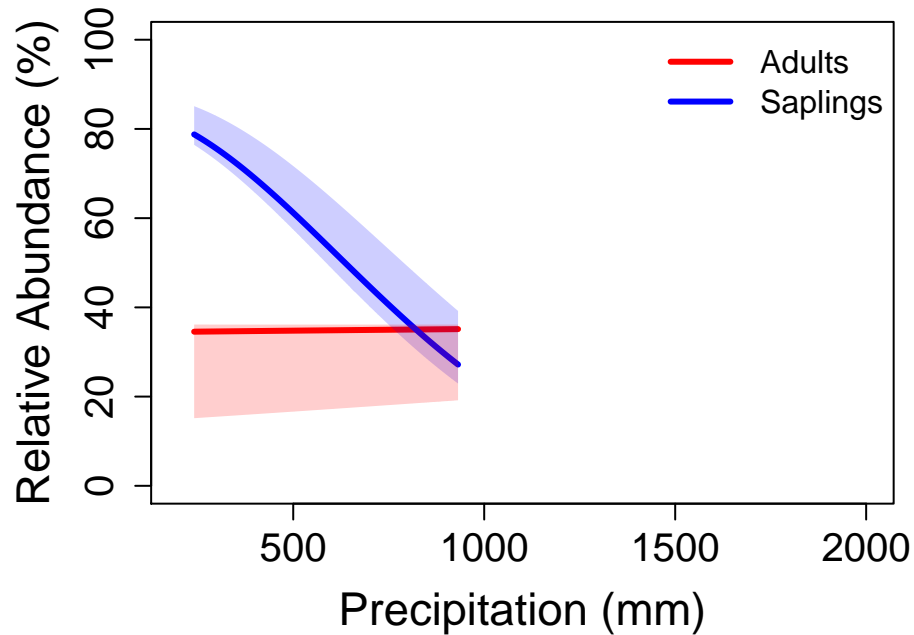
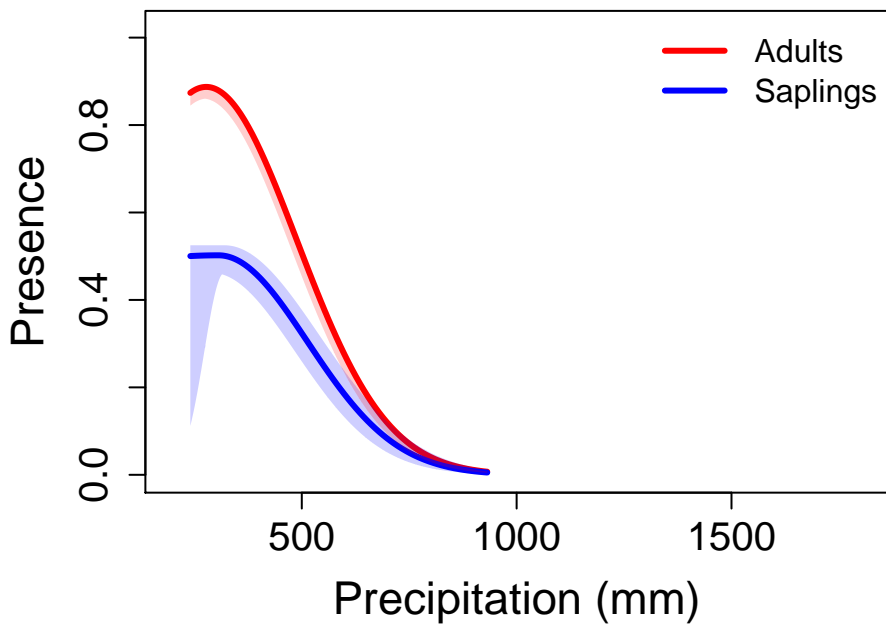


# Pinus contorta – lodgepole pine

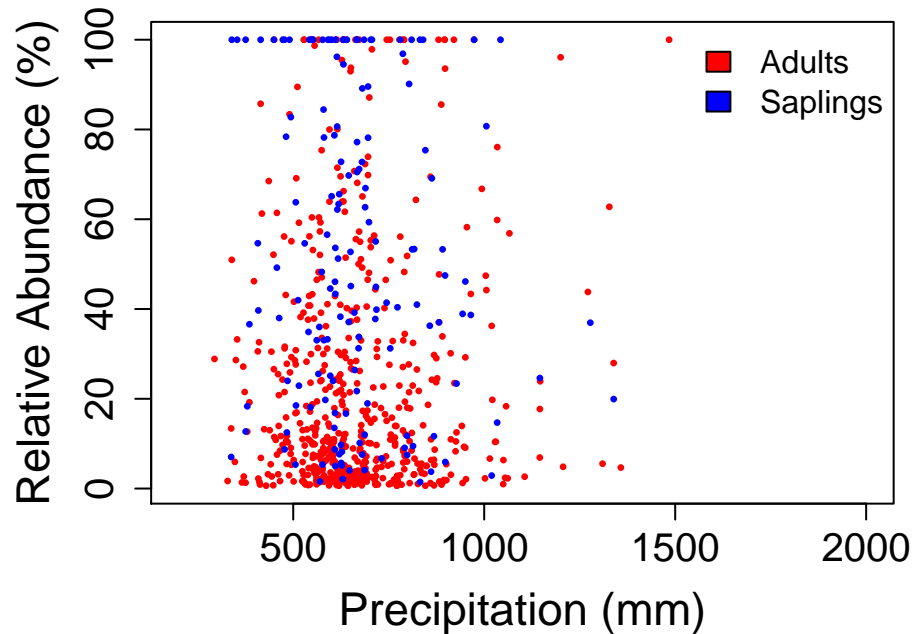
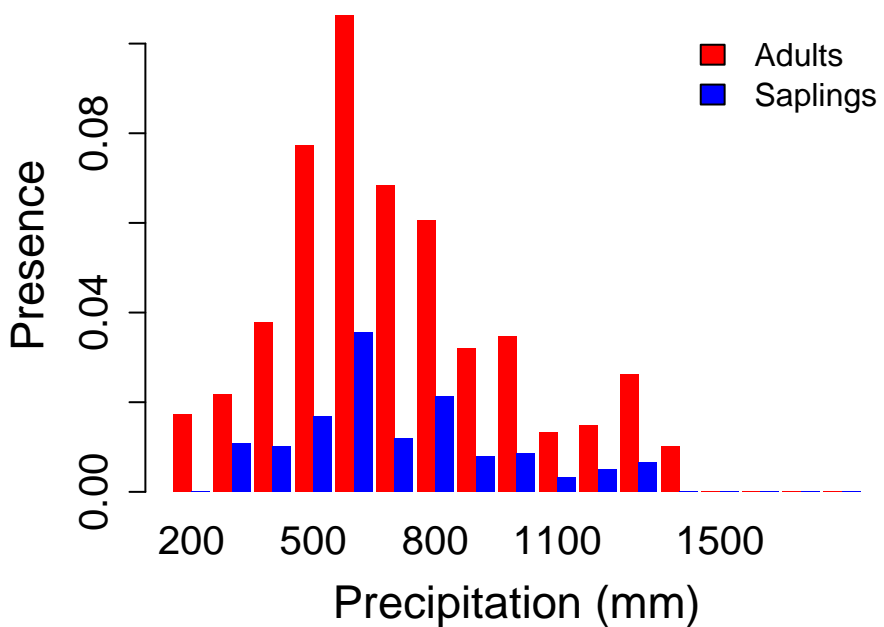
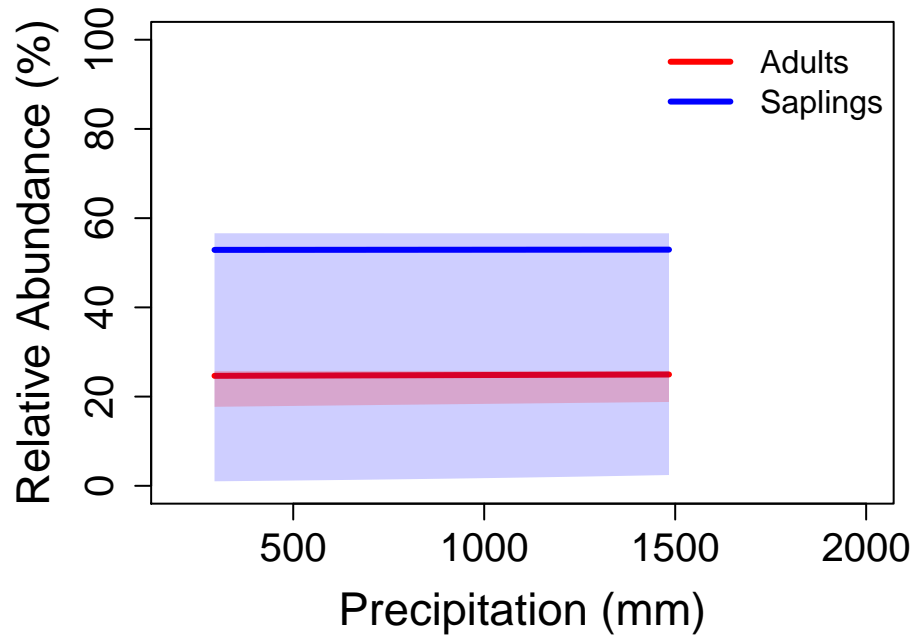
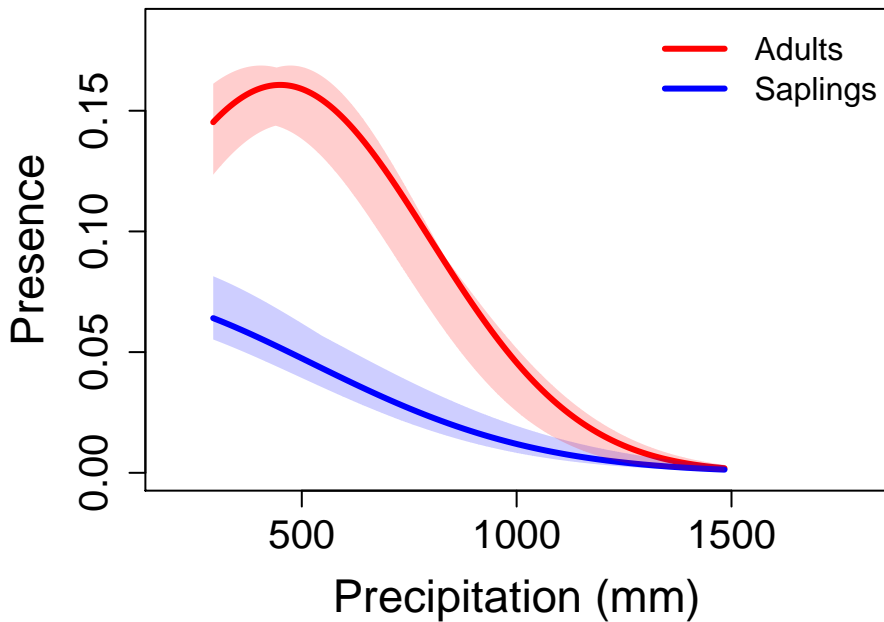




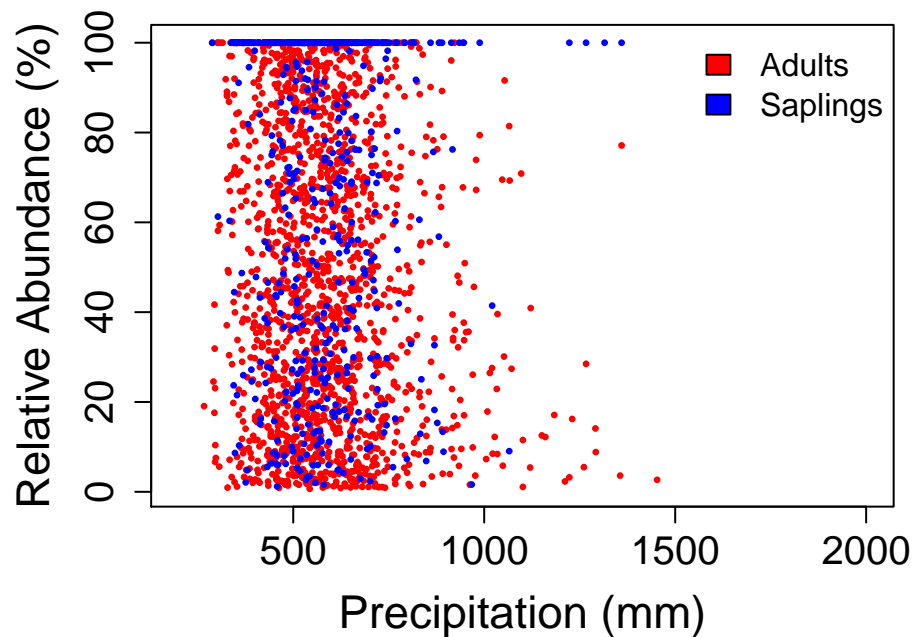
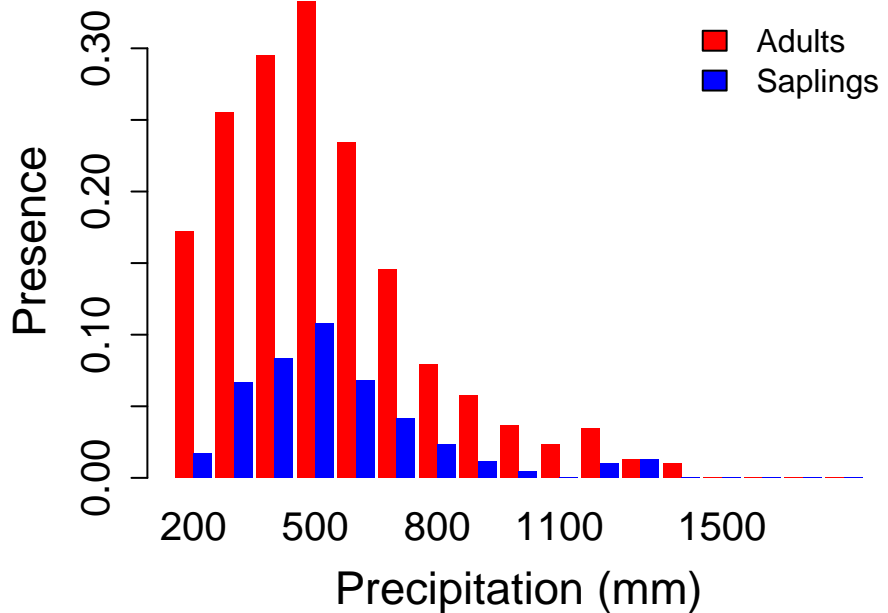
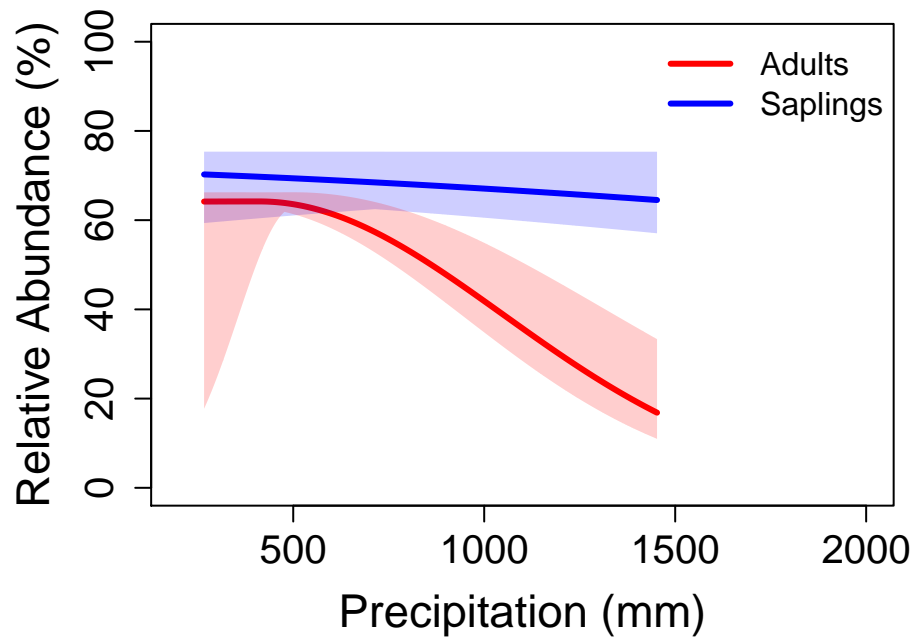
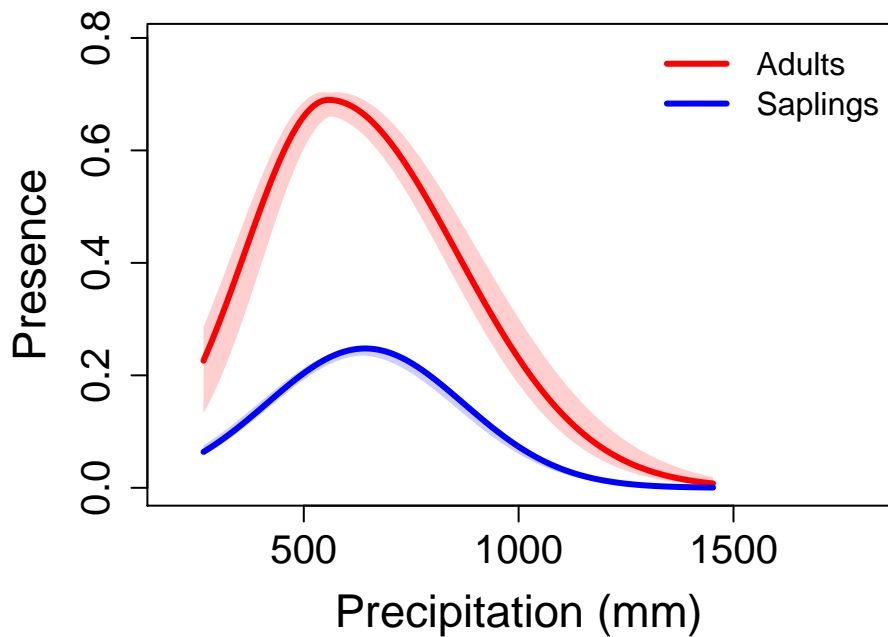
# Pinus edulis – Common or two-needle Pinyon



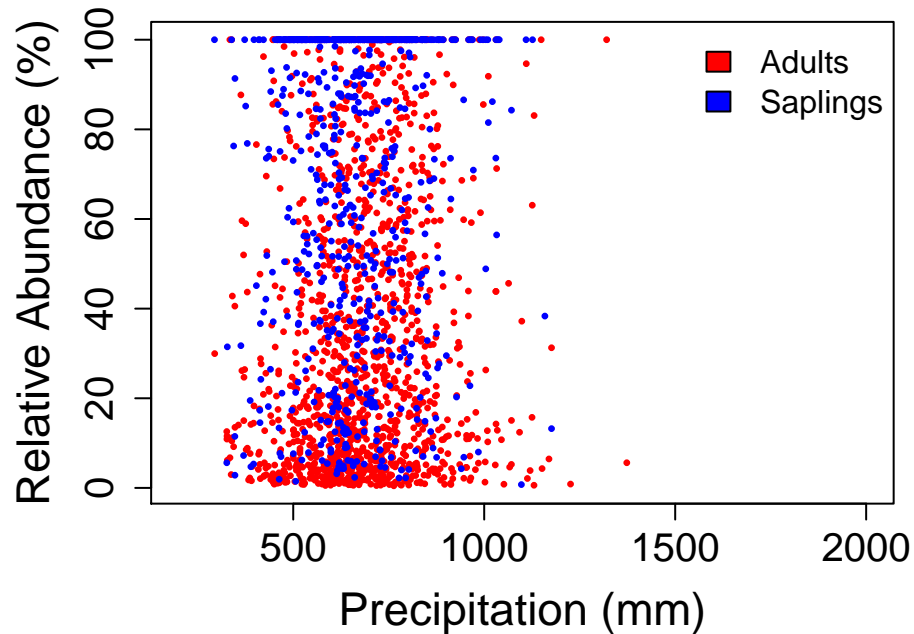
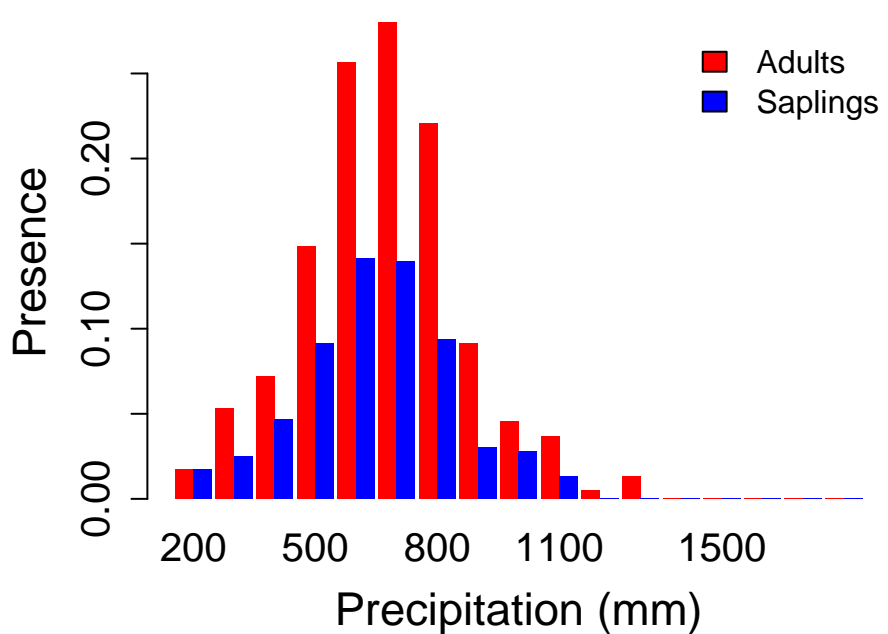
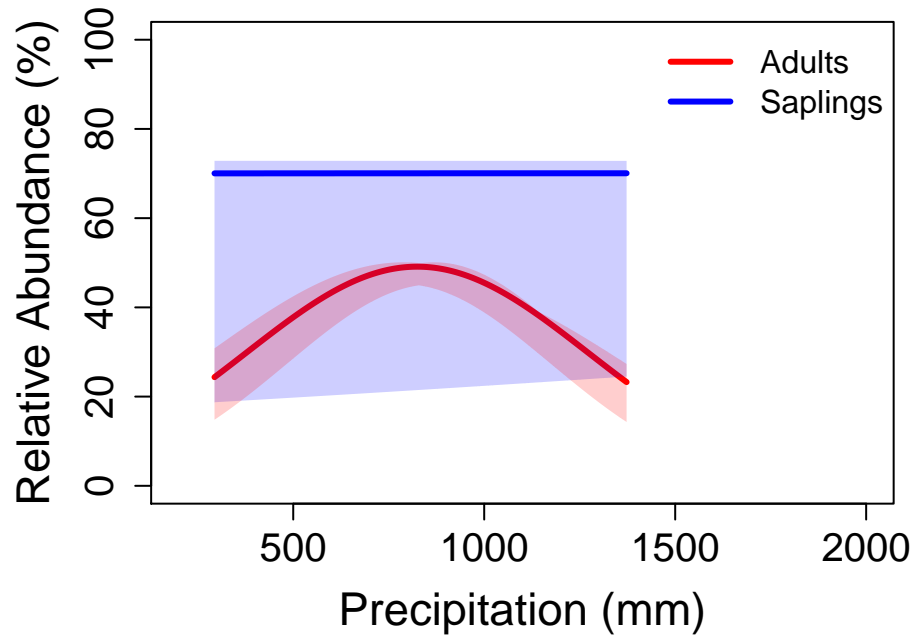
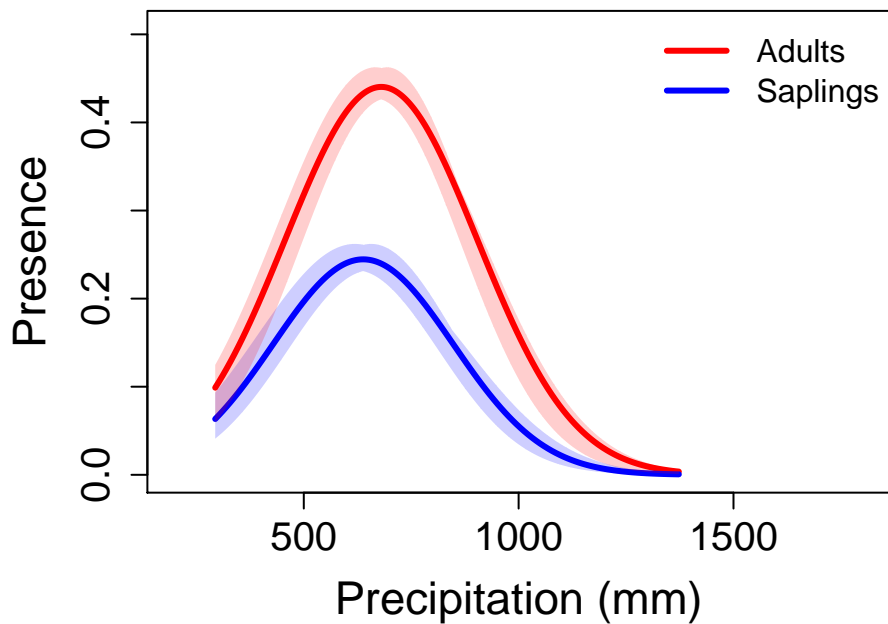
# Pinus flexilis – limber pine



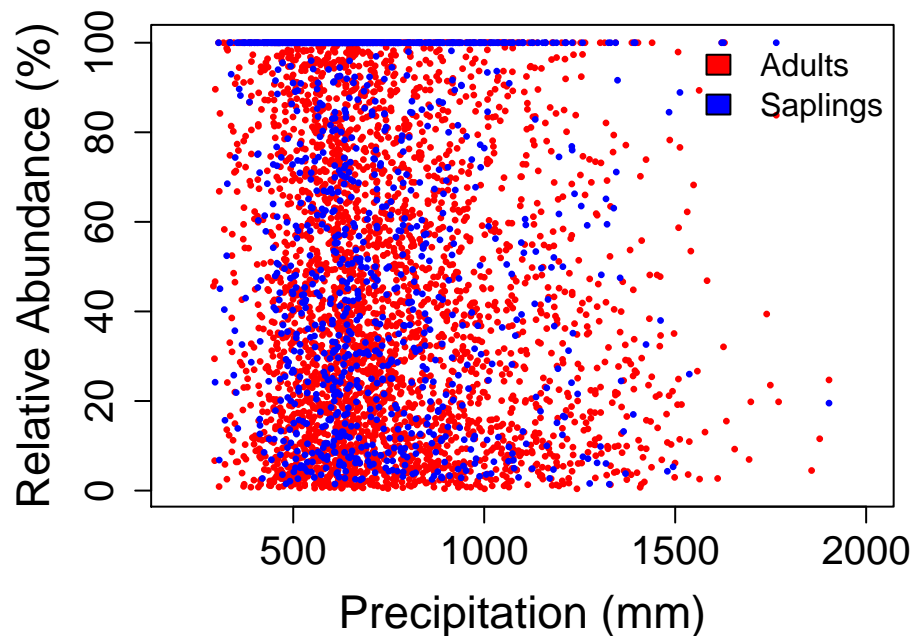
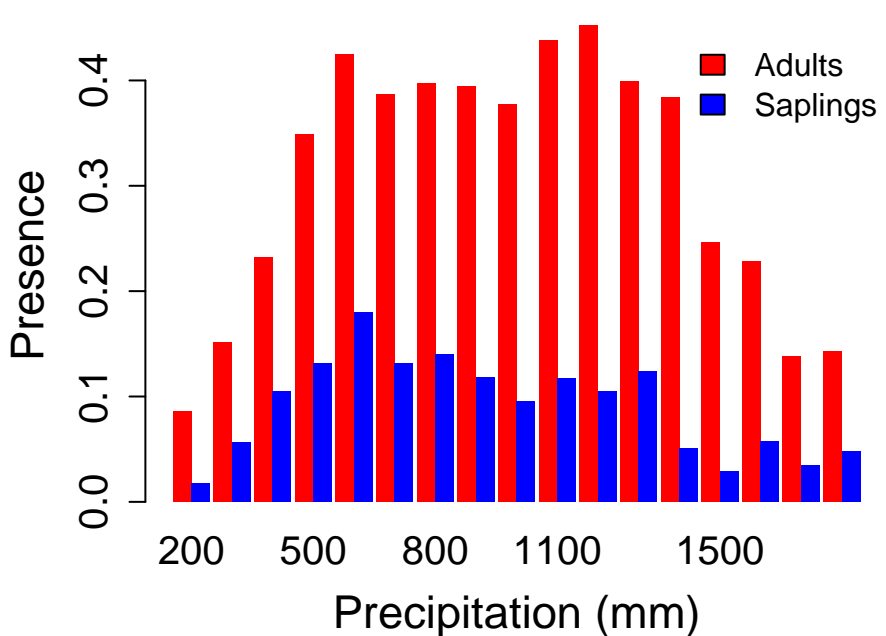
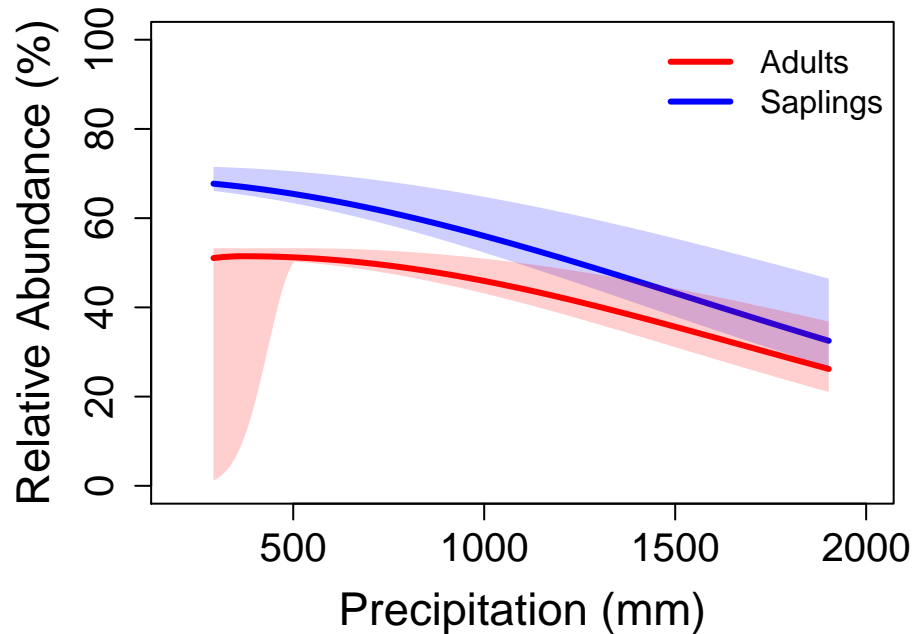
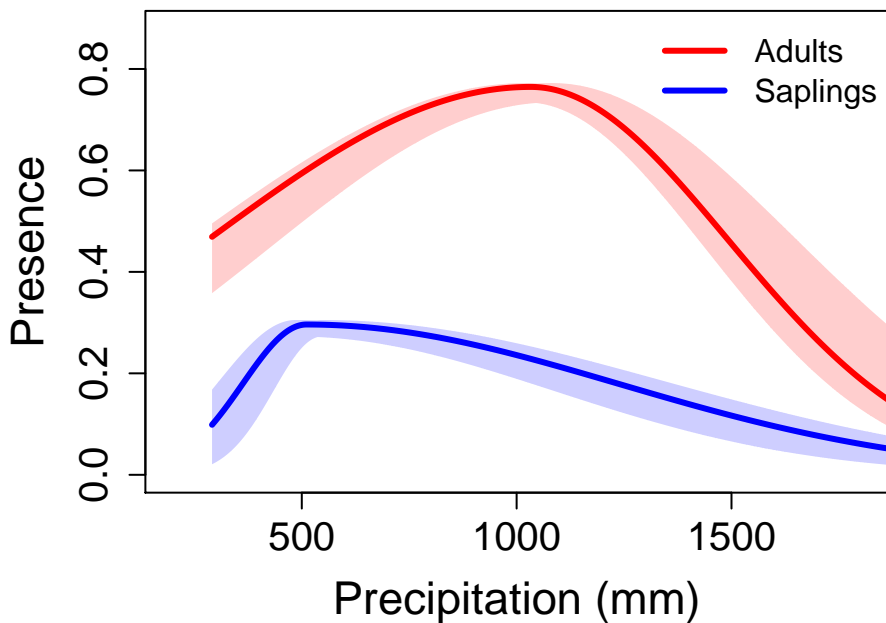
# Pinus ponderosa – ponderosa pine



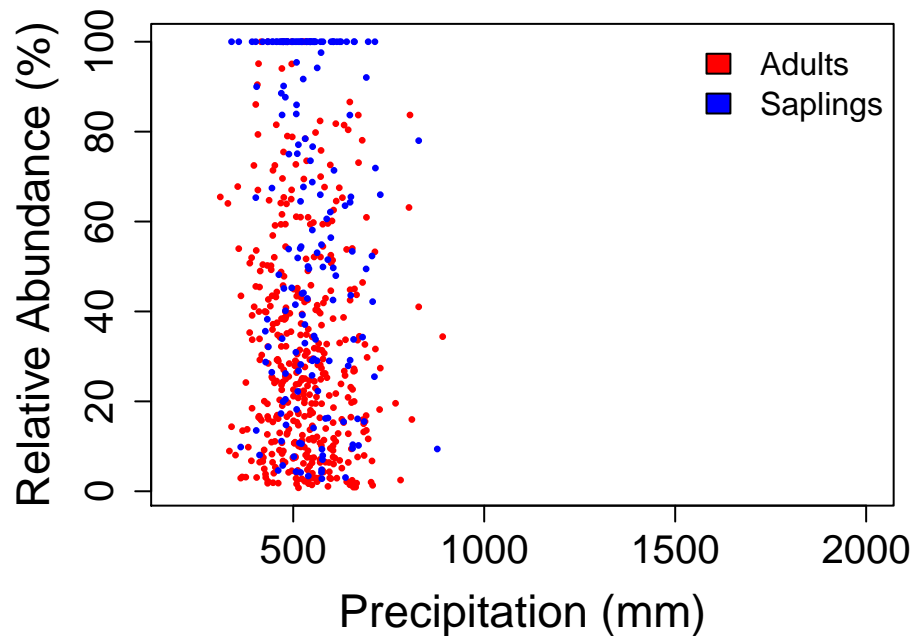
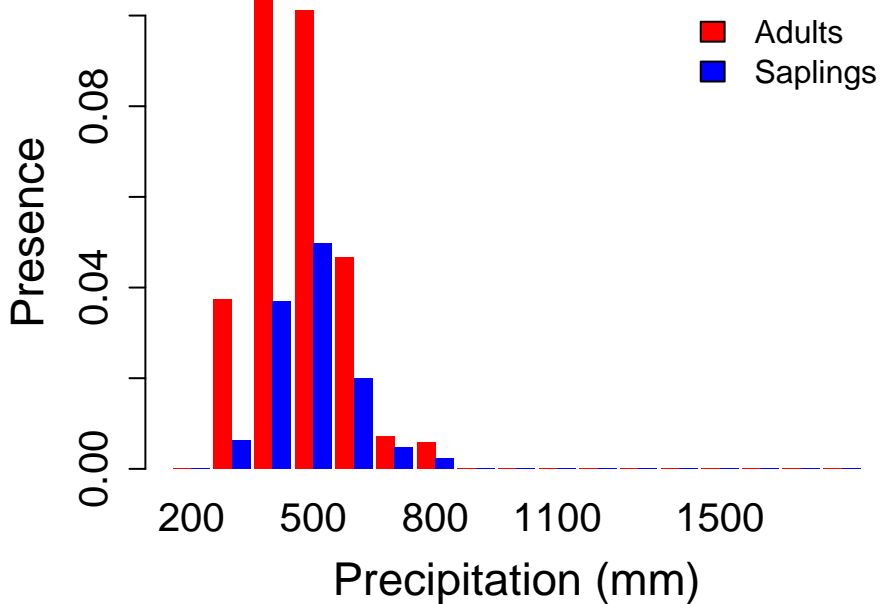
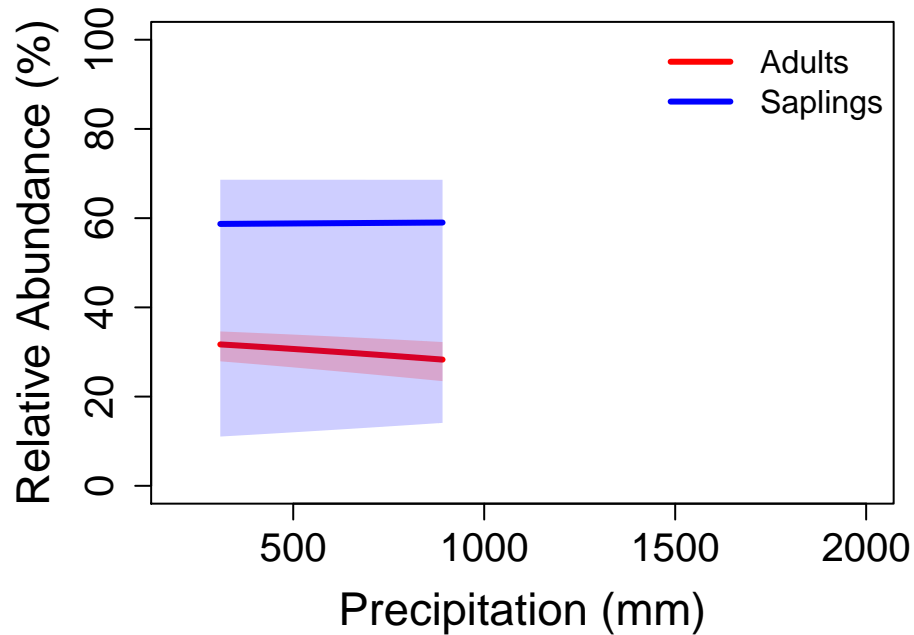
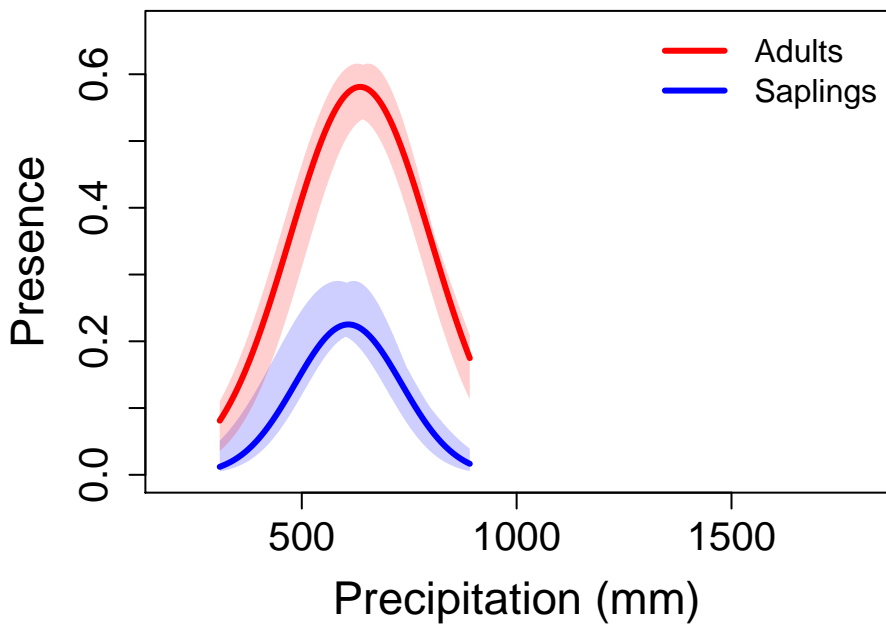
# Populus tremuloides – quaking aspen



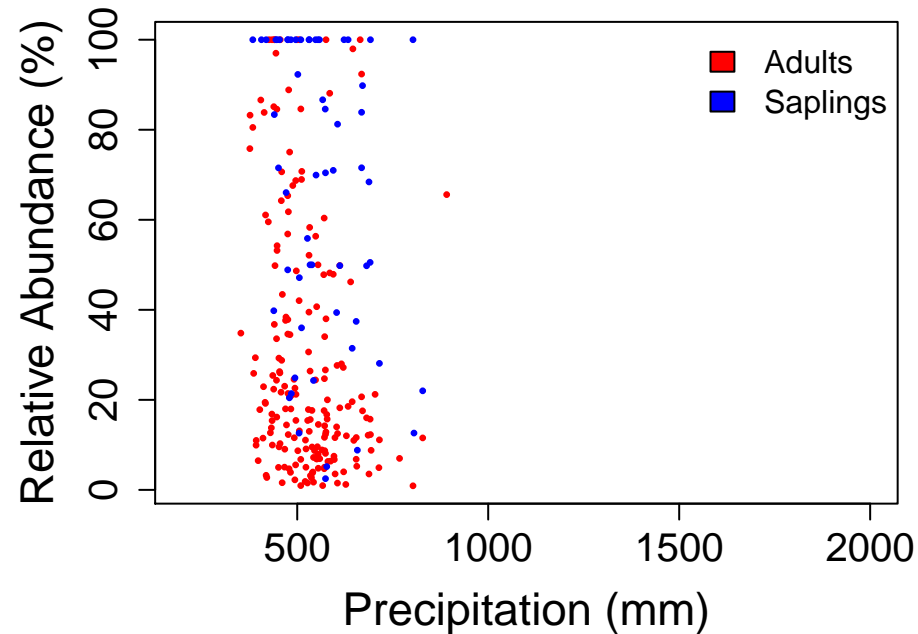
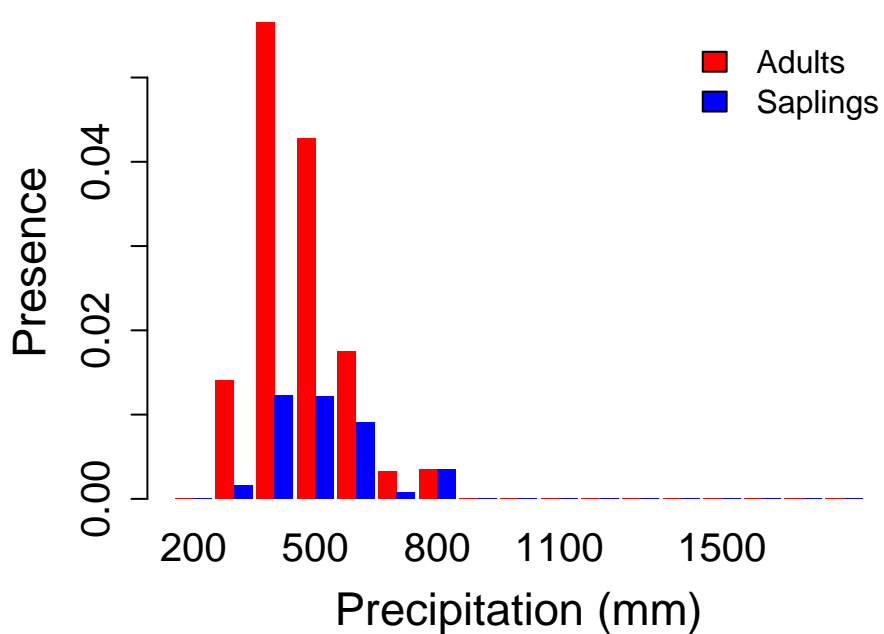
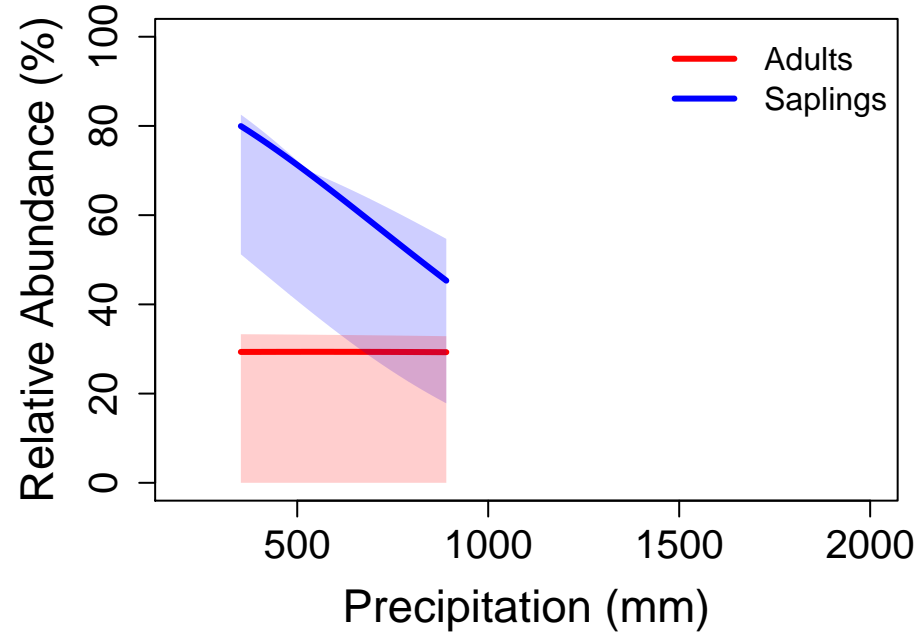
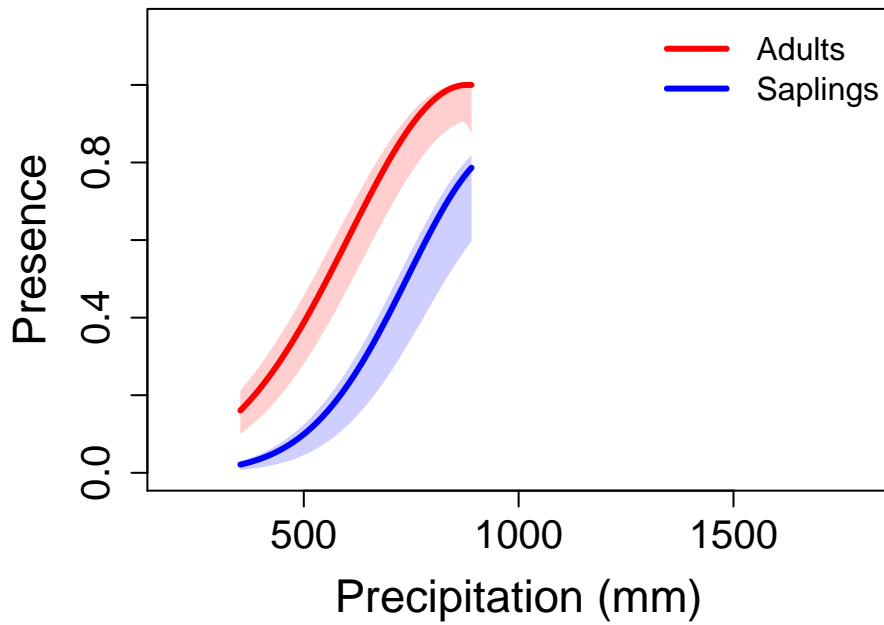
# Pseudotsuga menziesii – Douglas-fir



# Quercus arizonica – Arizona white oak



# Quercus emoryi - Emory oak



# Quercus gambelii – Gambel oak

